

Deep-Water Octocorals (Cnidaria, Anthozoa) from the Galápagos and Cocos Islands. Part I: Suborder Calcaxonia

Stephen D. Cairns¹

¹ Department of Invertebrate Zoology, National Museum of Natural History, Smithsonian Institution, P. O. Box 37012, MRC 163, Washington, D.C. 20013-7012, USA

Corresponding author: Stephen D. Cairns (cairnss@si.edu)

Academic editor: B. W. Hoeksema | Received 20 October 2017 | Accepted 12 December 2017 | Published 16 January 2018

<http://zoobank.org/F54F5FF9-F0B4-49C5-84A4-8E4BFC345B54>

Citation: Cairns SD (2018) Deep-Water Octocorals (Cnidaria, Anthozoa) from the Galápagos and Cocos Islands. Part 1: Suborder Calcaxonia. ZooKeys 729: 1–46. <https://doi.org/10.3897/zookeys.729.21779>

Abstract

Thirteen species of deep-water calcaxonian octocorals belonging to the families Primnoidae, Chrysogorgiidae, and Isididae collected from off the Galápagos and Cocos Islands are described and figured. Seven of these species are described as new; nine of the 13 are not known outside the Galápagos region. Of the four species occurring elsewhere, two also occur in the eastern Pacific, one off Hawaii, and one from off Antarctica. A key to the 22 Indo-Pacific species of *Callogorgia* is provided to help distinguish those species.

Keywords

Octocorals, Galápagos, Cocos Islands, Calcaxonia, *Callogorgia*

Introduction

Early in my career (1986) I was privileged to participate in a deep-sea submersible expedition to the Galápagos and Cocos Islands, which was sponsored by SeaPharm, Inc. and HBOI (Pomponi et al. 1988). It made rich collections from 27 stations from off the Galápagos (*JSL-I*-1911 to 1937) and eight stations off the Cocos Islands (*JSL-I*-1938 to 1945) at depths to 823 m (Figure 1). Also on board this expedition were

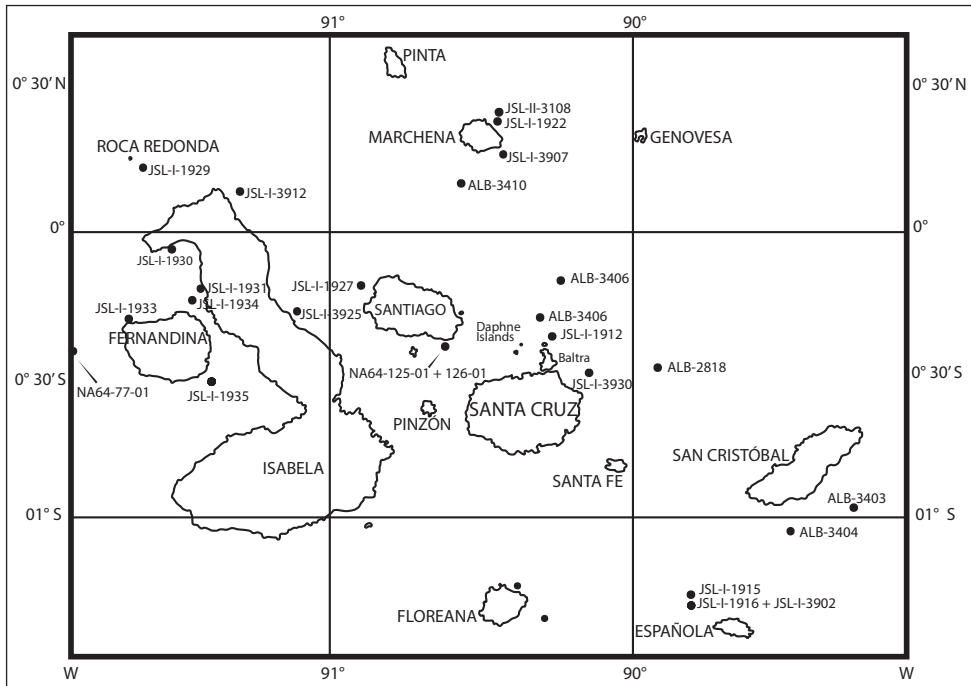


Figure 1. Map of the Galápagos Islands localities from where specimens are reported in this paper.

research scientists Shirley Pomponi and John Reed. Abundant deep-water invertebrates were collected at all stations, including many corals, but because the goal of the expedition was to seek biologically active compounds from these species, a 25-year sequestration was placed by the National Cancer Institute on all specimens collected. Nonetheless, as a participant in the expedition, I was given permission to publish on the Scleractinia (Cairns 1991a) and Stylasteridae (Cairns 1986, 1991b). Now, at the end of my career, I have come full circle to publish on the remaining deep-water corals collected by this expedition.

Although the 1986 *Johnson-Sea-Link* expedition was the first submersible expedition to sample the deep waters off the Galápagos, it was not the first to collect deep-water invertebrates from this region. As early as 1888 the *Albatross* had made 13 deep-water stations (*Alb* 2806 to 2819) off these islands, 14 more stations again in 1891 (*Alb* 3400–3413), and another 10 stations (*Alb* 4636–4646) in 1904, all these specimens being deposited at the NMNH. The *Johnson-Sea-Link* also made additional collections in the Galápagos in 1995 (*JSL-I*-3900 to 3985) and in 1998 (*JSL-II*-3084 to 3113). More recently the *E/V Nautilus* has made deep-water collections in July 2015. Deep-water octocorals from all of these cruises were examined to form a basis for this report.

Thirteen deep-water octocoral species are reported herein, i.e., those that belong to the suborder Calcaxonina: Primnoidae, Chrysogorgiidae, and Isididae. Approximately

an equal number of deep-water octocorals belonging to the families Alcyoniidae, Acanthogorgiidae, Plexauridae and the order Pennatulacea have also been collected from these islands and will be reported in later parts. Of these thirteen species, seven are described as new, four have range extensions, and only two had been previously reported from the Galápagos by Studer (1894).

Material and methods

As explained in the Introduction, this study is based on all the deep-water calcaxonian octocoral specimens collected by the *Albatross* and *John-Sea-Link I* and *II*, which are deposited at the NMNH. It also includes material collected by the *Nautilus*, which is deposited at the CDRS.

The methodology concerning sclerite preparation for SEM can be found in Cairns (2016). SEM stub numbers are in a series established by the author, and all are deposited at the NMNH. Morphological terminology follows the glossary of Bayer et al. (1983), as updated by Cairns (2012, 2016).

The following abbreviations are used in the text:

Museums / institutions

BM	British Museum (now The Natural History Museum, London)
CDRS	Charles Darwin Research Station, Galápagos
HBOI	Harbor Branch Oceanographic Institute, Ft. Pierce, Florida
NMNH	National Museum of Natural History, Smithsonian, Washington DC
USNM	United States National Museum (now the NMNH)

Vessels

<i>Alb</i>	USFWS <i>Albatross</i>
<i>GS</i>	R/V <i>Gilliss</i>
<i>JSL-I</i>	<i>Johnson-Sea-Link I</i> submersible (HBOI)
<i>JSL-II</i>	<i>Johnson-Sea-Link II</i> submersible (HBOI)
<i>NA</i>	<i>E/V Nautilus</i>

Other terms

L:W	ratio of length to width of a polyp or sclerite
SEM	scanning electron microscope

Systematic account

Subclass Octocorallia

Order Alcyonacea

Suborder Calcaxonia

Family Primnoidae Milne Edwards, 1857

Genus *Callozostron* Wright, 1885

Callozostron Wright 1885: 690–691; Wright and Studer 1889: 48; Bayer 1996: 151–152; Cairns and Bayer 2009: 32–33; Cairns 2016: 26–27 (key to species).

Type species. *Callozostron mirabile* Wright and Studer, 1889, by monotypy.

Diagnosis. Colonies unbranched, sparsely dichotomously branched, or pinnately branched. Polyps arranged in whorls, the bases of adjacent polyps sometimes fused. Polyps covered by eight longitudinal rows of body wall scales, which completely cover the polyp. At least four and up to 24 marginal and submarginal scales bear elongate slender apical spines; marginal scales do not fold over operculars. Coenenchymal scales similar to those of body wall, arranged in one layer. All scales thin, with a smooth pouter face and tuberculate inner face.

Distribution. Antarctic, Subantarctic, Antipodes, New Zealand, Clarion-Clipper-ton Fracture Zone, Galápagos, 744–4235 m deep.

Remarks. A discussion and key to the six species in this genus are given by Cairns (2016).

Callozostron carlottae Kükenthal, 1909

Figures 3h, 4

Callozostron carlottae Kükenthal 1909: 49–50; 1912: 334–336, pl. 22, figs 14–17, text-figs 43–47. Not: Bayer 1996: 159–161, figs 7–10 (but includes a complete synonymy); Cairns 2016: 27.

Material examined. *Nautilus* NA064-77-01-A, 1 branch, 1.82° C, CDRS, and SEM stubs 2376–2378, NMNH.

Types. Four specimens (?syntypes) are included in the original description. Their deposition is unknown.

Type locality. Antarctica (between 60–90°E), 3397 m depth (*Gauss* German South Polar Expedition of 1901–1903).

Distribution. Galápagos: east of Fernandina, 3381 m depth. Elsewhere: Antarctica, 3397 m depth.

Description. Although only one incomplete colony is available (Figure 3h), it appears to be unbranched and 9 cm in length. Its polyps are arranged in whorls of six or seven (Figure 4a), about five whorls occurring per cm branch length; the whorl diam-

eter is about 4 mm, including the marginal spines. The polyps are short and cylindrical (Figures 4b–d), only about 1.2–1.4 mm in height, not counting the marginal spines, which can be up to twice as long as the polyp. The actual body wall is relatively short (about 0.5 mm), the opercular scales making up the remaining length of the polyp.

The body wall scales (Figures 4f–i) are arranged in eight irregular longitudinal rows, the two distal marginal and submarginal body wall scales being quite different from the lower four or five tiers of scales, the latter (Figure 4f) being roughly elliptical to rectangular in shape, quite thin, and often having a slightly lobate distal margin. The body wall scales are slightly curved to fit the circumference of the polyp and are highly imbricate. Their outer face is perfectly smooth, their inner face covered with sparse small tubercles. There are eight marginal and usually eight submarginal scales. The marginal scales (Figures 4g, i) have a rectangular to trapezoidal base that is up to 0.6 mm in width, capped by a slender (0.1 mm in diameter basally, but attenuating to a point distally) elongate (up to 2.2 mm in length) spine, the spinose part thus contributing 75–80% of the length of the sclerite. The spine is smooth but itself covered with very small (about 15 μm in length) spines. The submarginal scales (Figure 4h) may be as large as the marginal scales, but some are only about half as long (0.75–0.90 mm in length, see below). The eight operculars (Figures 4b, e) are arranged in two alternating quartets of four, an inner quartet and an outer, the lateral edges of the outer operculars overlapping those of the inner. The opercular scales are isosceles triangular in shape with a pointed (not spinose) tip, and having a longitudinally concave, perfectly smooth outer surface and a sparsely tuberculate inner surface. They are slightly curved about 45° in order to fold over the polyp to form the operculum. The operculars are 0.7–1.0 mm in height, with a L:W of 1.9–2.6. The marginal and submarginal scales that are aligned with the four inner opercular scales are usually both large in size, whereas the submarginals associated with the outer opercular scales are often much smaller (see above) and may even be absent. The coenenchymal scales (Figure 4j) are irregular in shape but usually elongate, up to 0.65 in greater length. Like most of the other scales, they have a smooth outer surface and a sparsely tubercular inner surface, and are quite thin, and easily broken.

Comparisons. Despite the long distance between the Antarctic type locality and the Galápagos, this specimen is identified as *C. carlottae*, but it does differ in several points from the original description. The Galápagos specimen has larger polyps, and thus larger opercular and marginal spines, those of the Antarctic syntypes being only 0.6 mm and 0.8 mm in length, respectively. And the Antarctic syntypes have eight or nine polyps per whorl, whereas the Galápagos specimen has only six or seven. Otherwise, the two specimens are remarkably similar, the Galápagos specimen even showing the dimorphic-sized submarginal spines (Kükenthal 1912: fig. 43). The specimens reported by Bayer as *C. carlottae* are not considered conspecific, based on a difference in the size and number of rows of submarginal spines (see Cairns 2016), as well as having differently shaped marginal spines and thicker granular body wall scales.

Remarks. This is the first report of this species subsequent to its original description, and was collected at virtually the same depth.

Genus *Callogorgia* Gray, 1858

Callogorgia Gray 1858: 286; Bayer 1982: 119–123; 1998: 162–163; Cairns and Bayer 2002: 841–845; 2009: 40; Cairns 2010: 425; 2016: 58.

Caligorgia Wright and Studer 1889: 75–77; Versluys 1906: 55–58; Kükenthal 1919: 362–366.

Type species. *Gorgonia verticillata* Pallas, 1766, by monotypy.

Diagnosis. Colonies uniplanar, pinnately or dichotomously branched. Polyps cylindrical to clavate, arranged in whorls of up to 12, all polyps facing upward. Polyps covered with eight longitudinal rows of body wall scales, the number of scales per row decreasing from ab- to adaxial polyp side. Body wall scales granular, smooth, pitted, or covered with tall ridges (crystate). Inner side of opercular scales convex, covered with a multiply serrate keel.

Distribution. Indo-Pacific, Atlantic, 37–2472 m deep.

Remarks. The identification of the species of *Callogorgia* has been greatly facilitated by the availability of previously published dichotomous keys. The structure and characters used for the first published key were chosen by Kükenthal (1919) and later refined by Kükenthal (1924) and Bayer (1982). Since Bayer's key, which was limited to the Indo-Pacific species, at least one species (*C. cristata* (Aurivillius, 1931)) has been synonymized, two (*C. ventilabrum* Studer, 1878, *C. laevis* Thomson and Mackinnon, 1911) transferred to different genera, four described as new (*C. tessellata* Cairns, 2016, *C. dichotoma* Cairns, 2016, *C. galapagensis* sp. n., *C. arawak* Bayer et al., 2014), two previously overlooked (*C. gilberti* (Nutting, 1908), *C. modesta* (Studer, 1878)), and the characteristics of *C. kinoshitai* (Kükenthal, 1913) re-evaluated. Thus, a revised key is provided below, which relies heavily on the characters used in previously published keys. *C. dubia* (Thomson and Henderson, 1906), based on a poor description and no figures, is of doubtful attribution and is not considered in the key. Previously *C. elegans* (Kükenthal 1919, Bayer 1982) had been keyed as having 12–13 abaxial scales, but examination of the type in the BM by Bayer (pers. comm.) indicates that it has only six to eight abaxial body wall scales and a body wall sclerite formula of: 6–8:2:0:1. Keys to the five western Atlantic species were published by Cairns and Bayer (2002) and Bayer et al. (2014). Altogether, there are currently 28 valid species in the genus (Cairns and Bayer 2009; Taylor and Rogers 2015).

Key to the 22 Indo-Pacific species of *Callogorgia* (species included herein in bold face; species having ridged (crystate) abaxial body wall scales indicated with an asterisk)

- 1 Branching typically pinnate 2
- Branching dichotomous or quasi-dichotomous 13
- 2 Branches strictly opposite *C. formosa* (Kükenthal, 1907)
- Branches alternate 3

- 3 Scales in outer lateral body wall rows well developed, i.e., having the same or only slightly fewer than those in abaxial row 4
- Scales in outer lateral body wall rows sharply reduced in number, i.e., usually less than half the number as that in abaxial row 6
- 4 Coenenchymal scales elongate and not thick; outer surface of abaxial body wall scales on distal half of polyp highly ridged **C. galapagensis* sp. n.
- Coenenchymal scales irregular in shape and quite thick (tessellate); outer surface of body wall scales granular or pitted (not ridged) 5
- 5 Seven to nine scales in abaxial body wall scale rows; body wall scales pitted; polyps 1.4–1.8 mm in length *C. sertosa* (Wright and Studer, 1889)
- Nine to eleven scales in abaxial body wall scale rows; body wall scales granular; polyps 1.0–1.2 mm in length *C. tessellata* Cairns, 2016
- 6 Operculum low and inconspicuous *C. pennacea* (Versluys, 1906)
- Operculum tall and prominent 7
- 7 Abaxial opercular scales with two to four apical points **C. weltneri* (Versluys, 1906)
- Abaxial opercular scales with a single point 8
- 8 Eight or more scales in each abaxial body wall row 9
- Six to eight scales in each abaxial body wall row 11
- 9 Apex of opercular scales prolonged into a rod-like (cylindrical) point **C. ramosa* (Kükenthal and Gorzawsky, 1908)
- Apex of opercular scales not prolonged in a cylindrical point 10
- 10 Eight to ten scales in abaxial body wall scale rows **C. flabellum* (Ehrenberg, 1834)
- Eleven to thirteen scales in abaxial body wall scale rows **C. gilberti* (Nutting, 1908)
- 11 Polyps about 2 mm tall **C. robusta* (Versluys, 1906)
- Polyps 1.0–1.8 mm tall 12
- 12 Coenenchymal scales elongate; inner lateral and adaxial body wall scales present; eastern Pacific *C. kinoshitai* (Kükenthal, 1913)
- Coenenchymal scales polygonal; inner lateral and adaxial body wall scales absent; South Pacific *C. joubini* (Versluys, 1906)
- 13 Scales in outer lateral body wall rows well developed, i.e., having the same or only slightly fewer than those in abaxial row 14
- Scales in outer lateral body wall rows sharply reduced in number, i.e., usually less than half the number as that in abaxial row 15
- 14 Five or six scales in each abaxial body wall row *C. dichotoma* Cairns, 2016
- Ten scales in each abaxial body wall row *C. versluysi* (Thomson, 1905)
- Twelve or 13 scales in each abaxial body wall row *C. imperialis* Cairns, in press
- 15 Three scales in each outer lateral body wall row 16
- One or two scales in each outer lateral body wall row 17

- 16 Four polyps per whorl..... *C. elegans* (Gray, 1870)
- Two or three polyps per whorl *C. indica* (Thomson and Henderson, 1906)
- 17 Five scales in each abaxial body wall row 18
- Seven scales in each abaxial body wall row 19
- 18 Two or three polyps per whorl; eight to nine whorls per cm branch length;
body wall scales with low marginal ridges *C. minuta* (Versluys, 1906)
- Three or four polyps per whorl; 9–11 whorls per cm branch length; body wall
scales with distal margins strongly reflexed, exposing high crest-like ridges on
inner face *C. chariessa* Bayer, 1982
- 19 Two or three polyps per whorl; seven to eight whorls per cm branch length....
..... *C. similis* (Versluys, 1906)
- Four to six polyps per whorl; nine to ten whorls per cm branch length 20
- 20 Abaxial body wall scales with strong marginal ridges
..... **C. affinis* (Versluys, 1906)
- Abaxial body wall scales with only weak marginal ridges
..... *C. modesta* (Studer, 1878)

***Callogorgia galapagensis* sp. n.**

<http://zoobank.org/F21CD90F-41C8-4A0A-9B2B-6CF8E4E9E6A4>

Figures 2a, 5

Material examined. Types. Holotype: *JSL-I-1933*, large colony and SEM stubs 2295–2297, 2308–2311, USNM 1161744. Paratypes: *JSL-I-1915*, partial colony, USNM 1161750; *JSL-I-1930*, partial colony, USNM 1161746; *JSL-I-1934*, 1 branch, USNM 1161745; *JSL-I-1942*, 1 branch, USNM 1161748.

Type locality. *JSL-I-1933*: 0°17.072'S, 91°04.208'W (off northwest tip of Fernandina, Galápagos), 663–788 m deep.

Distribution. Galápagos: Tagus Cove between Isabela and Fernandina, north of Española, 308–633 m deep; Cocos Island, 628–656 m deep.

Description. Colonies are uniplanar and taller than broad, the holotype (Figure 2a) measuring 49 cm in height and 18 cm in width, with a broken basal branch diameter of 5.9 mm. Another colony fragment (*JSL-I-1915*) has a broken basal branch diameter of 8.9 mm, suggesting a colony height of close to 1 m. Branching is alternate pinnate (sympodial and geniculate), the terminal branchlets up to 13 cm in length. The polyps are arranged in whorls of five or six (Figure 5a); four to five whorls occur per cm branch length; the whorl diameter ranges from 2.5–3.1 mm. The polyps are 1.5–2.0 mm in length, slightly curved, and clavate (Figure 5b–d). The color of the colony and polyps is white.

There are eight longitudinal rows of body wall scales, decreasing in number from ab- to adaxial polyp side, the body wall sclerite formula being: 10–12:10–12:4–5:2. The distal five or six pairs of abaxial scales (Figure 5f) are narrow (0.31–0.35 mm



Figure 2. Colonies of various species. **a** *Callogorgia galapagensis*, holotype, USNM 1161744 **b** *Callogorgia kinoshitai*, Alb-3406, USNM 50960 **c** *Calyptrophora agassizii*, JSL-II-3108, USNM 1093041 **d** *Calyptrophora reedi*, holotype, USNM 1409027 **e** *Narella ambigua*, JSL-I-1927, USNM 1297223.

wide), each bearing four to seven prominent (up to 0.08 mm in height) longitudinal ridges that terminate as projections on the distal edge of the scale. More proximal abaxial body wall scales are broader (up to 0.48 mm) and flat, lacking radial ridges. The outer lateral body wall scales (Figure 5h) are sculpted similarly, the basal pairs being

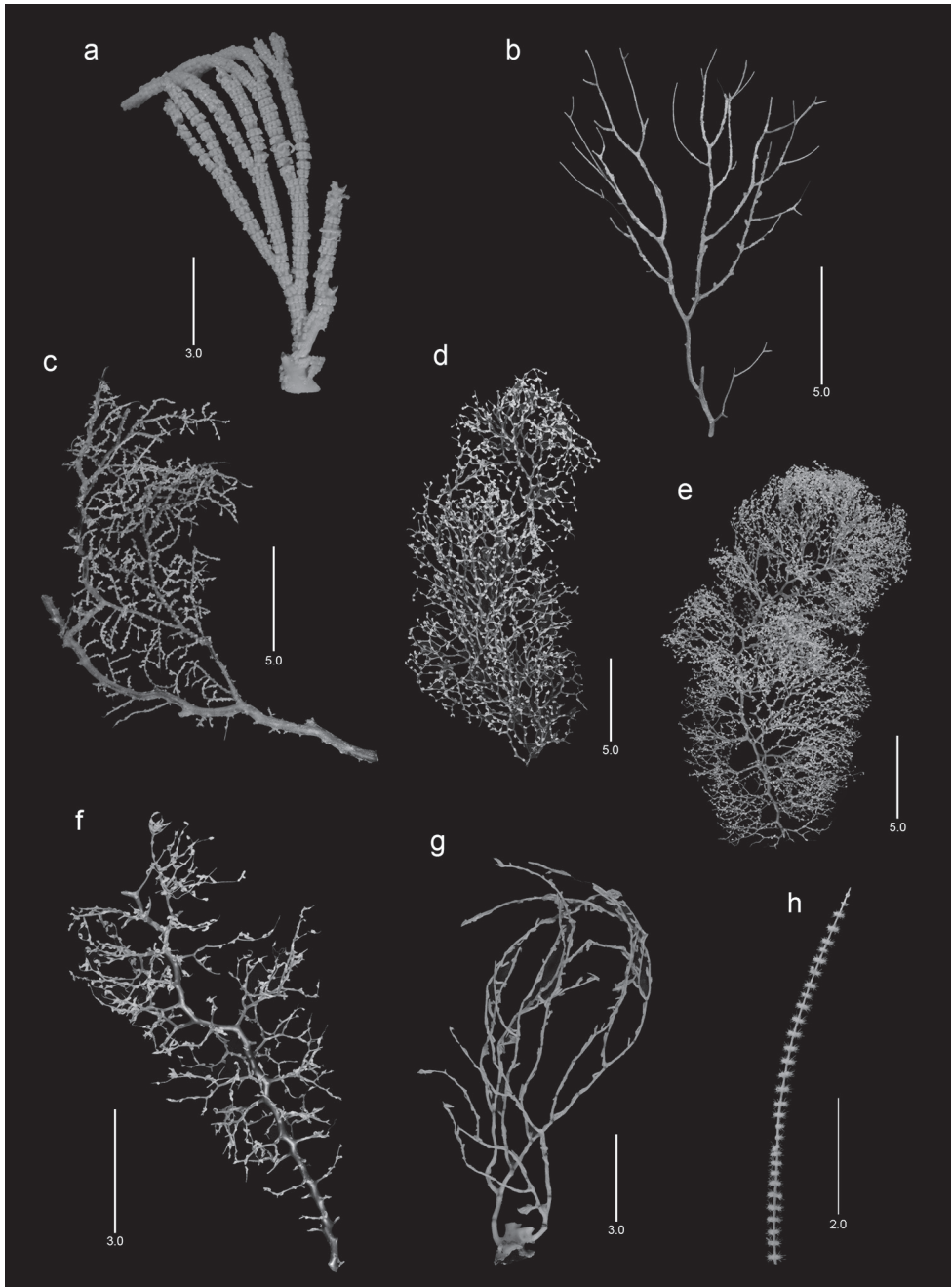


Figure 3. Colonies of various species. **a** *Narella enigma*, holotype, USNM 1409703 **b** *Plumarella abietina*, Alb-2818, USNM 49605 **c** *Parastenella pomponiae*, holotype, USNM 1410289 **d** *Chrysogorgia scintillans*, JSL-II-1927, USNM 89377 **e** *Chrysogorgia midas*, holotype, USNM 1160575 **f** *Chrysogorgia laevorsa*, holotype, USNM 1409029 **g** *Isidella tenuis*, holotype, USNM 89382 **h** *Callozostron carlottae*, NA64-77-01-A.

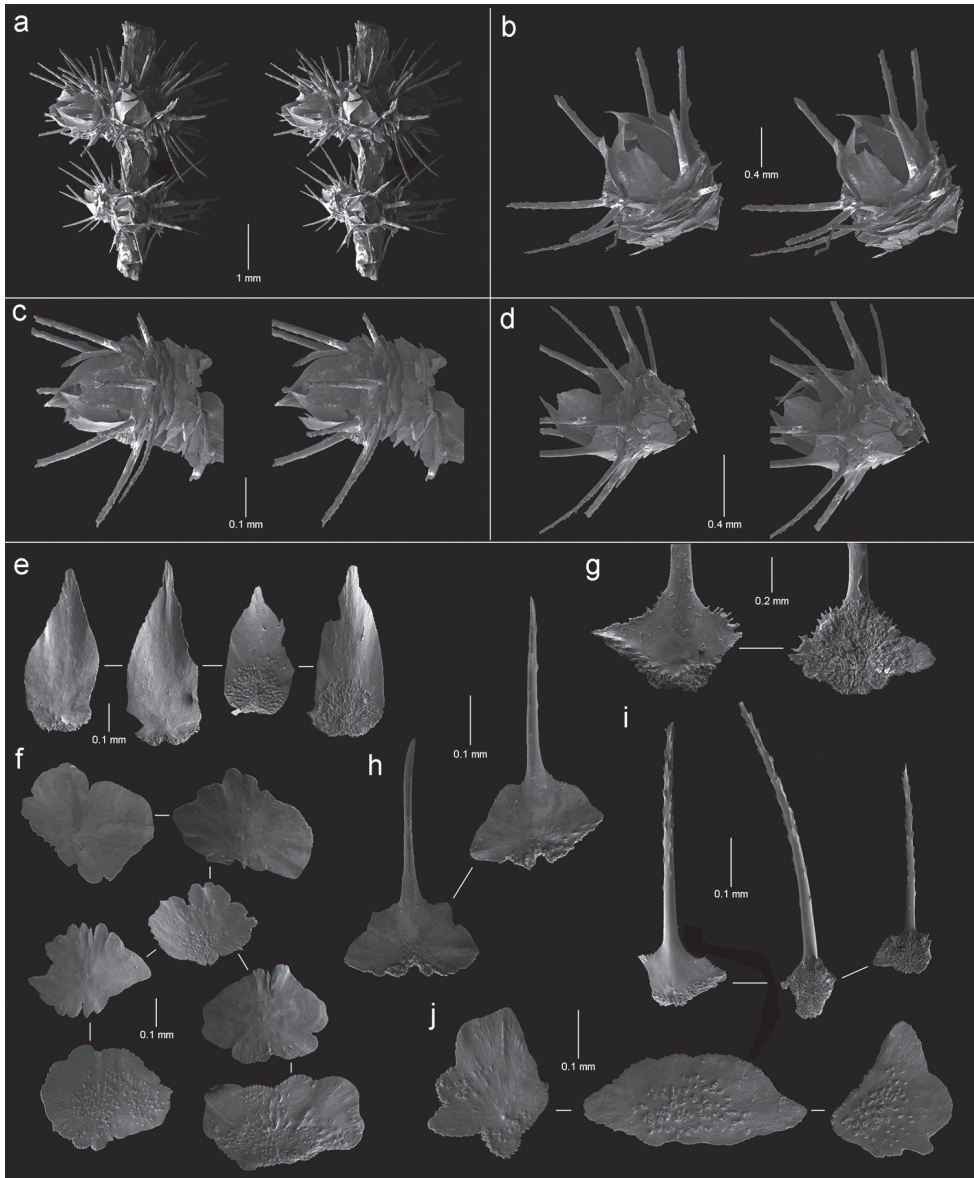


Figure 4. Polyps and sclerites of *Callozostoon carlottae* from NA64-77-01-A. **a** lateral stereo view of two polyp whorls **b–d** lateral stereo views of three polyps showing spinose marginal and submarginal scales and non-spinose proximal body wall scales **e** opercular scales **f** lower, non-spinose body wall scales **g** wide base of marginal scales **h** spinose submarginal scales **i** marginal scales **j** coenenchymal scales.

even wider than those on the abaxial face. The ridges of these distal scales are so tall and closely spaced that it is difficult to determine the lateral margins of the scales. The inner lateral body wall scales (Figure 5g) are even broader (up to 0.56 mm in width)

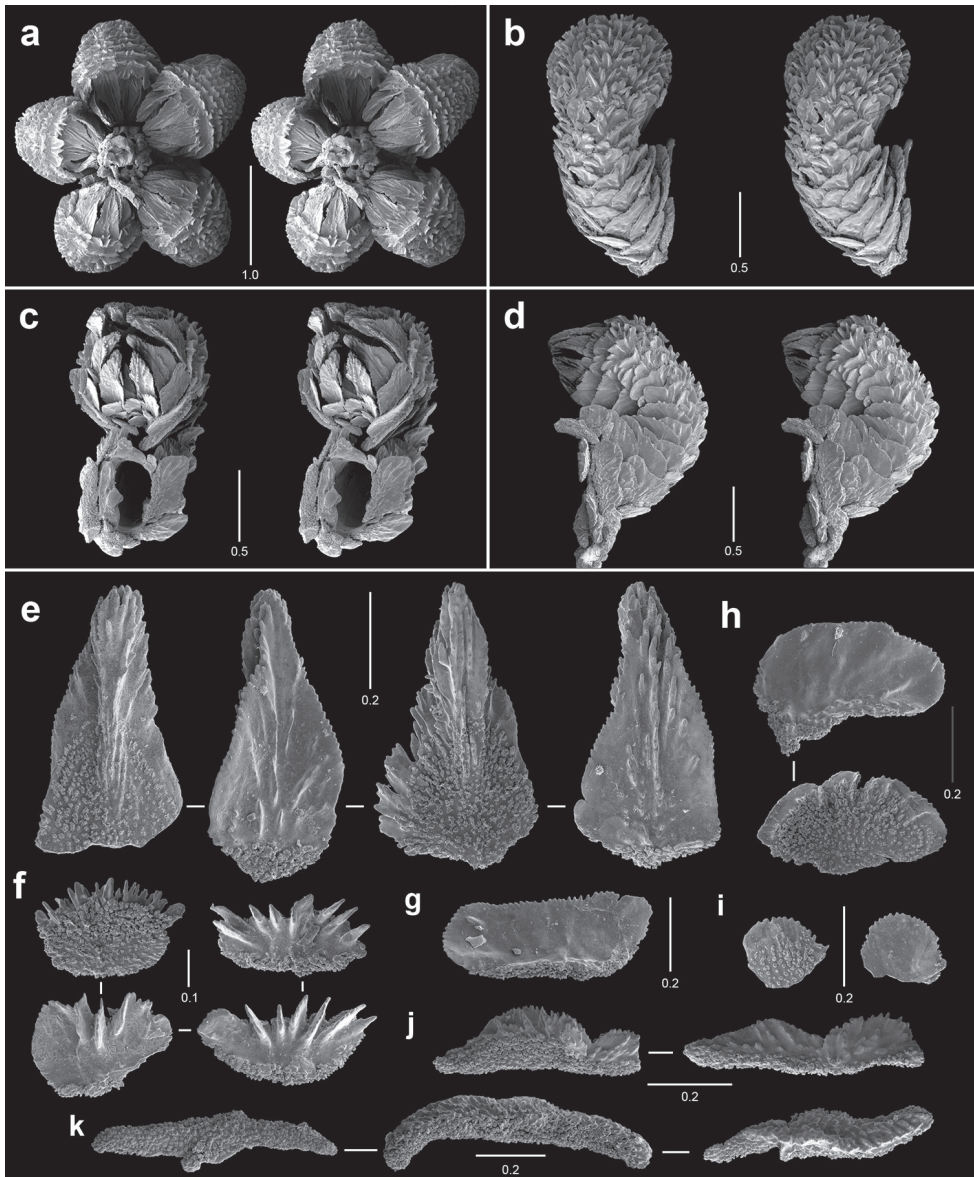


Figure 5. Polyps and sclerites of *Callogorgia galapagensis* from the holotype, *JSL-I-1933*, USNM 1161744. **a** apical stereo view of polyp whorl **b–d** abaxial, adaxial, and lateral stereo views of a polyp, respectively **e** opercular scales **f** abaxial body wall scales **g** inner lateral body wall scale **h** outer lateral body wall scales **i** adaxial body wall scales **j** infrabasal scales **k** coenenchymal scales.

and have a finely serrate distal edge. The two pairs of adaxial scales (Figure 5i) are small, only 0.22–0.25 mm in width, below which the polyp is naked (Figure 5c). At the junction of the lowest body wall scales and the branch coenenchymal sclerites is a pair

of crescentric infrabasal scales (Figure 5j) that forms a transition, each about 0.6 mm wide and 0.25 mm in height. The distalmost body wall scales in each row fold over the operculum as a short circumoperculum (Figure 5c). The opercular scales (Figure 5e) range in length from 0.50–0.65 mm, decreasing in length from ab- to adaxial polyp side, forming a prominent operculum; their L:W ranges from 1.7–2.25. Their outer surface is covered with tall serrate ridges and their edges are finely serrate. Their inner face is tuberculate, the distal third bearing a multiply serrated keel. The coenenchymal sclerites (Figure 5k) are elongate (L:W = 5–6), thick sclerites, arranged parallel to the branch axis, measuring up to 0.8 mm in length and 0.13–0.14 mm in width. Their outer surface is coarsely granular.

Comparisons. *Callogorgia galapagensis* belongs to a group of eight species that have highly cristate abaxial body wall scales, the other seven species listed in Cairns (2016), the Pacific component indicated in the key above by asterisks. The prominent ridges on these body wall scales often make it difficult to see the boundaries between adjacent rows of body wall scales. *Callogorgia galapagensis* can be distinguished from the other seven species by its sclerite formula, being the only species to have 10–12 abaxial and outer lateral body wall scales. This character is not used in the key above, and thus *C. galapagensis* keys closest to *C. sertosa* and *C. tessellata*, but can be distinguished by its unique sclerite formula.

Etymology. Named for the type locality of the species.

***Callogorgia kinoshitai* (Kükenthal, 1913), nom. correct.**

Figures 2b, 6

Callogorgia sertosa Nutting 1909: 715.

Callogorgia kinoshitae Kükenthal 1913: 264–266, text-figs E–F, pl. 8, fig. 10; Kükenthal 1919: 370; 1924: 270.

Callogorgia kinoshitae Bayer 1982: 122 (key); Cairns 2007b: 512 (listed); Cairns and Bayer 2009: 29 (listed).

Material examined. *Alb*-3406, 1 colony and SEM stubs 2300–2302, USNM 50960; *Alb*-3410, 1 colony, USNM 50959; *Alb*-4530, 1 colony, USNM 49611; *Alb*-4537, 3 colonies, USNM 30030, 43126, and 58986; *Desteiquer*, 36°37'12"N, 122°13'18"W, 1476–1609 m, 1 colony, USNM 75231; *Alb*-4357, USNM 30084 (syntype).

Types. Kükenthal (1913) established this species on the specimens described by Nutting (1909) as *C. sertosa*. Although Kükenthal examined some of those specimens and added information about them, he did not report any additional specimens or designate a type. The specimens reported by Nutting (1909) are thus considered as syntypes, and include those from *Alb*-4356, *Alb*-4357 (USNM 30084, SEM stubs 2298–2299), *Alb*-4358, *Alb*-4386, and *Alb*-4391, all presumably deposited at the NMNH, although only *Alb*-4357 could be located in 2017.

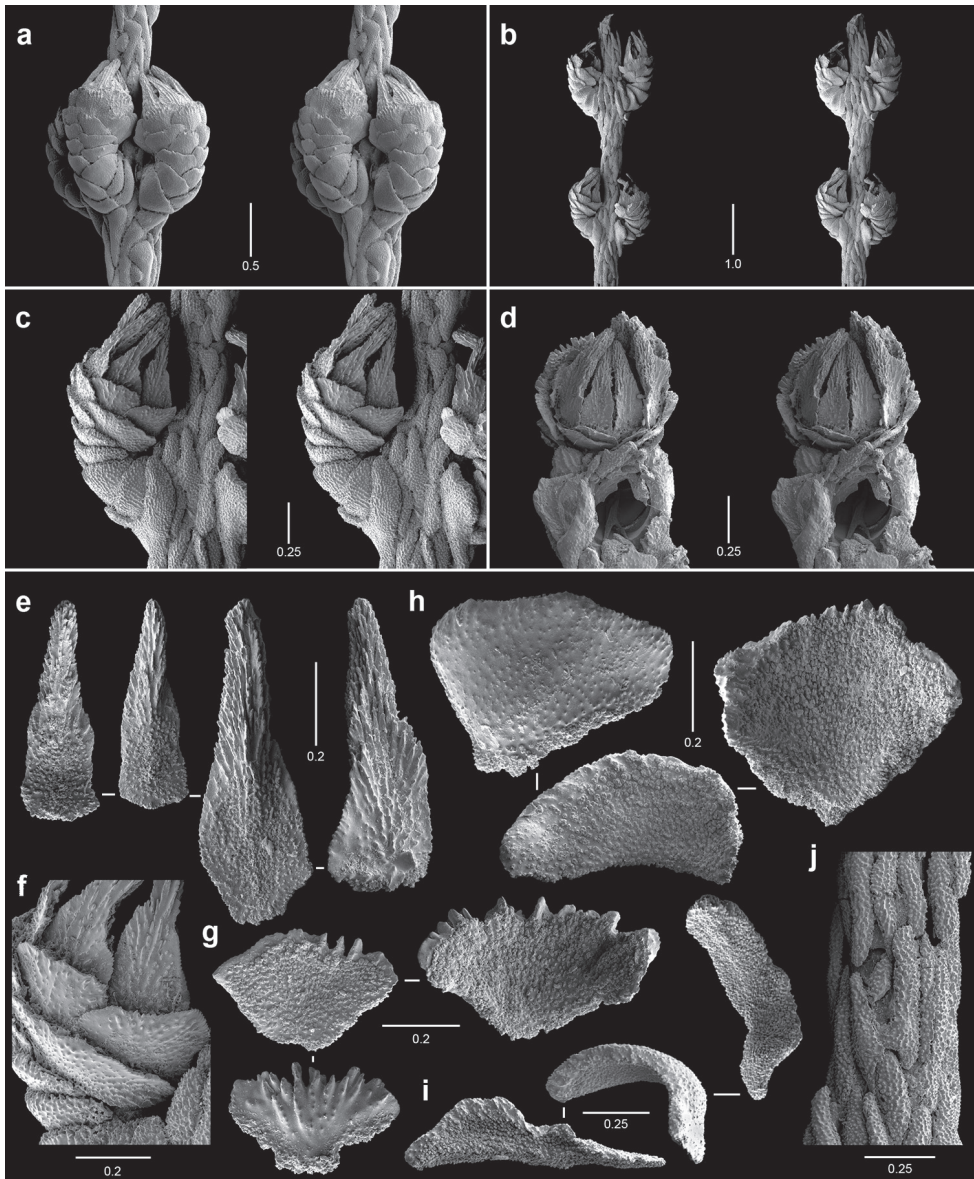


Figure 6. Polyps and sclerites of *Callogorgia kinoshitai* (**a** *Alb*-4357, USNM 30084 **b–j** *Alb*-3406, USNM 50960) **a–b** lateral stereo views of polyp whorls **c** lateral stereo view of a polyp **d** adaxial stereo view of a polyp **e** opercular scales **f** view of outer lateral scales, in situ **g** marginal scales **h** abaxial body wall scales **i** infrabasal scales **j** coenenchymal scales, in situ.

Type locality. As defined by the syntype series, the type-locality extends from northern Baja California (latitude 30°30'30"N) to just north of San Diego (latitude 33°02'15"N), and includes the bathymetric range of 219–2469 m.

Distribution. Galápagos: between Santa Cruz and Marchena, 605–1008 m deep. Elsewhere: northern Baja California to Monterey Bay (new records), California, 219–2469 m deep.

Description. Colonies are uniplanar and taller than wide, the largest Galápagos specimen (*Alb*-3406) a broken colony only 18 cm in height, but the largest syntype measuring up to 26 cm in height. Branching is alternate pinnate (sympodial and geniculate, Figure 2b), the terminal distal branchlets only about 4 cm in length. The polyps are arranged in whorls of two or three (Figures 6a, b), although Kükenthal (1919) reported a range of two to six, with four being the most common number. The whorl diameter is about 1.5 mm. The polyps are 1.3–1.5 mm in length, and slightly clavate (Figures 6c, d). The color of the colony and polyps is white.

There are eight longitudinal rows of body wall scales, decreasing in number from ab- to adaxial polyp side, the body wall sclerite formula being: 6–8:1–2:1–2:1–2. The marginal and submarginal abaxial body wall scales (Figure 6g) have a ctenate distal edge and increase in width and thickness from distal to proximal position. The basal-most abaxials are short but quite wide (up to 0.95 mm), curving around most of the basal part of the polyp and occupying the space normally reserved for the proximal outer and inner lateral scales. These scales serve as infrabasals (Figure 6i), forming a transition from the plate-like body wall scales (Figure 6h) to the thick elongate coenenchymal scales (Figure 6j). The outer (Figure 6f) and inner lateral body wall scales are quite wide (0.5–0.6 mm) and have a finely serrate distal edge. The adaxial scales (Figure 6d) are narrow, only about 0.3 mm in width. The outer surface of the body wall scales is relatively smooth, and covered with small, low granules. All body wall scales are curved to fit the circumference of the polyp body. The opercular scales (Figure 6d, e) range in length from 0.50–0.75 mm, decreasing in length from ab- to adaxial polyp side, forming a prominent operculum; their L:W ranges from 2.8–3.0. The relatively high L:W ratio is caused by an attenuate tip that is essentially round in cross section and covered on all surfaces by small spines arranged in longitudinal rows. The coenenchymal sclerites (Figure 6j) are elongate (L:W = 5–6) and thick, up to 0.55 mm in length and about 0.1 mm in width. They are longitudinally arranged in one layer on the branches. Their outer surface covered by low granules.

Comparisons. Although this species was originally identified as *C. sertosa* by Nutting (1909), that species differs in having more pairs of outer body wall scales, a pitted body wall outer surface texture, and a tessellate coenenchymal scale arrangement (Cairns 2016). As seen from the key above, *C. kinoshitai* is most similar to *C. joubini* (Versluys, 1906) (Indonesia, 520 m deep) but differs from that species in having inner and outer lateral scales and elongate (not polygonal) coenenchymal scales.

Remarks. Kükenthal (1919) described a sclerite formula of 7–8:7–8:4:2 for this species, but the syntype from *Alb*-4357 clearly has only two outer lateral scales and thus his sclerite formula is doubted.

Nomenclature. This species was clearly named after Kumao Kinoshita, and thus the name is herein changed to reflect a masculine ending.

Genus *Calyptrophora* Gray, 1866

Calyptrophora Gray 1866: 25; Bayer 2001:267–368; Cairns 2007b: 512 (listed); Cairns and Bayer 2009, 44–45; Cairns 2009: 420–426 (key to species); Cairns 2012: 42–43 (key to New Zealand species).

Type species. *Calyptrophora japonica* Gray, 1866, by monotypy.

Diagnosis. Colonies uniplanar to slightly bushy (lyrate, dichotomous, polychotomous, biplanar) or unbranched. Polyps arranged in whorls, the polyps facing either upward or downward. Polyps consist of two annular sclerite rings, each composed of two inseparably fused scales; a pair of crescent-shaped infrabasals also present. Articular ridge present between basal and buccal body wall scale. Distal margins of body wall scales often spinose, toothed, or lobate. Operculum composed of eight scales; keels usually present on inner face of opercular scales. Coenenchymal scales elongate and flat, sometimes quite thick (as plates). Small curved tentacular platelets often present.

Distribution. Tropical and temperate latitudes of Atlantic, Pacific, and Indian Oceans, 227–3531 m deep.

Remarks. Including the new species described herein, the genus contains 23 species, making it the fifth most species-rich genus within the primnoids. Bayer (2001) divided the genus into two species complexes, one having their polyps directed upward, the other having their polyps directed downward. Although helpful in grouping and identifying species, these two species groups do not seem to have phylogenetic validity (Cairns 2009, Cairns and Wirshing in review).

***Calyptrophora agassizii* Studer, 1894**

Figures 2c, 7

Calyptrophora agassizii Studer 1894: 63; Menneking 1905: 253–255, pl. 8, figs 5–6, pl. 9, figs 15–16; Versluys 1906: 112; Kükenthal 1919: 475; 1924: 317; Cairns 2009: 422–424 (key and phylogenetic analysis); Cairns and Bayer 2009: 31 (listed).

Material examined. *JSL-I-1922*, 1 colony, USNM 1297148. *JSL-I-1931*, 3 branches, USNM 1161747; *JSL-I-1935*, 1 branch, USNM 1161749; *JSL-II-3108*, 1 colony, USNM 1093041; *JSL-I-3907*, 1 colony, USNM 1297151; syntypes.

Types. Syntypes: several branches from which 99% of the polyps are detached, MCZ 4815, and SEM 1357–1358, NMNH. Mixed in with the type lot of *C. agassizii* were several branches of *Narella ambigua*, a species collected from the previous *Albatross* station (3403). These specimens were separated by me in 2008.

Type locality. *Alb-3404*: 1°03'S, 89°28'W (south of San Cristóbal, Galápagos), 704 m depth.

Distribution. Galápagos: west of Isabela, off Marchena and San Cristóbal, 509–1545 m deep.

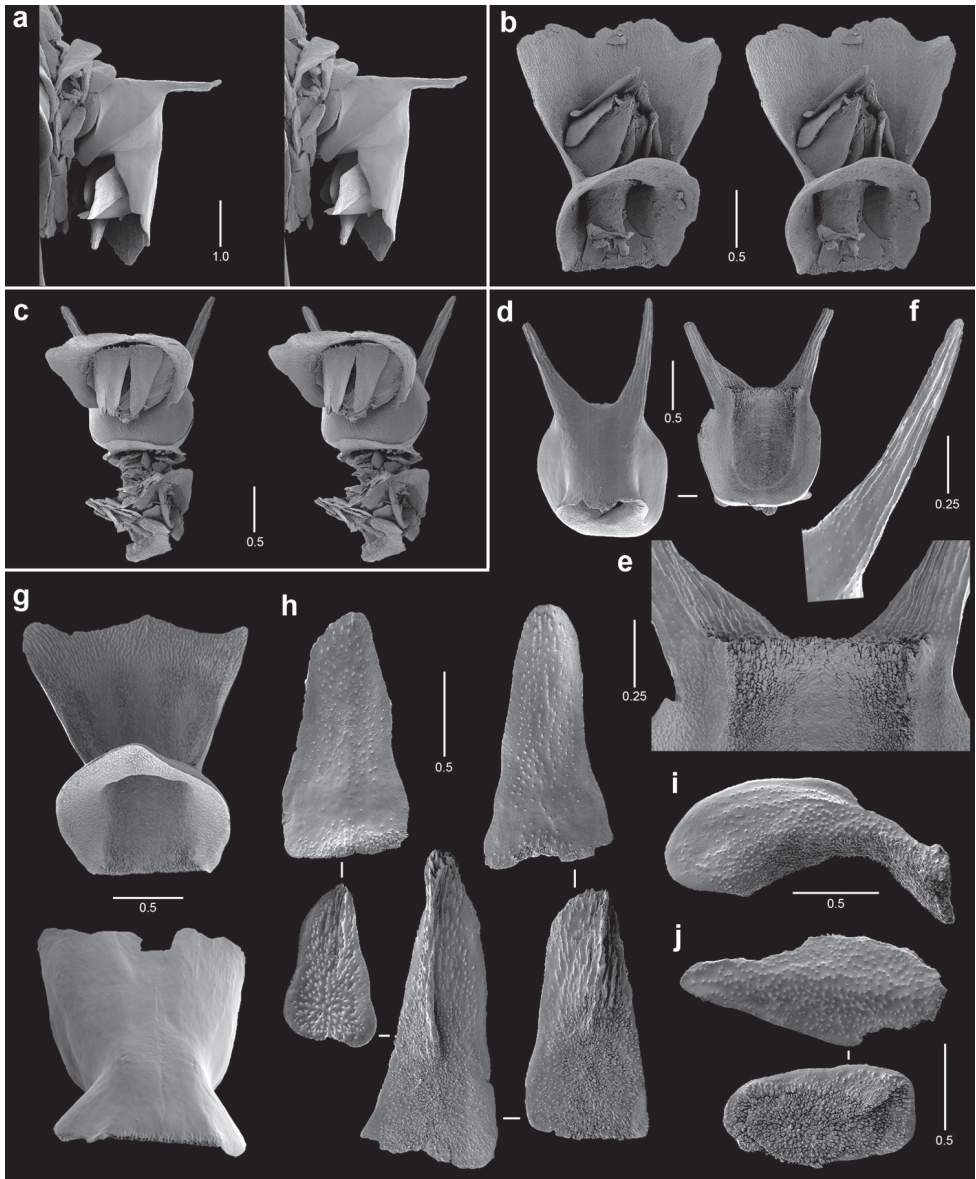


Figure 7. Polyps and sclerites of *Calyptrophora agassizii* from the holotype, *Alb-3404*, MCZ 4815. **a** lateral stereo view of a polyp **b–c** adaxial stereo views of a polyp **d** basal scales **e** articulating ridge of inner basal scale **f** longitudinal ridging on a basal spine **g** two buccal scales **h** opercular scales **i** infrabasal scales **j** coenenchymal scales.

Description. The colony is uniplanar, equally and dichotomously branched; the largest colony (*JSL-I-3108*, Figure 2c) is 13 cm tall and 10 cm in width, with a basal axis diameter of 1.1 mm. The colonies are quite flexible and weak; the polyps are poorly attached and often detached after collection. Polyps are directed downward,

and occur in whorls of four to six, the whorl diameter measuring 3.5–4.5 mm; the whorls are closely spaced, 4–4.5 whorls occurring per cm branch length. The horizontal length of the polyp is 1.8–2.2 mm. The pale yellow axis is slender, contributing to the flexibility of the colony.

The fused basal scale (Figures 7d–f) stands perpendicular to the branch and is up to 2.1 mm in height, the distalmost 0.9–1.1 mm consisting of two elongate spines (Figure 7 d, f). These spines are broad basally but attenuate to projections that are circular in cross section and bear low longitudinal ridges on all their surfaces (Figure 7f). The outer surface of the basal scale is smooth (Figure 7d); the articulating ridge (Figure 7e) is well developed, about 0.7 mm in length. The fused buccal scale (Figure 7g) is up to 2.2 mm in length and is oriented parallel to the branch. The distal edge of the buccal scale consists of several broad lobes (not spines or teeth), which form a translucent cowl (Figure 7b, c) up to 0.8 mm in length, which encircles and protects most of the operculum. Like the basal scales, the outer surface of the buccal scales is smooth, the inner face covered with low granules arranged in longitudinal rows near the distal edges. The paired, strongly curved infrabasals (Figure 7i) are about 1 mm in width and only 0.3 mm in height. The opercular scales (Figure 7h) range in length from 0.45–0.90 mm, decreasing in length from ab- to adaxial polyp side, forming a relatively small operculum that is encircled by the buccal cowl; their L:W ranges from 1.9–3.3. The operculars are thin, flat, and triangular, with a blunt apex; their outer surface is smooth to slightly granular, their inner surface covered by a longitudinal keel. The coenenchymal scales (Figure 7j) are thin, flat, and elongate, with blunt ends, and up to 0.8 mm in length. Their outer surface is covered with small, low granules.

Comparisons. Only four of the 23 species of *Calyptrophora* have polyps oriented in the downward direction (Cairns 2009). *Calyptrophora agassizii* easily differentiated from the others by having equal, dichotomous branching and keeled opercular scales.

Remarks. Several monographers have redescribed this species, but apparently based only on the type material. This is the first subsequent report of the species based on new material. The latitude reported by Studer (1894) for the type specimens is incorrect, it being 1°03'S, not north latitude.

Calyptrophora reedi sp. n.

<http://zoobank.org/FEE055B3-EE29-470E-9398-41A48442B5C0>

Figures 2d, 8

Material examined. Types. Holotype: colony and SEM stubs 2334–2337, *JSL-I-3930*, USNM 1409027. Paratype: *JSL-I-1922*, 1 denuded colony with many detached polyps, USNM 1409028; *Nautilus* NA-064-126-01-A, 1 branch, CDRS.

Type locality. *JSL-I-3930*: 0°29.755'S, 90°13.98'W (northeast coast of Santa Cruz, Galápagos), 450 m depth.

Distribution. Galápagos: off Santa Cruz, Santiago, and Marchena, 445–509 m depth.

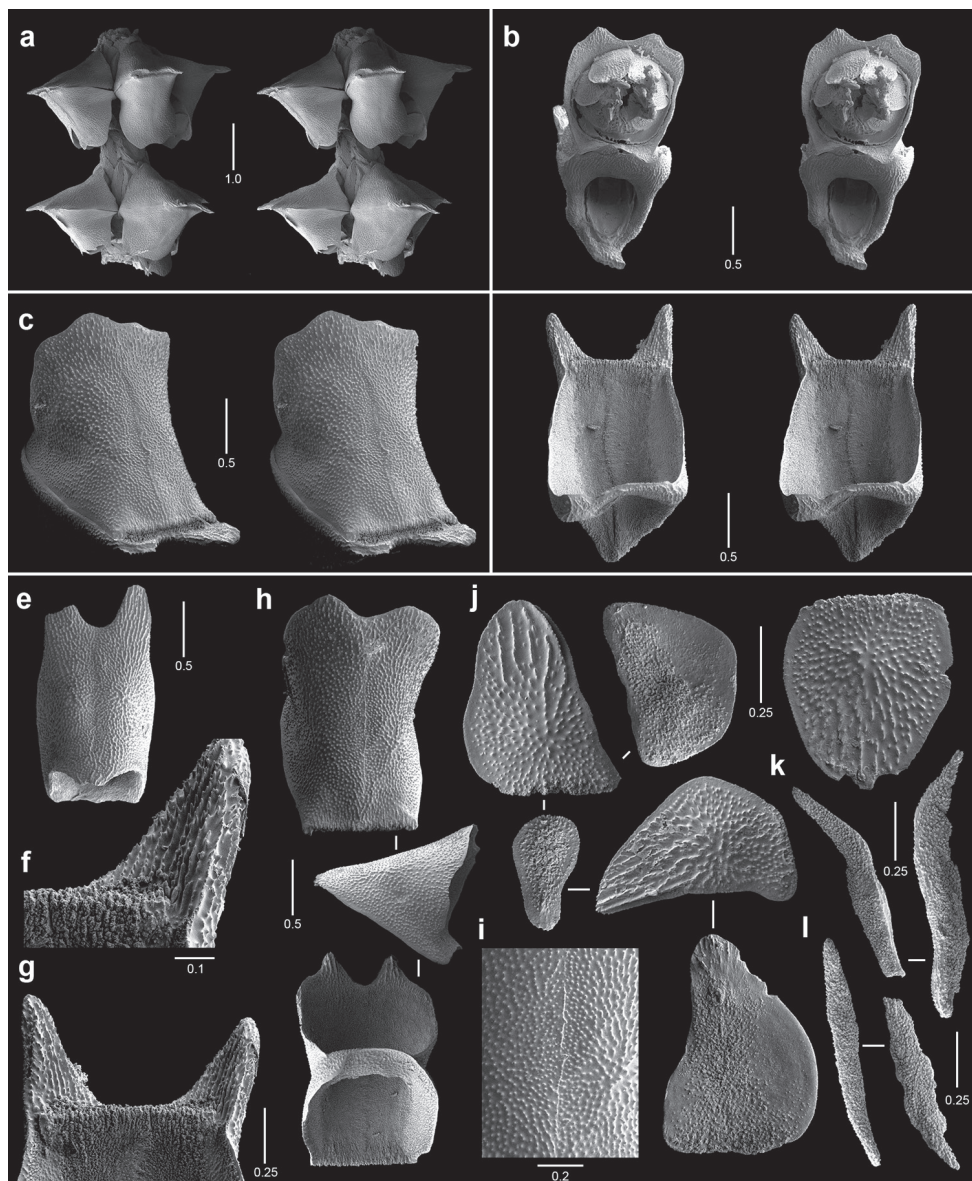


Figure 8. Polyps and sclerites of *Calyptrophora reedi* from the holotype, USNM 1409027. **a** lateral stereo view of two whorls **b** adaxial stereo view of a polyp **c** buccal stereo view of a polyp **d** stereo view of inner face of a basal scale **e** basal scale **f** ridged inner spine of basal scale **g** articulating ridge and spines of a basal scale **h** buccal scales **i** abaxial fusion of buccal scales **j** six opercular scales **k** two infrabasal scales **l** two coenenchymal scales.

Description. The colony is uniplanar, equally and sparsely dichotomously branched, some end branches up to 12 cm in length. The holotype (Figure 2d) is only 6.6 cm in height, whereas the paratype from *JSL-I-1922* is larger (20 cm) but poorly preserved. Polyps are directed downward, and occur in whorls of four to six

(Figure 8a), the whorl diameter measuring 4.0–5.5 mm; the whorls are closely spaced, about four polyps occurring per cm branch length. The horizontal length of a polyp is 2.2–2.4 mm. The axis is dark brown to bronze color.

The fused basal scale (Figures 8a, d, e) stands at roughly a 45° angle to the branch, and is 2.0–2.3 mm in height, including its distal spines. The distal spines (Figure 8d, f,) are flattened, with a broad base 0.30–0.35 mm in width, and extend 0.45–0.55 mm above the articulating ridge. Both inner and outer surfaces of the basal spines are covered with 6–11 thin, parallel spinose ridges. The straight articulating ridge is well defined (Figure 8d, f, g) and 0.70–0.75 mm in length. The outer surface of both basal and buccal scales is covered homogeneously with small but sharp spines. The fused buccal scale (Figure 8c, h) is 1.5–1.9 mm in length and slopes downward toward the branch surface, making the articular ridge and basal spines by far the highest point of the polyp. The distal edge of the buccal scale is smooth and usually bilobate, although the distal edges of some polyps are produced into two blunt teeth up to 0.3 mm in height (Figure 8h, lower figure); the buccal distal edge forms a cowl (Figure 8b) that completely enveloped the operculum. A low mid-dorsal (sagittal) ridge (Figure 8i) is often seen as a remnant of the dorsal fusion of the two young buccal scales. The abaxial opercular scale (Fig 8j, upper right) is almost elliptical in shape, up to 0.62 mm in height, and has a L:W as low as 1.15. The adaxial opercular (Figure 8j, lower left) is much smaller (0.35–0.45 mm in length) and triangular, having a L:W of about 1.7. The lateral operculars are asymmetrical, each having a lateral shoulder on their adaxial side. They range from 0.58–0.69 mm in height and have a L:W of 1.4–1.7. All opercular scales are quite thin and delicate, their outer surface covered with small spines often aligned as low ridges distally; their inner surface is tuberculate and not keeled (Figure 8j). The coenenchymal scales (Figure 8l) are straight, thick, and elongate, up to 1.1 mm in length and about 0.12 mm in width, with a L:W up to 10. They bear surface ornamentation like that of the body wall scales. Four thick, elongate coenenchymal scales (Figure 8k) surround the base of each polyp, each up to 1.2 mm in length with a L:W up to 6, and slightly curved to conform to the curvature of the polyp attachment of the branch, thus functioning as infrabasals.

Comparisons. Only four species in the genus have downward oriented polyps, the so called *wyvillei*-complex sensu Bayer (2001), *C. reedi* being very similar to *C. agassizii*, also known from the Galápagos. *Calyptrophora reedi* differs from that species primarily in the shape of its basal scales, which are not as long as those of *C. agassizii*, have a broader base, and a non-pointed (flat) tip.

Etymology. Named in honor of John Reed (HBOI), who participated in the *JSL-I* Galápagos expedition of 1986, during which this species was collected.

Genus *Narella* Gray, 1870

Narella Gray 1870: 49; Cairns and Bayer 2003: 618–619; 2007b: 84–86; Cairns and Bayer 2009: 43; Cairns and Baco 2007: 392–393; Cairns 2012: 14.
Stachyodes Wright and Studer 1889: 49; Versluys 1906: 86–88; Kükenthal 1919: 452–456.

Type species. *Primnoa regularis* Duchassaing and Michelotti, 1860, by monotypy.

Diagnosis. (from Cairns 2012): Colonies dichotomously branched (laterally), pinnate, or unbranched. Polyps arranged in whorls, all polyps facing downward. Each polyp covered with three (rarely four) pairs of abaxial body wall scales, one pair of basals, one or two pairs of medials, one pair of buccals, and one to four pairs of small adaxial scales, nevertheless leaving the adaxial side largely naked. Articular ridge present between basal and medial body wall scale. Distal margins of body wall scales often spinose, toothed, or lobate, often extending as a protective cowl. Opercular scale usually keeled. Coenenchymal scales often quite thick, of variable shape, sometimes ridged (i.e., “sail-scales”). Tentacular platelets often present.

Distribution. All ocean basins except Arctic, 128–4594 m deep.

Remarks. Previously (Cairns 2012) I stated that there were 43 valid species of *Narella*, but I inadvertently counted two junior synonyms within this tabulation, so, in fact, there are only 41 valid species. The new species described herein brings the total to 42. A unified key to all species known after 1924 (Kükenthal 1924) does not exist, but regional keys are available for 29 of these species: the seven western Atlantic species (Cairns and Bayer 2003), the nine Hawaiian species (Cairns and Bayer 2007b), the five Alaskan species (Cairns and Baco 2007), and the eight New Zealand species (Cairns 2012).

Narella ambigua (Studer, 1894)

Figures 2e, 9

Stachyodes ambigua Studer 1894: 63–64; Menneking 1905: 248–251, pl. 8, figs 1–2, pl. 9, figs 11–12; Versluys 1906: 103–104; Kükenthal 1919: 464 (key to species); 1924: 314.

Narella ambigua Cairns and Bayer 2007 (not 2008): 86 (listed); Cairns 2007b: 512 (listed); Cairns and Bayer 2009: 30 (listed).

Material examined. Branch fragments and detached polyps from *Alb*-3404, MCZ 79048, and USNM 1405230 (topotypic: possible syntypes); *Alb*-2818, 1 colony and SEM stubs 2312–2315, USNM 44165; *Gilliss*-21, 1 branch, USNM 57576; *JSL*-1-1927, 1 colony, USNM 1297223.

Types. As mentioned in the account of *Calyptrophora agassizii*, about 65% of the type lot (branches and detached polyps) of that species consisted of *Narella ambigua*. *Narella ambigua* was collected at the previous station (*Alb*-3403) to that of *C. agassizii* (*Alb*-3404), approximately 20 km to the northeast and bathymetrically 2 m shallower, both stations from off the southern coast of San Cristóbal. The *Narella* specimens were separated from the type lot of *C. agassizii* in 2008 and cataloged as MCZ 79048. Since the type of *S. ambigua* could not be found at the MCZ in 2008, the specimens cataloged as MCZ 79048 may serve as representative topotypic specimens, and may in fact be type material. A fragment of this colony is also deposited at the NMNH (USNM 1405230).

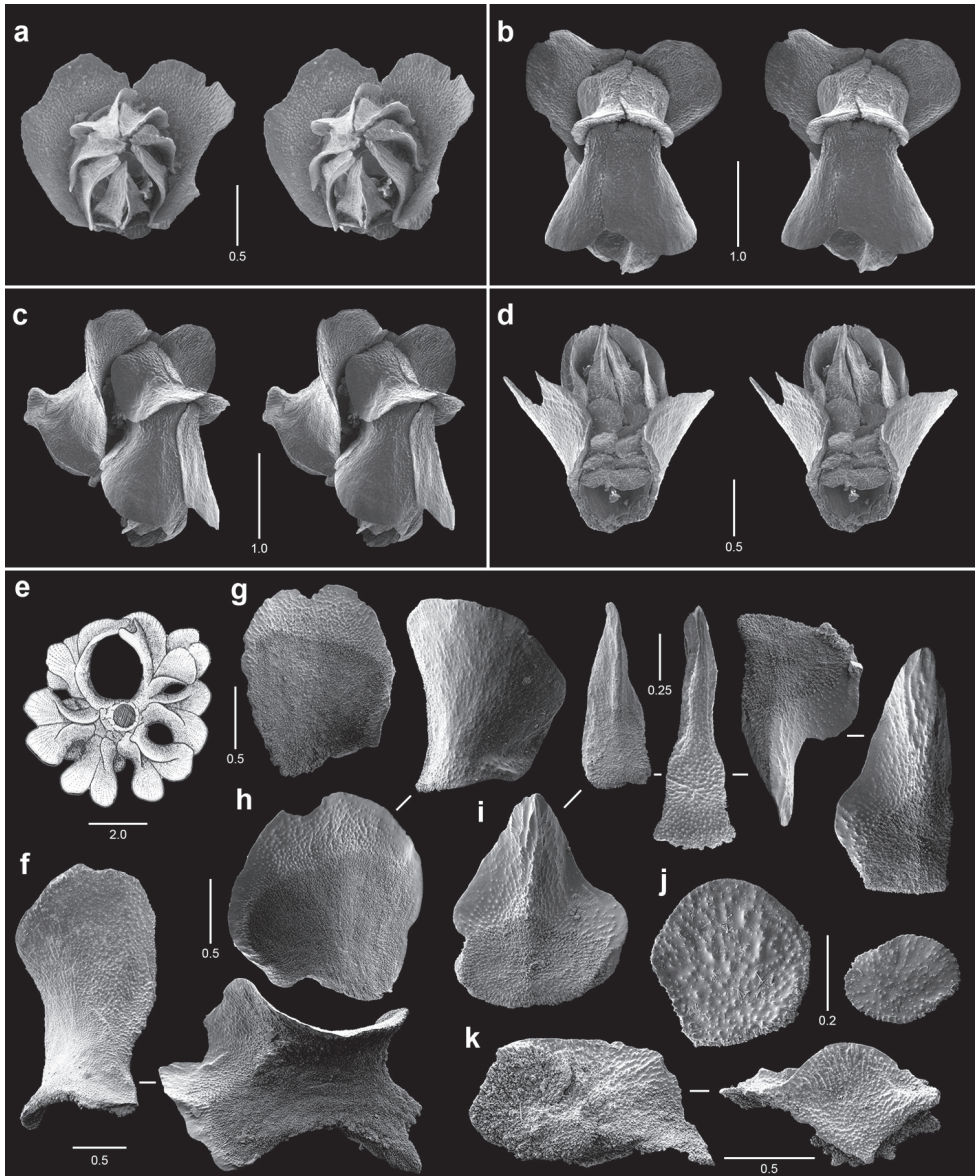


Figure 9. Polyps and sclerites of *Narella ambigua* from Alb-2818, USNM 44165. **a** opercular stereo view of a polyp **b–d** abaxial, lateral, and adaxial stereo views of a polyp, respectively **e** axial view (drawing) of a whorl showing polychaete tube **f** basal scales **g** medial scale **h** buccal scales **i** opercular scales **j** adaxial buccal scales **k** coenenchymal scales.

Type locality. Alb-3403: 0°58'30"S, 89°17'W (south of San Cristóbal, Galápagos), 702 m depth.

Distribution. Galápagos: off Santiago, Santa Cruz, and San Cristóbal, 702–741 m deep. Elsewhere: off Panama, 1463 m depth (herein, GS-21).

Description. The colony is uniplanar, and dichotomously (laterally) and sparsely branched (Figure 2e), large colonies being up to 28 cm in height and up to 1 cm in basal branch diameter. Terminal branches may be quite long, up to 15 cm. The axis is pale yellow. The polyps are arranged in whorls of five to seven (Figure 9e); whorls are not directly adjacent to one another and thus there are only approximately 2.5 whorls per cm branch length; the whorl diameter of terminal branchlets is about 6–7 mm. The horizontal length of a polyp is 2.5–3.0 mm.

The basal scales (Figure 9c, f) stand perpendicular to the branch and extend up to 2.8 mm in height, the distal 0.6–0.7 mm portion projecting beyond the junction with the medial scales as a broad lobate extension (Figure 9b). The lateral edge of one of the basal scales of a polyp will often enlarge and curve toward the corresponding enlarged basal scale of the adjacent polyp, forming a solid tube up to 3.5 mm in diameter that houses a commensal polychaete worm (Figure 9e). The dorso- and anterolateral faces of the basal scales are gently curved, not ridged. The medial scales (Figure 9g) are narrow, 0.9–1.1 mm in length, and have upturned edges proximally and distally (saddle-shaped). The buccal scales (Figure 9b, c, h) are longer (up to 1.6 mm) and about twice as wide as the medials, their distal edges rounded and smooth, forming a cowl (Figure 9a) up to 0.6 mm that encircles the operculum; the distal edges of the two buccal scales form a bilobate shape for the tip of each polyp, not unlike the distal edges of the basal scales. The ratio of the major body wall scales is about: 1:0.6:0.7. There are four pairs of small elliptical adaxial body wall scales (Figure 9d, j), ranging from 0.26 to 0.42 mm in greater diameter. The outer faces of all body wall scales are covered with small granules and thus look rather smooth. All of the opercular scales (Figure 9i) are roughly the same length, ranging from 1.0–1.3 mm in length, but the single abaxial opercular is quite broad (e.g., L:W = 1.2), whereas the single adaxial is quite slender (e.g., L:W = 3.0). The other six lateral operculars usually have a basal shoulder on their adaxial edges and thus have an intermediate L:W ratio. The outer surface of the operculars is granular like the body wall scales, whereas the inner surface bears a rounded keel. The coenenchymal scales (Figure 9k) are irregular to polygonal in shape, up to 1.4 mm in length, and have a flat to slightly concave outer surface.

Comparisons. *Narella ambigua* is easily distinguished from the somewhat similar *Paracalyptrophora enigma* by its long terminal branches, polychaete commensalism that causes highly modified basal scales, fewer polyp whorls per cm, non-toothed basal scales, lack of an articular ridge, and granular (not ridged) coenenchymal scales.

Remarks. Although discussed by several authors through the years (see synonymy), this is the first subsequent report of this species since its original description.

Genus *Paracalyptrophora* Kinoshita, 1908

Type species. *Calyptrophora kerberti* Versluys, 1906, by subsequent designation (Cairns and Bayer 2004).

Diagnosis. Colonies dichotomously branched in one plane, sometimes in a lyrate pattern and sometimes as two parallel fans. Polyps arranged in whorls of up to eight,

all polyps pointed downward. Each polyp covered with two (rarely three) unfused pairs of body wall scales. Articular ridge present between basal and buccal (or medial) body wall scales. Distal margins of buccal scales smooth or spinose. A pair of infrabasal scales often present. Coenenchymal scales elongate, granular, and sometimes ridged.

Distribution. Southwestern Pacific Ocean, Galapagos, Japan, Hawaii, North Atlantic, 150–1480 m deep.

Remarks. The genus diagnosis is herein expanded to accommodate a species having three pairs of body wall scales, otherwise similar to the genus *Narella*. The character placing it in *Paracalyptrophora* is its possession of an articular ridge, which is found in this genus as well as *Calyptrophora*, and is considered more significant than the number of body wall scales.

***Paracalyptrophora enigma* sp. n.**

<http://zoobank.org/14AC2E7D-3E1F-4701-92AD-F8B152150ADB>

Figures 3a, 10

Material examined. Types. Holotype: colony and SEM stubs 2338–2342, *JSL-I-1915*, USNM 1409703. Paratype: *JSL-I-1916*, 1 colony, USNM 1409707.

Type locality. 1°17.2'S, 89°48.7'W (northwest of Española, Galápagos), 653 m depth.

Distribution. Known only from northwest of Española, Galápagos, 547–653 m deep.

Description. The colony is uniplanar, equally and dichotomously branched, the largest colony (the holotype, Figure 3a) being 17 cm in length and having only 12 terminal branches, none longer than 4 cm. Its broken base is highly calcified and 10.5 mm in diameter. The entire corallum is white. The polyps are arranged in closely spaced (4.5–5 polyps per cm) whorls of seven or eight (Figure 10a), the higher number occurring on larger-diameter basal branches; the whorl diameter ranges from 4.5–6.0 mm. The horizontal length of a polyp is 2.5–2.7 mm.

The basal scales (Figures 10a, e) stand perpendicular to the branch or tilted slightly anteriorly, and extend up to 1.75 mm in length, the distal 0.23–0.28 mm of each basal scale projecting as wide, flat teeth, which are longitudinally ridged on their inner surface (Figure 10d). There is a horizontal articular ridge joining the basal to the medial scales (Figure 10d). Otherwise, the inner surface of the basal scale is highly tuberculate, and its outer surface is smooth and not ridged, as are all the body wall scales. The medial scales (Figure 10f) are as wide as the buccals, 1.10–1.15 mm in length; the distal and lateral 0.25 mm of their inner surface is smooth (but not ridged), the rest highly tuberculate. The buccal scales (Figure 10g) are slightly longer (1.12–1.25 mm) but much wider, curved around much of the operculum in a scalloped shape. The 0.5 mm distal, inner margins of these scales are also smooth and thin, forming a translucent cowl (Figure 10c) surrounding the operculum. The ratio of the major body wall scales is about: 1:0.67:0.77. There is at least one pair of rectangular adaxial scales (Figure 10c), each about 0.37 mm in width. The single abaxial opercular scale (Figure 10h, leftmost) is 0.85–0.90 mm in length and has two broad lateral lobes (producing a very low L:W of 0.75–0.85) and thus being symmetrical,

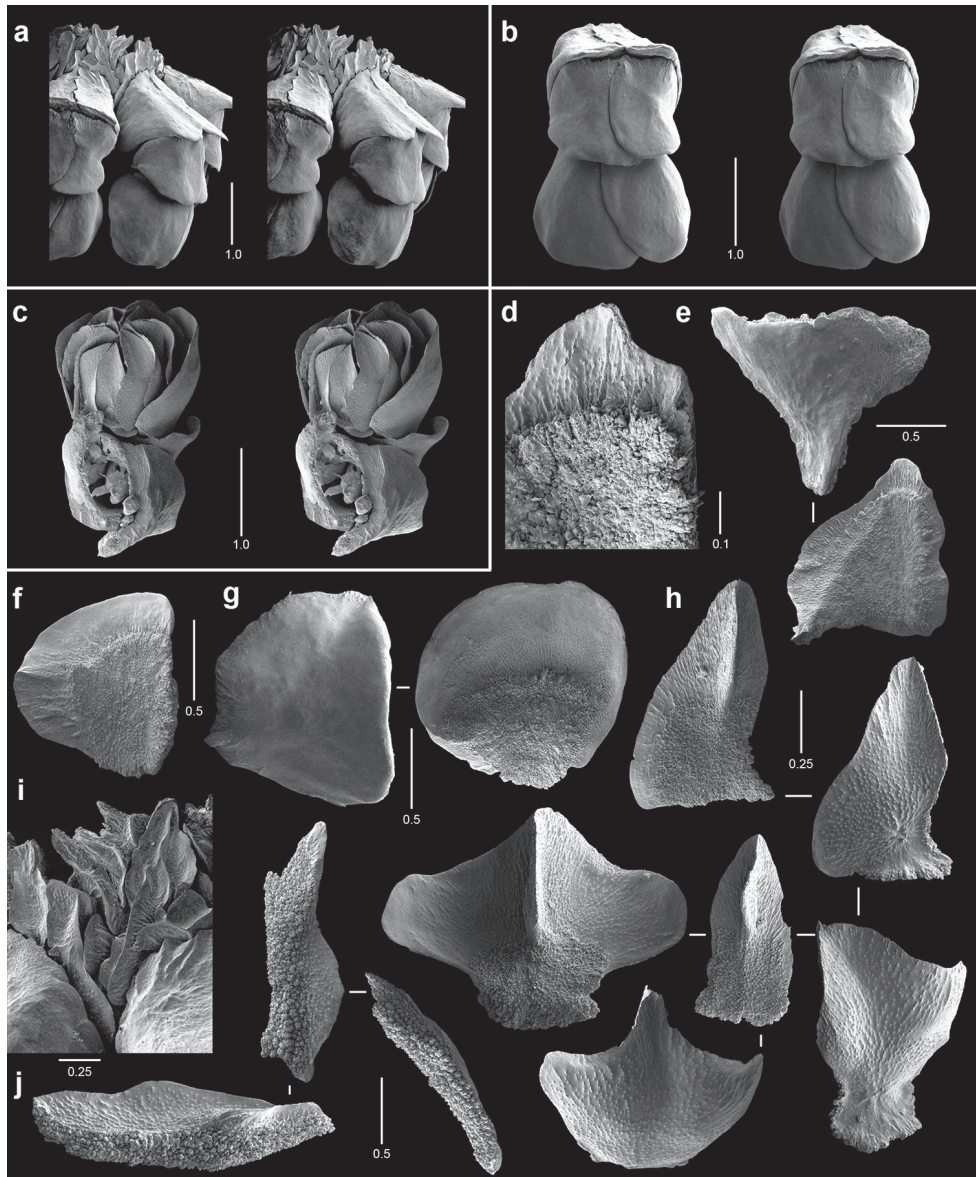


Figure 10. Polyps and sclerites of *Narella enigma* from the holotype, *JSL-I-1915*, USNM 1409703. **a** lateral stereo view of a whorl **b–c** abaxial and adaxial stereo views of a polyp, respectively **d** articular ridge and inner ridging on a basal spine **e** basal scales **f** medial scale **g** buccal scales **h** opercular scales **i** coenenchymal scales, in situ **j** coenenchymal scales.

and has a small rectangular base. The much smaller, symmetrical, paired adaxial operculars are 0.75–0.80 mm in length with a L:W of about 2.0. The five lateral operculars range in size from 0.90 to 1.05 mm in length and are asymmetrical, each having a lobe on their adaxial side, the L:W ranging from 1.5–1.6 (Figure 10h). The distal inner half of all oper-

cular scales bears a thin ridged keel, whereas the outer surface is covered with low pointed granules. The coenenchymal scales (Figure 10i, j) are elongate (L:W up to 8) and longitudinally crested (i.e., “sail scales”, Figure 10j), the crests up to 0.15 mm in height. The outer surface of these scales is covered with small granules much like that of the operculars.

Comparisons. Superficially this species resembles the genus *Narella*, in that it has three pairs of body wall scales, but the distal inner surface of the basal scales have an articular ridge, which is more consistent with the genus *Paracalyptrophora*, *P. enigma* being the only species in the genus with three pairs of body wall scales.

Etymology. Named “*enigma*” (Latin for inexplicable) because it is the only species in the genus to have three (not two) pairs of body wall scales.

Genus *Plumarella* Gray, 1870

Plumarella Gray 1870: 36; Kükenthal 1919: 340–343; Bayer 1981: 936 (key to genus); Cairns and Bayer 2009: 39–40; Cairns 2011: 7; 2016: 51–52.

Type species. *Gorgonia penna* Lamarck, 1815, by subsequent designation (Wright and Studer 1889).

Diagnosis. Colonies usually uniplanar and alternately pinnately branched, dichotomously branched, or bottlebrush in shape. Polyps arranged in alternate biserial fashion (nominate subgenus), crowded on all sides (subgenus *Dicholaphis*), paired (subgenus *Faxiella*), or arranged in whorls (subgenus *Verticillata*). Each polyp covered by eight rows of body wall scales, the adaxial scales usually somewhat smaller. Distal edges of marginal body wall scales do not overlap much of opercular scales. Inner surface of opercular scales may be smooth or ridged, but not keeled, except in subgenus *Faxiella*.

Distribution. Indo-Pacific, western Atlantic, Subantarctic, 10–3181 m deep.

Remarks. There are 37 species in the genus arranged in four subgenera, most listed in Cairns (2011: table 2), however, two new subgenera were recently added by Zapata-Guardiola and López-González (2012) and Zapata-Guardiola, López-González and Gili (2012).

Plumarella (Faxiella) abietina (Studer, 1894)

Figures 3b, 11

Amphilaphis abietina Studer 1894: 65; Menneking 1905: 255–260, pl. 8, figs 7–8, pl. 9, figs 17–20; Versluys 1906: 22; Cairns 2007b: 512 (listed); Cairns and Bayer 2009: 28 (listed); Cairns 2016: 58.

Thouarella (Amphilaphis) abietina Kükenthal 1919: 410–411; 1924: 290.

Not *Thouarella abietina* Pasternak 1981: 49–50 (= *T. vityazi* Zapata-Guardiola and López-González 2012).

Plumarella (Faxiella) abietina Zapata-Guardiola and López-González 2012: 372–375, figs 20–22.

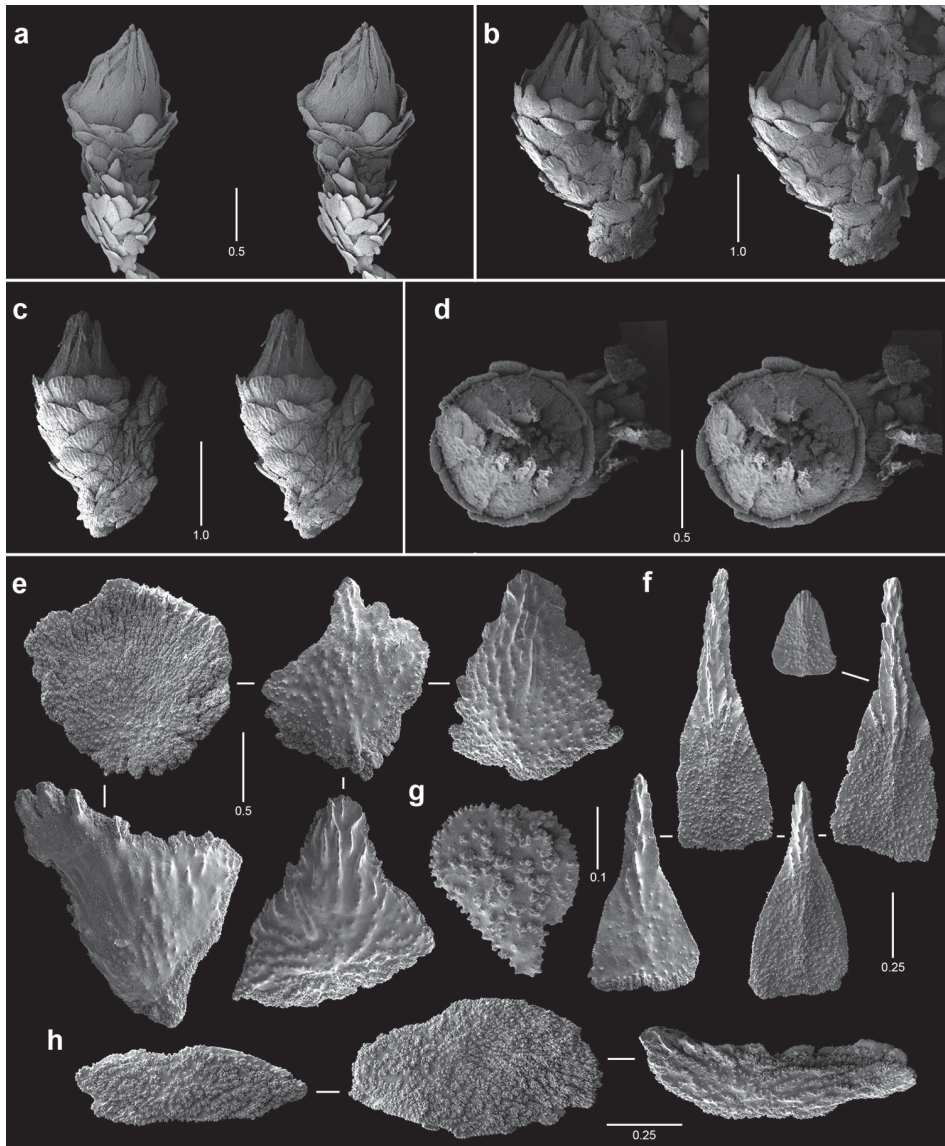


Figure 11. Polyps and sclerites of *Plumarella abietina* (**a** holotype, *Alb*-3399, MCZ 4802 **b–h** *Alb*-2818, USNM 49605) **a–d** abaxial, lateral, abaxial, and opercular stereo views of a polyp **e** body wall scales **f** opercular scales **g** adaxial scale **h** coenenchymal scales.

Material examined. *Alb*-2818, 1 colony in very poor condition (most of its polyps detached) and SEM stubs 2343–2346, USNM 49605; *JSL-I*-1929, 1 branch, USNM 1406397; holotype.

Types. Holotype: *Alb*-3399, MCZ 4802.

Type locality. 1°07'N, 81°04'W (lower continental slope off northwestern Ecuador, at same latitude as Galápagos Islands but about 860 km to the east), 3181 m depth.

Distribution. Galápagos: east of Santa Cruz and off Roca Redonda, 717–808 m deep. Elsewhere: off Ecuador, 3181 m depth.

Description. The colony is uniplanar to slightly bushy, the Galápagos specimen (*Alb*-2818, Figure 3b) measuring 12 cm in height, but it is part of a badly damaged colony that was probably larger. Branching is equal and dichotomous. The upward-directed polyps are usually arranged in pairs but may also occur in whorls of three as well as individually. Polyps are about 2.6 mm in length, about two pairs occurring per cm branch length.

The body wall scales (Figure 11e) are arranged in eight somewhat irregular longitudinal rows, the sclerite formula being: 5–6:4–5:4–5: variable. All marginal scales, except for the abaxial marginals, are roughly rectangular, 0.35–0.64 mm in width, and have a straight distal margin that covers only a small proximal part of the opercular scales. The distal edges of the two marginal scales project as small teeth. All body wall scales except for the adaxials become progressively larger and transform to triangular toward the base of the polyp. The adaxial body wall scales (Figure 11a, g) are small (0.25–0.35 mm in diameter) and random (variable) in arrangement, but cover the entire adaxial side of the polyp. The body wall scales are relatively thick, convex, and covered with low ridges; their distal edges are finely serrate. The opercular scales (Figure 11f) are triangular in shape (0.75–1.2 mm in length, L:W = 2.2–2.9), each with an elongate distal process, the length and L:W progressively decreasing from ab- to adaxial side; the operculum is quite prominent (Figure 11a–c). The outer opercular face is covered with granules basally and short serrate ridges distally; the inner face is also covered with serrate ridges raised into a keel-like structure distally, but having tubercles proximally. The coenenchymal scales (Figure 11h) are elongate (L:W about 4), with a granular outer surface and a tuberculate inner surface.

Comparisons. This is the deepest of the 37 known species in the genus. Only one other species occurs in this subgenus, *P. (F) delicatula* (Thompson and Rennet, 1931), known only from the New Zealand region at 650–2743 m depth (Cairns 2016). These species are compared by Cairns (2016).

Remarks. The specimens reported herein are only the second report of the species. It fits the re-description of the holotype given by Zapata-Guardiola and López-González (2012), except that the Galápagos specimen sometimes has polyps arranged in whorls of three.

Genus *Parastenella* Versluys, 1906

Stenella Wright and Studer 1889: 56 (junior homonym).

Stenella (*Parastenella*) Versluys 1906: 39, 45.

Parastenella Bayer 1961: 295; 1981: 936; Cairns 2007a: 245–247; 2007b: 518; Cairns and Bayer 2009: 45–46, figs 16A–G; Cairns 2010: 434; 2016: 94–96.

Type species. *Stenella dodderleini* Wright and Studer, 1889, by subsequent designation (Bayer 1956).

Diagnosis. Colonies uniplanar to slightly bushy; branching lateral and somewhat irregular. Polyps stand perpendicular to branch, arranged independently or in pairs or whorls of up to four. Eight marginal scales present, offset in position from opercular scales; marginal, and sometimes submarginal, scales fluted; nematocyst pads present on distal inner surface of fluted marginals. Body wall scales arranged in four to eight longitudinal rows. Operculum well developed, the distal inner surface of operculars prominently keeled. Coenenchymal scales flat to highly concave, sometimes ridged. Pinnular rodlets sometimes present.

Distribution. Cosmopolitan, except for eastern Atlantic, the Arctic, and off continental Antarctica, 475–3470 m depth.

Remarks. Including the new species described herein, there are eight species known in this distinctive genus. Accounts of *Parastenella* species are found in Cairns (2007b, 2010, 2016) and Cairns and Bayer (2009).

***Parastenella pomponiae* sp. n.**

<http://zoobank.org/3E4C0441-A172-4E29-8F5A-8CA4E035B7A1>

Figures 3c, 12

Material examined. Types. Holotype: colony and SEM stubs 2303–2305, *JSL-I-1922*, USNM 1410289. Paratypes: *JSL-I-1922*, 1 colony, USNM 1410290; *JSL-I-3912*, 1 branch, USNM 1410291; *Nautilus* NA064-125-01-A, 1 colony, CDRS.

Type locality. 0°23.68'N, 90°26.341'W (off northeastern Marchena), 475–578 m deep.

Distribution. Galápagos: off Marchena, Santiago, and Isabela, 446–578 m deep.

Description. The colony is uniplanar, the largest colony (the holotype, Figure 3c) measuring 44 cm in height, and having a basal branch diameter of 6.5 mm. Branching is lateral and somewhat irregular; the longest terminal branchlets are less than 2 cm in length. The axis is golden bronze and the polyps and coenenchyme are white. The polyps are 2.8–3.1 mm in height and stand perpendicular to the branches, arranged in pairs (Figures 12a, b), whorls of three, and often as singles; about five polyp whorls (or pairs) occur per cm branch length.

The body wall scales (Figure 12d) are arranged in eight rows, each row with six scales, the lateral edges of all scales overlapping with those of adjacent rows. The eight marginal scales form an asymmetrical rosette: six of the marginals consist of elongate scales (up to 0.9 mm in length and 0.4 mm wide) with broad shallow flutes, whereas the two adaxial marginals are much wider but shorter (up to 0.6 in length and 0.9 mm in width) and are flat (without a flute) or bear only a very shallow flute (Figure 11c). A nematocyst pad (Figure 12c) is present on the distal inner face of each fluted marginal. The body wall scales proximal to the marginals (Figure 12b) are never fluted and are elliptical in shape, about 0.60–0.85 mm in width; they have a concave granular outer surface, their lateral and distal edges turned upward. The opercular scales (Figures 12b, c, f) are fairly uniform in length (0.7–0.8 mm) but variable in width. The abaxial and

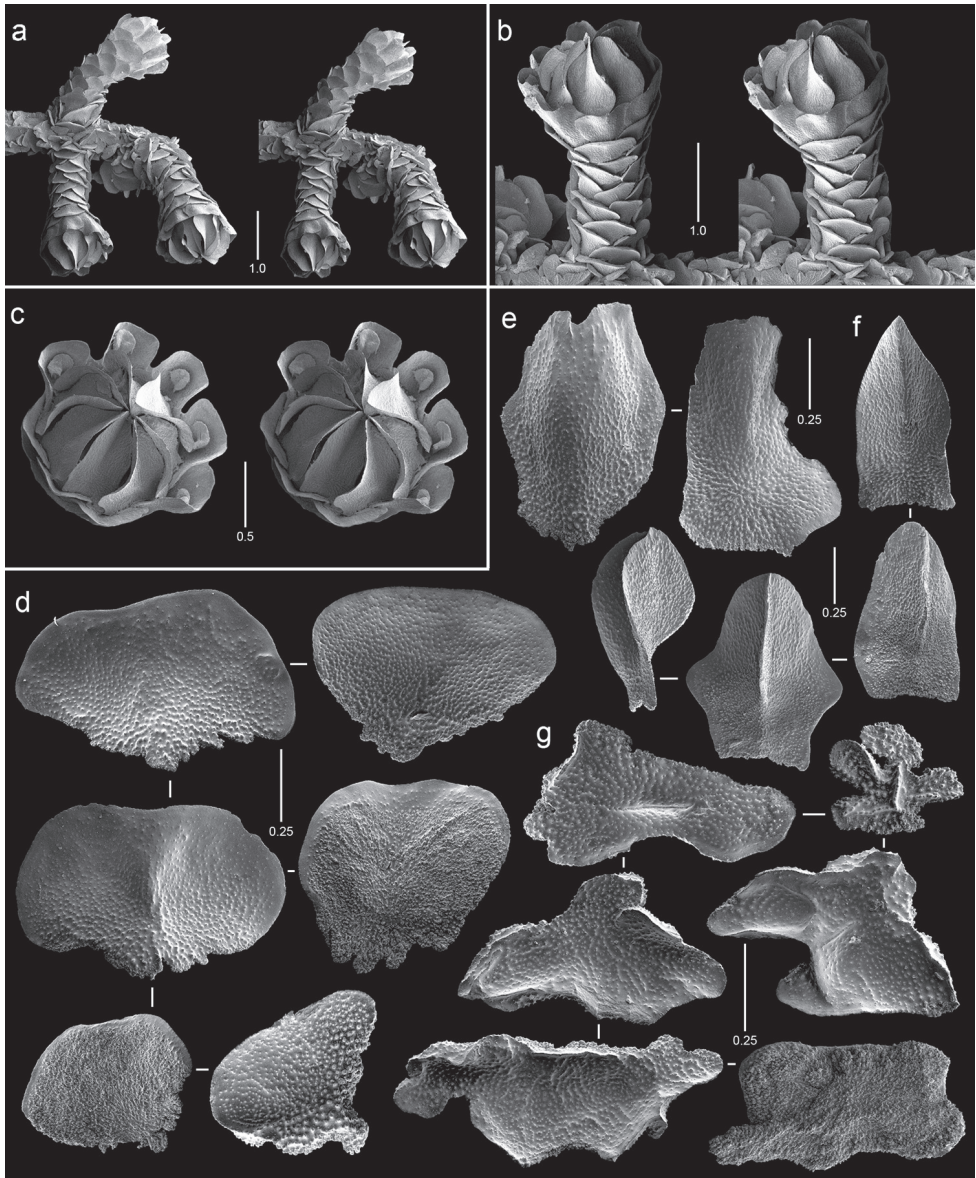


Figure 12. Polyps and sclerites of *Parastenella pomponiae* from the holotype, JSL-I-1922, USNM 1410289, **a** stereo view of paired polyps **b** lateral stereo view of a polyp **c** opercular stereo view of a polyp showing nematocyst pads **d** body wall scales **e** fluted marginal scales **f** opercular scales **g** coenenchymal scales.

adaxial operculars are symmetrical, the abaxial having two lateral lobes (H:W about 1.2), the adaxials lacking lobes (H:W about 2); the lateral operculars are asymmetrical, each having only one lobe on the adaxial lateral side. All opercular scales have a deeply longitudinally creased outer surface that corresponds to a sharply keeled inner surface.

The coenenchymal scales (Figure 12g) are irregular in shape, although usually longer than broad, and up to 1.1 mm in length. Their outer surface is concave, like that of the body wall scales, and bears low granules and occasionally short ridges.

Comparisons. *Parastenella pomponiae* is morphologically most similar to *P. ramosa* (Studer, 1894), known from the eastern Pacific from the Gulf of Alaska to Panama, but differs from that species in having eight (not five) rows of body wall scales, concave (not flat) coenenchymal scales, wider fluted marginal scales, and in lacking submarginal fluted body wall scales.

Etymology. Named in honor of Shirley Pomponi (formerly of HBOI), who participated in the *JSL-I* expedition of 1986, during which this species was collected.

Genus *Chrysogorgia* Duchassaing and Michelotti, 1864

Chrysogorgia Duchassaing and Michelotti 1864: 13; Versluys 1902: 17–33; Kükenthal 1919: 505–511 (key to species); 1924: 388–390 (key to species); Bayer 1956: F216; Bayer and Stefani 1988: 259 (key to genus and some species); Cairns 2001: 754–756; Pante and France 2010: 600 (key to genus); Pante et al. 2012: fig. 2. *Dasygorgia* Verrill 1883: 21.

Type species. *Chrysogorgia desbonni* Duchassaing and Michelotti, 1864, by monotypy.

Diagnosis. Branching from main branch sympodial in an ascending spiral, clockwise (R) or counterclockwise (L), usually following a repeated geometric branching formula, producing a bottlebrush colony, or dichotomous in one or more parallel planes. Branchlets repeatedly dichotomously branched, resulting in short terminal segments. Polyps large in relation to branchlets, standing perpendicular to branchlets and usually well separated. Sclerites consist of rods and scales. Axis with a brilliant metallic luster, usually golden or yellow in color, and thus referred to as the golden corals.

Distribution. Cosmopolitan, including off Antarctica (Pante et al. 2012: figs 4–5), 100–3860 m deep.

Remarks. In order to manage the relatively large number of species in the genus, now standing at 70, Versluys (1902) divided the genus into three groups based on the presence of rods or scales in the body wall and tentacles of each species, which he referred to as Groups A–C. Table 1 is a graphic representation of the four permutations of these two characters as divided between the two regions of the polyp. This table also lists the number of species currently assigned to each group, their geographic and depth ranges, and the branching formulas encountered within the group. A species having the fourth permutation, Group D, was not reported until 2015 (Cordeiro et al. 2015). Recent molecular evidence (Pante et al. 2012), based on three genes, supports the monophyly of the genus as well as groups B and C, but results in Group A being paraphyletic. Regardless of the true phylogeny of the species, the grouping of Versluys (1902), along with the branching formula, served to help distinguish the various species.

Table 1. The four species groups of *Chrysogorgia* determined by a combination of body wall and tentacular sclerite type.

	Body Wall Rods	Body Wall Scales
Tentacular Rods	Group A: 38 species: Indo-West Pacific, Atlantic; 100–3114 m. 2/5R, 1/4L, 3/8L, 1/3R, 2/5L, 1/3L, dichotomous, irregular, pinnate	Group B: 13 species: Indo-West Pacific, western Atlantic; 250–2271 m. 1/4R, 1/5R, 1/6R, 1/7R, 1/7R, 2/5R, biflabellate
Tentacular Scales	Group D: 1 species: off Brazil, 1300 m. dichotomous	Group C: 18 species: Indo-West Pacific, North Atlantic, Antarctic; 204–3860 m. 1/3L, 1/4L, 2/5L, 1/4R, flabellate

Chrysogorgia scintillans Bayer and Stefani, 1988

Figures 3d, 13

Chrysogorgia curvata Nutting 1908: 591, pl. 45, fig. 9.

Chrysogorgia scintillans Bayer and Stefani 1988: 270–276, figs 11–12.

Material examined. *JSL-I-1927*, 1 colony and SEM stubs 2327–2331, USNM 89377; *JSL-I-1942*, 1 colony, USNM 1160577; *JSL-I-3925*, 1 colony, USNM 1409700; holotype.

Types. The holotype is deposited at the NMNH (USNM 25371).

Type locality. *Alb-4153*: between Kauai and Moku Manu, 1758–1937 m deep.

Distribution. Galápagos: between Isabela and Santiago; Cocos Island, 628–768 m deep. Elsewhere: Hawaiian Islands, 1758–1937 m deep.

Description. The colony is biplanar (perhaps multiplanar), the largest colony examined (*JSL-I-1927*, Figure 3d) being 25 cm in height and 10 cm in width, and is somewhat bushy. The branching is dichotomous, the length of the internodes 6–7 mm, each internode bearing only one or sometimes two polyps. The polyps are 2.3–2.8 mm in height and project perpendicular to the branches (Figure 13a–c), having a relatively narrow body wall column and a much larger distal crown, made larger by the projecting sclerites that support the tentacles. The axis is a metallic bronze in color.

The body wall scales (Figure 13c, d) are transversely arranged and slightly curved to fit the circumference of the polyp. The body wall scales, called “slippers” by Bayer and Stefani (1988), are up to 0.65 mm in length and 0.07–0.10 mm in width, resulting a L:W ratio ranging from 4.5–6.0; these scales are quite thin (about 0.03 mm). Some body wall scales are often slightly irregular in shape but usually rounded on their distal ends; their inner and outer faces are smooth and their edges rounded. The tentacular scales (Figure 13e) are similar in shape to the body wall scales but somewhat smaller, i.e., 0.35–0.45 mm in length. The base of each tentacle bears a distinctive tear-dropped shaped region about 0.4 mm long and 0.18 mm in width that is devoid of sclerites (Figures 13a–c). These regions are surrounded by flattened scales that project around the lower edge of the tentacle and thus forming a support for it. These scales sometimes have a root-like or lobate base (Figure 13f). The pinular scales (Figure 13g) are 0.20–0.25 mm in length and are similar to the body wall scales, except that they have slightly serrate marginal edges. The coenenchymal scales

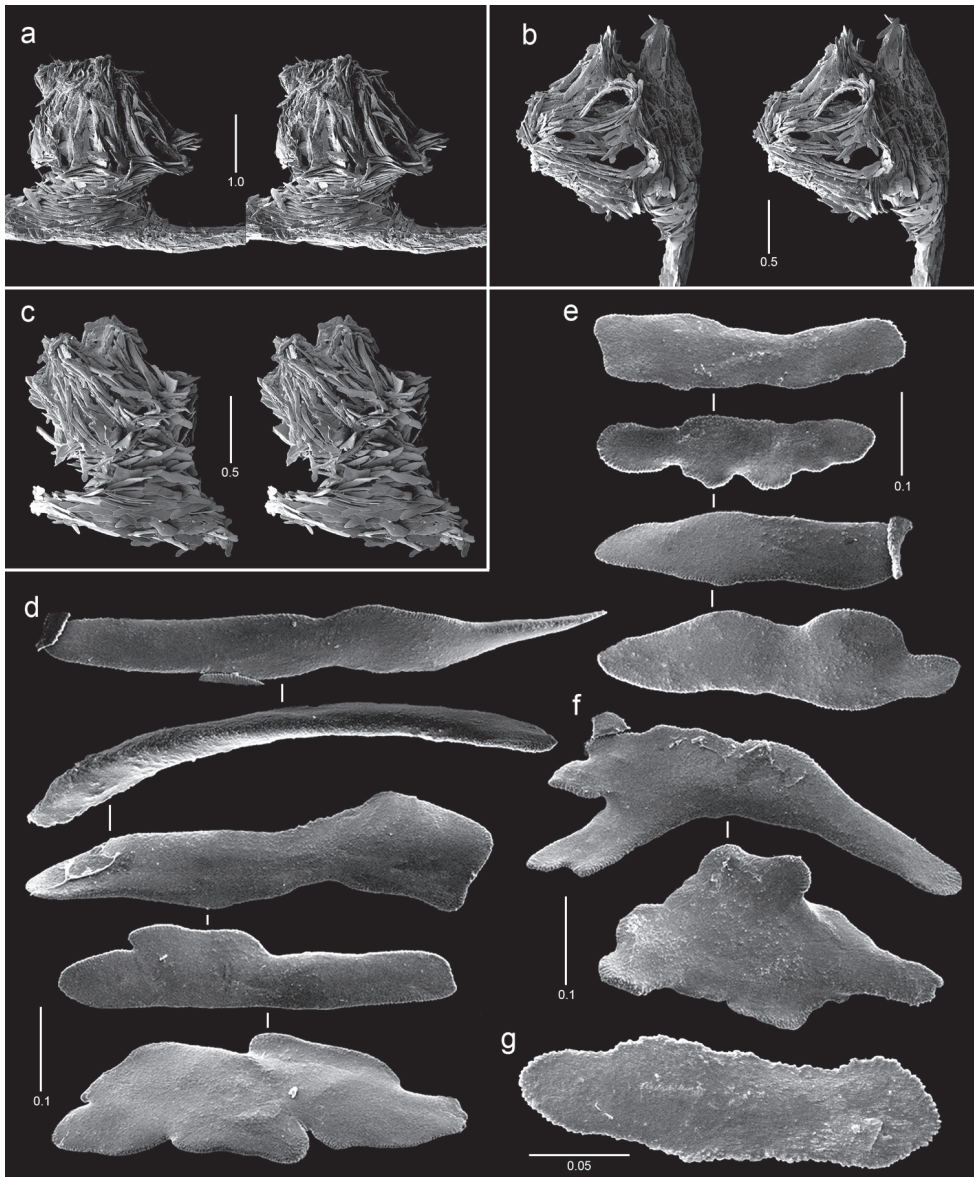


Figure 13. Polyps and sclerites of *Chrysogorgia scintillans* from JSL-I-1927, USNM 89377. **a–c** lateral stereo views of polyp showing regions devoid of sclerites **d** body wall scales **e** tentacular scales **f** scales in base of tentacle **g** pinnular scale.

(Figure 13c) are indistinguishable from the body wall scales, and are arranged longitudinally parallel to the branch axis.

Comparisons. *Chrysogorgia scintillans* belongs to “Group C” sensu Versluys (1902) (Table 1), i.e., species having sclerites in the form of scales in both tentacles and body wall. Currently there are 18 species known in this grouping (Cairns 2001; Pante and

Watling 2011), three of which, including *C. scintillans*, having flabellate or multi-flabellate colonies and non-spiral branching. As noted by Bayer and Stefani (1988: key), *C. scintillans* is most similar to *C. electra* Bayer and Stefani, 1988, another flabellate species, but differs in having larger polyps, smaller projections beneath the tentacle bases, and slightly different shaped to their body wall and coenenchymal scales.

***Chrysogorgia midas* sp. n.**

<http://zoobank.org/62A55FA8-2A1D-429A-8344-B065A33B5696>

Figures 3e, 14

Material examined. Types. Holotype: colony and SEM stubs 2316–2319, 2350–2316, *JSL-I*-1915, USNM 1160575. Paratypes: *Alb*-2818, many denuded branches (dry), USNM 51464; *JSL-I*-1912, distal colony, USNM 1160579; *JSL-I*-1916, distal colony, USNM 1160578; *JSL-I*-1929, 1 colony, USNM 1160585; *JSL-I*-1933, 1 branch, USNM 1160582; *JSL-I*-3902, 1 branch, USNM 1405908.

Type locality. 1°17'12"S, 89°48'42"W (north of Española, Galápagos), 650–662 m deep.

Distribution. Throughout Galápagos from Roca Redondo to Española, 560–816 m deep.

Description. The colony is bottlebrush in shape (Figure 3e), the holotype measuring 26 cm tall and 12–13 cm in maximum diameter, having a basal branch diameter of 2.5 mm. The branching is sympodial, the branching formula being consistently 1/3L. The orthostiche interval is 12–18 mm. The length of the internodes of the branchlets ranges from 4.0–5.9 mm, up to nine nodes occurring on each branchlet; each internode supports one polyp. The polyps are about 1.1 mm in length, cylindrical (Figures 14a, b), and when preserved in alcohol tend to curve toward the branch surface, the tentacles often adhering to the surface branch. The axis is bronze in color.

The body wall sclerites (Figure 14a–c) are slightly flattened, rotund rods 0.22–0.25 mm in length, having a L:W of 5–6. They are straight and longitudinally oriented. The tentacular sclerites (Figure 14d) are similarly shaped rods, but are slightly shorter (0.18–0.22 mm in length) and more elongate (L:W = 5–8), also longitudinally oriented along the tentacles. All of the rods bear low sparse granulation. The pinnular scales (Figure 14e) are 0.08–0.12 mm in length, about 0.005 mm in thickness, and have a L:W of 3.5–4.5. The coenenchymal scales (Figures 14a, f) are 0.13–0.17 mm in length, about 0.01 mm in thickness, and have a H:W of 3.5–5.0. They are longitudinally oriented along the branch axis.

Comparisons. Having rods in its body wall and tentacles places *C. midas* in *Chrysogorgia* Group A, the largest of the four groups of *Chrysogorgia*, consisting of 38 species (Table 1). *C. midas* is the only species in this group to have a 1/3L branching formula, this formula being much more common in Group C and in one species of Group B (see Cairns 2001).

Etymology. Named “*midas*” (from the Greek Midas, the mythical king at whose touch everything turned to gold) in allusion to the golden luster of the branch axis, characteristic of the genus.

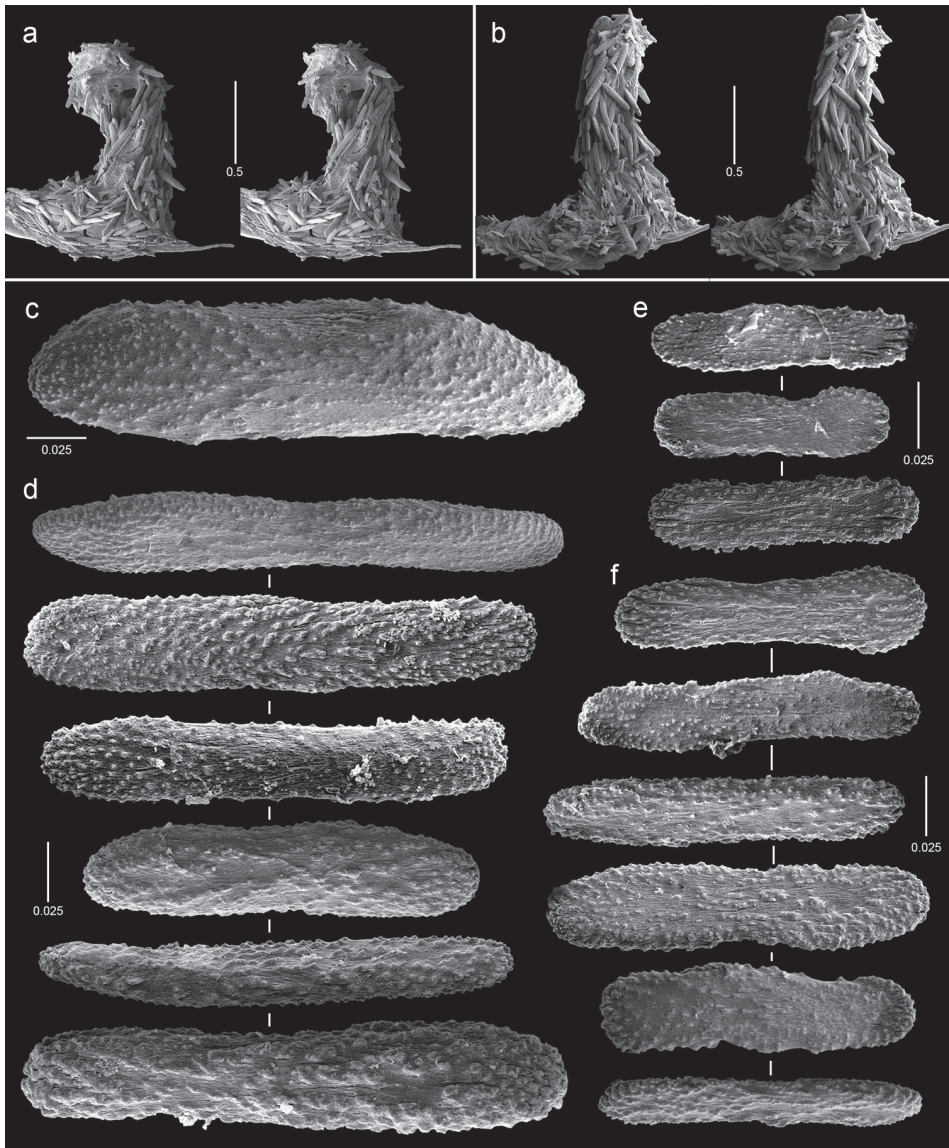


Figure 14. Polyps and sclerites of *Chrysogorgia midas* from the holotype, *JSL-I-1915*, USNM 1160575, **a–b** lateral stereo views of polyps **c** body wall spindle **d** tentacular flattened rods **e** pinnular scales **f** coenenchymal scales.

***Chrysogorgia laevorsa* sp. n.**

<http://zoobank.org/26185B5F-FCA3-4160-A271-48FE5EC2E73D>

Figures 3f, 15a, c–f

Material examined. Types. Holotype: colony and SEM stubs 2320–2322, *JSL-I-1929*, USNM 1409029. Paratypes: *Alb-2818*, 13 denuded stems, USNM 1409031; *JSL-I-1938*, 1 colony, USNM 1160584.

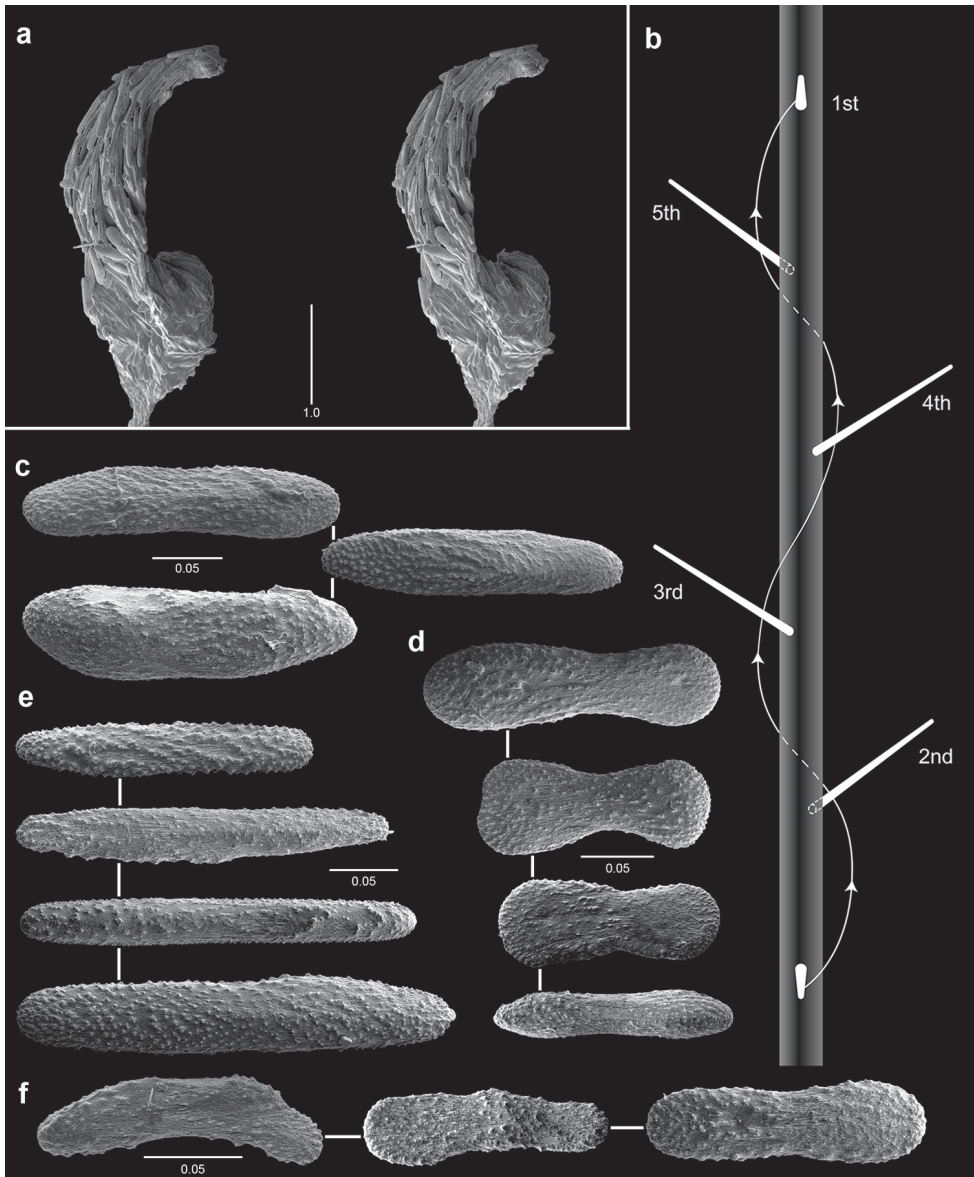


Figure 15. Polyps and sclerites of *Chrysogorgia laevorsa*, JSL-I-1929, USNM 1409029, **a** lateral stereo view of a polyp **b** diagram of 2/5R polyp arrangement, not found in *C. laevorsa* **c** upper body wall flattened rods **d** lower body wall flattened rods and waisted scales **e** tentacular flattened rods **f** pinnular scales.

Type locality. 0°14'40"N, 91°36'32"W (off Roca Redonda, Galápagos), 806 m depth.

Distribution. Galápagos: Roca Redonda, west of Santa Cruz, 717–806 m deep; Cocos Islands, 614–785 m deep.

Description. The colony is bottlebrush in shape (Figure 3f), the holotype 11 cm tall and 6 cm in maximum diameter, having a basal branch diameter of 2.3 mm.

Branching is sympodial, the branching formula being consistently $2/5L$. The orthostiche interval varies from 10 to 23 mm, the shorter intervals near the base of the colony, the higher intervals near the top. The length of the internodes on the branchlets is 3–5 mm, up to five or six nodes occurring on each branchlet; each internode supports two polyps. The polyps are 1.5–1.9 mm in length and cylindrical in shape, with a slightly swollen base (Figure 15a). The axis is metallic gold in color tinged with a greenish hue.

The upper body wall sclerites (Figure 15c), those associated with the cylindrical part of the polyp, consist of slightly flattened rotund rods that are 0.19–0.24 mm in length and having a L:W of 3.5–4.7. They are straight, longitudinally oriented, and uniformly covered with very small granules. Distal to the body wall are the tentacles, which may compose as much as half of the polyp length. They are also composed of slightly flattened rods (Figure 15c), but these rods are longer and more slender, 0.25–0.32 mm in length, with a L:W of 5.1–9.0. Like the upper body wall rods, they are straight and similarly granulated. The pinnular scales (Figure 15f) are smaller (0.073–0.16 mm in length) curved platelets, having a L:W of 3.4–4.5. The swollen base of the polyp is covered with flattened rods similar in shape to those of the tentacles (Figure 15d), as well as waisted scales 0.17–0.21 mm in length and having a L:W of 2.4–3.4. Otherwise, the coenenchyme seems to be devoid of sclerites.

Comparisons. Having rods in its body wall and tentacles places *C. laevorsa* in *Chrysogorgia* Group A, the largest of the four groups of *Chrysogorgia*, having 38 species. *Chrysogorgia laevorsa* is the only species in this group to have a $2/5L$ branching formula, whereas 14 species in this group have a $2/5R$ formula (Figure 15b). The $2/5L$ formula is found in only four species of *Chrysogorgia*, all belonging to Group C.

Etymology. Named *laevorsa* (from the Latin *laevorsus*, meaning “towards the left”) in allusion to the direction of the branching formula ($2/5L$).

Family Isididae Lamouroux, 1812

Subfamily Keratoisidinae Lamouroux, 1812

Genus *Isidella* Gray, 1858

Isidella Gray 1858: 283; Kükenthal 1919: 564; 1924: 414; Bayer 1956: F222; Bayer and Stefani 1987a: 51 (key to genus); 1987b: 941 (key to genus); Bayer 1990: 207–208; Etnoyer 2008: 543; Brugler and France 2008: 126–127 (inverted gene order); Watling et al. 2011: 76, fig. 2.11 (map); Dueñas et al. 2014: 20.

Type species. *Isis elongata* Esper, 1788, by monotypy.

Diagnosis. Colonies sparsely branched, dichotomously or trichotomously from nodes, resulting in a uniplanar colony; internodes long and hollow. Polyps non-retractile, cylindrical, armed with stout needles placed longitudinally in body wall. Spiny pharyngeal rodlets present.

Distribution. Northeast Atlantic (including Mediterranean), New England Seamounts, eastern Pacific from California to Alaska, Hawaii, Galápagos, 400–2593 m deep (France 2007).

Remarks. Including the species described below, there are currently six species in the genus, three of which occur in the Pacific. The genus was most recently keyed and discussed by Bayer (1990).

Using one or two mitochondrial genes and six species (most of them undescribed), France (2007) and Dueñas et al. (2014: Figure 2) indicated that *Isidella* was not monophyletic. Both papers imply that branching pattern, which has traditionally been used to distinguish keratoisidinine genera, is not a reliable character.

***Isidella tenuis* sp. n.**

<http://zoobank.org/3B9D476D-BB64-4348-B0F9-7883933E0375>

Figures 3g, 16

Isidella sp. Breedy and Cortés 2008: 73, 76.

Material examined. Types. Holotype: colony and SEM stubs 2355–2358, *JSL-I-1942*, USNM 89382. Paratypes: *JSL-I-1942* 4 colonies, USNM 1423001.

Type locality. 5°34.6'N, 87°04.25'W (off Cocos Island), 606–628 m deep.

Distribution. Known only from the type locality.

Description. The colony is uniplanar, the largest specimen (the holotype, Figure 3g) measuring 18 cm in height and 7 cm in width, with a basal branch diameter of 1.7 mm. The holotype shares a thin basal encrustation with another specimen (a paratype). Branching is always dichotomous from nodes, the internodes ranging from 9–14 mm in length. The internodes are white, not longitudinally grooved, and hollow, the central canal (Figure 16b) constituting about 35–40% of the branch diameter.

The polyps are uniserially placed (Figure 16a), their bases about 4–6 mm apart, but because of the length of the upturned polyps there is only 1–3 mm between adjacent polyps. The polyps are cylindrical and slender (Figure 16a), up to 3.3 mm in length and about 0.5 mm in diameter. Most of each polyp consists of eight elongate (up to 2.9 mm, L:W = 26–31), straight, cylindrical needles (Figure 16d), their pointed tips projecting beyond the tentacles. The sclerites bear numerous short (22–26 μ m in length) ridges about 5 μ m in height, which are arranged longitudinally on the sclerite (Figure 16e). Toward the base of the polyp are several shorter needles 0.95–1.0 mm in length (L:W = 17–19), these needles (Figure 16f) also being cylindrical but having blunt, flattened tips. Directly adjacent to the coenenchyme are also several even shorter needles (0.5 mm in length, L:W = about 13), also with flattened, blunt tips (Figure 16i). These two smaller size classes of needles allow for some flexibility of the polyp where it attached to the branch. The tentacular platelets (Figure 16h) are numerous, consisting of flat, blunt-tipped sclerites 0.095–0.1 mm in length and having a L:W of about 7. Their flat surfaces are fairly smooth, covered by small granules and

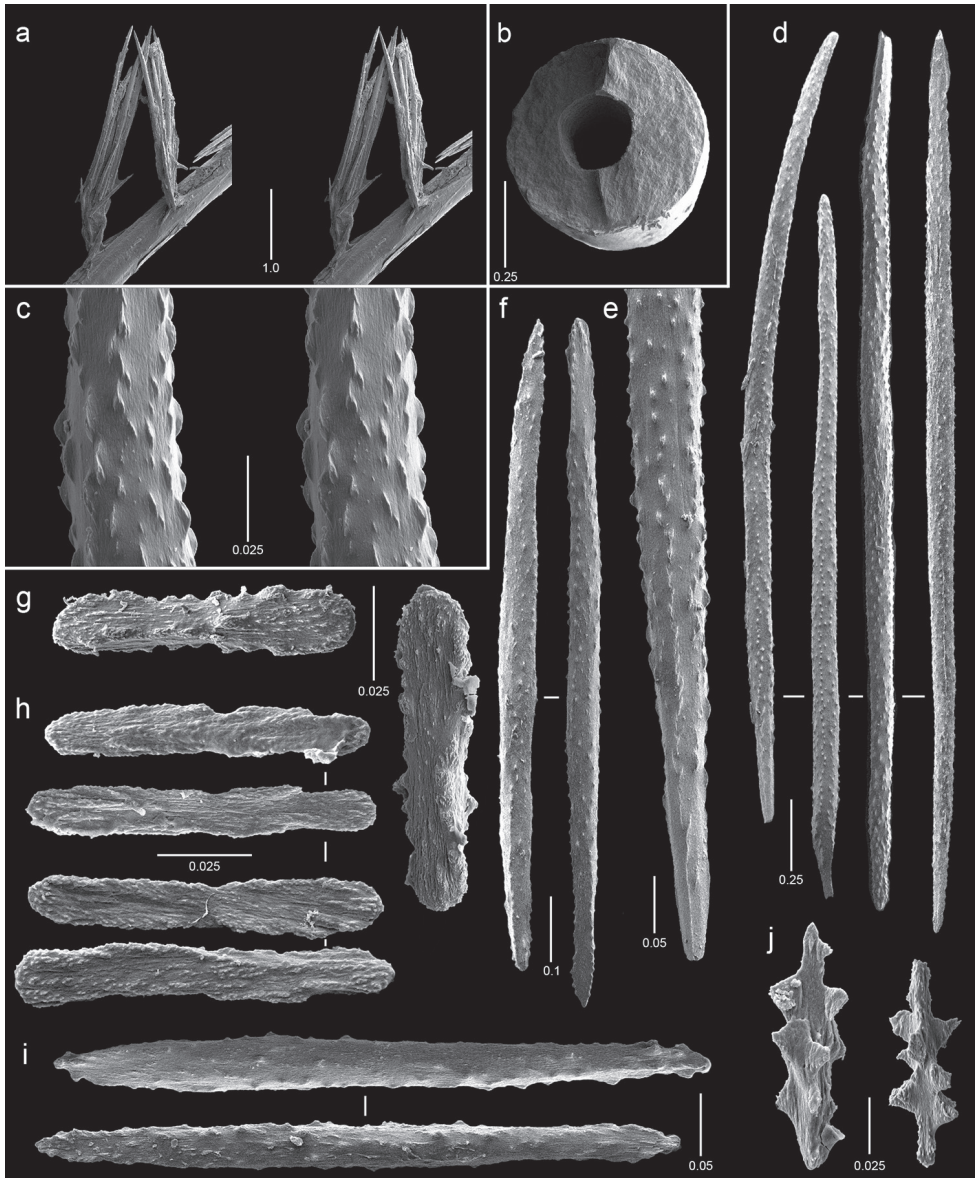


Figure 16. Polyps and sclerites of *Isidella tenuis*, holotype, *JSL-I-1929*, USNM 89382, **a** lateral stereo view of two polyps **b** cross section of internode showing hollow core **c** stereo view of ridged ornamentation of body wall needles **d** upper body wall needles **e** enlargement of upper body wall needle **f** lower body wall needles **g** two coenenchymal scales **h** tentacular platelets **i** basal body wall needles **j** pharyngeal rodlets.

low ridges. The pharyngeal sclerites (Figure 16j) are small (0.072–0.10 mm in length) rodlets that bear relatively tall spines. The coenenchymal sclerites (Figure 16g) are quite rare, consisting of flat, blunt-tipped scales (like those of the tentacles), but larger: 0.15–0.18 mm in length (L:W = 4–5).

Comparisons. *Isidella tenuis* differs from *I. trichotoma* Bayer, 1990 (Hawaii, 1920 m) in having dichotomous branching, much smaller coenenchymal and body wall sclerites, and differently shaped pharyngeal sclerites. *Isidella tenuis* differs from *I. tentaculatum* Etnoyer, 2008 (California to Alaska, 720–1050 m) in having needle-shaped body wall scales, differently shaped pharyngeal scales, smaller polyps, uniserial polyps, and blunt-tipped body wall sclerites.

Etymology. Named “*tenuis*” (Latin for thin) in reference to the slender polyps of the species.

Acknowledgments

I am grateful to John Reed for the gift of specimens collected on the three *JSL* expeditions to the Galápagos, and to Les Watling and Nicole Raineault (Ocean Exploration Trust) for facilitating the loan of three specimens collected by the *E/V Nautilus*. Molly Ryan executed the drawing of Figure 15b, and F. M. Bayer made the drawing of *Narella ambigua* (Figure 9e) as well as taking the SEM polyp images of *N. ambigua* (Figure 9a–d). I am thankful to Robert Ford for composing Figures 2–16, and to Freya Goetz for drafting Figure 1.

References

- Aurivillius M (1931) The Gorgonarians from Dr. Sixten Bock's expedition to Japan and Bonin Islands 1914. *Kungliga Svenska Vetenskaps-Akademiens Handlingar* 3(9)(4): 1–337.
- Bayer FM (1956) Octocorallia. In: Moore RC (Ed.) *Treatise on Invertebrate Paleontology, Part F, Coelenterata*. University of Kansas Press, Lawrence, F166–F189.
- Bayer FM (1961) The shallow-water Octocorallia of the West Indian Region. *Studies on the fauna of Curaçao and other Caribbean Islands* 12: 1–373.
- Bayer FM (1981) Key to the genera of Octocorallia exclusive of Pennatulacea (Coelenterata: Anthozoa), with diagnoses of new taxa. *Proceedings of the Biological Society of Washington* 94(3): 902–947.
- Bayer FM (1982) Some new and old species of the primnoid genus *Callogorgia* Gray, with a revalidation of the related genus *Fanellia* Gray (Coelenterata: Anthozoa). *Proceedings of the Biological Society of Washington* 95(1): 116–160.
- Bayer FM (1990) A new isidid octocoral (Anthozoa: Gorgonacea) from New Caledonia, with descriptions of other new species from elsewhere in the Pacific Ocean. *Proceedings of the Biological Society of Washington* 103(1): 205–228.
- Bayer FM (1996) The Antarctic genus *Callozostron* and its relationship to *Primnoella* (Octocorallia: Gorgonacea: Primnoidae). *Proceedings of the Biological Society of Washington* 109(1): 150–203.
- Bayer FM (1998) A review of the circumaustral gorgonacean genus *Fannyella* Gray, 1870 with descriptions of five new species. *Senckenbergiana biologica* 77(2): 161–204.

- Bayer FM (2001) New species of *Calyptrophora* (Coelenterata: Octocorallia: Primnoidae) from the western part of the Atlantic Ocean. *Proceedings of the Biological Society of Washington* 114(2): 367–380.
- Bayer FM, Cairns SD, Cordeiro RTS, Pérez CA (2014) New records of the genus *Callogorgia* (Anthozoa: Octocorallia) in the western Atlantic, including the description of a new species. *Journal of the Marine Biological Association of the United Kingdom* 95(5): 905–911. <https://doi.org/10.1017/S0025315414001957>
- Bayer FM, Grasshoff M, Verseveldt J (1983) Illustrated trilingual glossary of morphological and anatomical terms applied to Octocorallia. E. J. Brill, Leiden, 75 pp.
- Bayer FM, Stefani J (1987a) Isididae (Gorgonacea) de Nouvelle-Calédonie. Nouvelle clé des genres de la famille. *Bulletin du Muséum National d'Histoire Naturelle.*, Paris ser. 9, A (1): 47–106.
- Bayer FM, Stefani J (1987b) New and previously known taxa of isidid octocorals (Coelenterata: Gorgonacea), partly from Antarctic waters. *Proceedings of the Biological Society of Washington* 100(4): 937–991.
- Bayer FM, Stefani J (1988) A new species of *Chrysogorgia* (Octocorallia: Gorgonacea) from New Caledonia, with descriptions of some other species from the western Pacific. *Proceedings of the Biological Society of Washington* 101(2): 257–279.
- Breedy O, Cortés J (2008) Octocorals (Coelenterata: Anthozoa: Octocorallia) of the Isla del Coco, Costa Rica. *Revista de Biología Tropical* 56: 71–77.
- Brugler MR, France SC (2008) The mitochondrial genome of a deep-sea bamboo coral (Cnidaria, Anthozoa, Octocorallia, Isididae): Genome structure and putative origins of replication are not conserved among octocorals. *Journal of Molecular Evolution* 67(2): 125–136. <https://doi.org/10.1007/s00239-008-9116-2>
- Cairns SD (1986) Stylasteridae (Hydrozoa: Hydroida) of the Galápagos Islands. *Smithsonian Contributions to Zoology* 426: 1–42. <https://doi.org/10.5479/si.00810282.426>
- Cairns SD (1991a) A revision of the ahermatypic Scleractinia of the Galápagos and Cocos Islands. *Smithsonian Contributions to Zoology* 504: 1–32. <https://doi.org/10.5479/si.00810282.504>
- Cairns SD (1991b) New records of Stylasteridae (Hydrozoa: Hydroida) from the Galápagos and Cocos Islands. *Proceedings of the Biological Society of Washington* 104(2): 209–228.
- Cairns SD (2001) Studies on western Atlantic Octocorallia (Coelenterata: Anthozoa). Part 1: The genus *Chrysogorgia* Duchassaing & Michelotti, 1864. *Proceedings of the Biological Society of Washington* 114(3): 746–787.
- Cairns SD (2007a) Studies on western Atlantic Octocorallia (Gorgonacea: Primnoidae). Part 8. New records of Primnoidae from the New England and Corner Rise Seamounts. *Proceedings of the Biological Society of Washington* 120(3): 243–263. [https://doi.org/10.2988/0006-324X\(2007\)120\[243:SOWAOG\]2.0.CO;2](https://doi.org/10.2988/0006-324X(2007)120[243:SOWAOG]2.0.CO;2)
- Cairns SD (2007b) Calcaxonian Octocorals (Cnidaria: Anthozoa) from the Eastern Pacific seamounts. *Proceedings of the California Academy of Sciences* 58(25): 511–541.
- Cairns SD (2009) Review of Octocorallia (Cnidaria: Anthozoa) from Hawai'i and adjacent seamounts. Part 2. Genera *Paracalyptrophora* Kinoshita, 1908; *Candidella* Bayer, 1954; and *Calyptrophora* Gray, 1866. *Pacific Science* 63(3): 413–448. <https://doi.org/10.2984/049.063.0309>

- Cairns SD (2010) A review of the Octocorallia (Cnidaria: Anthozoa) from Hawai'i and adjacent seamounts, Part 3: The genera *Thouarella*, *Plumarella*, *Callogorgia*, *Fanellia*, and *Parastenella*. Pacific Science 64(3): 413–440. <https://doi.org/10.2984/64.3.413>
- Cairns SD (2011) A revision of the Primnoidae (Octocorallia: Alcyonacea) from the Aleutian Islands and Bering Sea. Smithsonian Contributions to Zoology 634: 1–55. <https://doi.org/10.5479/si.00810282.634>
- Cairns SD (2012) New Zealand Primnoidae (Anthozoa: Alcyonacea) Part 1. Genera *Narella*, *Narelloides*, *Metanarella*, *Calyptraphora*, and *Helicoprinoa*. NIWA Biodiversity Memoirs 126: 1–71.
- Cairns SD (2016) The Marine fauna of New Zealand: Primnoid octocorals (Anthozoa, Alcyonacea) Part 2. *Primnoella*, *Callozostxon*, *Metafannyella*, *Callogorgia*, *Fanellia* and other genera. NIWA Biodiversity Memoir 129: 1–131.
- Cairns SD, Baco A (2007) Review of five new Alaskan species of the deep-water octocoral *Narella* (Octocorallia: Primnoidae). Systematics and Biodiversity 5(4): 391–407. <https://doi.org/10.1017/S1477200007002472>
- Cairns SD, Bayer FM (2002) Studies on western Atlantic Octocorallia (Coelenterata: Anthozoa). Part 2: The genus *Callogorgia* Gray, 1858. Proceedings of the Biological Society of Washington 115(4): 840–867.
- Cairns SD, Bayer FM (2003) Studies on western Atlantic Octocorallia (Coelenterata: Anthozoa). Part 3: The genus *Narella* Gray, 1870. Proceedings of the Biological Society of Washington 116(3): 617–648.
- Cairns SD, Bayer FM (2004) Studies on western Atlantic Octocorallia (Coelenterata: Anthozoa). Part 4: The genus *Paracalyptraphora* Kinoshita, 1908. Proceedings of the Biological Society of Washington 117(1): 114–139.
- Cairns SD, Bayer FM (2007) A review of the Octocorallia (Cnidaria: Anthozoa) from Hawai'i and adjacent seamounts: the genus *Narella* Gray, 1870. Pacific Science 62(1): 83–115. [https://doi.org/10.2984/1534-6188\(2008\)62\[83:AROTOC\]2.0.CO;2](https://doi.org/10.2984/1534-6188(2008)62[83:AROTOC]2.0.CO;2)
- Cairns SD, Bayer FM (2009) A generic revision and phylogenetic analysis of the Primnoidae (Cnidaria: Octocorallia). Smithsonian Contributions to Zoology 629: 1–79. <https://doi.org/10.5479/si.00810282.629>
- Cairns SD, Stone RP, Moon H-W, Lee JH (2018) Primnoidae (Octocorallia: Calcaxonia) from the Emperor Seamounts, with notes on *Callogorgia elegans* (Gray, 1870). Pacific Science 72(1).
- Cairns SD, Wirshing HH (in review) A phylogenetic analysis of the Primnoidae (Anthozoa: Octocorallia: Calcaxonia), with a key to the genera and subgenera.
- Cordeiro RTS, Castro CB, Pérez CD (2015) Deep-water octocorals (Cnidaria: Octocorallia) from Brazil: family Chrysogorgiidae Verrill, 1883. Zootaxa 4058: 81–100. <https://doi.org/10.11646/zootaxa.4058.1.4>
- Duchassaing FP, Michelotti J (1860) Mémoire sur les coralliaires des Antilles. Mémoires de l'Académie des Sciences de Turin (2)19: 279–365 [reprint paged 1–89]
- Duchassaing FP, Michelotti J (1864) Supplément au mémoire sur les coralliaires des Antilles. Mémoires de l'Académie des Sciences de Turin (2)23: 97–206 [reprint paged 1–112] <https://doi.org/10.5962/bhl.title.105196>
- Dueñas LF, Alderslade P, Sánchez JA (2014) Molecular systematics of the deep-sea bamboo corals (Octocorallia: Isididae: Keratoisidinae) from New Zealand with descriptions of two

- new species of *Keratoisis*. Molecular Phylogenetics and Evolution 74: 15–28. <https://doi.org/10.1016/j.ympev.2014.01.031>
- Ehrenberg CG (1834) Beiträge zur physiologischen Kenntniss der Corallenthiere im allgemeinen und besonders des Rothen Meeres, nebst einem Versuch zur physiologischen Systematik derselben. Physikalische-Mathematische Abhandlungen der Königlischen Akademie der Wissenschaften zu Berlin (1832) 1: 225–380.
- Esper EJC (1788) Die Pflanzenthiere in Abbildungen nach der Natur mit Farben erleuchtet nebst Beschreibungen. Theil 1: Raspichen Buchhandlung, Nürnberg, 97–192.
- Etnoyer PJ (2008) A new species of *Isidella* bamboo coral (Octocorallia: Alcyonacea: Isididae) from northeast Pacific seamounts. Proceedings of the Biological Society of Washington 121(4): 541–553. <https://doi.org/10.2988/08-16.1>
- France SC (2007) Genetic analysis of bamboo corals (Cnidaria: Octocorallia: Isididae): Does lack of colony branching distinguish *Lepidisis* from *Keratoisis*? Bulletin of Marine Science 81(3): 323–333.
- Gray JE (1858) Synopsis of the families and genera of axiferous Zoophytes or barked corals. Proceedings of the Zoological Society of London for 1857: 278–294.
- Gray JE (1866) Description of two new forms of gorgonioid corals. Proceedings of the Zoological Society of London for 1866: 24–27.
- Gray JE (1870) Catalogue of the Lithophytes or Stony Corals in the Collection of the British Museum: 1–51.
- Kinoshita K (1908) Primnoidae von Japan. Journal of the College of Science, Imperial University, Tokyo, Japan. 23(12): 1–74.
- Kükenthal W (1907) Gorgoniden der Deutschen Tiefsee-Expedition. Zoologischer Anzeiger 31(7): 202–212.
- Kükenthal W (1909) Diagnosen neuer Alcyonarien (7. Mitteilung). Zoologischer Anzeiger 35(1/2): 46–53.
- Kükenthal W (1912) Die Alcyonarien der deutschen Süd-polar Expedition 1901–1903. Deutschen Süd-polar Expedition 1901–1903, Zoologie 5(3): 289–349.
- Kükenthal W (1913) Über die Alcyonarienfauna Californiens und ihre tiergeographischen Beziehungen. Zoologische Jahrbücher (Syst.) 35(2): 219–270. <https://doi.org/10.5962/bhl.part.16718>
- Kükenthal W (1919) Gorgonaria. Wissenschaftliche Ergebnisse der deutschen Tiefsee-Expedition auf dem Dampfer “*Valdivia*”, 1898–1899 13(2): 1–946.
- Kükenthal W (1924) Coelenterata: Gorgonaria. Das Tierreich 47. Walter de Gruyter & Co., Berlin, 478 pp.
- Kükenthal W, Gorzawsky H (1908) Diagnosen neuer japanischer Gorgoniden (Reise Doflein 1904–05). Zoologischer Anzeiger 32: 621–631.
- Lamarck JBPAdM (1815) Sur les polypiers corticifères. Mémoires du Muséum National d’Histoire Naturelle, Paris 1–2: 401–416, 467–476, 76–84, 157–164, 227–240.
- Lamouroux JVF (1812) Extrait d’un mémoire sur la classification des polypiers coralligènes non entièrement pierreux. Nouvelle Bulletin de la Société Philomatique, Paris 3(63): 181–188.
- Menckling F (1905) Über die Anordnung der Schuppen und das Kanalsystem bei *Stachyodes ambigua* (Stud.), *Caligorgia flabellum* (Ehrb.), *Calyptrophora Agassizii* (Stud.), *Amphilaphis abietina* (Stud.) und *Thouarella variabilis* (Stud.). Archiv für Naturgeschichte 71(3): 245–266.

- Milne Edwards H (1857) Histoire naturelle des coralliaires ou polypes proprement dits. Volume 1. Librairie Encyclopédique de Roret. Paris, 326 pp.
- Nutting CC (1908) Descriptions of the Alcyonaria collected by the U.S. Bureau of Fisheries Steamer *Albatross* in the vicinity of the Hawaiian Islands in 1902. Proceedings of the United States National Museum 34: 543–601. <https://doi.org/10.5479/si.00963801.34-1624.543>
- Nutting CC (1909) Alcyonaria of the Californian coast. Proceedings of the United States National Museum 35: 681–727. <https://doi.org/10.5479/si.00963801.35-1658.681>
- Pallas PS (1766) Elenchus Zoophytorum. P. van Cleef, Hague Comitum, 28 + 451 pp.
- Pante E, France SC (2010) *Pseudochrysogorgia bellona* n. gen., n. sp.: a new genus and species of chrysogorgiid octocoral (Coelenterata, Anthozoa) from the Coral Sea. Zoosystema 32(4): 595–612. <https://doi.org/10.5252/z2010n4a4>
- Pante E, France SC, Couloux A, Cruaud C, MacFadden CS, Samadi S, Watling L (2012) Deep-sea origin and in-situ diversification of chrysogorgiid octocorals. PLoS ONE 7(6): e38357. <https://doi.org/10.1371/journal.pone.0038357>
- Pante E, Watling L (2011) *Chrysogorgia* from the New England and Corner Rise Seamounts: Atlantic-Pacific connections. Journal of the Marine Biological Association of the United Kingdom 92(5): 911–927. <https://doi.org/10.1017/S0025315411001354>
- Pasternak FA (1981) Alcyonacea and Gorgonacea. In: Benthos of the Submarine Mountains of the Marcus-Necker and adjacent Pacific Regions. Academy of Sciences of the USSR, P.P. Shirshov Institute of Okeanology, 40–56.
- Pomponi SA, Reed JK, Rinehart KL (1988) 1986 expedition to Galápagos Islands, Cocos Islands, and Pearl Islands. Harbor Branch Oceanographic Institution, Ft. Pierce, 19 pp.
- Studer T (1878) Übersicht der Steinkorallen aus der Familie der Madreporaria aporosa, Eupsammia, und Turbinaria, welche auf der Reise S.M.S. *Gazelle* um die Erde gesammelt wurden. Monatsberichte der Königlich Preussischen Akademie der Wissenschaften zu Berlin, 1877: 625–654, pls. 1–4.
- Studer T (1894) Note préliminaire sur les Alcyonaires. Bulletin of the Museum of Comparative Zoology 25(5): 53–69.
- Taylor ML, Rogers AD (2015) Evolutionary dynamics of a common sub-Antarctic octocoral family. Molecular Phylogenetics and Evolution 84: 185–204. <https://doi.org/10.1016/j.ympev.2014.11.008>
- Thomson JA (1905) Appendix to the report on the Alcyonaria collected by Professor Herdman, at Ceylon, in 1902. In: Report to the Government of Ceylon on the Pearl Oyster Fisheries of the Gulf of Manaar. Part 4. Supplementary report 28: 167–186.
- Thomson JA, Henderson WD (1906) An account of the Alcyonarians collected by the Royal Indian Marine Survey Ship Investigator in the Indian Ocean. Part 1. The Alcyonarians of the deep sea. Indian Museum, Calcutta, 1–132.
- Thomson JA, Mackinnon DL (1911) The Alcyonarians of the “Thetis” expedition. Australian Museum Memoirs 4: 661–695. <https://doi.org/10.3853/j.0067-1967.4.1911.1509>
- Thomson JA, Renner NI (1931) Alcyonaria, Madreporaria, and Antipatharia. Australasian Antarctic Expedition Scientific Reports (C- Zoology and Botany) 9(3): 1–46.

- Verrill AE (1883) Report on the Anthozoa, and on some additional species dredged by the “Blake” in 1877–1879, and by the U.S. Fish Commission Steamer “Fish Hawk” in 1880–1882. Bulletin of the Museum of Comparative Zoology, Harvard 11: 1–72.
- Versluys J (1902) Die Gorgoniden der *Siboga*-Expedition I. Die Chrysogorgiidae. *Siboga*-Expedition Monographie 13: 1–120.
- Versluys J (1906) Die Gorgoniden der *Siboga*-Expedition. II. Die Primnoidae. *Siboga*-Expedition Monographie 13a: 1–187.
- Watling L, France SC, Pante E, Simpson A (2011) Chapter 2: Biology of Deep-Water Octocorals. *Advances in Marine Biology* 60: 41–122. <https://doi.org/10.1016/B978-0-12-385529-9.00002-0>
- Wright EP (1885) The Alcyonaria. Report of the Scientific Results of the Challenger, Narrative 1(2): 689–693.
- Wright EP, Studer T (1889) Report on the Alcyonaria collected by *H.M.S. Challenger* during the years 1873–76. Report on the Scientific Results of the Voyage of *H.M.S. Challenger* during the years 1873–76, *Zoology* 31(64): 1–314.
- Zapata-Guardiola R, López-González PJ (2012) Revision and redescription of the species previously included in the genus *Amphilaphis* Studer and Wright in Studer, 1887 (Octocorallia: Primnoidae). *Scientia Marina* 76(2): 357–380. <https://doi.org/10.3989/scimar.03278.18B>
- Zapata-Guardiola RP, López-González PJ, Gili J-P (2012) A review of the genus *Mirostenella* Bayer, 1988 (Octocorallia: Primnoidae) with a description of a new subgenus and species. *Helgoland Marine Research* 67: 229–240. <https://doi.org/10.1007/s10152-012-0318-z>

Appendix I

Station	Latitude	Longitude	Depth (m)	Date
JSL-I				
1912	0°21.877'S	90°15.747'W	806	Nov 14 1986
1915	1°17.2'S	89°48.7'W	650	Nov 15 1986
1916	1°18.715'S	89°48.809'W	545–562	Nov 16 1986
1922	0°23.683'N	90°26.341'W	475–578	Nov 19 1986
1927	0°10.50'S	90°53.25'W	708–782	Nov 21 1986
1929	0°14.675'N	91°36.526'W	804	Nov 23 1986
1930	0°03.057'S	91°33.927'W	333–478	Nov 23 1986
1931	0°10.303'S	91°24.675'W	441–528	Nov 24 1986
1933	0°17.072'S	91°40.208'W	663–788	Nov 25 1986
1934	0°15.16'S	91°27.93'W	252–308	Nov 25 1986
1935	0°29.737'S	91°23.806'W	391–488	Nov 26 1986
1938	5°24.49'N	87°09.83'W	614–785	Nov 30 1986
1942	5°34.60'N	87°04.25'W	606–628	Dec 2 1986
3902	1°18.763'S	89°48.82'W	554	Oct 17 1995
3907	0°20.517'N	90°23.788'W	530–576	Oct 19 1995
3912	0°08.581'N	91°23.708'W	489	Oct 21 1995
3925	0°17.100'S	91°05.046'W	768	Oct 28 1995
3930	0°29.749'S	90°13.981'W	450	Oct 30 1995
JSL-II				
3108	0°24.00'N	90°26.5'W	1545	Jul 21 1998
USFWS Albatross				
2818	0°29'S	89°54'30"W	717	Apr 15 1888
3399	1°07'00"N	81°04'W	3182	Mar 24 1891
3403	0°58'30"S	89°17'W	700	Mar 28 1891
3404	1°03'S	89°28'W	704	Mar 28 1891
3406	0°16'S	90°21'30"W	1008	Apr 3 1891
3410	0°19'N	90°34'W	805	Apr 3 1891
4153	23°05'N	161°52'W	1760–1837	Aug 5 1902
4357	32°N	117°W	245–284	Mar 15 1904
4530	36°45'N	121°55'W	1381–1752	May 27 1904
4537	36°45'N	121°55'W	1575–1942	May 31 1904
R/V Gilliss				
21	7°11'N	79°16'W	1463	Jan 18 1972
E/V Nautilus				
NA64–77–01	0°23.40'S	91°52.98'W	3381	Jul 3 2015
NA64–125–01	0°22.60'S	90°40.05'W	446	Jul 6 2015
NA64–126–01	0°22.59'S	90°49.06'W	445	Jul 6 2015

Description of the last-instar larva and pupa of a leaf-mining hispine – *Prionispa champaka* Maulik, 1919 (Coleoptera, Chrysomelidae, Cassidinae, Oncocephalini)

Chengqing Liao¹, Peng Liu¹, Jiasheng Xu¹, Charles L. Staines², Xiaohua Dai^{1,3}

1 Leafminer Group, School of Life and Environmental Sciences, Gannan Normal University, Ganzhou, Jiangxi 341000, China **2** Department of Entomology, National Museum of Natural History, Smithsonian Institution, P. O. Box 37012, Washington, DC 20013-7012, USA **3** National Navel-Orange Engineering Research Center, Ganzhou, Jiangxi 341000, China

Corresponding author: Xiaohua Dai (ecoinformatics@gmail.com; leafminer@vip.qq.com)

Academic editor: A. Eben | Received 17 September 2017 | Accepted 21 November 2017 | Published 16 January 2018

<http://zoobank.org/33C82A78-B840-42C3-9336-9E4BC9B3615D>

Citation: Liao C, Liu P, Xu J, Staines CL, Dai X (2018) Description of the last-instar larva and pupa of a leaf-mining hispine - *Prionispa champaka* Maulik, 1919 (Coleoptera, Chrysomelidae, Cassidinae, Oncocephalini). ZooKeys 729: 47–60. <https://doi.org/10.3897/zookeys.729.21041>

Abstract

The last-instar larva and pupa of *Prionispa champaka* Maulik, 1919 are described and figured in detail. The chaetotaxy of the head, mouthparts, legs, and dorsal and ventral surfaces of the body are given. The larva of *P. champaka* mine in the leaves of *Pollia japonica* Thunb. (Commelinaceae) and pupate in the base of the mid-ribs. The adults were also observed feeding on the leaves of *Pollia siamensis* (Carib.) Faden ex D. Y. Hong. The prominent diagnostic characters of immature stages of other species of the three genera of Oncocephalini (*Prionispa*, *Chaeridiona*, and *Oncocephala*) are discussed.

Keywords

Cassidinae, chaetotaxy, immature stages, leaf-mining hispines, morphology, Oncocephalini, *Pollia*, *Prionispa*

Introduction

The genus *Prionispa* Chapuis, 1875 is a member of the tribe Oncocephalini, Chapuis 1875 (Chrysomelidae: Cassidinae) and consists of 29 described species occurring in the oriental tropics (Staines 2015). Seven species are recorded from China, especially in Yunnan Province: *P. champaka* Maulik, 1919, *P. cheni* Staines, 2007 (replacement name for *Chaeridiona tuberculata* Chen & Yu in Chen et al. 1986), *P. clavata* (Yu, 1992) (as *C. clavata*, Hunan), *P. dentata* Pic, 1938, *P. houjayi* Lee et al., 2009 (Taiwan), *P. opacipennis* Chen & Yu, 1962, and *P. sincia* Gressitt, 1950 (Fujian). This genus can be distinguished from the other genera in Oncocephalini, such as *Chaeridiona* Baly, 1869 and *Oncocephala* Agassiz, 1846, by the following characters: head with a distinct longitudinal ridge but without protuberance between the antennal bases; antennae not striate, third antennomere longer than the anterior two antennomeres combined; the labial palpi with three palpomeres; and the pronotum without tubercles (Chen et al. 1986).

So far only five *Prionispa* species have been recorded with host plants: *P. champaka* feeding on the leaves of an unidentified Zingiberaceae (Hua 2002), *P. dentata* feeding on several plant species of the family Zingiberaceae (Hua 2002) and Commelinaceae (Chaboo et al. 2010), *P. fulvicollis* (Guérin-Méneville, 1830) infesting *Pollia thyrsiflora* Endl. ex Hasskarl (Commelinaceae) (Taylor 1937), *P. houjayi* infesting *Disporum kawakamii* Hayata (Liliaceae) (Lee et al. 2009), and *Prionispa tuberculata* Pic, 1926 associated with *Ipomoea batatas* Poir. (Convolvulaceae) (Mo 1956). In the present study, we found the larvae of *P. champaka* mining in the leaves of *Pollia japonica* Thunb. (Commelinaceae) in Jiangxi Province, China, and we also made some biological observations.

Materials and methods

Immatures of *Prionispa champaka* were collected on wild plants (natural host plants) that were placed in plastic zip-lock bags. Then larvae and pupae were reared and observed in the laboratory. Field-collected and laboratory-emerged adults were preserved as pinned specimens (Figs 1–3) and identified using the keys of Chen et al. (1986). Host plants from Jiangxi Province were identified by plant experts.

All immatures were collected at Anjishan Provincial Forest Park (Longnan County, Jiangxi Prov.) from 2015 to 2017, on *Pollia japonica* Thunb. (Commelinaceae). One adult was collected at Jiulianshan National Nature Reserve (Longnan County, Jiangxi Prov.) in July 2016 (without host plant note), and one adult was collected at Bawangling National Forest Park (Changjiang County, Hainan Prov.) in August 2016, on *Pollia siamensis* with feeding channels of adults.

Three mature larvae, three pupae, and three pupal exuviae were examined morphologically. Larvae and pupae were preserved in anhydrous ethanol. For microscopic study, heads of the larvae were separated from the rest of body and then the mouthparts were dissected. The photos of adults were made using a Cannon EOS 7D camera and



Figures 1–3. *Prionispa champaka*. **1** Dorsal view **2** Ventral view **3** Lateral view.

macro lenses; dissection of heads and mouthparts were done using a Motic SMZ-140 and Olympus SZX2-ILLT stereomicroscope; figures and examination were obtained using an Optika B-292 microscope and Cannon EOS 70D camera. Descriptions of immature stages follows Świętojańska et al. (2006). Terminology of the chaetotaxy of the head follows Borowiec and Świętojańska (2003).

All studied material (mature larvae, pupae and exuviae) and adults were deposited at the Leafminer Group, School of Life and Environmental Science, Gannan Normal University, China.

Result

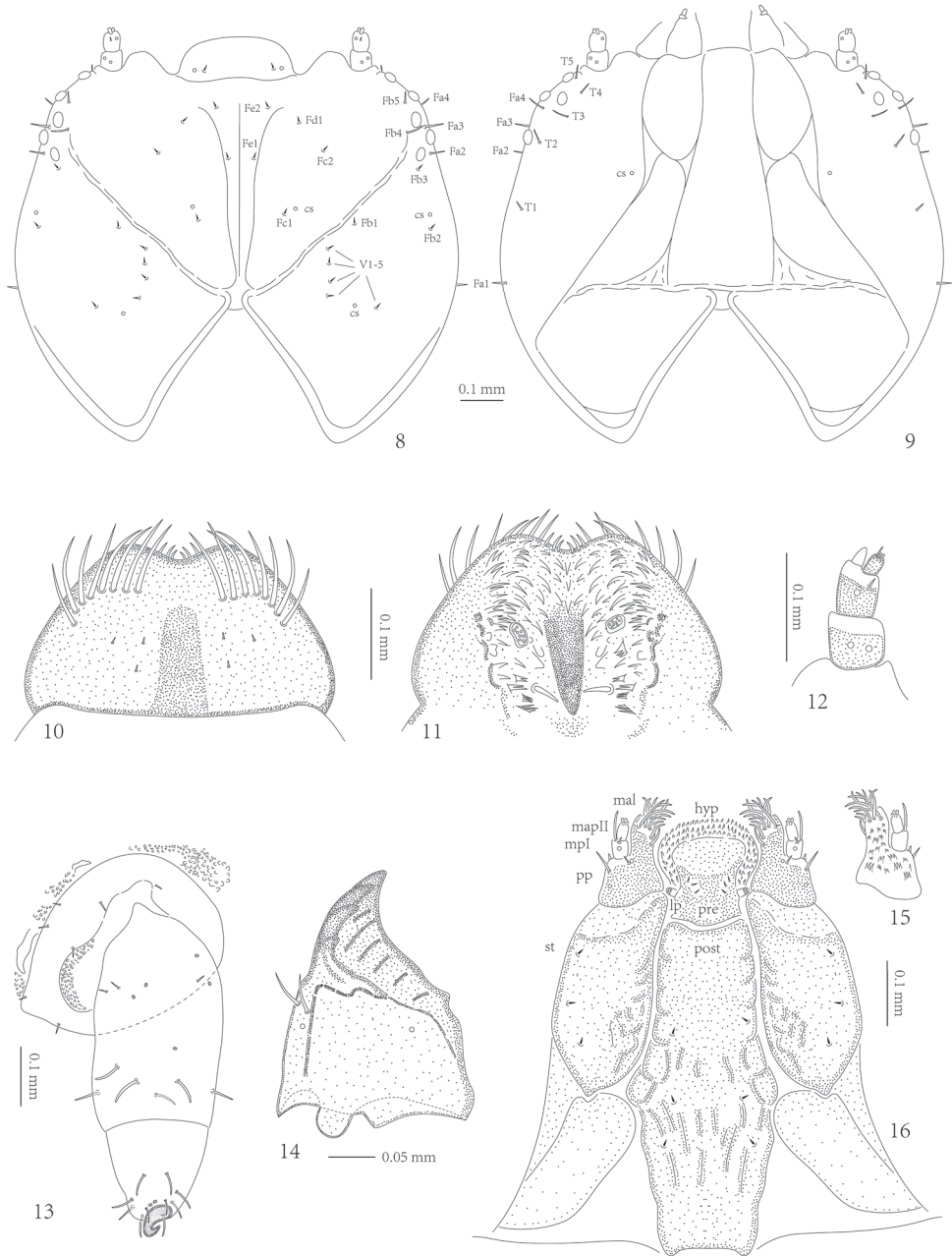
Description of *Prionispa champaka* Maulik, 1919

Mature larva (Figs 4–5, 8–18)

Length of mature larva 6.5–6.6 mm without head, width of body 1.8–1.9 mm across pronotum and 2.9–3.0 mm across abdominal segment IV. Body distinctly flattened dorso-ventrally, mature larvae are widest across abdominal segments IV–V (Figs 4–5, 17–18). Body yellowish, with dark brown head, brown spiracles, and pronotum basally with two irregular brown patches and a pale longitudinal line, brown trapezoidal patch on prosternum, brown legs and dark brown claws. Body of alcohol-preserved larvae somewhat lighter in color.



Figures 4–7. *Prionispa champaka*. **4** Larva, dorsal view **5** Larva, ventral view **6** Pupa, dorsal view **7** Pupa, ventral view.



Figures 8–16. *Prionispa champaka*, larva. **8** Dorsal view of head: cs - campaniform sensilla **9** Ventral view of head. **10** Dorsal view of labrum **11** Ventral view of labrum **12** Antenna **13** Leg **14** Mandible **15** Dorsum of palpiger and maxillary palp **16** Ventral views of maxillae and labium. Abbreviations: hyp - hypopharynx; lp - labial palp; mal - mala; mpI - first segment of maxillary palp; mpII - second segment of maxillary palp; post - postmentum; pp - palpifer; pre - prementum; st - stipes.

Body with four pairs of lateral scoli placed on abdominal segments V–VIII (Figs 4–5, 17–18). Lateral scoli triangular, without lateral branches but with one seta apically and three setae at base (two placed dorsally, one ventrally). Abdominal segments I–IV without lateral scoli but with two setae laterally and one seta ventrally. Granulation of body distinct in all examined larvae. Minute setae on anterior margin of each tergite and sternite; tergites and sternites covered with short pointed setae. Tergites of meso-, meta-thorax and abdominal segments I–II with two transverse grooves, tergites of abdominal segments III–VII and sternites I–VIII with one transverse groove (Figs 17–18). Asperites present at the anterior margin of pronotum and around each transverse groove.

Pronotum on each side with 14 setae arranged in a constant pattern (Fig. 17). Meso- and metanotum with six setae on anterior margin (two pairs in the middle and a pair laterally); a row of eight setae running across segment; three setae on each side laterally and three setae placed on each lateral margin. Abdominal tergites I–VII with four minute setae on anterior margin; two rows of setae running across segment, both with four setae; two setae placed close to each spiracle. Abdominal tergite VIII with four minute setae on anterior margin; one seta placed on each side laterally; three rows of setae running across segment: anterior with four setae, next with two, and posterior with two setae placed between spiracles (close to each other). Posterior margin of spiracle VIII with eight setae on each side.

Prosternum with two rows of setae medially (anterior with two setae, posterior with four setae) and four setae on each side at base of leg (Fig. 18). Meso- and metasternum with two setae on anterior margin; four setae medially; and three minute setae on each side at base of leg. Abdominal sternites I–VIII with a pair of minute seta on anterior margin medially; with rows of four setae running across segment medially; and two setae on each side of sternite laterally.

Nine pairs of distinct *spiracles* (Figs 4, 17): one placed on lateral margin of mesothorax anteriorly, and eight placed on abdominal tergites. Spiracles of thorax more elevated than those on abdomen, spiracles of abdominal tergites I–VII approximate same in size, but spiracles of abdominal tergite VIII form triangular tip of body.

Head well sclerotized, prognathous, partially retracted into pronotum (Figs 8–9). Epicranial stem absent; median endocarina wide, extending between frontal arms; frontal arms V-shaped, fronto-clypeal suture present; clypeus flat and with a pair of setae and one pair of campaniform sensilla. Frons with two short setae (Fd1 and Fe2) placed anteriorly, two short setae (Fc1 and Fc2) and one campaniform sensillum between median endocarina and frontal arm, one short seta (Fb3) and two long setae (Fb4 and Fb5) laterally close to frontal arm, one short seta on median endocarina (Fe1); vertex with seven short setae (Fb1, Fb2, and V1–5) and two campaniform sensilla (one between setae V4 and V5, one close to seta Fb2). One long seta (Fa1) placed on lateral margins close to pronotum, three long setae (Fa2, Fa3, and Fa4) close to stemmata. Temporal side with one campaniform sensillum and five setae: one shorter (T1), four longer (T2, T3, T4, and T5).

Six stemmata on each side of head (Figs 8–9). Antenna (Fig. 12) with three antennomeres, set in membranous ring; 1st antennomere stout, approximately as wide as

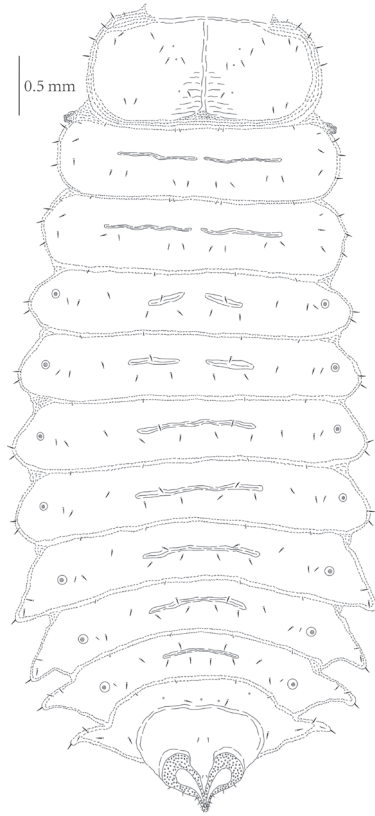


Figure 17. *Prionispa champaka*, last instar larva, dorsal view.

long, with two campaniform sensilla; 2nd antennomere slightly slender, longer than wide, with one small seta laterally and one campaniform sensillum dorsally, prominent sensory appendix at apex close to base of 3rd antennomere; 3rd antennomere distinctly longer than wide, with one small seta and two peg-like sensilla at apex.

Labrum approximately two times wider than long, anterior margin emarginate (Figs 10–11). Anterior margin with eight stout, long, pointed setae on each side. Dorsal surface of labrum with six short setae medially. Mid and anterior part of ventral surface (epipharyngeal area) with numerous stout spines; lateral parts with tiny spines; two irregular groups of a few small sensilla medially.

Mandibles heavily sclerotized, with four prominent teeth, followed by some tiny teeth (Fig. 14); two setae and two campaniform sensilla on dorsal side (one close to setae).

Maxillae and labium connate. Each stipes (st) with three short pointed setae laterally (Figs 15–16). Palpifer (pp) with three setae (one seta distinctly longer than others) and two campaniform sensilla ventrally, and numerous short spines dorsally. Maxillary palp (mp) with two palpomeres: first palpomere with one long seta and one short seta at apex, and one campaniform sensillum ventrally; second palpomere with a group of peg-like sensilla at apex. Mala (mal) with twelve long pointed setae apically. Hypophar-

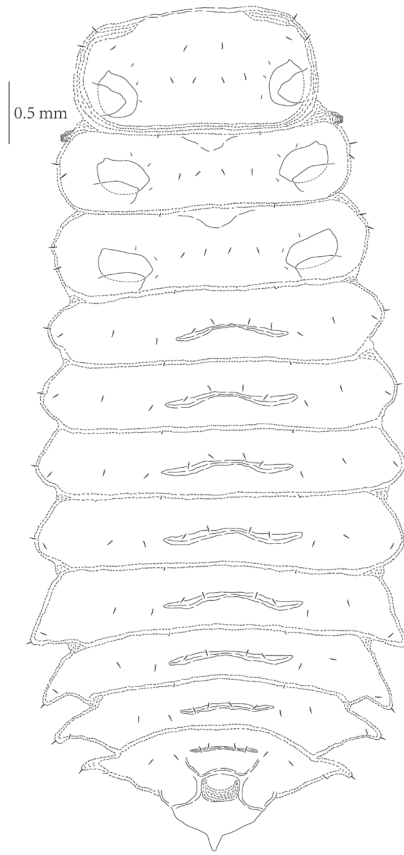


Figure 18. *Prionispa champaka*, last instar larva, ventral view.

ynx (hyp) covered with numerous spines. Labial palp (lp) with one palpomere, with a group of small peg-like sensilla at the apex. Prementum (pre) with three setae on each side. Postmentum (post) with three short setae placed on each side medially.

Legs stout, consist of three segments: coxa, femur, and tibiotarsus (Fig. 13). Tibiotarsus armed apically with heavily sclerotized, short, curved, single, simple claw. Coxa with four setae placed along base on internal surface, three setae placed dorsally. Femur with three short pointed setae and four campaniform sensilla placed in basal half, six long pointed setae and one campaniform sensillum placed around apical half. Tibiotarsus with nine long pointed setae and two campaniform sensilla: six setae around claw, three setae, and two sensilla above claw.

Pupa (Figs 6–7, 19–20)

Length of pupa 6.5 mm, width of body 2.0 mm across the base of pronotum and 3.0 mm across abdominal segment IV without lateral scoli. Body flattened dorso-ventrally, elongate-oval, color when alive as well as alcohol preserved pupa yellowish-brown (Figs 6–7).

Head with two distinct long and one short triangular processes on anterior margin (Figs 6–7, 19–20). Prothorax with a pair of two-branched lateral scoli, but meso- and metathorax without lateral scoli. Each short branch apically armed with pointed seta. Abdominal segments I–IV with single scoli on each side, these scoli basally with two to three very small tubercle-like branches. Abdominal segment V with one two-branched scoli laterally. Abdominal segments VI–VIII with five lateral scoli, usually the third and fourth scoli with a broad common stem. Each scoli or branch apically with one seta. Posterior lateral scoli of segments VI–VIII with lateral branch directed posteriorly without any seta. Segment VIII additionally with 14 (rarely 13 or 15) flattened long processes (more or less one-two processes shorter than others) placed at posterior border. Each process armed with single seta, regardless of their size or length.

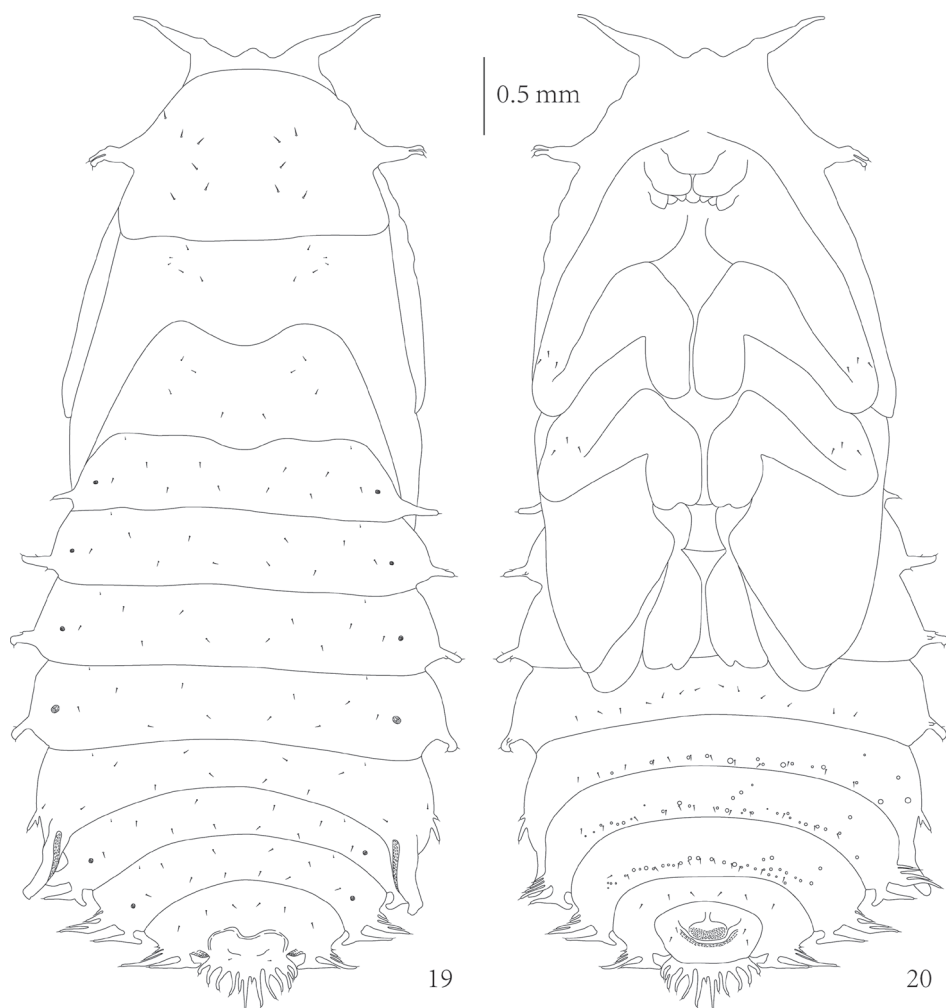
Pronotum with one pair of setae laterally and five setae on each side medially (Fig. 19). Mesonotum with five setae on each side medially (lateral two minute setae). Metanotum with a group of three setae on each side laterally and two setae medially. *Abdominal tergites* I–VII with two minute setae at anterior border; two rows of setae running across segment, both with four setae; one seta placed close to each spiracle. Abdominal tergite VIII with two rows of setae running across segment: anterior with six setae, and posterior with two setae (placed between spiracles).

In ventral view (Fig. 20): head and mouthparts without setae; each femur of legs with three setae placed at apex (hind legs were covered by the wings, invisible); visible abdominal sternites IV–VII with rows of twelve setae running across segment posteriorly; abdominal sternite VIII with rows of six setae running across segment anteriorly, and two setae placed on each side of anus.

Abdominal segments each with a pair of *spiracles* (Fig. 19). Spiracles of segments I–III and VI–VII similar in size. Spiracles of segment IV similar and approximately two times larger than others. Spiracles of segment VIII not elevated, and similar to spiracles of segment IV. Spiracles of segment V most prominent, elongated into long appendage (respiratory horns) with elongate-oval spiracular opening, directed posteriorly. Abdominal sternites V–VII each with one row of tubercles placed posteriorly (tubercles of sternite VII are the most developed), some of them very close to setae of each sternite.

Habitat and biological notes

There is little biological information known on *P. champaka*. It was reported to feed an unidentified host plant of the family Zingiberaceae from China (Hua 2002), but without any descriptions on larval mines and adult feeding patterns. At Anjishan Provincial Forest Park from 2015 to 2017, we collected eggs, larvae, pupae and adults of this species on the leaves of *Pollia japonica* from June to July, and only mature larvae, pupae and adults in August (Figs 21–27). Additionally, we collected only one adult in 31th October 2016. At Jiulianshan National Nature Reserve (Longnan County, Jiangxi Prov.), we collected only adults from 13–19th July 2016. At Bawangling National Forest Park (Changjiang County, Hainan Prov.), we collected only adults associated with



Figures 19–20. *Prionispa champaka*, pupa. **19** Dorsal view **20** Ventral view.

Pollia siamensis and its feeding channels from 4–11th August 2016. Chen et al. (1986) recorded adults of this species occurring in Yunnan Province from May to June. We consider the life cycle of *P. champaka* to be univoltine based on the information above.

The female of *P. champaka* bites a narrow line across the mid-rib of the lower canopy leaves on the plant, and then extends it along each side of the mid-rib in the same direction. The biting channel results in two short vertical lines and forms an elongate “U” shape. Subsequently, the female lays a single long egg sheath (usually comprising 5–8 eggs) at the base of the biting channel. Finally, the female covers this portion of the biting channel with feces (Figs 23–24). This shows the biting channel of the female as well as her secretion helps to protect the egg sheath. The length of the egg sheath is approximately 7–10 mm (average 8.5 mm, ten sheathes were measured), which is usually shorter than that of the female biting channel. The larvae are gregarious, usually developing in a common mine (Fig. 25). Freshly hatched larvae bore into the mesophyll of

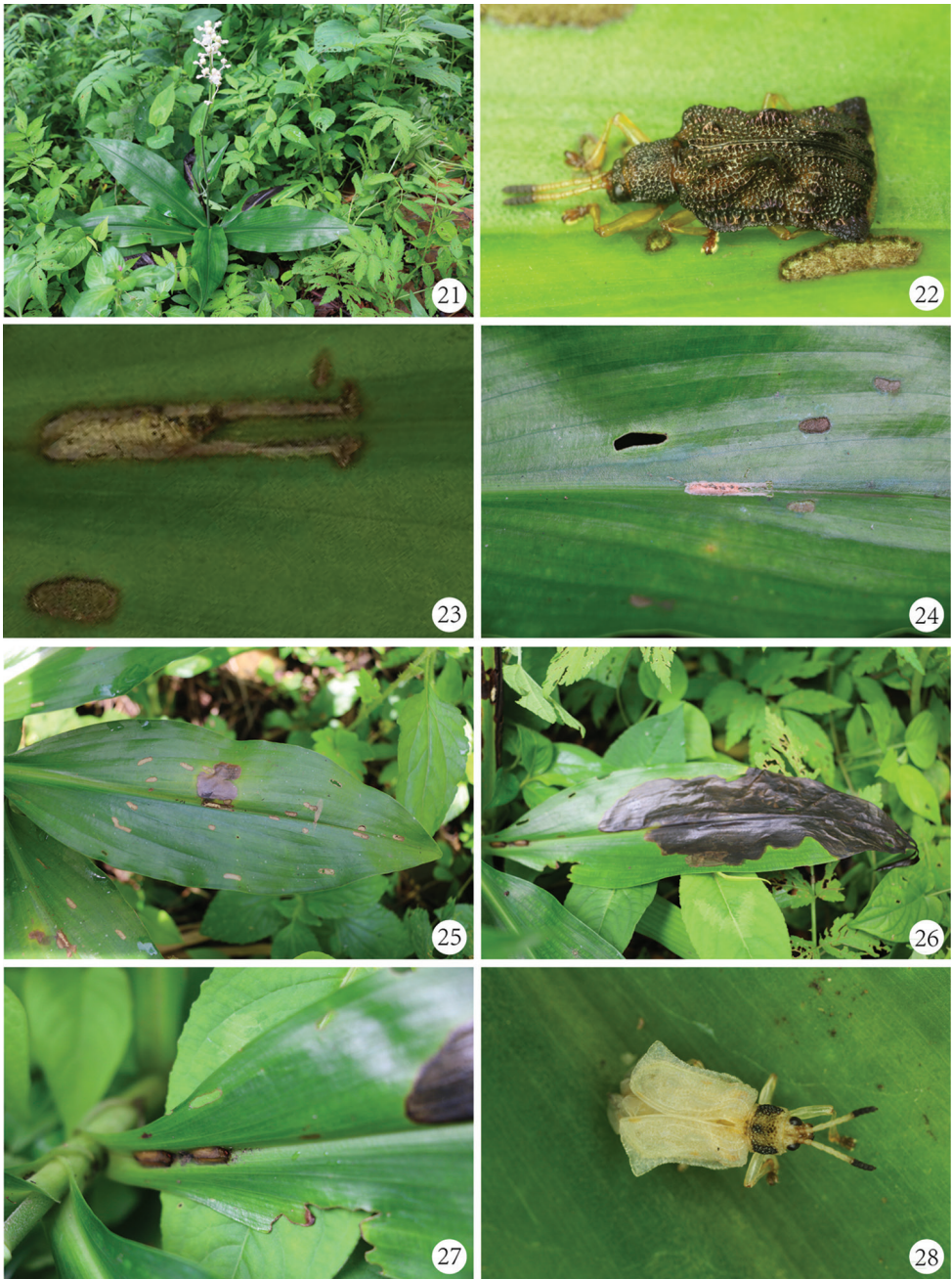
the upper leaf surface (Fig. 25). The larval mine is very broad and irregular in shape, even extending to the entire leaf (Fig. 26). The larvae deposit their feces in the mine. The mature larva leaves its original mine and builds a new one on the base of petiole (Fig. 27), in which it transforms into the pupa and then emerges as an adult. The pupal mine is an elongate channel with a distinct opening which closed by apex of pupal abdomen (Fig. 27). The freshly emerged adults are mostly white, with eyes and apical four antennomeres black, pronotum yellowish with three black longitudinal marks or completely black, and brownish tarsi (Fig. 28). Hours later, the body of adults becomes darker and harder (Fig. 22). Subsequently, the adults start to feed. The feeding channels are elongate-oval or linear striped, usually on the upper surface of leaves (Fig. 25).

Discussion

Immature stages of only four species in the tribe Oncocephalini have been described in detail. Świątojańska et al. (2006) described and compared the mature larvae and pupae of *C. picea* Baly, 1869 and *O. quadrilobata* Guérin-Ménéville, 1844. In this study, the authors indicated that the typical morphology of Old World leaf-mining hispines are a flattened body and at least abdominal segments with lateral scoli in the larval stage, and very long spiracles on the fifth abdominal segment in the pupal stage. Świątojańska and Kovac (2007) described the mature larva and pupa of *C. thailandica* Kimoto, 1998 with detailed habitat and biological notes. Lee et al. (2009) described the immature stages and adult of *P. houjyai*. Our study showed that the diagnostic characters are the lateral scoli of the thorax, the abdominal apex of the larva, and the processes on the head and pronotum of the pupa.

In the present study, a prominent diagnostic character of the larva of *P. champaka* was found: the lateral scoli on abdominal segments V–VIII. However, the lateral scoli of *P. houjyai* are present on all abdominal segments, as well as the meso- and metathorax (Lee et al. 2009). Presence of the lateral scoli on abdominal segments is variable between genera or within a genus, but at least some abdominal segments have lateral scoli, especially the posterior segments. The shape of abdominal apex is most similar to the tapering type of *C. thailandica* and *C. picea* but not the quadrate type of *P. houjyai*, indicating that this is not a constant character within the genus *Prionispa*. Furthermore, the larva of *P. champaka* has prominent labial palpi, highlighted as a unique character for *P. houjyai* (Lee et al. 2009). However, the labial palpi of *P. champaka* seem to be less prominent than those of *P. houjyai*.

The pupa of *P. champaka* is most similar to that of *P. houjyai*. These two species have a pair of prominent processes on the head and pronotum which is probably a constant character within the genus. The lateral scoli of the abdominal segments and the fifth abdominal spiracles also look very similar, but the opening of the fifth abdominal spiracle extends to the base of the spiracle. The most prominent difference from other species of these three genera is that the abdominal apex of *P. champaka* has 14 long flattened processes, whereas *P. houjyai* has only two wide flattened processes, *O. quadrilobata* has four flattened processes, and *C. thailandica* and *C. picea* respec-



Figures 21–28. Life stages of *Prionispa champaka*. **21** *Pollia japonica*, the host plant for *P. champaka* **22** Adult of *P. champaka* and its feeding channel **23–24** An egg sheath of *P. champaka* which laid and located on the mid-rib of upper surface of a leaf **25** A leaf with new mine of hatching larvae of *P. champaka* and some linear feeding channels of adults **26** Large larval mine of mature larvae **27** Two pupal mines of *P. champaka* located at the base of petiole on the upper surface **28** Freshly emerged adult.

tively have two and three slender processes (Lee et al. 2009; Świętojańska et al. 2006; Świętojańska and Kovac 2007).

It can be seen from above that the lateral scoli and abdominal apex of larva and pupa are the most important diagnostic characters between different species in these three genera as well as other Old World genera of leaf-mining hispines, such as *Dactylispa* Weise, 1897 (Chen et al. 1986; Kimoto and Takizawa 1994; Lee and Cheng 2007, 2010; Zaitsev 2012; Dai et al. 2012), *Platypria* Guérin-Méneville, 1840 (Kimoto and Takizawa 1994; Liao et al. 2014), *Dicladispa* Gestro, 1897 (Chen et al. 1986; Lee et al. 2010; Świętojańska et al. 2014).

The habits of immature stages of *P. champaka* are similar to other leaf-mining chrysomelids especially hispines. The mature larvae move to another location and build a new mine (called “pupal mine” or “pupal chamber”) for pupation (Hering 1951), the same as *P. houjayi* Lee et al. (on the lower surface of the leaf close to the mid-rib) (Lee et al. 2009), *O. promontorii* Péringuey, 1898 (on the lower surface away from the leaf base) (Chaboo et al. 2010), *C. thailandica* Kimoto (on the mid-rib on the upper surface of the leaf) (Świętojańska and Kovac 2007), *Platypria melli* Uhmann, 1954 (on a vein of the leaf especially the mid-rib on the upper surface) (Liao et al. 2014), *Notosacantha vicaria* (Spaeth, 1913) (on the mid-rib on the upper surface of the leaf) (Rane et al. 2000), and some species of genus *Dactylispa* (unpublished data). The pupa of *P. champaka* can close its pupal mine with the broadened and flat caudal end of the abdomen, as can *C. thailandica* (Świętojańska and Kovac 2007).

Acknowledgements

We thank every member of the Leafminer Group of Gannan Normal University for collection, laboratorial rearing, observation, and recording of leaf-mining hispines. We also thank Prof. Renlin Liu and his postgraduate Chao Fu (Gannan Normal University, China), and Dr. Xiaoya Yu (Qiannan Normal University for Nationalities) for identifying of the host plants. This study was funded by the National Natural Science Foundation of China (31760173, 41361009, 31260116), Natural Science Foundation of Jiangxi, China (20171BAB204023) and Innovation Team Project of Gannan Normal University.

References

- Borowiec L, Świętojańska J (2003) The first instar larva of *Cassida nebulosa* L. (Coleoptera: Chrysomelidae: Cassidinae) – a model description. *Annales Zoologici* 53: 189–200.
- Chaboo CS, Grobbelaar E, Heron HDC (2010) An African leaf miner, *Oncocephala promontorii* Péringuey, 1898 (Chrysomelidae: Cassidinae: Oncocephalini): Biological notes and host records. *Coleopterists Bulletin* 64(1): 21–29. <https://doi.org/10.1649/0010-065X-64.1.21>

- Chen SH, Yu PY, Sun CH, T'an CH, Zia Y (1986) Fauna Sinica (Insecta: Coleoptera: Hispididae). Science Press, Beijing, 653 pp. [In Chinese]
- Dai XH, Xu JS, Jiang ZM (2012) Bionomics of *Dactylispa approximata* on *Lophatherum gracile*. Northern Horticulture 22: 125–127. [in Chinese]
- Hering EM (1951) Biology of the leaf miners. Springer Science & Business Media, Berlin, 420 pp. <https://doi.org/10.1007/978-94-015-7196-8>
- Hua LZ (2002) List of Chinese Insects Vol. 2. Zhongshan University Press, Guangzhou, 612 pp.
- Kimoto S, Takizawa H (1994) Leaf beetles (Chrysomelidae) of Japan. Tokai University Press, Tokoyo, 539 pp.
- Lee CF, Cheng HT (2007) The Chrysomelidae of Taiwan 1. Sishow-Hills, Taipei, 199 pp. [in Chinese]
- Lee CF, Cheng HT (2010) The Chrysomelidae of Taiwan 2. Sishow-Hills, Taipei, 191 pp. [in Chinese]
- Lee CF, Świątojańska J, Staines CL (2009) *Prionispa boujayi* (Coleoptera: Chrysomelidae: Cassidinae: Oncocephalini), a newly recorded genus and new species from Taiwan, with a description of its immature stages and notes on its bionomy. Zoological Studies 51: 832–861.
- Liao CQ, Xu JS, Dai XH, Zhao XL (2014) Study on the biological characteristics of *Platypria melli*. Northern Horticulture 3: 118–120. [in Chinese]
- Mo TT (1956) Notes on *Oncocephala tuberculata* (Olivier) (Coleoptera: Hispididae). A leafminer of sweet potato (*Ipomoea batatas* Poir.) in West Java. Philippine Journal of Science 85: 517–519.
- Rane N, Ranade S, Ghate HV (2000) Some observations on the biology of *Notosacantha vicaria* (Spaeth) (Coleoptera: Chrysomelidae: Cassidinae). Genus 11(2): 197–204.
- Staines CL (2015) Tribe Oncocephalini. Catalog of the hispines of the World (Coleoptera: Chrysomelidae: Cassidinae). http://entomology.si.edu/Collections_Coleoptera-Hispines.html [accessed 14 September 2017]
- Świątojańska J, Chorzępa M, Ghate H (2006) Description of last instar larva and pupa of *Chaeridiona picea* Baly, 1869 and *Oncocephala quadrilobata* (Guérin, 1844) (Coleoptera: Chrysomelidae: Cassidinae: Oncocephalini) from India. Zootaxa 1341: 49–68. <http://dx.doi.org/10.11646/zootaxa.1341.1.3>
- Świątojańska J, Kovac D (2007) Description of immatures and the bionomy of the Oriental leaf beetle *Chaeridiona thailandica* Kimoto, 1998 (Coleoptera: Chrysomelidae: Cassidinae: Oncocephalini), a leaf-mining hispine beetle. Zootaxa 1637: 21–36.
- Świątojańska J, Borowiec L, Stach M (2014) Redescription of immatures and bionomy of the Palearctic species *Diclidispa testacea* (Linnaeus, 1767) (Coleoptera: Chrysomelidae: Cassidinae: Hispini), a leaf-mining hispine beetle. Zootaxa 3811(1): 1–33. <http://dx.doi.org/10.11646/zootaxa.3811.1.1>
- Yu P (1992) Coleoptera: Hispididae. In: Peng J, Liu Y (Eds) Iconography of forest insects in Hunan China. Academia Sinica & Hunan Forestry Institute, Hunan, China, 610–615. [in Chinese]
- Taylor THC (1937) The biological control of an insect in Fiji. An account of the coconut leaf-mining beetle and its parasite complex. The Imperial Institute of Entomology, London, 239 pp.
- Zaitsev YM (2012) The immature stages of the leaf-beetle genus *Dactylispa* (Coleoptera, Chrysomelidae) from Vietnam. Entomological Review 92(3): 305–314. <http://dx.doi.org/10.1134/S0013873812030074>

Two new genera of metalmark butterflies of North and Central America (Lepidoptera, Riodinidae)

Marysol Trujano-Ortega^{1,2}, Uri Omar García-Vázquez³, Curtis J. Callaghan⁴,
Omar Ávalos-Hernández¹, Moisés Armando Luis-Martínez¹,
Jorge Enrique Llorente-Bousquets¹

1 Museo de Zoología, Departamento de Biología Evolutiva, Facultad de Ciencias, Universidad Nacional Autónoma de México, Apdo. Postal 70–399, México 04510, Ciudad de México, México **2** Posgrado en Ciencias Biológicas, Universidad Nacional Autónoma de México, México **3** Facultad de Estudios Superiores Zaragoza, Universidad Nacional Autónoma de México, Batalla 5 de Mayo s/n, Ejército de Oriente, Ciudad de México 09230, México **4** Casa Picapau, Floresta de la Sabana. Carrera 7, 237–04, Bogotá, Colombia

Corresponding author: Marysol Trujano-Ortega (marysol_trujano@yahoo.com.mx)

Academic editor: T. Simonsen | Received 11 August 2017 | Accepted 31 October 2017 | Published 16 January 2018

<http://zoobank.org/C3539AD1-70E3-4600-B072-F361E7E69129>

Citation: Trujano-Ortega M, García-Vázquez UO, Callaghan CJ, Ávalos-Hernández O, Luis-Martínez MA, Llorente-Bousquets JE (2018) Two new genera of metalmark butterflies of North and Central America (Lepidoptera, Riodinidae). ZooKeys 729: 61–85. <https://doi.org/10.3897/zookeys.729.20179>

Abstract

Two new genera of Riodinidae (Insecta: Lepidoptera) are described, *Neoapodemia* Trujano-Ortega, **gen. n.** (*Neoapodemia nais* (W. H. Edwards, 1876), **comb. n.**, *N. chisosensis* Freeman, 1964, **comb. n.**) and *Plesioarida* Trujano-Ortega & García-Vázquez, **gen. n.** (*Plesioarida palmerii palmerii* (W. H. Edwards, 1870), **comb. n.**, *P. palmerii arizona* (Austin, [1989]), **comb. n.**, *P. palmerii australis* (Austin, [1989]), **comb. n.**, *P. hepburni hepburni* (Godman & Salvin, 1886), **comb. n.**, *P. hepburni remota* (Austin, 1991), **comb. n.**, *P. murphyi* (Austin, [1989]), **comb. n.**, *P. hypoglauca hypoglauca* (Godman & Salvin, 1878), **comb. n.**, *P. hypoglauca wellingi* (Ferris, 1985), **comb. n.**, *P. walkeri* (Godman & Salvin, 1886), **comb. n.**, *P. selvatica* (De la Maza & De la Maza, 2017), **comb. n.**). *Neoapodemia* Trujano-Ortega, **gen. n.** is distributed in the southwestern USA and northeastern Mexico, while *Plesioarida* Trujano-Ortega & García-Vázquez, **gen. n.** is present from the southern USA to Central America. Species of these genera were previously classified as *Apodemia* C. Felder & R. Felder but molecular and morphological evidence separate them as new taxa. Morphological diagnoses and descriptions are provided for both new genera, including the main distinctive characters from labial palpi, prothoracic legs, wing venation and genitalia, as well as life history traits. A molecular phylogeny of one mitochondrial gene (COI) and two nuclear

genes (EF-1a and wg) are also presented of most species of *Apodemia*, *Neoapodemia* Trujano-Ortega, **gen. n.**, *Plesioarida* Trujano-Ortega & García-Vázquez, **gen. n.**, and sequences of specimens from all tribes of Riodinidae. We compare the characters of *Apodemia*, *Neoapodemia* Trujano-Ortega, **gen. n.** and *Plesioarida* Trujano-Ortega & García-Vázquez, **gen. n.** and discuss the differences that support the description of these new taxa. This is a contribution to the taxonomy of the Riodinidae of North America of which the generic diversity is greater than previously recognized.

Keywords

Apodemia, molecular phylogeny, Papilionoidea, semiarid regions, taxonomy

Introduction

Butterflies of the family Riodinidae exhibit a great variation in wing shape, color, and pattern. They represent more than 8% of all butterflies and are found mainly in the New World, where they comprise approximately 133 genera and more than 1350 described species arranged in two subfamilies, Riodinae (1200 species) and Euselasiinae (176 species) (Espeland et al. 2015). This considerable diversity has caused some taxonomic confusion. While the position of the family Riodinidae in the phylogeny of Lepidoptera is well-resolved (Saunders 2010), the relationships between genera within the family are poorly understood (Kristensen 1976, de Jong et al. 1996, Ackery et al. 1999, Wahlberg et al. 2005). In recent years, this family has been subject to several studies attempting to clarify its internal relationships and taxonomy (Hall and Harvey 2002, Hall 2003, Sperling 2003, Campbell and Pierce 2003, Saunders 2010, Espeland et al. 2015).

Apodemia C. Felder & R. Felder, [1865] is a genus living in arid and semiarid regions of western North America ranging from southern Canada and the northeastern USA to Central America, with only one South American species in Brazil. DeVries (1997) noted that the genus is increasingly rare towards the southern end of its distribution. This genus currently contains 36 taxa with 16 described species and 26 subspecies, most of which belong to the *A. mormo* complex (DeVries 1997, Pelham 2008, Proshchek 2011, Warren et al. 2017). Thirteen (81%) of the 16 species of *Apodemia* are present in Mexico, of which seven species and four subspecies are endemic to the country (Callaghan and Lamas 2004, Llorente-Bousquets et al. 2013, De la Maza and De la Maza 2017a, b, Warren et al. 2017).

The original description of *Apodemia* is brief and refers to the antennal characters (Felder and Felder 1864–1867) and wing patterns. For this reason, following the original description, other authors defined additional characters to distinguish the genus (Godman and Salvin 1878–1901, DeVries 1997) and its type species *A. mormo mormo* C. Felder & R. Felder (Opler and Powell 1961). These characters include a less atrophied venation in the anterior wings, joint point of the trochanter and the coxa, the presence of two rows of spines in the tarsi, the large palpi and the sagittate signa in female genitalia. DeVries (1997) mentions that although this genus includes some butterflies similar to those of *Lasaia* H. Bates and *Emesis* [Fabricius], it can be distinguished by the leg configurations and the distinctive features of the veins.

Most of the taxonomic studies of *Apodemia* were published during the 20th century, and more than half of these are descriptions of subspecies (Emmel and Emmel 1998, Emmel et al. 1998). Recently, the genetic structure of some populations of *A. mormo* and its subspecies in the USA and Canada were studied (Proshek 2011, Proshek et al. 2013, 2015).

The first data on the phylogenetic relations between the species of *Apodemia* is presented based on molecular data. Also, two new genera are described that emerged from the phylogenetic analysis and are recognizable by their morphology.

Materials and methods

Taxon sampling

Eighty male specimens of 15 of the 16 species in the genus *Apodemia* and five *Emesis* species were examined. The material was collected in 2015–2017 in Mexico and gathered from Mexican as well as international scientific collections (Suppl. material 1). These specimens were selected in order to cover the phylogenetic diversity and the geographic distribution of the genus, with an emphasis on type localities. Specimens from *A. selvatica* De la Maza & De la Maza were not reviewed; however, its characteristics are discussed based on the original description (De la Maza and De la Maza, 2017b). Specimens examined came from the following scientific collections: Colección Nacional de Insectos del Instituto de Biología, México (CNIN-IBUNAM), Colección Lepidopterológica del Museo de Zoología de la Facultad de Ciencias, UNAM, Mexico (MZFC); Colección Lepidopterológica del Museo de Zoología de la FES Zaragoza, UNAM, Mexico (MZFZ); McGuire Center for Lepidoptera and Biodiversity, Florida Museum of Natural History, University of Florida, USA (MGCL) and Colección de Curtis Callaghan, Colombia (CJC).

Morphological procedures

The length of the right anterior wing from the base to the upper apex was measured. Labial palpi and legs were dissected using an Olympus SZX9 stereoscopic microscope, with a planar objective 1.5. The structures and wings were diaphanized by soaking them in alcohol and 5.25% NaClO solution (bleach). Then they were digitized and sketched using an Olympus DP12 camera attached to the microscope. Morphological terminology follows Comstock and Needham (1918), Harvey and Clench (1980), DeVries (1997), Penz and DeVries (1999, 2006) and Hall (1999, 2005). The following abbreviations were used: forewing (FW), hind wing (HW), dorsal (D), ventral (V). Male genitalia were extracted using an enzymatic digestion technique modified from Knölke et al. (2005). If needed, genitalia were soaked a few seconds in a hot potassium hydroxide solution (KOH 10%) to complete the cleaning. All structures were preserved in micro vials with glycerin solution and acetic acid at 4%. Terminology of

genitalia descriptions follows Klots (1956), Eliot (1973), Harvey (1987), Penz and DeVries (1999, 2006) and Hall (2008). Digital images of dorsal and ventral views of the genitalia were taken using focus stacking of light microscopy with a Leica Z16 APO-A stereoscopic microscope, a Leica DFC490 HD camera, and the Leica Application Suite program. Cornuti images were taken with a ZEISS microscope AXIO Zoom. V16, with an AxioCam MRc5 camera, and the Zeiss Efficient Navigation program. All images were taken at the Instituto de Biología-UNAM.

Molecular procedures

Twenty-six specimens of *Apodemia* including eleven of the 16 currently recognized species were collected. Species not included were *Apodemia chisosensis* H. Freeman, *A. virgulti* (Behr), *A. castanea* (Prittwitz), *A. planeca* De la Maza & De la Maza, and *A. selvatica*. Some species (*Apodemia chisosensis*, *A. castanea*, and *A. virgulti*) were excluded due to the lack of sequences from nuclear genes which are more informative in generic level. Two other species (*A. planeca* and *A. selvatica*) have been recently described (De la Maza and De la Maza 2017a, b) and we did not have fresh tissue suitable for DNA extraction (Suppl. material 2). To evaluate the monophyly of *Apodemia*, sequences from 31 other riordinid species were included, representing all tribes of the family according to the most recent phylogeny of Riordinidae (Espeland et al. 2015). With the exception of three sequences of *Emesis*, other sequences of outgroups were taken from GenBank (Suppl. material 2).

DNA was extracted from legs or abdomen using the DNeasy Blood & Tissue kit (Qiagen, Valencia, CA, USA). Partial sequences of 623 bp of the mitochondrial gene Cytochrome Oxidase I (COI) were obtained. Also, two nuclear loci, 495 bp of the gene Elongation factor 1 α (EF-1a), and 402 bp of wingless (wg) were sequenced. These loci were selected because it has been shown previously they are informative at different levels of divergence within riordinid butterflies (Campbell et al. 2000, Campbell and Pierce 2003, Espeland et al. 2015, Proshek et al. 2015). Primer sequences for COI were taken from Proshek et al. (2013), for EF-1a from Monteiro and Pierce (2001), and for wg from Brower and De Salle (1998). All gene regions were amplified via polymerase chain reaction (PCR) in a 25 μ L reaction volume containing 0.5–1.0 μ L deoxynucleoside triphosphates (dNTPs; 10 mM), 18–19.25 μ L double-distilled water, 0.2–0.5 μ L each primer (10 mM), 2.5 μ L 1X PCR buffer, 1.2 mM MgCl₂ (Fisherbrand, Pittsburgh, PA, USA), 0.15 μ L Taq DNA polymerase (Fisherbrand), and 1.0–1.5 μ L template DNA. For COI, DNA was denatured at 94 °C for 2 min, followed by 38–40 cycles of 94 °C for 30 s, 48–50 °C for 45 s, and 72 °C for 45 s. A final extension phase of 72 °C for 7 min terminated the protocol. For EF-1a and wg, DNA was processed according to a touchdown protocol suggest by Espeland et al. (2015) with an initial denaturation for 3 min at 94 °C, 20 cycles of 94 °C for 50 s, annealing temperature starting at 49 °C and ramping down 0.5° for every cycle for 40 s, 72 °C for 1 min, another 20 cycles of 94 °C for 50 s, annealing temperature (48–52 °C) for

40 s, and 72 °C for 1 min, and a final extension of 72 °C for 5 min. Double-stranded PCR products were checked by electrophoresis on a 1% agarose gel. PCR products were purified with polyethylene glycol precipitation (Lis 1980). DNA templates were sequenced in both directions with the Big Dye Terminator version 3.1 cycle sequencing kit (Applied Biosystems, Inc.) and an ABI 3100 automated DNA sequencer (Applied Biosystems, Inc.) using the amplification primers. Sequences were assembled and edited in the STADEN PACKAGE version 1.6.0 (Whitwham and Bonfield 2005).

Phylogenetic inferences

Sequences were aligned using the MUSCLE algorithm (Edgar 2004) included in the software MEGA version 7 (Kumar et al. 2016). Sequences were uploaded to GenBank and accession numbers are listed in Suppl. material 2. Prior to the concatenated analysis, independent ML analyses were conducted for each gene. The phylogeny of the concatenated data set ($n = 56$ individuals, including outgroups) was inferred using Bayesian inference and maximum likelihood (ML) phylogenetic methods. For both methods, partitioned analyses were used to improve phylogenetic accuracy. The best-fitting substitution models and partitioning schemes were selected simultaneously using the Bayesian Information Criterion in the software PARTITIONFINDER version 1.1.1 (Lanfear et al. 2012). Bayesian inference analyses were conducted using MRBAYES version 3.2.1 (Ronquist et al. 2012). Four runs were conducted using the 'nruns = 4' command, each with three heated and one cold Markov chains with sampling every 1000 generations for 50 million generations. Output parameters were visualized using TRACER version 1.4 (Rambaut and Drummond 2007) to identify stationarity and convergence. Convergence between runs was assessed using AWTY (Nylander et al. 2008). After discarding the first 12.5 million generations (25%) as burn-in, parameter values of the samples were summarized from the posterior distribution on the maximum clade credibility tree using TREEANNOTATOR version 1.4.8 (Drummond and Rambaut 2007) with the posterior probability limit set to 0.1 and mean node heights summarized. Maximum likelihood analyses were conducted using RAxML version 7.2.6 (Stamatakis 2006) under the GTRCAT model, with 1000 nonparametric bootstrap replicates to assess nodal support. Nodes were considered strongly supported if their Bayesian posterior probability was ≥ 0.95 and their bootstrap value was $\geq 80\%$ (Huelsenbeck and Rannala 2004).

Genetic distances

Finally, to obtain an estimate of genetic distances, pairwise genetic distances for COI were computed between and within the major clades obtained in the phylogenetic analysis (see results). The corrected pairwise genetic distances were calculated using the K2P model with MEGA version 7 (Kimura 1980, Kumar et al. 2016).

Results

Phylogenetic inferences

The results showed some incongruence between loci, but the major differences were between poorly-supported clades (Suppl. material 3–5). The final concatenated data set consisted of 1520 aligned nucleotide positions. The partitions and models that best fit the data were GTR+G (COI second positions, wg first and second positions, EF-1a third positions), and GTR+I+G (COI first and third positions, wg third positions, and EF-1a first and second positions). ML and Bayesian inference analyses resulted in highly congruent phylogenetic trees. The recovered relationships between the genera of Riodinidae were in agreement with recently published phylogenies (e.g., Espeland et al. 2015), thus providing a solid platform for the evaluation of the monophyly of *Apodemia*.

In the phylogenetic analyses, four clades can be distinguished (Fig. 1). The monophyly of *Apodemia* was not supported, as *Apodemia phyciodoides* W. Barnes & Benjamin was more related to *Emesis* than to other *Apodemia*. The rest of the species of *Apodemia* were included into three strongly supported clades. The first clade (*Apodemia* clade), included the North American taxa of the *A. mormo* complex: *A. mormo* and *A. mejicanus* (Behr), also *A. duryi* (W. H. Edwards) and *A. multiplaga* Schaus. The second clade included *A. nais*; and the third clade (Mexico clade) was composed by the *Apodemia* taxa distributed mostly in Mexico and Central America: *A. hepburni* Godman & Salvin, *A. hypoglaucia* Godman & Salvin, *A. murphyi* Austin, *A. palmerii* W. H. Edwards and *A. walkeri* Godman & Salvin.

The relationships between the four major clades were as follows: the *Apodemia* clade was the sister group of *A. nais*, and this clade *Apodemia* + *A. nais* was the sister group of the clade *Emesis* + *A. phyciodoides* (*Emesis* clade). These relationships were strongly supported in the Bayesian analysis, but less supported in the ML analysis. The Mexico clade was the sister group of the rest of the species of *Apodemia* and *Emesis*.

Genetic distances within major clades ranged from 0.9% in *A. nais* to 9.8% in *Emesis* + *A. phyciodoides*, whereas distances between genera ranged from 7.4% in Mexico clade versus *A. nais* to 10.5% in the *Apodemia* clade versus *Emesis* clade. The genetic distance between *Apodemia* clade and Mexico clade was 8.7% (Table 1).

Descriptions of new genera

Diagnosis of *Plesioarida* Trujano-Ortega & García-Vázquez gen. n. and *Neoapodemia* Trujano-Ortega gen. n. are presented, comparing both with *Apodemia* (Table 2). The morphology of both genera is described, including photographs and illustrations of the structures; distribution maps of these new genera are also given. The extent of genetic divergence between them and the phylogenetic position within the Riodinidae are discussed. The morphologic examination of the specimens revealed that the genital structures of the species *A. phyciodoides*, *A. planeca*, and *A. castanea* are distinct from

Table 1. Corrected pairwise genetics distances calculated with K2P model. Among (below diagonal) and within (diagonal) all major clades obtain in the phylogenetic analysis (see results) using only COI gene.

	<i>Apodemia</i> clade	Mexico clade	<i>A. nais</i>	<i>Emesis</i> clade
<i>Apodemia</i> clade	0.055			
Mexico clade	0.087	0.050		
<i>Apodemia nais</i>	0.081	0.074	0.010	
<i>Emesis</i> clade	0.104	0.095	0.093	0.100

Table 2. Comparison of selected morphological characters for the *Apodemia*, *Plesioarida*, and *Neoapodemia*.

Character	<i>Apodemia</i>	<i>Neoapodemia</i> gen. n.	<i>Plesioarida</i> gen. n.
Labial palpus			
Length of the first segment	Longer than the third segment	As long or longer than the third segment	As long or longer than the third segment
Length of the second segment	More than 2.5 the length of the first segment	Twice the length of the first segment	From 2 to 2.5 the length of the first segment
Anterior wing			
Vein Sc+R1 originates	in the second third of the discal cell [†]	in the last third of the discal cell	in the last third of the discal cell
Prothoracic legs			
Trochanter-coxa joint	Beyond half of the coxa	Beyond half of the coxa	At the middle of the coxa
Number of tarsomeres	Three tarsomeres	Three tarsomeres	Two tarsomeres [‡]
Shape of the last tarsomere	Conic	Wide at the base, elongated and tapering toward the apex, with blunt end	Wide at the middle, oval-shaped, elongated, pointy at the end
Femur + trochanter length	Less than 3/4 the length of the tibia	More than 3/4 the length of the tibia	Less than 3/4 the length of the tibia
Tibia	Wider than the tarsus	Wider than the tarsus	As wide as the tarsus
Male genitalia (lateral view)			
Posterior margin of the uncus	Blunt	Blunt with a middle groove	Rounded
Tegumen	Wide	Wide	Narrow
Tegumen margins	Dorsal margin longer than anterior margin	Dorsal margin longer than anterior margin	Dorsal margin shorter than anterior margin
Posterior projection of the mid region of the vinculum hump-shaped	Evident, sclerotized	Evident, sclerotized	Less evident, slightly sclerotized
Length of the dorsal process of the valve	As long or shorter than the posterior margin of the uncus [§]	Shorter than the posterior margin of the uncus	Beyond the posterior margin of the uncus
Cornuti	Simple plate, long, strongly sclerotized	Multiple long spines, wide and sclerotized, jointed at the base (crest like), and flatten laterally	Multiple long spines, wide and sclerotized, in separated bulbs
Host plant			
	<i>Eriogonum</i> spp. (Polygonaceae) and <i>Krameria glandulosa</i> (Krameriaceae)	<i>Ceanothus fendleri</i> (Rhamnaceae)	<i>Prosopis</i> spp. and <i>Acacia</i> spp. (Fabaceae)
Habitat			
	Xerophile shrubland and Deciduous tropical forest	Coniferous forest	Xerophile shrubland, Deciduous tropical forest, and Evergreen tropical forest

[†] Except in *A. multiplaga*; [‡] Except in *P. h. hypoglaucia*; [§] Except in *A. multiplaga*.

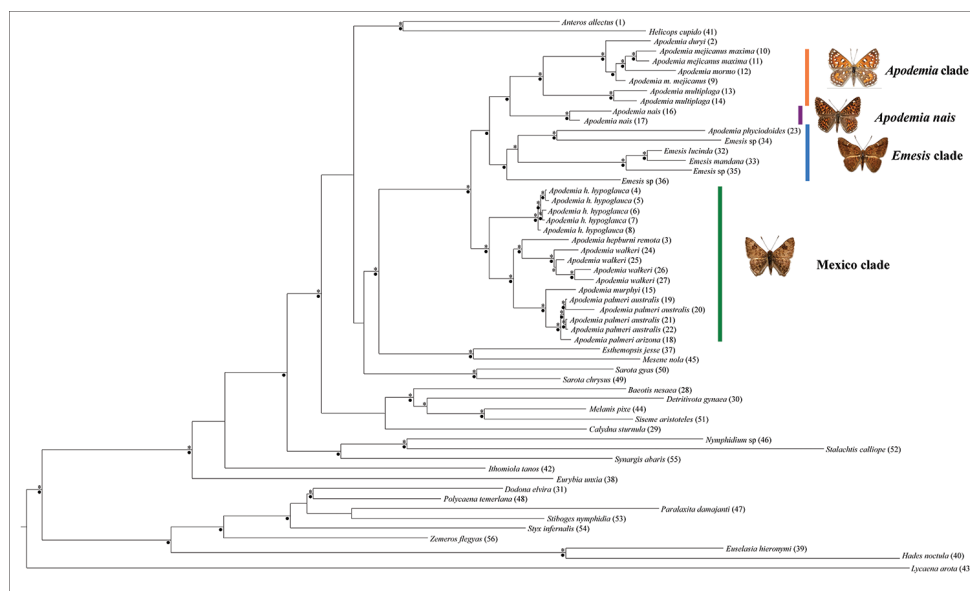


Figure 1. Phylogenetic relationships based on partial sequences of the mtDNA (COI), and nuclear genes (EF-1a, wg). Bayesian posterior probabilities and bootstrap values of major nodes are indicated with black dots for well-supported nodes. Vertical lines correspond to the major clades found in this study.

the other species of *Apodemia*; suggesting these are not congeneric with the *Apodemia* species of Central and North America. The inclusion of these three species in *Apodemia* is being evaluated (Seraphim et al. submitted, Trujano-Ortega unpublished data); therefore, the morphology of *Apodemia* reported here excludes these species.

Plesioarida Trujano-Ortega & García-Vázquez, gen. n.

<http://zoobank.org/627AB6DD-9174-4175-A5AB-B6B34E586540>

Figs 2–6

Type species. *Apodemia walkeri* Godman & Salvin, 1886 by present designation.

Diagnosis. The species of this new genus can be distinguished from other Riodinidae by a combination of characters (Table 2). Labial palpi are long, slender, pointed apically and projected forward and upward, the second segment is a little more than twice the length of the third segment, the third segment is barely visible from dorsal view (Fig. 2). Radial veins originate near the end of the discal cell, costal vein runs parallel to Sc+R1; these veins get close but never fuse together. Vein R4 reaches wing margin at the apex (Fig. 3). Prothoracic legs of males are slender and trochanter inserts at the middle of the coxa; tibia is as wide as *tarsus* and smaller than the length of the femur plus the trochanter. Most of the species present two tarsomeres, the second tarsomere is oval-shaped and the apex pointed, except *P. hypoglaucia* comb. n. which has three tarsomeres with the last one oval-shaped (Fig. 4). Tegumen of male genitalia is typically oval-shaped, narrow

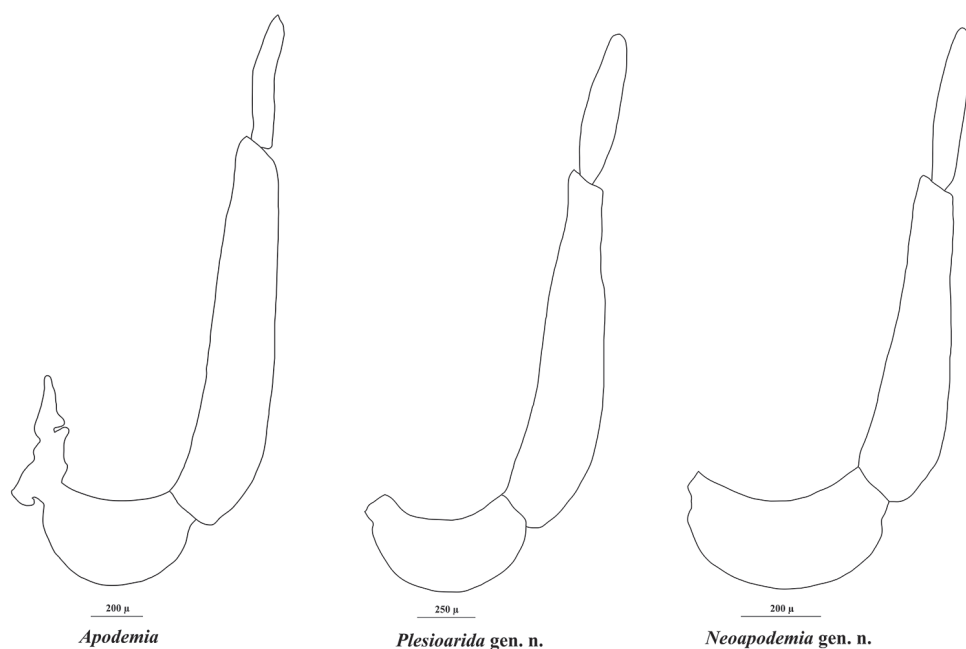


Figure 2. Left male palpus of *Apodemia*, *Plesioarida*, and *Neoapodemia*.

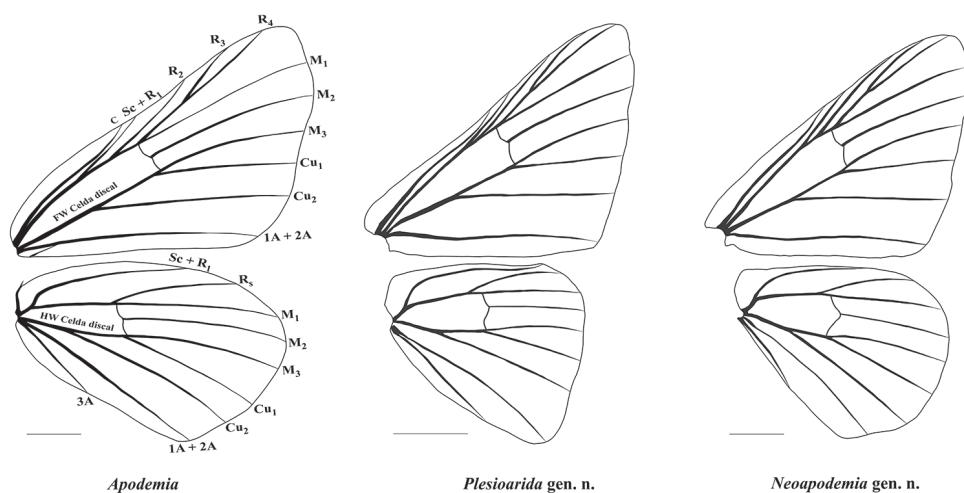


Figure 3. Wing venation of *Apodemia*, *Plesioarida*, and *Neoapodemia*. Upper, forewing; lower, hind wing. Vein abbreviations (black lettering): **Sc** subcostal, **R** radial, **M** median, **Cu** cubital, **A** anal. Scale bars: 3 mm.

and slightly sclerotized, posterior half is a hyaline area that Hall (1999) named ‘windows’ through which the subscaphum can be observed; the uncus is rounded and with setae in the posterior margin. The vinculum is a narrow band not covering the whole margin of the tegumen, is mostly straight and convex toward the saccus, a little hump-shaped in the mid region. Valvae are bifurcated, the dorsal process is conical, elongated, and with a sharp

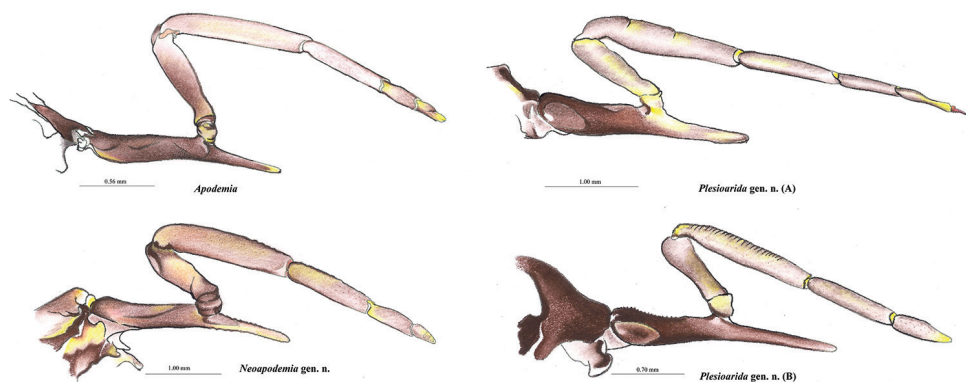


Figure 4. Prothoracic legs of males of *Apodemia*, *Plesioarida*, and *Neoapodemia*.

end projected forward and exceeding the posterior margin of the uncus, the ventral process is shorter and blunt with many setae. Aedeagus is long and sigmoid, wider in the anterior edge, slender and pointed on the posterior edge, where it opens dorsally. Cornuti are a series of wide, strongly sclerotized spines that originate from individual bulbs (Fig. 5).

Description. Male. Anterior wing length: 10–15 mm. *Head.* Ringed antennae with 30 to 32 flagellomeres of the same width, with white scales at the base of each flagellomere. Widen abruptly in the apical 10 flagellomeres to form the antennal club, which is dark and iridescent dorsally. Sometimes white or brown scales are present at the sides, ending in a whitish or yellowish tip, with a nudum from flagellomere 20 to the apex. Labial palpi white with black or brown scales mainly in the third segment. *Wings* (Figs 3, 6) with four radial veins. Three distinct shapes of anterior wings, rounded toward the apex (*P. palmerii* comb. n.), elongated and triangular (*P. walkeri* comb. n.) and triangular with the external margin curved and the apex slightly sickle-like (*P. hypoglauca* comb. n.). Background color in both wings varies from brown to dark gray. Some species present a series of white spots outlined with black in the anterior margins and a series of submarginal black dots, sometimes with white scales and occasionally with reddish scales toward the base of the anterior and posterior wings. In grayish species spots are black. *Legs.* Prothoracic legs with dense long scales generally whitish, mid and hind legs with multiple short and dense spines in the interior margin of the tibia and *tarsus*. *Abdomen.* Dark in the dorsum with reddish or whitish scales outlining each segment. Ventrally with dense scales varying from whitish as in *P. hypoglauca* comb. n. to brown-orange as in *P. palmerii* comb. n. *Genitalia.* Genital capsule small, uncus rounded with a groove of variable depth which gives it a lobulated or straight appearance. Tegumen oval-shaped and sclerotized in the anterior region; with large ‘windows’ that reach the gnathi. Gnathi are slender, sclerotized, slightly twisted ending in an upward hook. Vinculum generally is straight or slightly curved near the tegumen, a little wider near the valve, this swelling is weakly sclerotized and hard to notice, curved before the saccus and anteriorly projected. Dorsal processes of the valve conic and membranous toward the transtilla but strongly sclerotized toward the apex, which is a small upward hook, with setae lengthwise. The

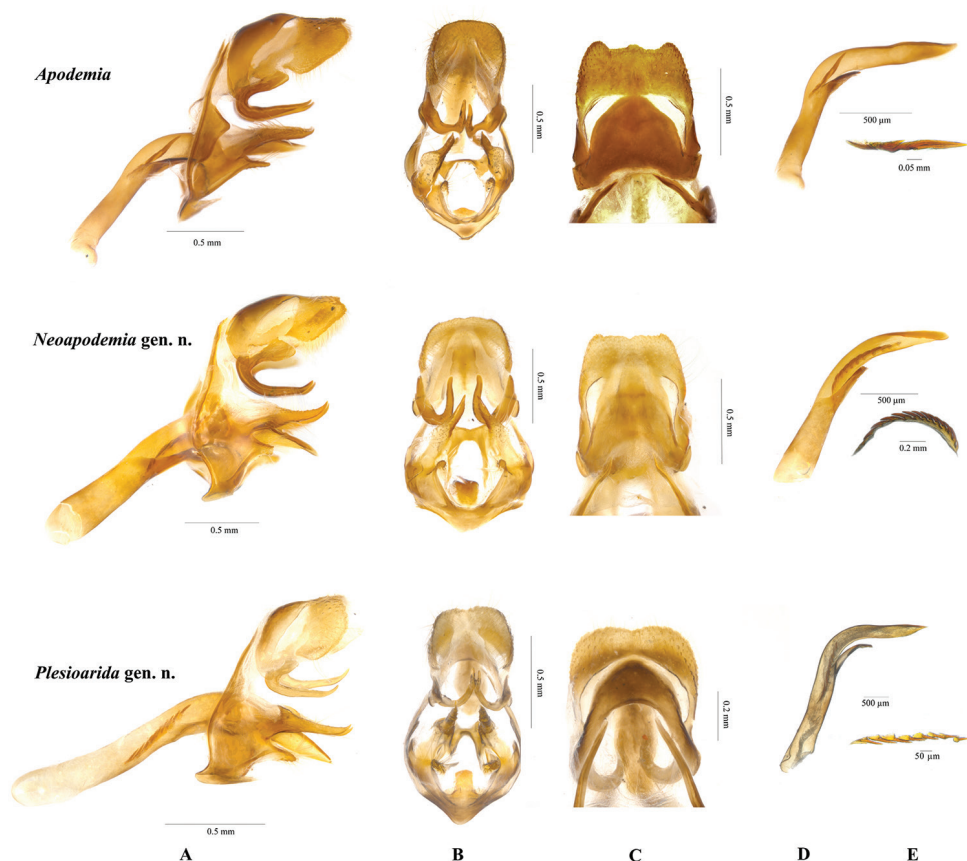


Figure 5. Male genitalia of *Apodemia*, *Plesioarida*, and *Neoapodemia*. **A** lateral view **B** ventral view **C** dorsal view **D** aedeagus **E** cornuti.

ventral process is long and blunt, of variable lengths but always with multiple mostly long setae. Aedeagus is slender toward the distal portion with a pointed tip, widening toward the anterior portion, straight or sinuous. Cornuti are thick sclerotized spines apparently each surging from independent bulbs forming a line.

Etymology. The name comes from the Greek *plesios* meaning near or close to and the Latin *aridus* meaning dry, in reference to the desert and semiarid habitats of most of the species.

Distribution and habitat. This genus is distributed below 1750 m in the Pacific slope from central Arizona and in the Atlantic slope from the south of Texas to the dry forests of Guanacaste in the northeast of Costa Rica (DeVries 1997) (Fig. 7). In the USA, it has been collected in arid regions, in xerophilic shrubland of Arizona, California, and New Mexico, with isolated records in the south of Texas in Río Grande Valley (Warren et al. 2017). In Mexico it can be found in deserts and semiarid regions of Baja California Sur and part of Baja California Norte in the Chihuahuan Desert and in the Mexican Plateau, regions where xerophilic shrubland is dominant. It is also

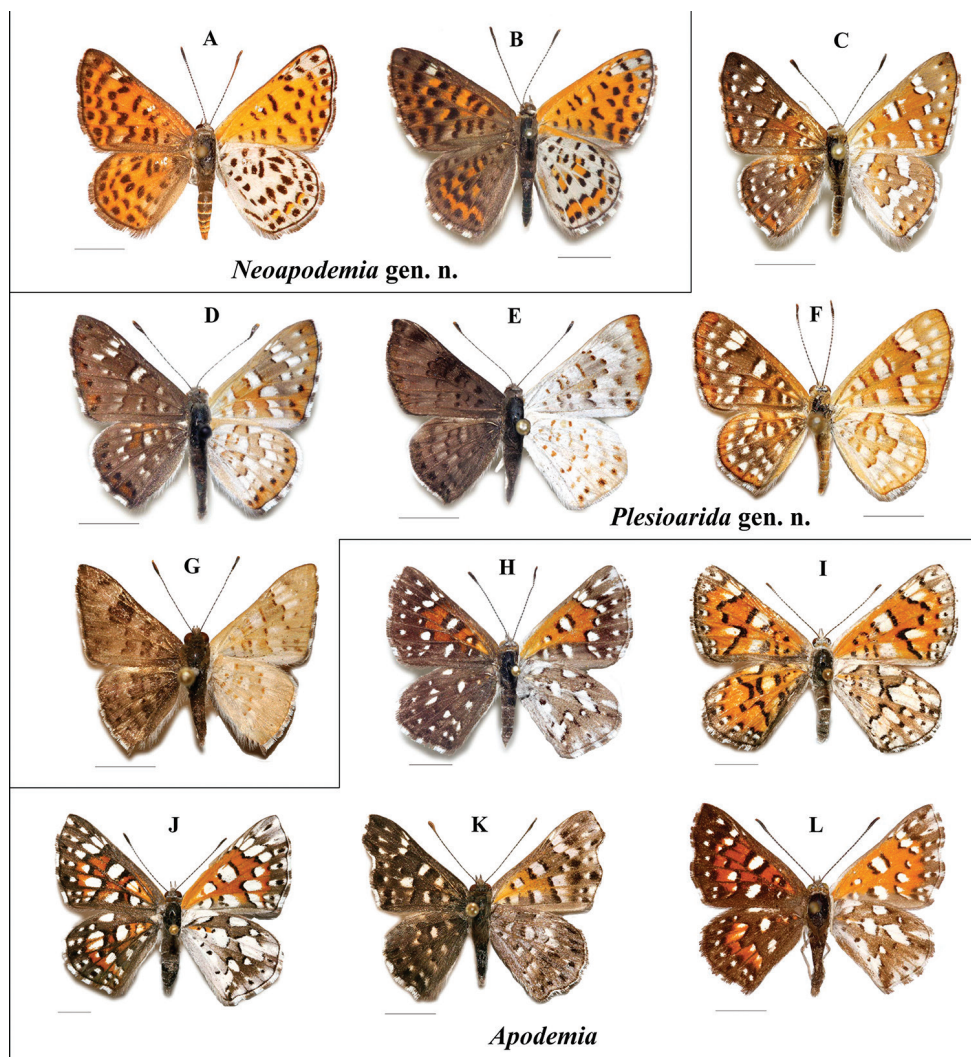


Figure 6. Wing color patterns of *Apodemia*, *Plesioarida* and *Neoapodemia* **A** *Neoapodemia chisosensis* comb. n. **B** *Neoapodemia nais* comb. n. **C** *Plesioarida murphyi* comb. n. **D** *Plesioarida h. hepburni* comb. n. **E** *Plesioarida h. hypoglaucia* comb. n. **F** *Plesioarida p. palmerii* comb. n. **G** *Plesioarida walkeri* comb. n. **H** *Apodemia m. mormo* **I** *Apodemia duryi* **J** *Apodemia mejicanus* **K** *Apodemia multiplaga* **L** *Apodemia virgulti*. Scale bars: 5 mm. Additional data of the specimens in the photos are shown in Suppl. material 6.

distributed in the deciduous tropical forest of the west of Mexico in the Pacific coast and the Balsas Basin, as well as in the east in the coastal plain of the Gulf of Mexico and the Yucatan Peninsula. Its distribution in deciduous tropical forests extends through Central America to Costa Rica. Finally, *P. selvatica* comb. n. and some populations of *P. walkeri* comb. n. inhabit the tropical forests in the south of Mexico in Veracruz and Chiapas. De la Maza and De la Maza (2017b) mention that *P. selvatica* comb. n. probably is present in Guatemala and Belize.

Natural history. Larvae of the species of *Plesioarida* Trujano-Ortega & García-Vázquez gen. n. are associated with the family Fabaceae, particularly with species of the genera *Prosopis* spp. and *Acacia* spp. (Ferris 1985, Austin 1988, DeVries 1997).

A proposed classification of *Plesioarida* gen. n.

Plesioarida Trujano-Ortega & García-Vázquez, gen. n. Type species: *Apodemia walkeri* Godman & Salvin, [1886], Biol. Centr. Amer., Lepid. Rhop. 1(45): 468, no. 6, by present designation.

hepburni comb. n. (*Apodemia*).

Apodemia hepburni Godman & Salvin, 1886. Type Locality: "Mexico, Pinos Altos in Chihuahua".

h. hepburni Godman & Salvin, 1886, comb. n. (*Apodemia*).

h. remota Austin, 1991, comb. n. (*Apodemia*). Type Locality: "México: Baja California Sur; Arroyo San Bartolo".

hypoglauca comb. n. (*Apodemia*).

Lemonias hypoglauca Godman & Salvin, 1878. Type Locality: "Mexico".

h. hypoglauca Godman & Salvin, 1878, comb. n. (*Apodemia*).

h. wellingi Ferris, 1985, comb. n. (*Apodemia*). Type Locality: "México: Yucatán; Pisté".

murphyi comb. n. (*Apodemia*).

Apodemia murphyi Austin, [1989]. Type Locality: "México: Baja California Sur; Arroyo San Bartolo".

palmerii comb. n. (*Apodemia*).

Lemonias palmerii Edwards, 1870. Type Locality: "Utah"

p. palmerii W. H. Edwards, 1870

= *p. marginalis* Skinner, 1920

p. arizona Austin, [1989], comb. n. (*Apodemia*). Type Locality: "Arizona: Cochise County, Arizona State Route 90, 10.8 miles north of Arizona State Route 82"

p. australis Austin, [1989], comb. n. (*Apodemia*). Type Locality: "México: Durango: 1 mi. S Nombre de Dios".

selvatica comb. n. (*Apodemia*).

Apodemia selvatica De la Maza & De la Maza, 2017. Type Locality: "Estación Chajul" [México, Chiapas].

walkeri comb. n. (*Apodemia*).

Apodemia walkeri Godman & Salvin, 1886. Type Locality: "Mexico, Acapulco" [Guerrero]

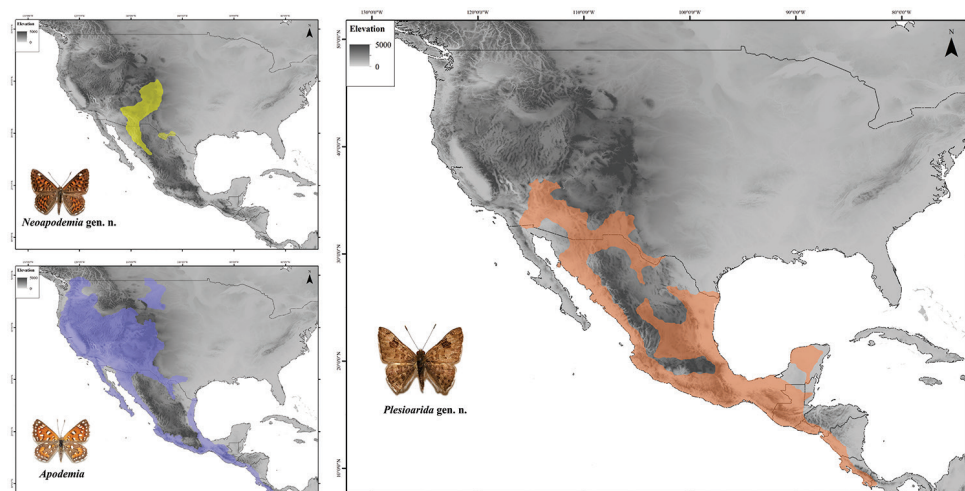


Figure 7. Known distribution of *Apodemia*, *Plesioarida*, and *Neoapodemia*. Black lines represent countries' limits.

***Neoapodemia* Trujano-Ortega, gen. n.**

<http://zoobank.org/749DBAD0-54D3-4AA0-8095-704228745AD0>

Figs 2–6

Type species. *Chrysophanus nais* Edwards, 1876 by present designation.

The original generic name for *Apodemia nais*, *Chrysophanus* Hübner, 1818, is unavailable, having been suppressed by the ICZN. In 1886, Godman and Salvin proposed the generic name *Polystigma*, with *Chrysophanus nais* W.H. Edwards as its type species. However, *Polystigma* Godman & Salvin, 1886 is invalid, being a junior homonym of *Polystigma* Kraatz, 1880 (Coleoptera). Therefore, we propose the name *Neoapodemia* for this taxon.

Diagnosis. This genus contains two species that can be distinguished from other Riodinidae by the presence of the labial palpi that are medium sized, slender, sharp apically and projected upward and forward; the second segment is twice the length of the third segment; third segment and apical third of the second segment are visible from dorsal view (Fig. 2, Table 2). Radial veins originate near the end of the discal cell, costal vein parallel to Sc+R1 separated by at least twice the width of R1 in the closest portion. Vein R4 reaches the margin in the wing apex (Fig. 3). Prothoracic legs of male are slender, trochanter joint beyond the middle of the coxa, tibiae are slightly wider than the tarsi and the length of the femur + trochanter is nearly the same as tibia length. Tarsus with three tarsomeres, the third tarsomere is small, wide at the base tapering toward the apex but with a blunt end (Fig. 4). Male genitalia with tegumen typically oval-shaped, wide, strongly sclerotized in the dorsal region, posterior half hyaline; the uncus is rectangular with a groove in the distal margin, with setae. Gnathi are wide, curved and ending in a sharp tip projected dorsally. Vinculum is a wide sclerotized band not covering the whole margin of the tegumen, generally straight and convex toward the

saccus, with an evident swallowing in the mid region. Valvae bifurcated, dorsal process conical of variable width and setae all along, ending in a sharp tip projected dorsally, this process is shorter than the posterior edge of the uncus; the ventral process is short and with a rounded tip, projected anteroventrally, also with setae. Cornuti are a series of long, flatten laterally, strongly sclerotized spines, joined at the base in a crest-like shape (Fig. 5).

Description. Male. Anterior wing length: 15–18 mm. *Head.* Ringed antennae with 40 flagellomeres with white scales at the base of each flagellomere. Widen in the apical 18–22 flagellomeres, where a nudum is present and it extends to the apex ending in a whitish or yellowish tip. The antennal club is formed by the apical 10–12 flagellomeres, black dorsally and sometimes with a line of white scales. Labial palpi white with black or brown scales in the third segment.

Wings (Figs 3, 6). Triangular with four radial veins. In dorsal view, background color varies in both wings from brown to copper-orange, margins are darker and costal and external margins are outlined with black. External margin with a line of seven rounded dots and a line of rectangular spots in the submarginal area which cross the wing from the costal to the anal margin in both wings. Three subapical white spots, the first two are just short lines and the third is squared and large, situated in the R4 cell. After the spots is an irregular band of black spots in the postmedian area going into the median area. Discal cell with four black bands, with the most external one larger and wider than the remainder. Under the discal cell are three other bands in the postbasal and submedian areas. White and black fringe present in diverse patterns. Particularly, *N. nais* comb. n. presents copper-orange scales in the discal cell and between the lines of black spots on both wings. Ventrally, anterior wing is orange, lighter and brighter than dorsal view, with the same pattern of black spot as in dorsal side, white spot of R4 cell extends till the apex; the black dots forming the marginal line are surrounded by white scales, as the dots approach the tornus the white scales are present only in the posterior margin. The posterior wing is white at the base and with essentially the same pattern of black spots as in dorsal view, however the base of *N. nais* comb. n. is white-greyish and the white scales over the veins provide a less uniform pattern to the wing than in *N. chisosensis* comb. n. This species presents three orange spots in the posterior margin of the line of submarginal spots, while in *N. nais* comb. n. the orange area is between the line of black submarginal and marginal spots, getting wider as it approaches the tornus. This species also presents an orange area along the costal margin just before the apex and another one in the anterior margin of the irregular band of black spots in the median area.

Legs. Prothoracic legs have dense and long scales generally white or whitish; mid and hind tibiae and tarsi with a series of multiple short and dense white, whitish or yellowish spines in the inner margin.

Abdomen. Dorsum of abdomen dark of brown with orange and whitish scales outlining each segment. Ventrally, the abdomen is bright white in *N. chisosensis* comb. n. and whitish in *N. nais* comb. n.

Genitalia. Generally strongly sclerotized, genital capsule medium sized. The margin of the uncus in dorsal view presents great variation, it can be rounded or straight with

a groove of variable depth. Dorsal processes of the valve are conic and membranous toward the transtilla but narrower in *N. nais* comb. n. than in *N. chisosensis* comb. n.; the ventral process is also narrower and longer in *N. nais* comb. n. Aedeagus of *N. nais* comb. n. is wide, short and sclerotized, of uniform width all along, with a more sclerotized plate in the dorsum and ending in a sharp tip in the posterior edge where it opens dorsally. In *N. chisosensis* comb. n. aedeagus is narrower, longer and less curved, it slightly widens in the anterior edge and makes narrow toward the posterior edge, with a more sclerotized dorsal plate ending in a blunt tip. Cornuti are a series of long, flattened laterally, strongly sclerotized spines, joined at the base in a crest-like shape (Fig. 5E).

Etymology. The name is a combination of the Greek prefix *neo*, meaning new, and *Apodemia*, in reference to the genus from which it separates.

Distribution and habitat. This genus has a disjunct distribution. *Neoapodemia nais* comb. n. is distributed in montane areas with medium to high elevations (1600–2300 m), mostly in the southern and southwestern Rocky Mountains in the USA. In USA inhabits chaparral and open areas of coniferous forests in northern and central Colorado, southeastern New Mexico, and central and southeastern of Arizona where its presence appears to be sporadic (Scott 1986, Brock and Kaufman 2006). In Mexico it can be found in the Sierra Madre Occidental in the states of Sonora, Chihuahua, and Durango (Warren et al. 2017). On the other hand, the distribution of *N. chisosensis* comb. n. is restricted to western Texas in the Chisos Mountains in Big Bend National Park, where it inhabits the chaparral of submontane shrubland.

Natural history. Larvae of *Neoapodemia* Trujano-Ortega, gen. n. can be found feeding on plants of the Rosaceae family, *Prunus havardii* (W. Wight) S.C. Mason, and the Rhamnaceae, *Ceanothus fendleri* A. Gray (Scott 1986, Brock and Kaufman 2006, Warren et al. 2017).

A proposed classification of *Neoapodemia* gen. n.

Neoapodemia Trujano-Ortega, gen. n. Type species: *Chrysophanus nais* W. H. Edwards, 1876, Trans. Am. Entomol. Soc. 5(3/4): 291–292, by present designation.

= *Polystigma* Godman & Salvin, [1886]. Biol. Centr. Amer., Lepid. Rhop. 1(45): 469. Type-species: *Chrysophanus nais* W. H. Edwards, 1876, Trans. Am. Entomol. Soc. 5(3/4): 291–292, by monotypy. Preoccupied by *Polystigma* Kraatz, 1880, Dtsche. Entomol. Z. 24(2): 191.

nais comb. n. (*Apodemia*).

Chrysophanus nais W. H. Edwards, 1876. Type Locality: “Southern California... Prescott, Arizona”.

chisosensis comb. n. (*Apodemia*).

Apodemia chisosensis Freeman, 1964. Type Locality: “Chisos Mountains, elevation 5400 ft., Texas”

Taxonomic remarks

The phylogenetic analysis based on molecular data shows three well-supported clades which are also distinguished by their morphology. The clade *Neoapodemia* is more related to the clade of *Apodemia* (*sensu stricto* excluding *A. castanea* and *A. phyciodoides*) than with *Plesioarida*. Besides the phylogenetic position, the proposed genera can be easily distinguished morphologically as well as with *Apodemia* and *Emesis*. Labial palpi of *Apodemia*, *Plesioarida* and *Neoapodemia* are slender, long and projected upward and forward, while *Emesis* present small labial palpi, close to the head and directed upward. The second segment of labial palpi in *Neoapodemia* is smaller in proportion with the third segment and only one third is visible in dorsal view, in contrast with *Apodemia* in which the second segment is long and half or more of it is visible in dorsal view. *Plesioarida* differs from both genera having only part of the third segment visible in dorsal view. Regarding wing veins patterns, radial veins of *Neoapodemia* and *Plesioarida* originate near the end of the discal cell, whereas in *Apodemia* these veins originate at the middle of the discal cell. Veins C and Sc+R1 are closer in *Plesioarida* and *Apodemia* than in *Neoapodemia*, which present a clear separation between these veins. The number and shape of the tarsomeres of prothoracic legs are useful characters for separating the genera. *Emesis* has only one tarsomere, *Plesioarida* has two (except *P. hypoglaucia* comb. n. which has three) and an oval-shaped tip, *Neoapodemia* and *Apodemia* presents three tarsomeres; the last tarsomere in *Apodemia* is conical, while *Neoapodemia* the last tarsomere is smaller than in *Plesioarida*, wide at the base, tapering toward the apex and ending in a blunt tip.

Apodemia and *Neoapodemia* present large genital capsules, more similar than with those of *Plesioarida*. However, *Neoapodemia* gnathi are slightly twisted and the posterior tip is hooked and strongly projected upward; while gnathi of *Apodemia* are straight. The genital capsule of *Plesioarida* is smaller and rounded, with tegumen with a marked hyaline area; gnathi are slim and twisted. Vinculum is straight in *Apodemia*; convex in *Neoapodemia*, which makes it appear larger; and straight near tegumen and convex toward the saccus in *Plesioarida*. Dorsal processes of *Plesioarida* differ from the other two genera because are long and exceed the posterior margin of the uncus. The ventral processes of the valves of *Neoapodemia* are shorter than those of *Apodemia* and *Plesioarida*, which are also slender. Aedeagus bends in a smooth angle in *Neoapodemia*, but in a marked angle in *Plesioarida*, in both genera this bending appears near the posterior tip of the aedeagus. In *Apodemia* the bending angle is marked (approximately 45°), nearly at half of aedeagus or closer to the anterior tip. The cornuti are one of the most important differences. The cornuti of *Apodemia* are simple, long, and sclerotized; *Plesioarida* presents a series of aligned spines that surge from individual bulbs; finally, *Neoapodemia* has long, strong, sclerotized spines, flattened laterally and joined at the base, forming a crest. *Emesis* genitalia are diverse and the cornuti are simple when present.

The phylogenetic analysis with molecular data suggests that *A. phyciodoides* is part of *Emesis*. However, we took a conservative approach and decided that *A. phyciodoides* should remain in *Apodemia* until morphology was reviewed. Considering that *Emesis*

need a taxonomical review and that the *Emesis* + *A. phyciodoides* clade was well supported only by Bayesian but not ML method.

Natural history characters also help to distinguish between these groups. For example, it is noteworthy that each genus has distinct host plants (Ferris 1985, Scott 1986, Austin 1988, DeVries 1997, Brock and Kaufman 2006, Warren et al. 2017), which is evidence of differences in their life histories. Although none of these genera is exclusive of an environment, some of their species are characteristic of specific habitats. For example, *Apodemia* inhabits desert areas and shrubland environments (although *A. multiplaga* is from deciduous tropical forests). *Neoapodemia* is recorded from coniferous forest, chaparral, and submontane shrublands. *Plesioarida* inhabits desert areas and deciduous tropical forests.

Conclusions

Our results show that *Apodemia* is paraphyletic with respect to *Emesis*; furthermore, the morphological evidence and the preliminary molecular analysis (Trujano-Ortega unpublished data) suggest polyphyly. This is because, historically, diverse unrelated lineages have been placed within *Apodemia* and reassigned posteriorly. Harvey and Clench (1980) created the genus *Dianesia* for *Apodemia carteri* and suggested that *A. castanea* is not congeneric with North and Central American *Apodemia*. More recently, Penz and DeVries (2006) reassigned *Apodemia paucipuncta* to the recently described genus *Hallonympha*.

In a previous analysis of the phylogenetic relations of Riodinidae at the tribe or subfamily level, *Apodemia* and *Emesis* appear always closely related based on morphological evidence (Stichel 1910–1911, Harvey 1987) and molecular evidence (Saunders 2010, Espeland et al. 2015, Proshchek et al. 2015). These two genera were grouped in the same tribe Emesini of Stichel (1910–1911). However, the taxonomic scale of these studies and the lack of recent material in scientific collections limited the resolution of lower taxonomic scale and the inclusion of Mexican and Central American species. That is why the two genera proposed here remained unnoticed. The morphological characters shared by *Apodemia*, *Emesis*, *Neoapodemia*, and *Plesioarida* are evident, as suggested by Harvey (1987), who analyzed the immature stages (pupae). These genera are more related to each other than with the genera of any other tribe of Riodinidae. Therefore, these two new genera should be included in a new tribe as mentioned by Espeland et al. (2015) for several *Incertae sedis* groups, like *Emesis-Apodemia*. The biogeographic patterns of these new genera are an interesting topic for further study. Espeland et al. (2015) proposed two independent dispersal events for these genera, from the Neotropical to the Nearctic region. One event of the ancestor of *Apodemia* mainly to the southwestern USA and the other event of the ancestor of *Calephelis*, to the eastern and central USA.

We consider that each of these genera is well supported by the morphological and molecular evidence. In order to resolve these phylogenetic relations a more extensive sampling is required, joined with a detailed review of the morphology of most species, including *Emesis* species. Also, the species *A. phyciodoides*, *A. castanea*, and *A. planeca* must be assigned to the correct genera in order to stabilize *Apodemia*. This can only be achieved with the use of diverse character systems and sufficient sampling. This study

contributes to the systematics and classification of Riodinidae. It adds two genera to the family: *Neoapodemia* which, as *Apodemia*, is exclusive to North America, and *Plesioarida* of North and Central America.

Acknowledgements

We thank the following individuals and institutions for allowing access to the collections under their care and for the stimulating discussions: A. D. Warren, J. Miller, and A. Sourakov (McGuire Center for Lepidoptera & Biodiversity, Gainesville, FL), R. K. Robbins (National Museum of Natural History, Smithsonian Institution, Washington DC), A. Zaldívar, C. Mayorga, and A. Ibarra (IBUNAM), C. Pozo (ECOSUR-Chetumal), and M. Luna (FES-Zaragoza). Many people helped to collect *Apodemia* samples for this study. We thank all of them, and especially A. Arellano-Covarrubias, J. Hernandez-Jerónimo, A. Contreras-Arquieta, T. K. O'Connor, A. D. Warren, J. C. Pavón-Vázquez, and D. Huerta. J. L. Salinas-Gutiérrez, and J. Shuey facilitated sample acquisition from Central America. Collecting permits were provided by the Secretaría de Medio Ambiente y Recursos Naturales, Dirección General de Fauna Silvestre to M. Trujano-Ortega (FAUT-0247). We also thank T. K. O'Connor, A. D. Warren, N. Manríquez and J. J. Morrone for their comments, which helped us to improve the manuscript, and N. Seraphim, L. Kaminski, and A. V. L. Freitas for the sequences provided and the discussions about *A. castanea*. M.T.O. thanks Julieta Brambila, J. Martínez Noble, and A. Warren for the support given during her research stay in Florida, USA. The authors thank Dr. N. Grishing for sharing his laboratory protocols and M. Rosado for the illustrations of the legs. We are very grateful with S. Guzmán for the technical advice on image capture at the LANABIO (IBUNAM) and to A. Nieto-Montes de Oca for allowing access to his laboratory at the F. Ciencias, UNAM where DNA was extracted. DNA sequences were uploaded to Genbank with the assistance of J. C. Pavón-Vázquez. This paper was partially supported by grants from CONABIO (JF065 and PJ016) to A. Nieto-Montes de Oca; from DGAPA, UNAM (PAPIIT no. IN221016) to U. García, and DGAPA, UNAM (PAPIIT no. IN212418) and CONACyT (284966) to JLB; from WWF-Alianza Carlos Slim (L039) to V. Souza; from CONACyT (CVU 131802) and from Becas Mixtas Program to M. Trujano-Ortega. Funding for international research visits was provided by PAEP-UNAM to M. Trujano-Ortega. Lastly, we thank the Posgrado en Ciencias Biológicas of the Universidad Nacional Autónoma de México, this work is part of the Ph. D. research project of M. Trujano-Ortega.

References

- Ackery PR, De Jong R, Vane-Wright RI (1999) The butterflies: Hedyloidea, Hesperoidea and Papilionoidea. In: Kristensen NP (Ed.) *Lepidoptera, moths and butterflies*. 1. Evolution, systematic and biogeography. *Handbuch der Zoologie/Handbook of Zoology*, 4(35), De Gruyter, Berlin, New York, 264–300.

- Austin GT (1988) *Apodemia palmerii* (Lycaenidae: Riodininae): Misapplication of names, two new subspecies and a new allied species. *The Journal of Research on the Lepidoptera* 26: 125–140.
- Brock J, Kaufman K (2006) *Butterflies of North America*. Houghton Mifflin, Singapore, 392 pp.
- Brower AVZ, De Salle R (1998) Patterns of mitochondrial versus nuclear DNA sequence divergence among nymphalid butterflies: the utility of wingless as a source of characters for phylogenetic inference. *Insect Molecular Biology* 7: 73–82. <https://doi.org/10.1046/j.1365-2583.1998.71052.x>
- Callaghan CJ, Lamas G (2004) Riodinidae. Checklist: Part 4A. Hesperioidea—Papilionoidea. In: Heppner JB (Ed.) *Atlas of Neotropical Lepidoptera* 5A. Association for Tropical Lepidoptera/Scientific Publishers, Gainesville, 141–170.
- Campbell DL, Brower AVZ, Pierce NE (2000) Molecular evolution of the wingless gene and its implications for the phylogenetic placement of the butterfly family Riodinidae (Lepidoptera: Papilionoidea). *Molecular Biology and Evolution* 17: 684–696. <https://doi.org/10.1093/oxfordjournals.molbev.a026347>
- Campbell DL, Pierce NE (2003) Phylogenetic relationships of the Riodinidae: implications for the evolution of ant association. In: Boggs C, Ehrlich PR, Watt WB (Eds) *Butterflies as Model Systems*. Chicago University Press, 395–408.
- Comstock JH, Needham JG (1918) The wings of Insects. *American Naturalist* 32: 231–257. <https://doi.org/10.1086/276835>
- De Jong R, Vane-Wright RI, Ackery PR (1996) The higher classification of butterflies (Lepidoptera): problems and prospects. *Entomologica Scandinavica* 27: 65–101. <https://doi.org/10.1163/187631296X00205>
- De la Maza R, De la Maza J (2017a) Una nueva especie de *Apodemia* C. y R. Felder, de la cuenca inferior del Río Balsas, Michoacán, México (Lepidoptera-Riodinidae). *Revista de la Sociedad Mexicana de Lepidopterología, nueva serie* 4: 31–36.
- De la Maza R, De la Maza J (2017b) Una nueva especie de *Apodemia* C. y R. Felder, de la Selva Lacandona, Río Lacantún, Chiapas, México (Lepidoptera-Riodinidae). *Revista de la Sociedad Mexicana de Lepidopterología, nueva serie* 4: 37–44.
- DeVries PJ (1997) *The Butterflies of Costa Rica and their Natural History. II: Riodinidae*. Princeton Univ. Press, New Jersey, 368 pp.
- Drummond AJ, Rambaut A (2007) BEAST: Bayesian evolutionary analysis by sampling trees. *BMC Evolutionary Biology* 7: 214. <https://doi.org/10.1186/1471-2148-7-214>
- Edgar RC (2004) MUSCLE: a multiple sequence alignment method with reduced time and space complexity. *BMC Bioinformatics* 5: 113. <https://doi.org/10.1186/1471-2105-5-113>
- Eliot JN (1973) The higher classification of the Lycaenidae (Lepidoptera): a tentative arrangement. *Bulletin of the British Museum of Natural History, Entomology* 28: 373–506. <https://doi.org/10.5962/bhl.part.11171>
- Emmel TC, Emmel JF (1998) Two new geographically restricted subspecies of *Apodemia mormo* (Lepidoptera: Riodinidae) from the vicinity of San Bernardino, California. In: Emmel TC (Ed.) *Systematics of Western North American Butterflies*. Mariposa Press, Gainesville, 795–800.
- Emmel TC, Emmel JF, Pratt G (1998) Five new subspecies of *Apodemia mormo* (Lepidoptera: Riodinidae) from southern California. In: Emmel TC (Ed.) *Systematics of Western North American Butterflies*. Mariposa Press, Gainesville, 801–810.

- Espeland M, Hall J, DeVries P, Lees D, Cornwall M, Yu-Feng Hsu, Li-Wei Wu, Campbell D, Talavera G, Vila R, Salzman S, Ruehr S, Lohman D, Pierce N (2015) Ancient Neotropical origin and recent recolonisation: Phylogeny, biogeography and diversification of the Riodinidae (Lepidoptera: Papilionoidea). *Molecular Phylogenetics and Evolution* 93: 296–306. <https://doi.org/10.1016/j.ympev.2015.08.006>
- Felder C, Felder R (1864–1867) *Apodemia*. *Reise der Österreichischen Fregatte Novara* 2: 302.
- Ferris CD (1985) A new subspecies of *Apodemia hypoglaucia* (Godman & Salvin) from the Yucatan Peninsula (Lycaenidae: Riodinidae). *Bulletin of the Allyn Museum* 94: 1–7.
- Godman FD, Salvin O (1878–1901) *Biologia Centrali Americana*. Insecta. Lepidoptera-Rhopalocera. Bernard Quaritch, Dulau, London, 240 pp.
- Hall JPW (1999) A Revision of the Genus *Theope*: its Systematics and Biology (Lepidoptera: Riodinidae: Nymphidiini). Scientific Publishers, Gainesville, 127 pp.
- Hall JPW (2003) Phylogenetic reassessment of the five forewing radial-veined tribes of Riodininae (Lepidoptera: Riodinidae). *Systematic Entomology* 28: 23–38. <https://doi.org/10.1046/j.1365-3113.2003.00196.x>
- Hall JPW (2005) A Phylogenetic Revision of the *Napaeina* (Lepidoptera: Riodinidae: Mesosemiini). *Entomological Society of Washington, Washington, DC*, 235 pp.
- Hall JPW (2008) *Theope* revisited: a synopsis of new discoveries, with the description of three new species (Lepidoptera: Riodinidae: Nymphidiini). *Proceedings of the Entomological Society of Washington* 110: 144–158. <https://doi.org/10.4289/0013-8797-110.1.144>
- Hall JPW, Harvey DJ (2002) Basal subtribes of the Nymphidiini (Lepidoptera: Riodinidae): phylogeny and myrmecophily. *Cladistics* 18: 539–569. <https://doi.org/10.1111/j.1096-0031.2002.tb00292.x>
- Harvey DJ (1987) The higher classification of the Riodinidae (Lepidoptera). PhD thesis, University of Texas, Austin, USA.
- Harvey DJ, Clench HK (1980) *Dianesia*, a new genus of Riodinidae from West Indies. *Journal of Lepidopterist Society* 34: 127–132.
- Huelsenbeck JP, Rannala B (2004) Frequentist properties of Bayesian posterior probabilities of phylogenetic trees under simple and complex substitution models. *Systematic Biology* 53: 904–913. <https://doi.org/10.1080/10635150490522629>
- Kimura M (1980) A simple method for estimating evolutionary rate of base substitutions through comparative studies of nucleotide sequences. *Journal of Molecular Evolution* 16: 111–120. <https://doi.org/10.1007/BF01731581>
- Klots AB (1956) Lepidoptera. In: Tuxen SL (Ed.) *Taxonomists's Glossary of Genitalia in Insects*. Copenhagen, Munksgaard, 97–110.
- Knölke S, Erlacher S, Hausmann A, Miller MA, Segerer AH (2005) A procedure for combined genitalia dissection and DNA extraction in Lepidoptera. *Insect Systematics and Evolution* 35: 401–409. <https://doi.org/10.1163/187631204788912463>
- Kristensen NP (1976) Remarks on the family-level phylogeny of butterflies (Insecta, Lepidoptera, Rhopalocera) Zeit. *Journal of Zoological Systematics and Evolutionary Research* 14: 25–33. <https://doi.org/10.1111/j.1439-0469.1976.tb00515.x>
- Kumar S, Stecher G, Tamura K (2016) MEGA7: Molecular Evolutionary Genetics Analysis version 7.0 for bigger datasets. *Molecular Biology and Evolution* 33: 1870–1874. <https://doi.org/10.1093/molbev/msw054>

- Lanfear R, Calcott B, Ho SYW, Guindon S (2012) PartitionFinder: combined selection of partitioning schemes and substitution models for phylogenetic analyses. *Molecular Biology and Evolution* 29: 1695–1701. <https://doi.org/10.1093/molbev/mss020>
- Lis JT (1980) Fractionation of DNA fragments by polyethylene glycol induced precipitation. *Methods in Enzymology* 65: 347–353. [https://doi.org/10.1016/S0076-6879\(80\)65044-7](https://doi.org/10.1016/S0076-6879(80)65044-7)
- Llorente-Bousquets J, Vargas-Fernández I, Luis-Martínez A, Trujano-Ortega M, Hernández-Mejía BC, Warren AD (2013) Diversidad de Lepidoptera en México. *Revista Mexicana de Biodiversidad Supplement* 85: S353–S371. <https://doi.org/10.7550/rmb.31830>
- Monteiro A, Pierce NE (2001) Phylogeny of *Bicyclus* (Lepidoptera: Nymphalidae) Inferred from COI, COII, and EF-1a Gene Sequences. *Molecular Phylogenetics and Evolution* 18: 264–281. <https://doi.org/10.1006/mpev.2000.0872>
- Nylander J, Ronquist F, Huelsenbeck JP, Nieves-Aldrey J (2004) Bayesian phylogenetic analysis of combined data. *Systematic Biology* 53: 47–67. <https://doi.org/10.1080/10635150490264699>
- Opler P, Powell JA (1961) Taxonomic and distributional studies on the Western components of the *Apodemia mormo* complex (Riodinidae). *Journal of Lepidopterists Society* 15: 145–171.
- Pelham JP (2008) A catalogue of the butterflies of the United States and Canada with a complete bibliography of the descriptive and systematic literature. *The Journal of Research on the Lepidoptera* 40: 1–652.
- Penz CM, DeVries PJ (1999) The higher level phylogeny of the tribe Lemoniini (Lepidoptera: Riodinidae): a preliminary assessment using adult morphology. *American Museum Novitates* 2384: 1–32.
- Penz CM, DeVries PJ (2006) Systematic position of *Apodemia paucipuncta* (Riodinidae) and a critical evaluation of the nymphidiine tramilla. *Zootaxa* 1190: 1–50.
- Proshok B (2011) Taxonomy and Conservation of *Apodemia mormo* (Lepidoptera: Riodinidae) in North America. Master Science thesis, University of Alberta, Canada.
- Proshok B, Crawford LA, Davis CS, Desjardins S, Henderson AE, Sperling FA (2013) *Apodemia mormo* in Canada: population genetic data support prior conservation ranking. *Journal of Insect Conservation* 17: 155–170. <https://doi.org/10.1007/s10841-012-9494-z>
- Proshok B, Dupuis JR, Engberg A, Davenport K, Opler PA, Powell JA, Sperling FA (2015) Genetic evaluation of the evolutionary distinctness of a federally endangered butterfly, Lange's Metalmark. *BMC Evolutionary Biology* 15: 73. <https://doi.org/10.1186/s12862-015-0354-9>
- Rambaut A, Drummond AJ (2007) Tracer v1.5. <http://beast.bio.ed.ac.uk>
- Ronquist F, Teslenko M, van der Mark P, Ayres DL, Darling A, Heohna S, Larget B, Liu L, Huelsenbeck JP (2012) MrBayes 3.2: efficient Bayesian phylogenetic inference and model choice across a large model space. *Systematic Biology* 61: 539–542. <https://doi.org/10.1093/sysbio/sys029>
- Saunders JW (2010) Molecular Phylogenetics of the Riodinidae (Lepidoptera). PhD thesis, University of Florida, USA.
- Scott JA (1986) The Butterflies of North America, a natural history and field guide. Stanford University Press, California, 583 pp.
- Sperling F (2003) Butterfly molecular systematics: from species definitions to higher-level phylogenies. In: Boggs CL, Watt WB, Ehrlich PR (Eds) *Butterflies: Ecology and evolution taking flight*, University of Chicago Press, Chicago, 431–458.

- Stamatakis A (2006) RAxML-VI-HPC: maximum likelihood-based phylogenetic analyses with thousands of taxa and mixed models. *Bioinformatics* 22: 2688–2690. <https://doi.org/10.1093/bioinformatics/btl446>
- Stichel H (1910–1911) *Lepidoptera Rhopalocera, fam. Riodinidae* Lep. In: Wytzman J (Ed.) *Genera Insectorum*, Wytzman, Brussels, 239–452.
- Wahlberg N, Braby MF, Brower AVZ, De Jong R, Lee MM, Nylin S, Pierce NE, Sperling FAH, Vila R, Warren AD, Zakharov EV (2005) Synergistic effects of combining morphological and molecular data in resolving the phylogeny of butterflies and skippers. *Proceedings of the Royal Society of London (B)* 272: 1577–1586. <https://doi.org/10.1098/rspb.2005.3124>
- Warren AD, Davis KJ, Grishin NV, Pelham JP, Stangeland EM (2017) Interactive Listing of American Butterflies. <http://www.butterfliesofamerica.com/>
- Whitwham A, Bonfield JK (2005) Staden package. <http://sourceforge.net/projects/staden>

Supplementary material 1

Specimens examined for morphological revision

Authors: Marysol Trujano-Ortega, Uri Omar García-Vázquez, Curtis J. Callaghan, Omar Ávalos-Hernández, Moisés Armando Luis-Martínez, Jorge Enrique Llorente-Bousquets

Data type: MS Word file.

Explanation note: Location data for specimens.

Copyright notice: This dataset is made available under the Open Database License (<http://opendatacommons.org/licenses/odbl/1.0/>). The Open Database License (ODbL) is a license agreement intended to allow users to freely share, modify, and use this Dataset while maintaining this same freedom for others, provided that the original source and author(s) are credited.

Link: <https://doi.org/10.3897/zookeys.729.20179.suppl1>

Supplementary material 2

Collection and voucher data for Riodinids genetic samples used in this study

Authors: Marysol Trujano-Ortega, Uri Omar García-Vázquez, Curtis J. Callaghan, Omar Ávalos-Hernández, Moisés Armando Luis-Martínez, Jorge Enrique Llorente-Bousquets

Data type: MS Word file.

Explanation note: Voucher data and GenBank accession numbers of samples used in the molecular analyses. The table is arranged alphabetically by species name and voucher number.

Copyright notice: This dataset is made available under the Open Database License (<http://opendatacommons.org/licenses/odbl/1.0/>). The Open Database License (ODbL) is a license agreement intended to allow users to freely share, modify, and use this Dataset while maintaining this same freedom for others, provided that the original source and author(s) are credited.

Link: <https://doi.org/10.3897/zookeys.729.20179.suppl2>

Supplementary material 3

Maximum likelihood tree of the relationships among *Apodemia* and selected species in the Riodinidae inferred with Cytochrome Oxidase I (COI). Numbers near branch nodes are bootstrap branch support

Authors: Marysol Trujano-Ortega, Uri Omar García-Vázquez, Curtis J. Callaghan, Omar Ávalos-Hernández, Moisés Armando Luis-Martínez, Jorge Enrique Llorente-Bousquets

Data type: Molecular data.

Explanation note: Tree inferred with Cytochrome Oxidase I gene.

Copyright notice: This dataset is made available under the Open Database License (<http://opendatacommons.org/licenses/odbl/1.0/>). The Open Database License (ODbL) is a license agreement intended to allow users to freely share, modify, and use this Dataset while maintaining this same freedom for others, provided that the original source and author(s) are credited.

Link: <https://doi.org/10.3897/zookeys.729.20179.suppl3>

Supplementary material 4

Maximum likelihood tree of the relationships among *Apodemia* and selected species in the Riodinidae inferred with Wingless (wg). Numbers near branch nodes are bootstrap branch support

Authors: Marysol Trujano-Ortega, Uri Omar García-Vázquez, Curtis J. Callaghan, Omar Ávalos-Hernández, Moisés Armando Luis-Martínez, Jorge Enrique Llorente-Bousquets

Data type: Molecular data.

Explanation note: Tree inferred with Wingless gene.

Copyright notice: This dataset is made available under the Open Database License (<http://opendatacommons.org/licenses/odbl/1.0/>). The Open Database License (ODbL) is a license agreement intended to allow users to freely share, modify, and use this Dataset while maintaining this same freedom for others, provided that the original source and author(s) are credited.

Link: <https://doi.org/10.3897/zookeys.729.20179.suppl4>

Supplementary material 5

Maximum likelihood tree of the relationships among *Apodemia* and selected species in the Riodinidae inferred with gene Elongation factor 1 α (EF-1a). Numbers near branch nodes are bootstrap branch support

Authors: Marysol Trujano-Ortega, Uri Omar García-Vázquez, Curtis J. Callaghan, Omar Ávalos-Hernández, Moisés Armando Luis-Martínez, Jorge Enrique Llorente-Bousquets

Data type: Molecular data.

Explanation note: Tree inferred with Elongation factor 1 α gene.

Copyright notice: This dataset is made available under the Open Database License (<http://opendatacommons.org/licenses/odbl/1.0/>). The Open Database License (ODbL) is a license agreement intended to allow users to freely share, modify, and use this Dataset while maintaining this same freedom for others, provided that the original source and author(s) are credited.

Link: <https://doi.org/10.3897/zookeys.729.20179.suppl5>

Supplementary material 6

Data of the photographs shown in the Figure 6

Authors: Marysol Trujano-Ortega, Uri Omar García-Vázquez, Curtis J. Callaghan, Omar Ávalos-Hernández, Moisés Armando Luis-Martínez, Jorge Enrique Llorente-Bousquets

Data type: MS Word file.

Explanation note: Location data and credits for the images.

Copyright notice: This dataset is made available under the Open Database License (<http://opendatacommons.org/licenses/odbl/1.0/>). The Open Database License (ODbL) is a license agreement intended to allow users to freely share, modify, and use this Dataset while maintaining this same freedom for others, provided that the original source and author(s) are credited.

Link: <https://doi.org/10.3897/zookeys.729.20179.suppl6>

A sibling species of *Platythyrea clypeata* Forel, 1911 in southeast Asia (Hymenoptera, Formicidae, Ponerinae)

Natthaporn Phengsi¹, Weeyawat Jaitrong², Jiraporn Ruangsittichai³,
Salinee Khachonpisitsak⁴

1 Biological Science Program, Department of Biology, Faculty of Science, Burapha University, 169 Long-Hard Bangsaen Road, Sanesuk, Mueang, Chon Buri, 20131 Thailand **2** Natural History Museum, National Science Museum, Technopolis, Khlong 5, Khlong Luang, Pathum Thani, 12120 Thailand **3** Department of Medical Entomology, Faculty of Tropical Medicine, Mahidol University, 420/6 Ratchawithi Road, Ratchathewi, Bangkok, 10400 Thailand **4** Department of Biology, Faculty of Science, Burapha University, 169 Long-Hard Bangsaen Road, Sanesuk, Mueang, Chon Buri, 20131 Thailand

Corresponding author: Salinee Khachonpisitsak (salineek@buu.ac.th)

Academic editor: B. Fisher | Received 2 October 2017 | Accepted 29 November 2018 | Published 16 January 2018

<http://zoobank.org/FA5E9B29-4174-4CC0-AF1E-6F22C27BC925>

Citation: Phengsi N, Jaitrong W, Ruangsittichai J, Khachonpisitsak S (2018) A sibling species of *Platythyrea clypeata* Forel, 1911 in southeast Asia (Hymenoptera, Formicidae, Ponerinae). ZooKeys 729: 87–102. <https://doi.org/10.3897/zookeys.729.21378>

Abstract

A new species of the rarely collected ant genus *Platythyrea* Roger, 1863 closely related to *Platythyrea clypeata* Forel, 1911 is described and illustrated based on the worker caste under the name *Platythyrea janyai* sp. n. This species is distributed in southern Thailand and western Malaysia, while *P. clypeata* is distributed in Sri Lanka, Vietnam, Laos, and Thailand in the areas north of the Isthmus of Kra. *Platythyrea clypeata* is newly recorded from Thailand from dead wood on the forest floor. The type series of *P. janyai* was also collected from rotten wood on the forest floor.

Keywords

new species, taxonomy, Thailand, *Platythyrea*, Ponerinae

Introduction

Platythyrea Roger, 1863 is a ponerine genus of the tribe Platythyreini, with *Pachycondyla punctata* Bingham, 1903 as the type species (Bolton 2003, Schmidt and Shattuck 2014). The genus is mainly pantropical in distribution, with some species also occurring in subtropical regions of the New World, Africa, Asia, and Australia (Bolton 2003, Schmidt and Shattuck 2014, Antweb 2017). Members of the genus are reported to nest in hollow branches or other preformed cavities in live or fallen trees, and to forage on tree trunks or other vegetation (Brown 1975, Ito 1994, 2016, Djiéto-Lordon et al. 2001, Molet and Peeters 2006, Yéo et al. 2006). Some large African species nest at the base of termite mound or under rocks (Brown 1975, Schmidt and Shattuck 2014).

At present, 38 extant species have been described within the genus with 9, 17, 6, and 8 species from the Neotropical, Ethiopian, Australian and Oriental regions, respectively (Schmidt and Shattuck 2014, Antweb 2017). Six species have been recorded in southeast Asia (*Platythyrea bidentata* Brown, 1975; *P. clypeata* Forel, 1911; *P. inermis* Forel, 1910; *P. parallela* (F. Smith, 1859); *P. quadridenta* Donisthorpe, 1941; and *P. tricuspidata* Emery, 1900). Jaitrong and Nabhitabhata (2005) recorded only three species, *Platythyrea parallela*, *P. quadridenta*, and *P. tricuspidata* from Thailand. A recent examination of *Platythyrea* specimens from Laos, Thailand, and western Malaysia recognised an additional two closely related species from these areas; one is new to science and is described herein, and the other (*P. clypeata*) is new to Thailand and is redescribed based on the worker and dealate queen.

Materials and methods

Holotype and paratypes of the new species are point-mounted and were examined along with other specimens of *Platythyrea* deposited in the Ant Museum, Faculty of Forestry, Kasetsart University, Bangkok, Thailand and the Natural History Museum of the National Science Museum, Thailand. Two dealate queens of *P. clypeata* collected from Laos were compared with the high resolution images of the *P. clypeata* holotype (alate queen) available on Antweb (2017). The holotype, paratype, and non-type workers of the new species were compared with workers from the colony from Laos to which the dealate queen belonged.

Most morphological observations were made with a ZEISS Discovery.V12 stereomicroscope. Multi-focused montage images were produced using NIS element 3.7 from a series of source images taken by a Nikon MNB42100 digital camera attached to a Nikon ECLIPSE E600 microscope. The holotype and paratypes were measured using a micrometre. All measurements are expressed in millimetres to the hundredths place.

Abbreviations used for the measurements and indices are as follows:

TL Total length in profile, roughly measured from the anterior margin of the head to the tip of the gaster in outstretched specimens.

HL	Maximum head length in full-face view, measured from the anterior clypeal margin to the midpoint of a line drawn across the posterior margin of the head.
HW	Maximum head width in full-face view, measured just behind the eyes.
SL	Scape length excluding the basal constriction and condylar bulb.
EL	Eye length, the maximum length of the eye in profile.
WL	Weber's length, the diagonal length of the mesosoma in profile from the anterior margin of the pronotum to the posteroventral angle of the metapleuron, excluding the neck.
PL	Petiole length measured from the anterior margin of the peduncle to the posterior-most point of the tergite in profile.
PH	Petiole height, the maximum height of the petiole in profile view.
PW	Petiole width, the maximum width of the petiole in dorsal view.
CI	Cephalic index. $HW/HL \times 100$.
EI	Eye index. $EL/HW \times 100$.
SI	Scape index. $SL/HW \times 100$.

Abbreviations of the type depositories and others are as follows:

AMK	Ant Museum, Faculty of Forestry, Kasetsart University, Bangkok, Thailand
THNHM	Natural History Museum of the National Science Museum, Pathum Thani, Thailand
MHNG	Muséum d'Histoire naturelle de la Ville de Genève, Switzerland

The general terminology of the worker ants follows Hölldobler and Wilson (1990) and Bolton (1994). For the important characters of the worker in the genus *Platythyrea* used in this paper, see Brown (1975), Bolton (2003) and Schmidt and Shattuck (2014). Queen and male characters of the genus, see Brown (1975) and Yoshimura and Fisher (2007).

In addition to morphometric measurements, Scanning Electron Microscope images of *Platythyrea* were made at Microscopic Center, Faculty of Science, Burapha University with a LEO 1450 VP scanning electron microscope on gold coated specimens.

Taxonomy

Platythyrea janyai sp. n.

<http://zoobank.org/E162024F-7730-41E9-9C3F-4667A2C3ECDD>

Figs 1, 5B1–B3

Holotype. Worker from Southern Thailand, Phatthalung Province, Si Banphot District, Riang Thong Waterfall, Khao Pu Khao Ya National Park, 28.IX.2007, W. Jaitrong leg., Colony no. WJT07-TH-2060 (THNHM-I-02392) deposited in THNHM.

Paratypes. Three workers, same data as the holotype (THNHM-I-02393 to THNHM-I-02395).

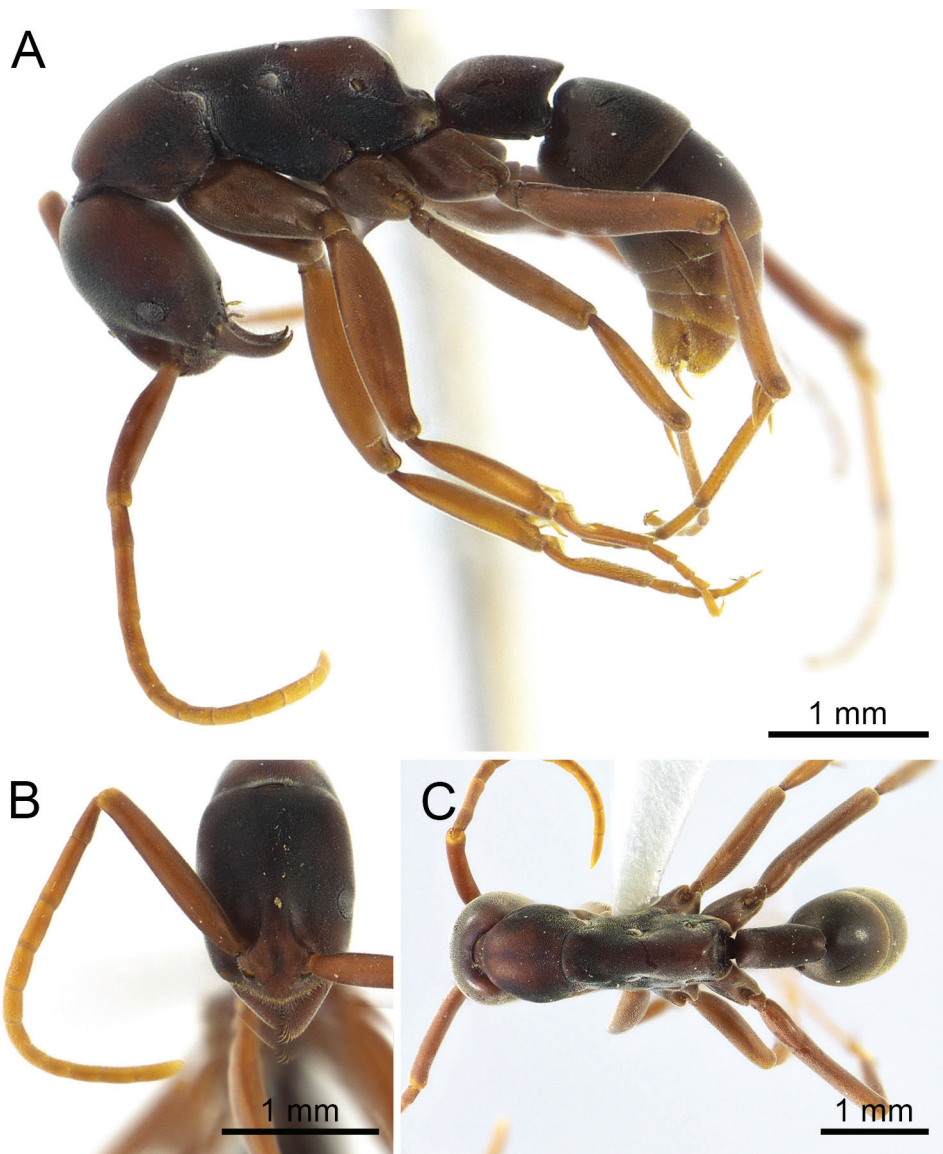


Figure 1. *Platythyrea janyai* sp. n. (holotype worker, THNHM-I-02392). **A** Body in profile view **B** Head in full-face view **C** Body in dorsal view.

Non-type material examined. Two workers from Southern Thailand, Trang Province, Na Yong District, Khao Chong Botanical Garden, 7.XI.2014, W. Jaitrong leg., Colony No. WJT071114-2 (THNHM-I-02421 to THNHM-I-02422); one worker from western Malaysia, Selangor, Ulu Gombak, 22.III.2013, F. Ito leg. (THNHM-I-02465).

Measurements and indices. Holotype. TL 6.63 mm; HL 1.42 mm; HW 1.06 mm; SL 1.39 mm; EL 0.20 mm; WL 2.21 mm; PL 0.73 mm; PH 0.53 mm; PW 0.40 mm;

CI 74, EI 18, SI 131. **Paratypes** (n = 3). TL 6.67–6.96 mm; HL 1.45 mm; HW 1.06 mm; SL 1.42 mm; EL 0.20 mm; WL 2.31 mm; PL 0.79 mm; PH 0.53 mm; PW 0.40 mm; CI 72, EI 18, SI 134.

Worker description. *Head.* Head in full-face view subrectangular, clearly longer than broad, with sides weakly convex, occipital corner round, and posterior margin almost straight; antenna relatively long; scape slender, clearly extending beyond posterolateral corner of head; antennal segment II narrow, 1.6 times as long as segment III; III longer than each of segments IV–XII; clypeus broad, in profile with median portion distinctly convex, in full-face view lateral portion narrow and anterior margin clearly convex; mandible triangular, masticatory margin with a large apical tooth, followed by 9–10 smaller teeth, larger and smaller teeth alternating, but the series as a whole decreasing in size toward basal tooth; basal margin of mandible without denticle; eye slightly convex, located laterally anterior to mid-length of head, relatively large, 0.20 mm in maximum diameter, with eleven ommatidia on longest axis, distance between mandibular base and anterior margin of eye 1.5 times as long as maximum eye length; with head in profile, distance between posterior margin of eye and occipital corner of head 3.4 times as long as distance between mandibular base and anterior margin of eye; frontal lobes relatively close to each other, with roundly convex lateral margins; antennal socket horizontal, in plane of transverse axis of head, and in dorsal view, half concealed by frontal lobe.

Mesosoma elongate, in profile with weakly convex dorsal outline; promesonotal suture distinct; metanotal groove absent; mesopleuron not clearly demarcated from mesonotum, but can be separated from metapleuron by a shallow furrow; metapleuron not demarcated from lateral face of propodeum; propodeum with almost straight dorsal outline; propodeal junction rounded; declivity of propodeum shallowly concave; seen from back propodeal declivity tapering above; propodeal spiracle opening elliptical; legs very long.

Petiole cylindrical and sessile, clearly longer than high and broad, its dorsal outline almost straight; with petiole in profile posterodorsal corner with acute angles overhanging declivity of petiole; declivity of petiole shallowly concave; in dorsal view petiole rectangular, its posterior margin concave medially; subpetiolar process weakly developed, subtriangular, located anteroventrally; ventral outline of petiole weakly convex.

Sculpture. Head (including antennal scape), mesosoma, petiole and gaster finely and densely micropunctate; coxae and femora superficially reticulate but shiny.

Pubescence white, very short and fine, distributed over whole body and appendages, longer and more oblique on anterior clypeal margin, tip of mandible and hypopygium; setae absent.

Colouration. Dorsum of head dark brown, while lateral face of head reddish brown; mesosoma, petiole and gaster dark brown to reddish brown (tip of gaster yellowish); antenna and legs yellowish brown (funicular segments paler than scape).

Ecology. The type series and all material examined of *P. janyai* were collected from small dead wood on the forest floor in lowland rainforests.

Etymology. The specific name is dedicated to Mr Janya Jareanrattawong of the Royal Forest Department, Thailand who kindly helped W. Jaitrong in ant collecting in southern Thailand.

Distribution. Southern Thailand (Phatthalung and Trang Provinces) and western Malaysia.

***Platythyrea clypeata* Forel, 1911**

Figs 2, 3, 5A1-A3

Platythyrea clypeata Forel, 1911: 378; Brown 1975: 50; Bolton 1995: 336; Xu and Zeng 2000: 214; Schmidt and Shattuck 2014: 51. Senior synonym of *P. thwaitesi*: Brown, 1975: 8.

Platythyrea thwaitesi Donisthorpe, 1931: 496. Junior synonym of *P. clypeata*: Brown 1975: 8.

Type. The syntype alate queen from “Pays de Moïs”, Cochinchina française (S.E. Asia), deposited in MHNG (not examined).

Non-type material examined. Nine workers, eastern Thailand, Chachoengsao Province, Tha Takiab District, Khao Ang Reu Nai Wildlife Sanctuary, 27.IX.2002, W. Jaitrong leg., Colony no. WJT270902-1 (THNHM-I-02423 to THNHM-I-02431); three workers, same locality, date and collector, Colony no. WJT270902-1 (THNHM-I-02432 to THNHM-I-02434); six workers, eastern Thailand, Sa Kaeo Province, Khao Ang Reu Nei Wildlife Sanctuary, 26.VI.2003, W. Jaitrong leg., Colony no. WJT03-TH-228 (THNHM-I-02435 to THNHM-I-02440); 23 workers and one male, eastern Thailand, Chanthaburi Province, Soi Dao District, 14.V.2008, W. Jaitrong leg., Colony no. WJT08-E065 (THNHM-I-02441 to THNHM-I-02453). Ten workers and one dealate queen, Laos, Vientiane, Pak Ngum District, Ban Phang Dang, ca. 300 m alt, 14.VI.2010, W. Jaitrong leg., Colony no. WJT-LAO-143 (THNHM); one dealate queen from same locality and collector, 12.VI.2010 (THNHM).

Measurements and indices. TL 5.74–6.20 mm; HL 1.29–1.39 mm; HW 0.86–0.89 mm; SL 1.12–1.18 mm; EL 0.10 mm; WL 1.85–2.05 mm; PL 0.66–0.73 mm; PH 0.46–0.53 mm; PW 0.40–0.43 mm; CI 61–69, EI 11, SI 125–138.

Worker redescription. *Head.* Head in full-face view rectangular, clearly longer than broad, with sides weakly convex or almost parallel, occipital corner roundly convex, and posterior margin feebly concave; antennal scape slender, relatively short, slightly extending beyond posterolateral corner of head (by 1/4 of its length); clypeus narrow, in profile with median portion distinctly convex, in full-face view lateral portion relatively broad and anterior margin clearly convex; mandible triangular, its masticatory margin with a large apical tooth, followed by ten smaller teeth (including basal tooth), large and smaller teeth alternating, but the series as a whole decreasing in size; basal margin of mandible without denticle; eye flat, located laterally at anterior to mid-length of head, very small, 0.10 mm in maximum diameter, with five omma-

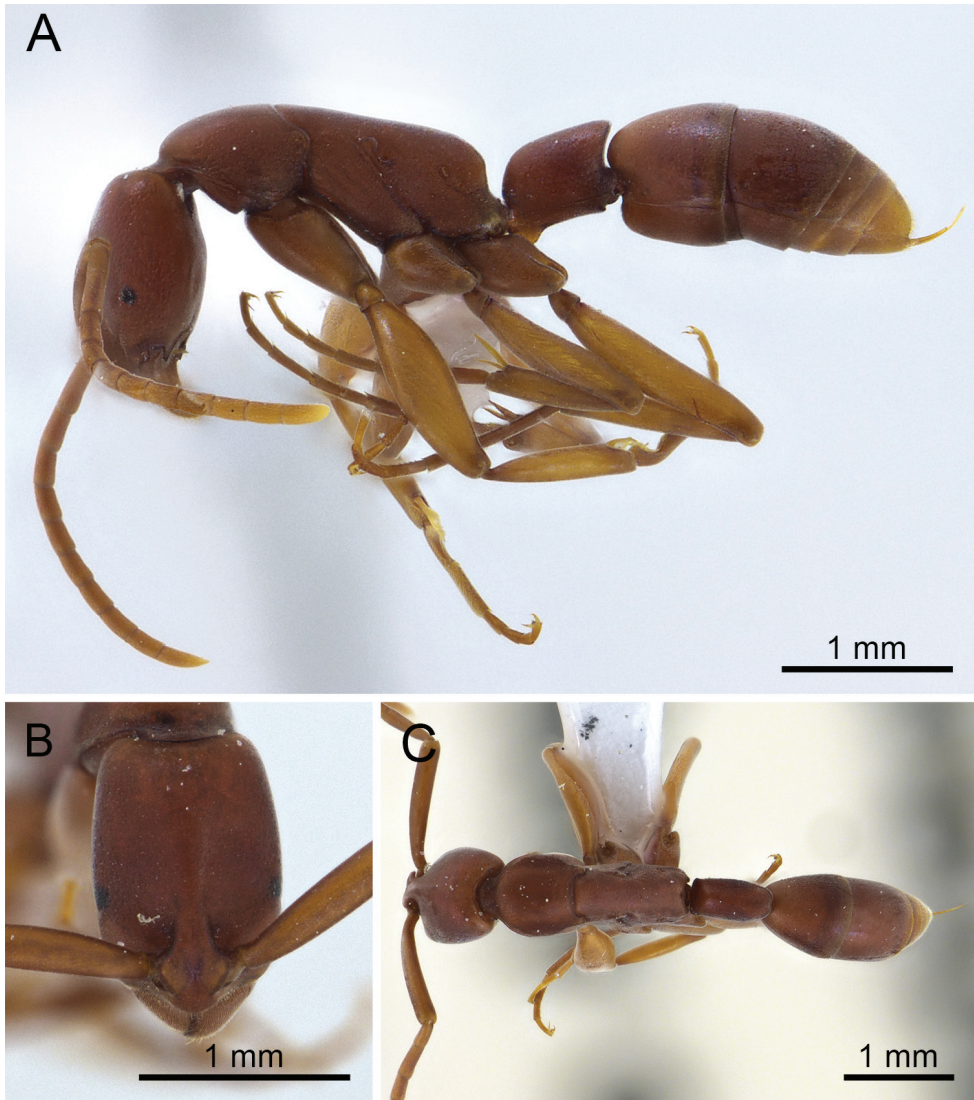


Figure 2. *Platythyrea clypeata* (non-type worker from Chanthaburi Province, THNHM-I-02445). **A** Body in profile view **B** Head in full-face view **C** Body in dorsal view.

tidia along longest axis; distance between mandibular base and anterior margin of eye approximately three times as long as maximum eye length; with head in lateral view, distance between posterior margin of eye and occipital corner of head 2.7 times as long as distance between mandibular base and anterior margin of eye; frontal lobes close to each other and rounded; frontal carinae strongly narrowed posteriorly.

Mesosoma elongate, in profile with almost straight dorsal outline; promesonotal suture distinct; mesopleuron demarcated from mesonotum and metapleuron by shallow furrows; propodeum in profile with almost straight dorsal outline; propodeal junction



Figure 3. *Platythyrea clypeata* (queen from Laos, Colony no. WJT10-LAO143). **A** Body in profile view **B** Head in full-face view **C** Body in dorsal view.

obtusely angulated; declivity of propodeum shallowly concave; seen from back propodeal declivity rounded above; propodeal spiracle opening elliptical; legs relatively long.

Petiole cylindrical and sessile, slightly longer than high and clearly longer than broad, its dorsal outline almost straight; in profile posterodorsal corner forming an acute angle; declivity deeply concave; in dorsal view node rectangular, slightly narrower posteriorly, its posterior margin convex and with shallow median concavity; subpetiolar process developed, located anteroventrally, subtriangular, its apex truncate and pointed forward; ventral outline of petiole feebly concave.

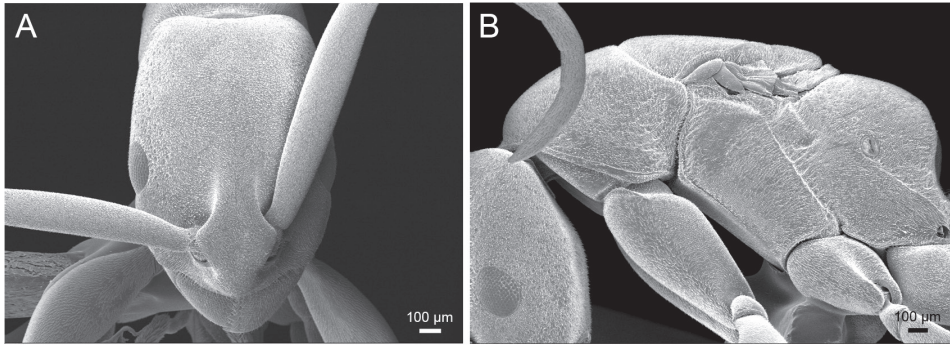


Figure 4. SEM images of *Platythyrea clypeata* (dealate queen from Laos, Colony no. WJT10-LAO143). **A** Head in full-face view **B** Mesosoma in profile view.

Sculpture. Dorsum of head finely punctate; lateral face of head behind, above and below eye punctate with dense foveae; dorsum of mesosoma with fine micropunctures similar to those on dorsum of head; lateral faces of pronotum, metapleuron and propodeum punctate with sparse shallow foveae; petiole finely micropunctate; gastral tergites I and II finely reticulate; antennal scape finely micropunctate; coxae microreticulate with smooth and shiny interspaces.

Pubescence white, very short and fine; setae present on tip of gaster.

Colouration. Head, mesosoma, petiole, and gaster reddish brown to dark brown (tip of gaster yellowish); antenna and legs yellowish brown to reddish brown (flagellum paler than scape).

Measurements and indices ($n = 2$). TL 7.49 mm; HL 1.52 mm; HW 1.06 mm; SL 1.32 mm; EL 0.20 mm; WL 2.31 mm; PL 0.79 mm; PH 0.73 mm; PW 0.46 mm; CI 69, EI 18, SI 125.

Dealate queen description. Body size slightly larger than worker. **Head.** Head in full-face view rectangular, clearly longer than broad with convex sides and almost straight posterior margin, occipital corner roundly convex; antennal scape extending beyond posterolateral corner of head by approximately 1/4 of its length; eye relatively large and convex, located anterior to mid-length of head, 0.20 mm in maximum diameter with ca. 17 ommatidia on the longest axis; frontal lobe and frontal carina similar to those in worker caste; distance between anterior margin of eye and mandibular base almost as long as eye length; ocelli clearly absent.

Mesosoma in profile with slightly convex dorsal outline; pronotum long and broad; mesoscutum trapezoidal, anterior edge clearly convex in dorsal view, separated from mesoscutellum by a shallow but wide suture and from pronotum by narrow suture; parapsidal lines indistinct, relatively long, straight and running anteriorly to mid-length of mesoscutum; mesoscutellum almost as long as broad; metanotum very short, separated from mesoscutellum and propodeum by deep grooves; propodeum relatively long; mesopleuron broad, anepisternum not demarcated from katepisternum; propodeal junction obtusely angulated; declivity of propodeum shallowly concave; seen from back propodeal declivity rounded above.

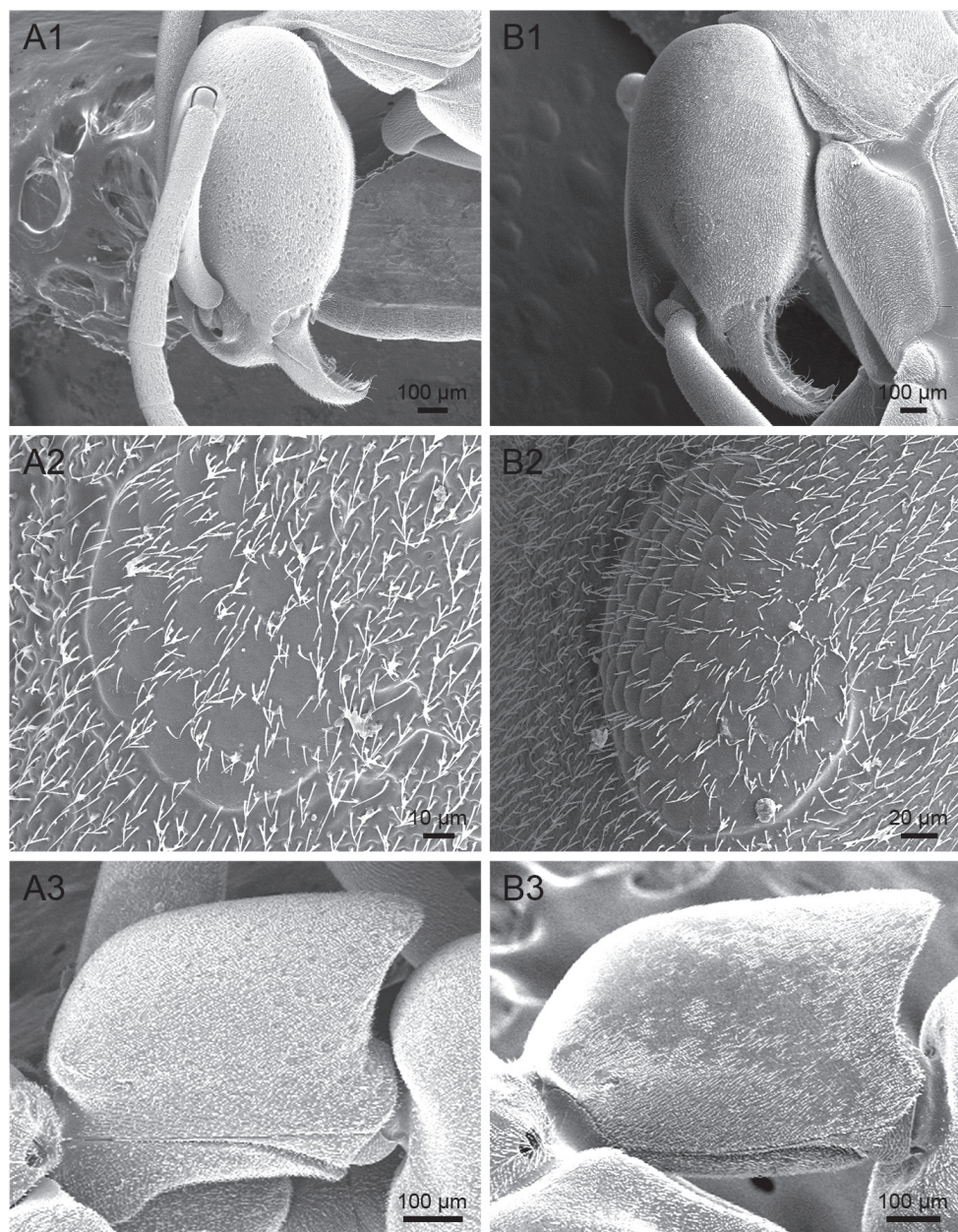


Figure 5. SEM images of *Platythyrea clypeata* (A1–A3) and *P. janyai* (B1–B3). A1, B1 Sculpture on lateral face of head A2, B2 Ommatidia of eye A3, B3 Petiole in profile view.

Petiole in profile view relatively short, rhombus, almost as long as high, its anterior margin weakly convex while posterior margin concave; declivity of petiole shallowly concave; subpetiolar process low and subtriangular, located anteroventrally, its apex pointed forward; ventral outline of petiole feebly concave. Gaster larger than in worker.

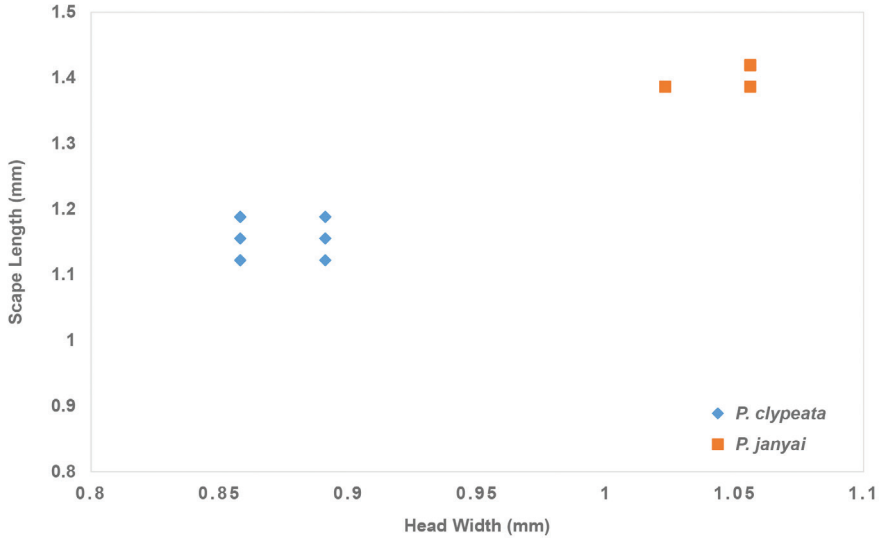


Figure 6. Scape length against head width in the worker.

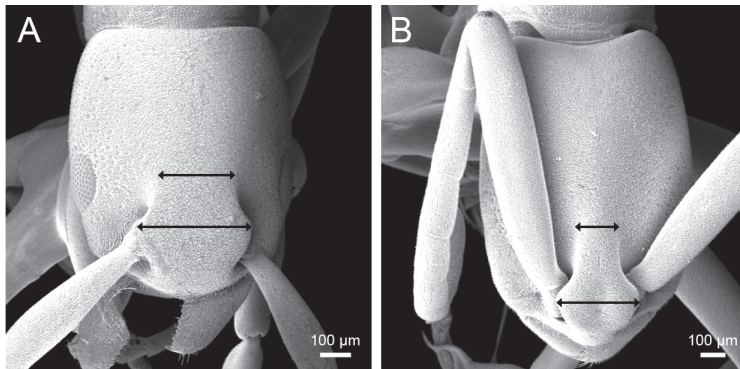


Figure 7. Frontal view focusing on the frontal carinae. **A** Frontal carinae very widely spaced **B** Frontal carinae relatively narrowly separated.



Figure 8. Dorsal view focusing on the petiole. **A** Posterior margin of petiole with two spines, teeth or blunt angles **B** Posterior margin of petiole with three spines, teeth or blunt angles **C** Posterior margin of petiole without distinct spines, teeth or blunt angles.

Sculpture, colouration, and setae similar to those of worker caste.

Distribution. Sri Lanka, Vietnam, China (?) and Thailand (new record).

Ecology. *Platythyrea clypeata* occurs in lowland (200–300 m alt) and inhabits primary and disturbed forests. All colonies of this species were collected from dead wood on the forest floor in an advanced stage of decomposition.

Key to the southeast Asian species of genus *Platythyrea* based on the worker caste

- 1 Frontal carinae very widely spaced, not continuing beyond level of posterior margin of antennal insertions (Fig. 7A); propodeal spiracle opening circular... **2**
- Frontal carinae relatively narrowly separated, extending far beyond level of posterior margin of antennal insertions where space between them is very narrow (Fig. 7B); propodeal spiracle opening elliptical..... **6**
- 2 In dorsal view, posterior margin of petiole with 2-3 distinct spines, teeth or blunt angles (Fig. 8A, B) **3**
- In dorsal view, posterior margin of petiole without distinct spines, teeth or sharp angles (Fig. 8C) **5**
- 3 In dorsal view, posterior margin of petiole clearly concave with distinct lateral blunt angles; petiole almost as long as high **4**
- In dorsal view, posterior margin of petiole with 3 distinct spines; petiole longer than high (Fig. 8B) *P. tricuspidata*
- 4 In profile view, propodeum armed with a pair of short teeth or tubercles (Fig. 9); lateral face of pronotum punctate with dense foveae *P. quadridenta*
- In profile view, propodeum unarmed; dorsum curving evenly into declivity (see fig. 28 in Brown 1975); lateral face of pronotum punctate with sparse foveae..... *P. bidentata*
- 5 In dorsal view, petiole clearly longer than broad; antennal scape relatively short, not reaching posterolateral corner of head..... *P. paravarella*
- In dorsal view, petiole almost as long as broad; antennal scape relatively long, slightly extending beyond posterolateral corner of head *P. inermis*
- 6 Head relatively shorter (CI 72–74); eye clearly larger (EL 0.20 mm with 11 ommatidia on longest axis); eye convex; dorsum and lateral face of head finely micropunctate without foveae; in profile view petiole clearly longer than high and in dorsal view node of petiole anteriorly as broad as posteriorly; ventral outline of petiole weakly convex *P. janyai* sp. n.
- Head relatively longer (CI 61–69); eye clearly smaller (EL 0.10 mm with 5 ommatidia on longest axis); eye flat; dorsum and lateral face of head finely punctate with dense shallow foveae; in profile view petiole slightly longer than high and in dorsal view node of petiole slightly narrower posteriorly; ventral outline of petiole feebly concave..... *P. clypeata*

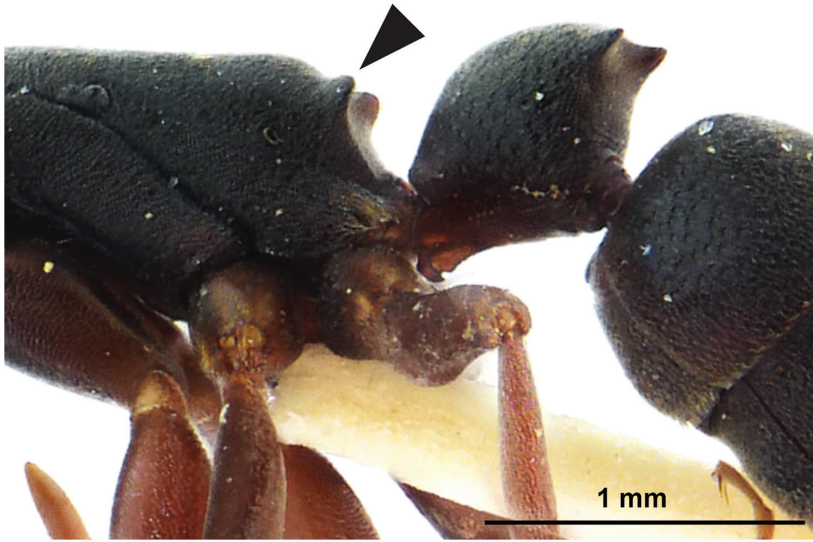


Figure 9. Profile view focusing on the propodeal junction of *P. quadridenta* from Thailand.

Discussion

Two dealate queens of the *P. clypeata* species group collected from Laos were compared with the high-resolution images of the *P. clypeata* holotype (alate queen from “Pays de Mois, Cochinchina française”) available on Antweb (2017). They have similar body sizes to those mentioned in Brown (1975: 50) and external morphological characteristics to the *P. clypeata* holotype. Additionally, Brown (1975) pointed out that alate queen of *P. clypeata* (holotype) completely lacks ocelli, which has also been observed in the Lao specimens (Fig. 4A). Workers of the *P. clypeata* species group collected from Eastern Thailand agree in most characters with the workers of a colony with a dealate queen (WJT-LAO-143) from Laos, while workers collected from Southern Thailand and western Malaysia differ from Laos and Eastern Thailand specimens. Thus, we here identify the specimens collected from Laos and Eastern Thailand as *P. clypeata* and those from Southern Thailand and western Malaysia as a new species, *P. janyai* sp. n. (see Fig. 5 for comparison).

The new species and *P. clypeata* are very similar in general appearance as they share the following characteristics: body reddish brown; frontal lobe narrow; frontal carinae closely spaced and strongly narrowed posteriorly; mandible triangular, its masticatory margin with a large apical tooth, followed by 9–10 smaller teeth, large and smaller teeth alternating; propodeal spiracle opening elliptical; in dorsal view posterior margin of petiole convex without spines. However, *P. janyai* can be easily separated from *P. clypeata* by the following characteristics: head relatively shorter (CI 72–74 in *P. janyai*; CI 61–69 in *P. clypeata*); eye clearly larger (EL 0.20 mm with eleven ommatidia on longest axis in *P. janyai*; EL 0.10 mm with five ommatidia on longest axis in *P. clypeata*); eye convex (flat in *P. clypeata*); dorsum and lateral face of head finely micropunctate

without foveae (finely punctate with dense shallow foveae in *P. clypeata*); in profile view petiole clearly longer than high and in dorsal view node of petiole anteriorly as broad as posteriorly (slightly longer than high and in dorsal view node of petiole slightly narrower posteriorly in *P. clypeata*); ventral outline of petiole weakly convex (feebly concave in *P. clypeata*). Fig. 6 shows ratio of HW/SL in the workers of *P. clypeata* (37 specimens) and *P. janyai* (6 specimens) from throughout their distribution ranges; no overlapping is observed in HW / SL between the species. *P. janyai* is distinctly allopatric with *P. clypeata* in distribution. It occurs in Malay Peninsula (S Thailand and W Malaysia). On the other hand, *P. clypeata* is recorded from Sri Lanka, Vietnam, Laos, and east Thailand (Brown 1975).

Xu and Zeng (2000) identified a worker from China as *P. clypeata*. It has a body size much larger than the holotype (alate queen) of *P. clypeata* (HW 1.20 mm in the Chinese specimen; HW 1.00 mm in the holotype). In general, queens in this genus are slightly larger than workers, with corresponding modifications of thoracic sclerites (Ito 1994, Schmidt and Shattuck 2014). Thus, the Chinese specimen should be re-identified.

Acknowledgments

This work was supported by Grant for Graduate Student 2016–2017 from Faculty of Science, Burapha University, Thailand. We would like to express our heartfelt gratitude to Prof. Frederick William Henry Beamish (Burapha University, Thailand) for his comments and reading through an earlier draft of this paper. We also thank Assoc. Prof. Decha Wiwatwitaya (Kasetsart University, Thailand) and Prof. Fuminori Ito (Kagawa University, Japan), who kindly allowed Weeyawat Jaitrong to examine the *Platythyrea* specimens in their collections and Yudthana Samung (Mahidol University, Thailand) for imaging assistance in this paper. Sincere thanks are also extended to one anonymous reviewer, Prof. Seiki Yamane (Kagoshima University Museum, Japan) and Dr. Brian Fisher (Subject editor) for their valuable comments.

References

- Antweb (2017) *Platythyrea*. Downloaded from <https://www.antweb.org/description.do?subfamily=ponerinae&genus=platythyrea&rank=genus> [accessed on 20 June 2017]
- Bingham CT (1903) The fauna of British India, including Ceylon and Burma. Hymenoptera, Vol. II. Ants and Cuckoo-wasps. Taylor and Francis, London, 506 pp.
- Bolton B (1994) Identification guide to the ant genera of the world. Harvard University Press, Cambridge, 222 pp. <https://doi.org/10.1093/aesa/88.4.593>
- Bolton B (1995) A new general catalogue of the ants of the world. Harvard University Press, Cambridge, 504 pp. <https://doi.org/10.1086/419489>
- Bolton B (2003) Synopsis and classification of Formicidae. *Memoirs of the American Entomological Institute* 71: 1–370.

- Brown Jr WL (1975) Contributions toward a reclassification of the Formicidae. V. Ponerinae, tribes Platythyreini, Cerapachyini, Cyldromyrmecini, Acanthostichini and Aenictogitini. Search Agriculture, Entomology (Itaca) 5(1): 1–115.
- Djiéto-Lordon C, Orivel J, Dejean A (2001) Consuming large prey on the spot: the case of the arboreal foraging Ponerine ant *Platythyrea modesta* (Hymenoptera, Formicidae). Insectes Sociaux 48(4): 324–326. <https://doi.org/10.1007/PL00001784>
- Donisthorpe H (1931) Descriptions of some new species of ants. Annals and Magazine of Natural History 10(8): 494–501. <http://dx.doi.org/10.1080/00222933108673428>
- Donisthorpe H (1941) Descriptions of new species of ants from New Guinea. Annals and Magazine of Natural History 11(7): 129–144. <http://dx.doi.org/10.1080/00222934108527147>
- Emery C (1900) Formiche raccolte da Elio Modigliani in Sumatra, Engano e Mentawai. Annali del Museo Civico di Storia Naturale di Genova (2) 20(40): 661–688. <https://doi.org/10.5962/bhl.part.9035>
- Forel A (1910) Fourmis des Philippines. Philippine Journal of Science Section D. General Biology, Ethnology and Anthropology 5: 121–130.
- Forel A (1911) Fourmis nouvelles ou intéressantes. Bulletin de la Société Vaudoise des Sciences Naturelles 47: 331–400. <http://doi.org/10.5281/zenodo.25597>
- Hölldobler B, Wilson EO (1990) The Ants. Harvard University Press, Cambridge, 732 pp. <http://dx.doi.org/10.1046/j.1420-9101.1992.5010169.x>
- Ito F (1994) Colony Composition of two Malaysian Ponerine ants, *Platythyrea tricuspidata* and *P. quadridenta*: sexual reproduction by workers and production of queens (Hymenoptera: Formicidae). Psyche 101: 209–218. <http://dx.doi.org/10.1155/1994/19319>
- Ito F (2016) Nesting and reproductive biology of *Platythyrea* sp. (*pararella*-group) in the Bogor Botanic Gardens, West Java, Indonesia (Hymenoptera: Formicidae). Asian Myrmecology 8: 111–117. <http://dx.doi.org/10.20362/am.008013>
- Jaitrong W, Nabhitabhata J (2005) A list of known ant species of Thailand (Hymenoptera: Formicidae). The Thailand Natural History Museum Journal 1(1): 9–54.
- Molet M, Peeters C (2006) Evolution of wingless reproductives in ants: weakly specialized ergatoid queen instead of gamergates in *Platythyrea conradti*. Insectes Sociaux 53(2): 177–182. <https://doi.org/10.1007/s00040-005-0856-3>
- Roger J (1863) Die neu aufgeführten Gattungen und Arten meines Formiciden-Verzeichnisses nebst Ergänzung einiger früher gegebenen Beschreibungen. Berliner Entomologische Zeitschrift 7. <https://dx.doi.org/10.1002/mmnd.18630070116>
- Schmidt CA, Shattuck SO (2014) The higher classification of the ant subfamily Ponerinae (Hymenoptera: Formicidae), with a review of Ponerine ecology and behavior. Zootaxa 3817(1): 1–242. <http://dx.doi.org/10.11646/zootaxa.3817.1.1>
- Smith F (1859) Catalogue of hymenopterous insects collected by Mr. A. R. Wallace at the islands of Aru and Key. Journal of the Proceedings of the Linnean Society of London, Zoology 3: 132–158. <https://doi.org/10.1111/j.1096-3642.1859.tb00077.x>
- Xu ZH, Zeng G (2000) Discovery of the worker caste of *Platythyrea clypeata* Forel and a new species of *Probolomyrmex* Mayr in Yunnan, China. Entomological Sinica 7: 213–217. <https://doi.org/10.1111/j.1744-7917.2000.tb00410.x>

- Yéo K, Molet M, Peeters C (2006) When David and Goliath share a home: compound nesting of *Pyramica* and *Platythyrea* ants. *Insectes Sociaux* 53: 435–438. <https://doi.org/10.1007/s00040-005-0890-9>
- Yoshimura M, Fisher BL (2007) A revision of male ants of the Malagasy region: key to sub-families and treatment of the genera of Ponerinae. *Zootaxa* 1654: 21–40. <https://doi.org/10.1371/journal.pone.0033325>

Supplementary material I

Data label of holotype of *Platythyrea janyai* sp.n.

Authors: Natthaporn Phengsi, Weeyawat Jaitrong, Jiraporn Ruangsittichai, Salinee Khachonpisitsak

Data type: Data label.

Explanation note: Close up of the label of Holotype of *Platythyrea janyai* sp.n.

Copyright notice: This dataset is made available under the Open Database License (<http://opendatacommons.org/licenses/odbl/1.0/>). The Open Database License (ODbL) is a license agreement intended to allow users to freely share, modify, and use this Dataset while maintaining this same freedom for others, provided that the original source and author(s) are credited.

Link: <https://doi.org/10.3897/zookeys.729.21378.suppl1>

Distribution of endangered Italian gudgeon *Romanogobio benacensis* (Cypriniformes, Cyprinidae, Gobioninae) with remarks on distinguishing morphological characters

Dušan Jelić^{1,2}, Mišel Jelić³, Petar Žutinić³, Ivana Šimunović¹,
Primož Zupančič⁴, Alexander M. Naseka^{4,5}

1 Croatian Institute for Biodiversity, Maksimirska cesta 129/5, HR-10000 Zagreb, Croatia **2** BIOTA j.d.o.o./ Ltd, Braće Radića 128A, HR-43290 Grubišno Polje, Croatia **3** University of Zagreb, Faculty of Science, Department of Biology, Rooseveltov trg 6, HR-10000 Zagreb, Croatia **4** Dinaric Research Institute, Dolsko 14, SI-1262 Dol pri Ljubljani, Slovenia **5** Faculty for Biology and Soil, Saint Petersburg State University, Universitetskaya Emb. 7/9, Saint Petersburg 199034, Russia

Corresponding author: Dušan Jelić (jelic.dusan@gmail.com)

Academic editor: M. Bichuette | Received 26 August 2017 | Accepted 20 October 2017 | Published 16 January 2017

<http://zoobank.org/F9BA4C98-F57C-4138-961D-900C329A6A16>

Citation: Jelić D, Jelić M, Žutinić P, Šimunović I, Zupančič P, Naseka AM (2018) Distribution of endangered Italian gudgeon *Romanogobio benacensis* (Cypriniformes; Cyprinidae; Gobioninae) with remarks on distinguishing morphological characters. ZooKeys 729: 103–127. <https://doi.org/10.3897/zookeys.729.20615>

Abstract

Distribution data on many freshwater fish species in Croatia are scarce and species identifications are difficult, requiring further detailed studies. This paper presents a report of the Italian gudgeon *Romanogobio benacensis* from the Mirna River in the Istra Peninsula in Croatia, in the south-east from its previously known distribution range. The identification of *R. benacensis* in Croatia was supported by a morphological comparison with *R. benacensis* from Italy and Slovenia, the common gudgeon *Gobio gobio*, and the Danubian gudgeon *Gobio obtusirostris* from geographically close locations. A combination of character states (number of scales between anus and anal-fin origin, branched pectoral-fin rays, lateral-line scales, total, abdominal, and caudal vertebrae, and the size and number of lateral blotches) distinguishes *R. benacensis* from both *G. gobio* and *G. obtusirostris*. The phylogenetic analyses using mitochondrial sequences of cytochrome b gene confirmed that specimens from the Mirna River belong to *R. benacensis*. Also, Reka River system (Adriatic Sea basin) in Slovenia is inhabited by a possibly introduced Danubian gudgeon, *G. obtusirostris*, and not by *R. benacensis*.

Keywords

Adriatic basin, freshwater fish, genetic barcoding, morphology, paleo-Po River, trans-Adriatic paleo-dispersal

Introduction

The richness of Croatian freshwater ichthyofauna manifests in at least 147 native fish and lamprey species, many of which are endemic (Mrakovčić et al. 2006, Jelić et al. 2008, Jelić 2011b). The number of fish species in Croatian freshwater environments is continuously increasing as a result of new species descriptions (Zupančič and Bogutskaya 2002, Marčić et al. 2011, Bogutskaya et al. 2012) and re-discovery of the previously described species (Jelić 2011a, Jelić and Jelić 2015). For example, *Télestes miloradi* Bogutskaya, Zupančič, Bogut & Naseka, 2012, an endemic species whose description is based on material deposited in a museum, collected more than 100 year ago, and which had been considered extinct, was recently re-discovered in nature (Jelić and Jelić 2015).

Another example is the Italian gudgeon *Romanogobio benacensis* (Pollini, 1816), which was firstly recorded in Croatia in 2011 (Jelić 2011a). This cyprinid fish species, belonging to Palearctic subfamily Gobioninae, was originally described as *Cyprinus benacensis* from specimens collected in Lake Garda in the Po drainage (Italy). Later, the Italian gudgeon was considered a subspecies of the common gudgeon *Gobio gobio* (Linnaeus) (Bianco and Taraborelli 1984, Bianco 1988, Pizzul et al. 1993, Bănărescu et al. 1999) or a valid species *Gobio benacensis* (Kottelat 1997, Bianco and Ketmaier 2001, 2005, Kottelat and Persat 2005). Currently, the species is assigned to *Romanogobio* Bănărescu (Kottelat and Freyhof 2007, Zupančič et al. 2008). Systematic position of the Italian gudgeon within *Romanogobio* is supported by phylogenetic reconstructions using mitochondrial DNA (mtDNA) sequences of genes coding for cytochrome b (cytb) (Bianco and Ketmaier 2005) and the cytochrome c oxidase subunit I (COI) (Geiger et al. 2014). However, the basal node in the *Romanogobio* clade which shows divergence between *R. benacensis* and the remaining subclades was not supported, thus preventing Bianco and Ketmaier (2005) to consider *Romanogobio* as a supported clade in comparison with the *Gobio* Cuvier clade.

Based on some diagnostic morphological characters, the Italian gudgeon is considered more similar to *Gobio* than to *Romanogobio* (Bianco and Ketmaier 2005, Kottelat and Freyhof 2007, Bianco 2014). According to Bianco and Ketmaier (2005), a single character discriminating *R. benacensis* and *G. gobio* was the number of scales between the anus and the anal-fin origin, 2–4 in the former species and 4–8 in the latter. Kottelat and Freyhof (2007) added that in *R. benacensis* the distance between the anus and the anal-fin origin is distinctly smaller than the eye diameter, while in *Gobio* it is equal to or greater than the eye diameter. Further, in *R. benacensis* the scales on the abdomen extend only to a point between the pectoral and pelvic-fin bases, while in *Gobio* they sometimes extend to a level of the posterior end of the pectoral-fin base. However, systematic position of *R. benacensis* is controversial, since some of the morphological

characters of *R. benacensis* do correspond to those diagnostic of the genus *Gobio*, while others are typical for *Romanogobio* (Kottelat and Freyhof 2007).

For nearly two centuries after its description, *R. benacensis* was considered an Italian endemic species, native in the Padano-Venetian district from the Isonzo River in the north to the Marecchia River in the south (e.g. Bianco and Taraborelli 1986, Bianco 1991, Bianco and Ketmaier 2005). First finding of Italian gudgeon outside of Italian territory was reported by Povž et al. (2005) in the lower reaches of Vipava River in the Soča (Isonzo) drainage (Slovenia). Crivelli (2006) cited a personal communication by M. Povž that *R. benacensis* was also found in the Reka River in the Adriatic basin in Slovenia. This was published later by Zupančič (2008) and Povž et al. (2015). However, no diagnostic characters of specimens from the Reka River were given to support this identification. Kottelat and Freyhof (2007) presumed that the Italian gudgeon probably occurs elsewhere in the northern Adriatic basin. Out of the native range, the Italian gudgeon was introduced and established in the Arno, Tiber, and Ombrone rivers in central Italy (Bianco 1994, Bianco and Ketmaier 2005).

In recent years, *G. gobio* was introduced in Italy and became invasive species in river systems down to the Badolato River in the south, making a serious threat to *R. benacensis* (Bianco and Ketmaier 2005). Phylogenetic inferences on mtDNA sequences of cytb (Bianco and Ketmaier 2005) and COI (Geiger et al. 2014) genes showed that the examined specimens of *G. gobio* from the Po drainage shared identical haplotypes with *G. gobio* from the Rhône drainage. However, Bianco and Ketmaier (2005) and Bianco (2009) indicated possible introductions of Danubian *G. gobio* in Italy (which refers to the Danubian gudgeon *Gobio obtusirostris* Valenciennes according to the recent taxonomic concept). *Gobio gobio* and *G. obtusirostris* are larger-sized fishes (SL up to 125–130 mm vs. 80–110 in *R. benacensis*) and, if successfully established, they might cause a considerable decline in populations, and even extirpation, of *R. benacensis* (Bianco and Ketmaier 2005, Bianco 2009). The latter species is thought to be represented only by genetically “pure” populations in its native range in the Tagliamento River in Italy (Bianco and Ketmaier 2005) and the Adriatic basin in Slovenia (Crivelli 2006, Bianco 2009, 2014). *Romanogobio benacensis* is considered an endangered species both globally (EN B2ab(i,ii,iii,iv,v), Crivelli 2006) and in Italy (Bianco et al. 2013).

Although four species of the subfamily Gobioninae (gudgeons) have been reported in Croatia (Mustafić et al. 2005, Freyhof and Kottelat 2007, Jelić 2011a), their systematic status is uncertain (e.g., species in the *R. albipinnatus* group *sensu* Freyhof and Kottelat 2007). Mustafić et al. (2005) reported *G. gobio*, *G. uranoscopus* (Agassiz), *G. albipinnatus* Lukasch, and *G. kesslerii* Dybowski. Later, these species were assigned to *G. obtusirostris*, the Danubian longbarbel gudgeon *R. uranoscopus*, the Danubian white-finned gudgeon *R. vladkovi* (Fang), and the Kessler’s gudgeon *R. kesslerii*, respectively (Freyhof and Kottelat 2007, Jelić 2011a). In the previous studies, gudgeons in the Istra Peninsula (Mirna River; Fig. 1) were identified as *G. gobio obtusirostris* (Leiner et al. 1995) (= *G. obtusirostris*) and *G. gobio* (Mustafić et al. 2005). The main aim of this study was to investigate which gobionine species occurs in the Istra Peninsula (Croatia) and to confirm the presence of *R. benacensis* in Croatia. Gudgeon individuals collected

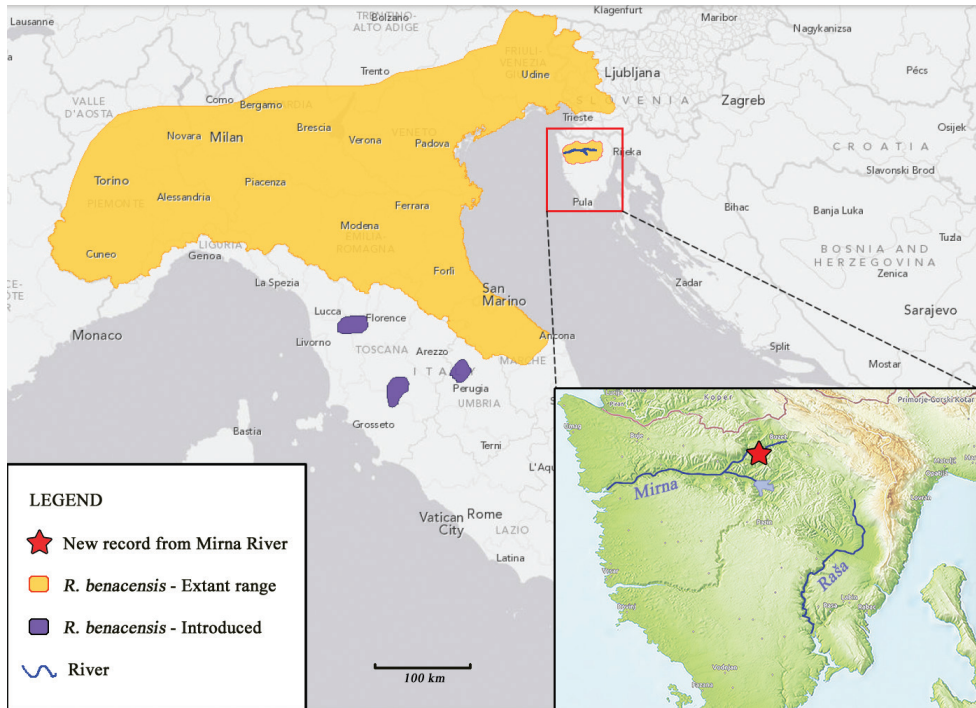


Figure 1. Map of distribution of *Romanogobio benacensis* in South-West Europe.

during an ichthyological survey in the Istra Peninsula was preliminary identified as *R. benacensis* by using morphological characters (Jelić 2011a). In the present paper, samples of *R. benacensis* from different localities in Italy, Slovenia, and Croatia were described using morphological and molecular characters to support their identification in comparison with *G. obtusirostris* and *G. gobio*.

Materials and methods

Morphological analysis

Measurements were made according to Naseka and Freyhof (2004). All measurements were made point-to-point with a digital calliper and recorded to the nearest of 0.1 mm. Vertebrae counts are given according to Naseka (1996). Last two rays in dorsal and anal fins based on a single pterygiophore were counted as 1½ ray. Unbranched rays in dorsal and anal fins were counted from radiographs. In total, 30 morphometric indices were used for descriptions and statistical analyses as in Table 1 and 18 meristic characters as in Table 2 were examined. All characters were obtained from specimens of both sexes and combined in analyses and tables. A Mann-Whitney U Test and a Discriminant Function Analysis (DFA) were performed using STATISTICA v6.0 and

Table 1. Morphometric characters in *Gobio gobio*, *Gobio obtusirostris*, and *Romanogobio benacensis*.

	<i>Gobio gobio</i> , Elba River (n = 2)		<i>Gobio obtusirostris</i> , Danube drainage (n=17)		<i>Gobio obtusirostris</i> , River (n=7)		<i>Romanogobio benacensis</i> , Mirna River (n=4)		<i>Romanogobio benacensis</i> , Po and Adige drainages (n=19)	
	range	SD	range	SD	range	SD	range	SD	range	SD
SL, mm	69.5–72.4	37.6–93.6	70.7		90.8–98.3	94.7	62.3–83.5	76.1	49.0–94.7	67.7
% SL										
Body depth at dorsal-fin origin	21.6–23.5	17.9–23.8	21.0	2.01	21.2–24.7	23.3	1.04	24.4–27.7	26.0	1.53
Caudal peduncle depth	8.7–9.6	8.2–10.9	9.7	0.75	9.7–11.0	10.2	0.48	10.4–11.2	10.8	0.33
Body width at dorsal-fin origin	13.9–16.5	11.4–16.5	13.9	1.45	14.7–17.7	16.1	1.09	12.8–17.9	15.3	2.38
Width of caudal peduncle	3.0–4.0	3.0–5.9	4.0	0.75	4.2–5.6	4.7	0.52	3.5–5.0	4.3	0.64
Predorsal length	50.0–50.2	46.3–50.2	48.8	1.19	47.1–50.3	48.6	1.12	46.8–51.4	48.4	2.03
Postdorsal length	40.3–42.4	40.1–42.7	41.3	0.87	41.5–43.4	42.7	0.82	41.0–41.5	41.3	0.24
Preanal length	50.1–50.4	47.3–52.4	50.2	1.37	48.2–51.3	49.6	0.99	49.9–51.4	50.7	0.72
Preadal length	70.8–71.7	68.4–74.1	71.7	1.46	70.1–73.5	71.6	1.17	67.1–70.6	69.3	1.62
Distance between pectoral fin and pelvic-fin origin	24.3–24.8	21.8–27.2	24.9	1.61	24.7–26.4	25.2	0.57	24.8–30.4	27.5	2.37
Distance between pelvic fin and anal-fin origin	20.7–22.3	20.7–23.3	21.8	0.87	21.3–23.9	22.6	0.87	18.7–22.2	20.4	1.80
Distance between anus and anal-fin origin	6.3–7.1	5.1–10.1	6.8	1.21	5.8–8.0	6.6	0.72	2.5–4.5	3.4	0.88
Caudal peduncle length	20.0–22.4	17.8–22.6	20.6	1.36	18.2–22.4	20.9	1.37	19.7–23.8	21.3	1.75
Dorsal-fin length	13.1–14.3	11.9–14.3	13.3	0.81	12.1–13.6	13.0	0.53	13.8–16.3	15.0	1.26
Dorsal-fin depth	24.2–24.9	21.0–26.2	23.4	1.72	20.9–22.0	21.5	0.48	21.7–25.6	23.7	1.78
Anal-fin length	8.2–8.7	7.7–9.5	8.6	0.51	6.9–8.7	8.0	0.66	10.0–13.1	10.8	1.51
Anal-fin depth	19.0–19.4	15.8–20.8	18.4	1.50	15.8–17.2	16.5	0.45	17.9–20.5	18.9	1.10
Pectoral-fin length	20.1–22.1	18.7–23.2	21.3	1.32	18.6–21.5	19.7	1.07	21.0–22.4	21.8	0.65
Pelvic-fin length	17.1–18.3	15.8–18.3	17.2	0.92	15.9–16.4	16.1	0.20	16.0–18.5	17.5	1.07
Head length	27.7–27.8	24.4–29.9	27.4	1.82	25.6–28.1	26.7	0.91	23.9–26.1	25.2	0.99
Eye diameter	6.4–6.8	4.9–6.8	6.1	0.62	5.3–5.9	5.5	0.23	5.6–6.6	6.0	0.42
% HL										
Head depth at nape	55.9–56.7	53.3–62.5	57.5	2.61	58.5–64.1	61.6	2.12	60.0–62.1	61.0	0.88
Snout length	40.4–41.1	36.7–41.6	38.8	1.67	40.0–43.8	42.1	1.16	43.2–44.1	43.5	0.39
Eye diameter	23.1–24.4	19.1–26.2	22.8	1.84	19.2–21.6	20.7	0.90	22.8–26.2	23.9	1.51
Postorbital distance	42.1–42.6	42.1–46.8	44.7	1.64	44.3–48.7	46.3	1.58	42.3–45.4	43.8	1.67
Maximum head width	50.4–54.8	48.8–55.8	51.7	2.31	56.7–63.2	59.8	2.60	56.7–58.6	57.8	0.78
Interorbital width	27.9–30.7	26.1–34.5	29.5	2.10	32.1–36.3	34.1	1.25	31.6–35.9	33.5	1.88
Length of upper jaw	24.7–25.9	20.3–26.5	24.5	1.75	25.2–28.4	26.8	1.17	25.4–28.1	26.7	1.36
Length of lower jaw	36.0–36.1	32.2–36.1	34.9	1.22	33.1–36.1	34.4	1.10	33.1–39.9	35.3	3.13
Barbel length	26.3–27.6	24.3–34.3	27.5	2.63	21.8–28.4	25.4	2.21	30.3–39.7	35.1	4.48
Caudal peduncle depth	31.4–34.7	31.4–41.2	36.0	2.58	34.4–40.7	38.1	2.24	41.5–44.5	42.8	1.48

Table 2. Meristic characters in *Gobio gobio*, *Gobio obtusirostris*, and *Romanogobio benacensis*.

	<i>Gobio gobio</i> , Elba River, n=2	<i>Gobio obtusirostris</i> , Reka River, n=7			<i>Gobio obtusirostris</i> , Danube drainage, n=17 (n=53 for vertebral counts)			<i>Romanogobio benacensis</i> , Mima River, n=4			<i>Romanogobio benacensis</i> , Po and Adige drainages, n=19		
		range	Mean	SD	range	Mean	SD	range	Mean	SD	range	Mean	SD
Unbranched dorsal-fin rays	3	3	3		3	3		4	4		3–4	3.7	0.48
Branched dorsal-fin rays	7½	7½	7½		7½	7½		7½	7½		7½	7½	
Branched anal-fin rays	6½	6½	6½		6½	6½		6½	6½		6½	6½	
Branched pectoral-fin rays	15–16	15–16	15.6	0.51	15–18	15.6	0.84	13–15	13.8	0.96	12–15	13.3	0.67
Branched pelvic-fin rays	7	7	7.0		7	7.0		7	7.0		7	7.0	
Scales in lateral row	42	41–43	41.4	0.79	40–42	41.3	0.73	38–39	38.5	0.58	37–40	38.8	0.73
Total lateral-line scales	42	41–42	41.3	0.49	39–42	41.0	1.0	37–39	38.3	0.96	37–40	38.5	0.87
Lateral-line scales to posterior margin of hypurals	39–42	38–40	39	0.58	38–40	38.9	0.81	35–36	35.8	0.50	34–37	36.4	0.80
Scales above lateral line	6	6	6.0		6	6.0		6	6.0		6	6.0	
Scales below lateral line	4	4–5	4.1	0.38	4	4.0		3–4	3.8	0.50	3–4	4.1	0.28
Scales between anus and anal-fin origin	6–9	4–7	5.4	1.27	4–7	6.1	0.71	2–3	2.3	0.50	1–5	3.7	0.85
Circumpeduncular scales	16	15–16	15.7	0.49	13–16	15.3	0.84	13–16	14.3	1.26	12–15	13.6	0.79
Predorsal scales	18–19	15–21	17.9	2.27	14–20	17.3	1.64	13–17	15.5	1.91	14–18	15.8	1.15
Total vertebrae	39–40	38–40	39.3	0.5	38–41	39.1	0.79	36–38	37.0	0.82	36–38	37.2	0.4
Abdominal vertebrae	20	20–21	20.6	0.53	20–22	20.5	0.54	19–20	19.5	0.59	18–20	19.1	0.46
Caudal vertebrae	19–20	18–19	18.7	0.49	17–20	18.5	0.68	16–18	17.5	1.0	17–18	17.9	0.32
Predorsal abdominal vertebrae	11	11	11	0.0	10–11	10.8	0.43	10–11	10.5	0.58	9–11	10.4	0.60
Prenal caudal vertebrae	2–3	1–2	1.3	0.49	1–3	1.6	0.58	0–2	1.3	0.96	1–2	1.4	0.50

PRIMER v6.1.9 to identify the most important characters that contribute to the differentiation of the two species and visualise the classification of the Reka and Mirna specimens into one of them.

(Abbreviations: SL, standard length; HL, lateral head length including skin fold; HDBI, Croatian Biological Research Society; NMW, Naturhistorisches Museum Wien; PZC, private collection of Primož Zupančič)

Examined material

***Romanogobio benacensis*. Adriatic basin, Croatia:** HDBI 1292, 3, SL 76.8–83.5 mm, Mirna River, Kamenita Vrata, coll. D. Jelić, 19.06.2011; HDBI 1323, 1, SL 62.3 mm, Mirna River, coll. D. Jelić, 2011. **Adriatic basin, Italy:** NMW 3522–23, 2, SL 59.4–65.4 mm, Turin, coll. Steindachner, 1910; NMW 15278, 1, SL 51.3 mm, Garda Lake basin, Adige River near Rovereto; NMW 53302, 5, SL 77.2–85.6 mm, Milan, coll. Steindachner, 1864; NMW 53303, 4, SL 78.0–94.7 mm, Milan, coll. De Filippi, 08.07.1845; NMW 53304, 3, SL 67.0–68.3 mm, Italy, Garda Lake, coll. Bellotti, 1888; NMW 84845, 4, SL 33.2–67.8 mm, T. Malone, 1 km upstream on the road Rivarossa-Argentera, Torino Prov., coll. Balma, 02.1987.

***Gobio gobio*. North Sea basin, Elbe drainage:** NMW 92127, 2, SL 69.5–72.4 mm, Czech Republic, Elba River near Celakovice, coll. Oliva, 1951.

***Gobio obtusirostris*. Danube drainage:** HDBI 1331, SL 83.7 mm, Croatia, Sava system, Kupa [Kolpa] River at Ozalj, coll. D. Jelić, 2011; HDBI 1356, 3, SL 66.5–82.9 mm, Croatia, Sava drainage, Kupa River at Ozalj, coll. D. Jelić, 2011; NMW 65533, 11 (from many), SL 48.5–75.9 mm, Romania, Timis River at Urseni, coll. Bănărescu, 1963; NMW 80989, 6 (from 20), SL 71.0–75.6 mm, Austria, Raba system, Pinka River near Badersdorf, coll. Jungwirth, 1982; NMW 87485, 6, SL 75.3–88.4 mm, Slovenia, Sava system, Drtiščica tributary of Kamniška Bistrica River, coll. Krištofek, 3.4.1988; NMW 90626, 3, SL 25.6–27.0 mm, Austria, Drau River near Linz, pond near Nörsach, coll. Kofler, 02.04.1991; NMW 90825, 4, SL 77.6–99.6 mm, Slovenia, Sava system, Dobravščica and Psata tributaries of Kamniška Bistrica River, coll. Povž, 03.04.1991; NMW 90828, 3, SL 72.4–93.6 mm, Slovenia, Drava system, Rožnodolski [Pekrski potok] tributary near Maribor, coll. Povž, 3.4.1991; NMW 91507, 16 (from 20), SL 37.6–91.6 mm, Austria, Mur River downstream from Graz, coll. Schulz, 1993; **Adriatic basin, Slovenia:** PZC 677, 7, SL 90.8–98.3 mm, Reka drainage, unnamed creek at Zarečje, 45.57°N, 14.21°E, coll. Zupančič, 07.04.2007.

DNA extraction, gene amplification, and sequencing

Besides species identification based on morphological features, species were characterised using sequences of cytochrome b gene (cytb), which is commonly used mtDNA

genetic marker for species affiliation of European cyprinids (e.g. Zardoya and Doadrio 1998, Bianco and Ketmaier 2005, Perea et al. 2010). Total DNA was extracted from pectoral fin tissue with the Qiagen DNeasy Blood and Tissue Kit (Qiagen, Germany) following the manufacturer protocol. After extraction, total genomic DNA was stored on -20°C until the polymerase chain reaction (PCR) was conducted. The primers used for cytochrome b were GluF and ThrR (Machordom and Doadrio 2001). The PCR was carried out with the HotStarTaq Master Mix Kit (Qiagen). PCR reactions were prepared in a total volume of 50 μL comprised of 2.5 U HotStarTaq DNA Polymerase, 1.5 mM MgCl_2 , 200 μM each dNTP, 0.2 μM of each primer and 20 ng of DNA template. The amplification process was conducted with the same conditions as described in Perea et al. (2010). Purification and sequencing of the PCR products were prepared by Macrogen Inc. (Seoul, South Korea) using the same primers used for gene amplification. Purified PCR products were sequenced on ABI 3730XL DNA Analyzer (Applied Biosystems, Foster City, USA). Sequence chromatograms were analysed using SEQUENCHER (version 5.3; Gene Codes Corp., Ann Arbor, USA) and aligned by eye.

The obtained sequences in this study (1141 base pairs long, bp) were examined using Nucleotide Basic Local Alignment Search Tool (Nucleotide BLAST; <http://blast.ncbi.nlm.nih.gov/Blast.cgi>) to screen for the most similar sequences in the GenBank nucleotide database (National Center for Biotechnology Information, U.S. National Library of Medicine, USA).

The Median-Joining (MJ) haplotype network (Bandelt et al. 1999) was used to infer the intraspecific relations in *R. benacensis* with cytb sequences obtained in this study and 342 bp sequences which were downloaded from the GenBank (Bianco and Ketmaier 2005). The MJ network was computed using PopART (Population Analysis with Reticulate Trees) v1.7 (Leigh and Bryant 2015).

Phylogenetic tree reconstructions were conducted using the cytb sequences obtained in this study and the available sequences belonging to *Gobio* and *Romanogobio* (1141 bp) from the GenBank (Briolay et al. 1998, Zardoya and Doadrio 1998, 1999, Madeira et al. 2005, Saitoh et al. 2006, Yang et al. 2006, Perea et al. 2010, Liu et al. 2010, Tang et al. 2011; Table 5). Sequences originating from the tench *Tinca tinca* (Linnaeus), the European bitterling *Rhodeus amarus* (Pallas) and the stone moroko *Pseudorasbora parva* (Temminck & Schlegel) were used as an outgroup. Newly obtained sequences in this study were deposited in the GenBank under accession numbers shown in Table 5 (will be available for publication). Phylogenetic reconstructions were inferred using three methods (Maximum Likelihood – ML, Bayesian Inference – IB and Maximum Parsimony – MP). The best-fit evolutionary model used in ML and IB was computed using jModelTest2 (version 2.1.6; Darriba et al. 2012) with the Bayesian information criterion (BIC) as implemented on the Cipres Science Gateway (version 3.1; <http://www.phylo.org>; Miller et al. 2010). Best-fit model of nucleotide substitution was Generalised Time Reversible (GTR) (Tavaré 1986) with a gamma distributed rate variation among sites (+G) and a significant proportion of invariant sites (+I). The ML was run using RAXML-HPC2 Workflow on XSEDE (version 8.2.8;

Stamatakis 2014) on the Cipres Science Gateway with optimized parameters. For ML analysis, 200 search replicates to find the ML tree and 1000 nonparametric bootstrap replicates under the GTRGAMMA model were applied. The IB was run in MrBayes 3.2 (Ronquist et al. 2012) on the Cipres Science Gateway. Two independent runs with four MCMC chains were run for 50 million generations and sampled every 5000 generations, with temperature parameter set to 0.2 and the first 12.5 million generations discarded as burn-in. The convergence of runs was screened using AWTY (Nylander et al. 2008) while effective sample sizes of parameters were checked using TRACER 1.5 (Drummond and Rambaut 2007). The MP analysis was performed in MEGA 6.06 (Tamura et al. 2013). The MP tree was obtained using the Subtree-Pruning-Regrafting algorithm (Nei and Kumar 2000) with search level 1 in which the initial trees were obtained by the random addition of sequences (10 replicates). Nodes in phylogram which have bootstrap values $P \geq 70$ in ML and MP, and posterior probabilities (pp) values ≥ 0.95 in IB were considered supported.

Three user trees (“Tree 1: *R. benacensis* sister taxon for *R. kesslerii* and *R. banaticus*”, “Tree 2: *R. benacensis* sister taxon for all *Romanogobio*”, and “Tree 3: *R. benacensis* sister taxon for all *Gobio*”) were analysed using tree topology tests [1sKH – one sided KH test based on pairwise SH tests (Shimodaira and Hasegawa 1999, Goldman et al. 2000, Kishino and Hasegawa 1989); SH – Shimodaira-Hasegawa test (2000); ELW – Expected Likelihood Weight (Strimmer-Rambaut 2002); 2sKH – two sided Kishino-Hasegawa test (1989)]. All topology tests were computed in TREE-PUZZLE v5.3rc16 (Schmidt et al. 2002).

Results

Comparative morphological description of *R. benacensis* from the Mirna River

Comparative morphological analysis of *R. benacensis* ($n = 23$), *G. gobio* ($n = 2$) and *G. obtusirostris* ($n = 24$) was performed based on number of available specimens. See Fig. 2a for general appearance and Table 1 for morphometric data. Below, only those characters demonstrating some difference between the species are discussed.

The body is relatively deep, the depth at the dorsal-fin origin is 24–28, averaging 26% SL (22–28, averaging 25% SL, in the Po samples) in contrast to 18–25, averaging 21–23% SL in *G. obtusirostris*.

The anus is located close to the anal-fin origin, the distance between the anus and the anal-fin origin is 3–5, averaging 3% SL (3–6, averaging 4% SL, in the Po samples) in contrast to 5–10, averaging 7% SL in *G. obtusirostris* where the anus is usually located about the midway between the pelvic and anal-fin origins (Table 2). The number of scales between the anus and the anal-fin origin is 1–5, commonly 2–4, in *R. benacensis* vs. 4–7 in *G. obtusirostris* and 6–9 in *G. gobio*.

The dorsal fin has 4 unbranched rays in all specimens from Mirna and Soča rivers and in 14 (of 19) specimens from the Po drainage (Table 2, Fig. 3). This is the first known example of a species with commonly 4 unbranched dorsal-fin rays in the Gobioninae.

Contrary, in *G. obtusirostris* and *G. gobio*, the number of unbranched dorsal-fin rays is always 3. In all species examined in this study the dorsal fin has $7\frac{1}{2}$ branched rays and the anal fin has 3 simple and $6\frac{1}{2}$ branched rays. The number of branched pectoral-fin rays is 12–15 in *R. benacensis* vs. 15–18 in *G. obtusirostris* and *G. gobio* (Table 2).

In *R. benacensis* from the Mirna River, scales along the midline of the belly extend forward to the middle of the pectoral-fin base. In *R. benacensis* from the Po drainage, scales along the midline of the belly extend forward from much behind the pectoral-fin base to the anterior end of the pectoral-fin base, commonly to the posterior end of the pectoral-fin base (Table 3). In *G. gobio*, the breast and throat are more scaled; scales along the midline of the belly extend forward from the middle of the pectoral-fin base to a point in front of the anterior end of the pectoral-fin base. In *G. obtusirostris*, the throat and breast are less scaled similarly to *R. benacensis*; scales along the midline of the belly extend forward from a point much behind the pectoral-fin base to the anterior end of the pectoral-fin base (Table 3).

The lateral line is complete, with 37–39 total scales averaging 38.6 (36–40 averaging 38.8 in the Po samples). These counts are lower than in *G. gobio* and *G. obtusirostris* which have a range of 39–42 scales, and averages of 42.0 and 41.3, respectively. Other scale counts can be also seen in Table 2. No epithelial keels on scales were found in specimens of *R. benacensis*.

The barbel is reaching the vertical through the middle of the pupil to the posterior margin of the eye (Table 4). Similar character states are also typical to *R. benacensis* from the Po drainage: the barbel is reaching the vertical through the middle of the pupil to behind the posterior margin of the eye, more frequently between the posterior margin of the pupil and the posterior margin of the eye. On average, the barbel is longer in *R. benacensis* than in *G. gobio* and *G. obtusirostris* (30–39% HL, averaging 35 in *R. benacensis* from the Mirna River and 26–37% HL, averaging 32.5 in *R. benacensis* from the Po drainage vs. 22–28% HL, averaging 25 in *G. obtusirostris* from the Reka River and 24–34% HL, averaging 27.5 in *G. obtusirostris* from the Danube drainage) (Table 1). In *G. obtusirostris*, the barbel is commonly reaching the vertical through the anterior margin of the pupil to the posterior margin of the pupil (Table 4).

Total vertebrae are 36–38, 19–20 abdominal, and (16)18 caudal including 0–2 preanal. 10–11 predorsal vertebrae. The vertebral counts in the Mirna samples of *R. benacensis* are similar to those in the Po samples, the most frequent vertebral formulae are 19+18 (17), 20+17 (2), and 20+18 (2) (Table 2). *G. gobio* and *G. obtusirostris* differ by higher average numbers of total, abdominal, and caudal numbers, the most frequent vertebral formulae are 21+18 (18), 20+19 (15), 20+18 (9), and 21+19 (8).

Laterally (examined on both sides) with 7–8, usually 7 roundish dark blotches. The size of a blotch varies but it is relatively large: the size of the blotch below the dorsal-fin origin is about (close to) or larger than the horizontal eye diameter. The same pattern of the blotches, 5–8, usually 6 or 7, is found in the examined specimens from the Po and Soča drainages. In *G. gobio* and *G. obtusirostris*, the blotches are smaller and more numerous, 7–11, usually 8 or 9, and the size of the blotch below the dorsal-fin origin is about the half horizontal eye diameter (Fig. 2).

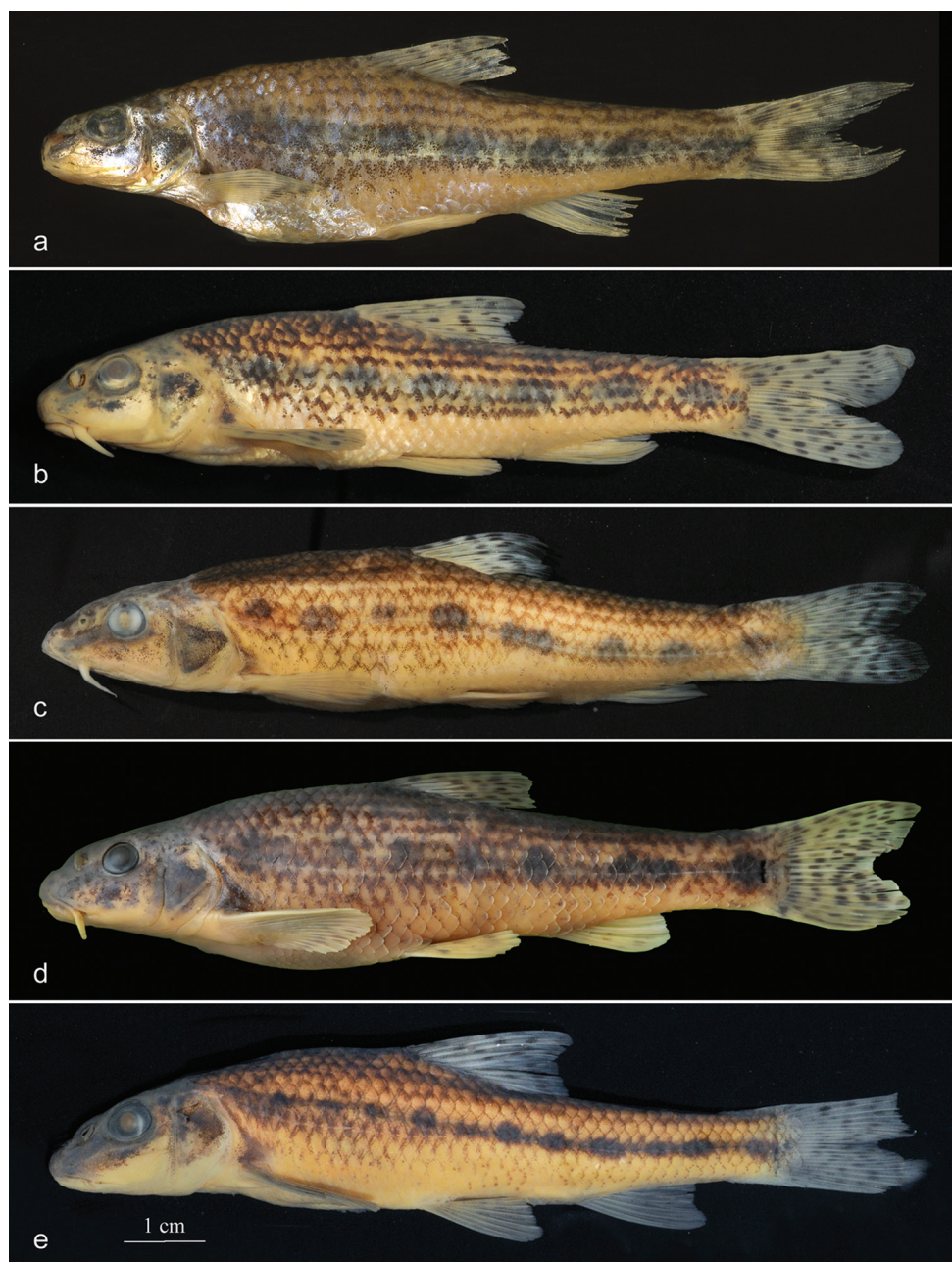


Figure 2. Lateral view of *Romanogobio benacensis* from the Mirna River (HDBI 1323), 62.3 mm SL (**a**) and the Po drainage (NMW 84845), 50.9 mm SL (**b**); *Gobio obtusirostris*, the Reka River (PZC), 98.3 mm SL (**c**) and the Sava River (NMW 87485), 88.4 mm SL (**d**); and *Gobio gobio*, the Elbe River (NMW 92127), 72.4 mm SL (**e**). Scale bar 1 cm.

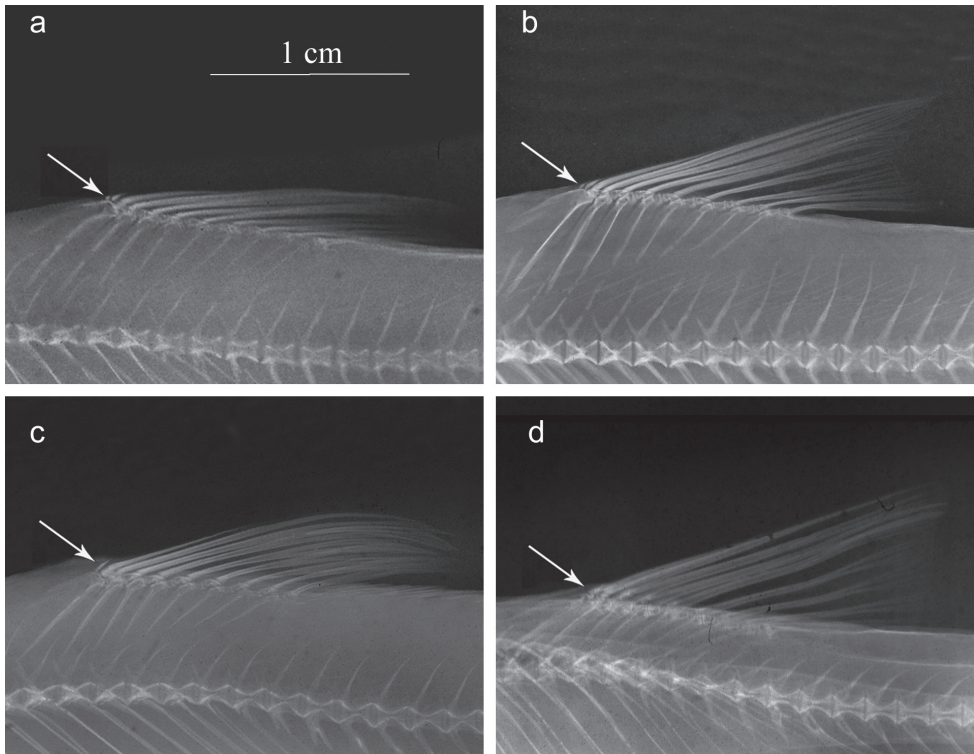


Figure 3. Radiographs of unbranched dorsal-fin rays. Specimens as **a–d** in Fig. 2. Arrow shows presence (**a–b**) or absence (**c–d**) of smallest anteriormost unbranched ray.

Statistical analysis

A Mann-Whitney U test revealed seven morphometric and nine meristic characters different on a statistically significant (0.01%) level between the samples of typical *G. obtusirostris* (Danube specimens) and typical *R. benacensis* (Po and Adige specimens): the body depth at the dorsal-fin origin, the distance between the pelvic fin and the anal-fin origin, the distance between the anus and the anal-fin origin, the dorsal-fin length, the anal-fin length, the interorbital width, the barbel length, the number of unbranched dorsal-fin rays, the number of branched pectoral-fin rays, the numbers of scales in lateral series, total lateral-line scales and lateral-line scales to the posterior margin of hypurals, the number of circumpeduncular scales, the number of scales between the anus and the anal-fin origin, and the numbers of total and abdominal vertebrae.

These 16 distinguishing characters were used for a DFA in order to classify the Reka and Mirna samples into one of the two species. DFA statistics values are as follows: Wilks' Lambda 0.00721, approx. F (45, 78) = 7.3894, $p < 0.0000$. The Mirna specimens are the closest to Italian *R. benacensis* (Fig. 5) (Squared Mahalanobis Distance equals 21.5024 vs. 74.7999 between *G. obtusirostris* from the Danube and Italian *R. benacensis*).

Table 3. Number of specimens of *Gobio gobio*, *Gobio obtusirostris*, and *Romanogobio benacensis* showing character states of the development (presence) of scales on the ventral side (throat and breast). Each character state refers to the anteriormost scale along the ventral midline.

Species and locality	In front of pectoral-fin base	Anterior end of pectoral-fin base	Middle of pectoral-fin base	Posterior end of pectoral-fin base	Behind pectoral-fin base
<i>Gobio gobio</i> , Elba River	1		1		
<i>Gobio obtusirostris</i> , Reka River		1		3	3
<i>Gobio obtusirostris</i> , Danube drainage		1		13	3
<i>Romanogobio benacensis</i> , Mirna River			4		
<i>Romanogobio benacensis</i> , Po drainage		1	4	10	4

Table 4. Character states of the position of the posteriormost extremity of the barbel in *Gobio gobio*, *Gobio obtusirostris*, and *Romanogobio benacensis*.

Species and locality	Barbel reaching to vertical of:					
	anterior margin of pupil	middle of pupil	posterior margin of pupil	between pupil and posterior margin of eye	posterior margin of eye	behind posterior margin of eye
<i>Gobio gobio</i> , Elba River		2				
<i>Gobio obtusirostris</i> , Reka River	4	1	2			
<i>Gobio obtusirostris</i> , Danube drainage	3	6	2	6		
<i>Romanogobio benacensis</i> , Mirna River		1	2		1	
<i>Romanogobio benacensis</i> , Po drainage		4	4	8	1	1

Phylogenetic tree inference

Two unique cytb haplotypes were detected in four specimens from the Mirna River (Table 5) Haplotype 1 originates from three specimens (HDBI 1323/tissue 771, HDBI 1292/tissue ID 772, and HDBI 1292/tissue ID 773) whereas Haplotype 2 was observed in one specimen (HDBI 1292/tissue ID 774). Haplotype 1 and Haplotype 2 have 99% similarity score (1136 identical nucleotide positions in 1141 bp sequence alignment). Nucleotide BLAST search using Haplotype 1 resulted in 99% similarity score (337 identical nucleotide positions in 342 bp alignment) with GenBank entry AY641522 designated as “strain TAG” of *G. benacensis* in Bianco and Ketmaier (2005), validating morphological determination of *R. benacensis* in this study. The second top match in BLAST search using Haplotype 1 was GenBank entry AY641524 designated as “strain OMB” of *G. benacensis* in Bianco and Ketmaier (2005) with similarity score 328/342 (96%). The 342 bp sequence alignment of *R. benacensis* were analysed with the MJ haplotype network (Fig. 6). Haplotypes 1 and 2 from Croatia differ by five mutational steps

from the “strain TAG” and can be considered as members of this strain. There are nine mutational steps between “strain TAG” and “strain OMB”, confirming there are two strains in *R. benacensis* (Bianco and Ketmaier (2005)). The sequences obtained in Bianco and Ketmaier (2005) (342 bp) were not used in further phylogenetic tree reconstruction in this study to avoid inclusion of significant proportion of missing sites in the final sequence alignment (1141 bp). The ML, IB and MP provided congruent trees with no supported contradictions (Fig. 7). Results of phylogenetic reconstruction indicated *Romanogobio* and *Gobio* as two statistically supported clades (P (ML) = 70, pp (IB) = 0.97, P (MP) = 91, and P (ML) = 100, pp (IB) = 1, P (MP) = 100, respectively). High statistical support was also observed for the node showing divergence between these two clades (P (ML) = 93, pp (IB) = 1, P (MP) = 80). Results of phylogenetic inference showed that *R. benacensis* belongs to the clade of *Romanogobio* (Fig. 7).

All topology tests (Table 6) indicated that best topology is presented in “Tree 1: *R. benacensis* sister taxon for *R. kesslerii* and *R. banaticus*” vs. “Tree 2: *R. benacensis* sister taxon for all *Romanogobio*” and “Tree 3: *R. benacensis* sister taxon for all *Gobio*”.

Discussion

Morphological data in this study confirm observations of the previous authors (Bianco and Taraborelli 1984, Bianco and Ketmaier 2005, Kottelat and Freyhof 2007) that *R. benacensis* differs from *G. gobio* and *G. obtusirostris* by a shorter distance between the anus and the anal-fin origin. However, this character is not completely discriminating in this study – there are specimens of both *R. benacensis* (including all examined specimens from the Soča River) and *Gobio* with 4 or 5 scales between the anus and the anal-fin origin. However, the length of the distance between the anus and the anal-fin origin is still diagnostic: in *R. benacensis*, the distance between the anus and the anal-fin origin (3–5% SL) is smaller than the eye diameter (6–8% SL) while in *G. gobio* and *G. obtusirostris* this distance (5–10% SL) is equal or larger than the eye diameter (5–7% SL). Kottelat and Freyhof (2007) also stated a difference in the scale pattern on the abdomen in *R. benacensis*; the scales extend only to a point between the pectoral and pelvic-fin bases vs. a level of the posterior end of the pectoral-fin base in *Gobio*. However, our data (Table 3) did not confirm this character to be clearly diagnostic for the two taxa.

Romanogobio benacensis also differs from *G. gobio* and *G. obtusirostris* by a number of character states which includes often four (vs. three) unbranched dorsal-fin rays, lower numbers of branched pectoral-fin rays (12–15 vs. 15–18), lateral-line scales (total number 37–40 vs. 39–42), total vertebrae (36–38 vs. 38–41), abdominal vertebrae (18–20 vs. 20–22), and caudal vertebrae (16–18 vs. 17–20) (Table 2).

Some of the morphological characters of *R. benacensis* do correspond to those diagnostic of the genus *Gobio*. As shown by Kottelat and Freyhof (2007), *R. benacensis* does not have epithelial crests on scales on the dorsal surface of the body, a shallow caudal peduncle, and a long distance between the anus and the anal-fin origin, the characters typical for *Romanogobio*. As to the position of the anus (in relation to anal-

Table 5. List of species used for phylogenetic tree inference on cytb sequences. Data on catalogue numbers of analysed specimens, localities, GenBank Accession numbers, sequences lengths, and references are shown.

Species	Catalogue no.	Locality	Accession No.	Sequence length (bp)	Reference
<i>Romanogobio benacensis</i>	HDBI 1323/tissue ID 771	Croatia: Mirna River, Kamenita Vrata	xxx	1141	This study
<i>Romanogobio benacensis</i>	HDBI 1292/tissue ID 772	Croatia: Mirna River, Kamenita Vrata	xxx	1141	This study
<i>Romanogobio benacensis</i>	HDBI 1292/tissue ID 773	Croatia: Mirna River, Kamenita Vrata	xxx	1141	This study
<i>Romanogobio benacensis</i>	HDBI 1292/tissue ID 774	Croatia: Mirna River, Kamenita Vrata	xxx	1141	This study
<i>Gobio obtusirostris</i>	HDBI/tissue ID 775	Bosnia and Herzegovina: Boračko Lake	xxx	1141	This study
<i>Gobio gobio</i>	MEL	Italy: Meletta River	AY641521	342	Bianco and Ketmaier (2005)
<i>Romanogobio benacensis</i>	TAG	Italy: Tagliamento River	AY641522	342	Bianco and Ketmaier (2005)
<i>Gobio gobio</i>	ASS	Italy: Assino River	AY641523	342	Bianco and Ketmaier (2005)
<i>Romanogobio benacensis</i>	OMB	Italy: Ombrone River	AY641524	342	Bianco and Ketmaier (2005)
<i>Gobio gobio</i>	BAD	Italy: Badolato River	AY641525	342	Bianco and Ketmaier (2005)
<i>Gobio gobio</i>		France: Rhone River	Y10452	1141	Briolay et al. (1998)
<i>Gobio lozanoi</i> Doadrio and Madeira, 2004		Spain: Tajo River	AF045996	1141	Zardoya and Doadrio (1998)
<i>Gobio obtusirostris</i>		Greece: Gallikos River	AF090750	1141	Zardoya and Doadrio (1999)
<i>Romanogobio bananescui</i> (Dimovski and Grupche, 1974)		Greece: Aliakmon River	AF090751	1141	Zardoya and Doadrio (1999)
<i>Romanogobio ciscaucasicus</i> (Berg, 1932)	Gobio_ciscaucasicus	Russia: Kuma River	AF095607	1141	Zardoya and Doadrio (1999)
<i>Romanogobio uranoscopus</i>	G.ura.34	Romania: Valsan River/Valsanesti	AY426593	1141	Madeira et al. (2005)
<i>Gobio lozanoi</i>	G.go.13FR.ADOUR	France: Adour River	AY426572	1141	Madeira et al. (2005)
<i>Gobio gobio</i>	G.go.33Czech.R	Czech Republic	AY426592	1141	Madeira et al. (2005)
<i>Gobio gobio</i>		Czech Republic: Plana	AB239596	1141	Saitoh et al. (2006)
<i>Gobio gobio</i>	Gobio_gobio (2)	Germany: Rhine River	AY953007	1141	Yang et al. (2006)
<i>Gobio obtusirostris</i>	Gobio_gobio (1)	Romania	EF173619	1141	Luca et al. (direct submission)
<i>Gobio obtusirostris</i>	MNCN_AT4759	Slovenia: Sevnica River	HM560092	1141	Perea et al. (2010)

Species	Catalogue no.	Locality	Accession No.	Sequence length (bp)	Reference
<i>Romanogobio kesslerii</i>	WL*0653a	Ukraine: middle Dniestr River close to type locality	AY952328	1141	Witte (direct submission)
<i>Romanogobio banaticus</i> (Bănărescu, 1960)	WL*0626a	Romania: middle Nera River (Danube drainage)	AY952329	1141	Witte (direct submission)
<i>Romanogobio banaticus</i>	WL*0626b	Romania: middle Nera River (Danube drainage)	AY952330	1141	Witte (direct submission)
<i>Romanogobio uranoscopus</i>	WL*0624a	Romania: middle Nera River (Danube drainage)	AY952331	1141	Witte (direct submission)
<i>Romanogobio macropterus</i> (Kamensky, 1901)	WL*0628a	Turkey: Aras River	AY952332	1141	Witte (direct submission)
<i>Gobio macrocephalus</i> Mori, 1930	Gobio_macrocephalus	China: Yanji, Tumenjiang River	AY953006	1141	Yang et al. (2006)
<i>Gobio cynocephalus</i> Dybowski, 1869	Gobio_cynocephalus	China: Fuyuan, Amur River	AY953005	1141	Yang et al. (2006)
<i>Romanogobio tenuicorpus</i> (Mori, 1934)	Romanogobio_tenuicorpus	China: Yellow River	AY953004	1141	Yang et al. (2006)
<i>Gobio huanghensis</i> Luo, Le and Chen, 1977	Gobio_huanghensis	China	FJ904648	1141	Qi et al. (direct submission)
<i>Gobio soldatovi</i> Berg, 1914	IHCAS:0210055	China: Kaiyuan, Liahe River	EU934491	1141	Liu et al. (2010)
<i>Romanogobio tenuicorpus</i>	CTOL00130	n/a	JN003327	1141	Tang et al. (2011)
<i>Romanogobio ciscaucasicus</i>	CTOL00128	n/a	JN003325	1141	Tang et al. (2011)
<i>Romanogobio tanaiticus</i> Nas-eka, 2001	CTOL00129	n/a	JN003324	1141	Tang et al. (2011)
<i>Gobio cynocephalus</i> Dybowski, 1869	CTOL00112	n/a	JN003328	1141	Tang et al. (2011)
<i>Gobio coriparoides</i> Nichols, 1925	CTOL00375	n/a	JN003326	1141	Tang et al. (2011)
<i>Tinca tinca</i>	<i>Tinca tinca</i>	Bosnia and Herzegovina: Trebišnjica River, Ravno	HM560230	1141	Perea et al. (2010)
<i>Rhodeus amarus</i>	<i>Rhodeus amarus</i>	Czech Republic: Libečovka River, Elbe River	HM560156	1141	Perea et al. (2010)
<i>Pseudorasbora parva</i>	<i>Pseudorasbora parva</i>	Turkey: Kizilirmak River, Kirschir	HM560155	1141	Perea et al. (2010)

Table 6. Comparison of user trees (“Tree 1: *Romanogobio benacensis* sister taxon for *Romanogobio kesslerii* and *Romanogobio banaticus*”, “Tree 2: *R. benacensis* sister taxon for all *Romanogobio*”, and “Tree 3: *R. benacensis* sister taxon for all *Gobio*”). The columns show the results and p-values of the following tests: 1sKH - one sided KH test based on pairwise SH tests (Shimodaira and Hasegawa 1999, Goldman et al., 2000, Kishino and Hasegawa 1989); SH - Shimodaira-Hasegawa test (1999); ELW - Expected Likelihood Weight (Strimmer and Rambaut 2002); 2sKH - two sided Kishino-Hasegawa test (1989). Plus signs denote the confidence sets. Minus signs denote significant exclusion. All tests used 5% significance level. 1sKH, SH, and ELW performed 1000 resamplings using the RELL method. 1sKH and 2sKH are correct to the 2nd position after the the decimal point of the log-likelihoods.

Tree	log L	difference	S.E.	p-1sKH	p-SH	c-ELW	2sKH
1	-8489.12	0.00	<--- best	1.0000 +	1.0000 +	0.7078 +	best
2	-8491.32	2.20	2.8840	0.2040 +	0.5230 +	0.2036 +	+
3	-8499.39	10.27	8.1588	0.1010 +	0.1250 +	0.0887 +	+

fin base), it is closer to the anal fin in *R. benacensis* than even in *Gobio*; a position of the anus at (or close to) the anal-fin origin is a plesiomorphic feature in the Gobi-oninae (Naseka 1996). The genus *Romanogobio* also differs from *Gobio* in having the supraethmoid wide (wider than long) vs. elongated (longer than wide); a high and oval second infraorbital (Fig. 4a) vs. narrow and rod-shaped (Fig. 4b), and a relatively high number of vertebrae both total and in the regions (the modal vertebral formula 42:(11)20(5)+3(21)(18) vs. 39:(11)21 (5)+(1)18(17) (Naseka 1996, Naseka et al. 2002). As shown above, *R. benacensis* possess low vertebral counts which are even lower than those found in the examined *Gobio* species. But the shape of the supraethmoid and infraorbitals are similar to that typical of *Romanogobio*.

As shown above in the results of the morphological analysis, the examined sample from the Reka River is *G. obtusirostris*, not *R. benacensis*. This was not expected having in mind the current hydrological features of the Reka River which drains into the Adriatic Sea. The Reka River (Notranjska Reka) originates in Croatia and flows 54 km through western Slovenia, disappears in the Škocjanske jame underground cave system and reappears again after 38 km as a part of the Timavo River in Italy flowing into the Adriatic Sea. Although results in this study indicates that *R. benacensis* is not present in the Reka River, further analyses using more specimens are needed for a final systematic conclusions. Also, the native status of *G. obtusirostris* in the Reka River is unclear. It could be a non-native species similar to an introduced chub *Squalius cephalus* (Linnaeus).

The morphological data discussed above confirmed that gudgeons from the Mirna River can be assigned to *R. benacensis*.

Phylogenetic reconstruction in this study (Fig. 7) indicated *Gobio* and *Romanogobio* as two statistically supported clades; with *R. benacensis* as a member of *Romanogobio* clade. Although results of Bianco and Ketmaier (2005) and Geiger et al. (2012) questioned the phylogenetic recognition of *Romanogobio* as a distinct clade in respect to *Gobio*, the monophyletic status of *Romanogobio* was shown by Madeira et al. (2005) and in comprehensive studies on Gobionine phylogeny (Yang et al. 2006, Tang et al. 2011). Difference in statistical supports for clades *Romanogobio* and *Gobio* among studies in which cytb was applied

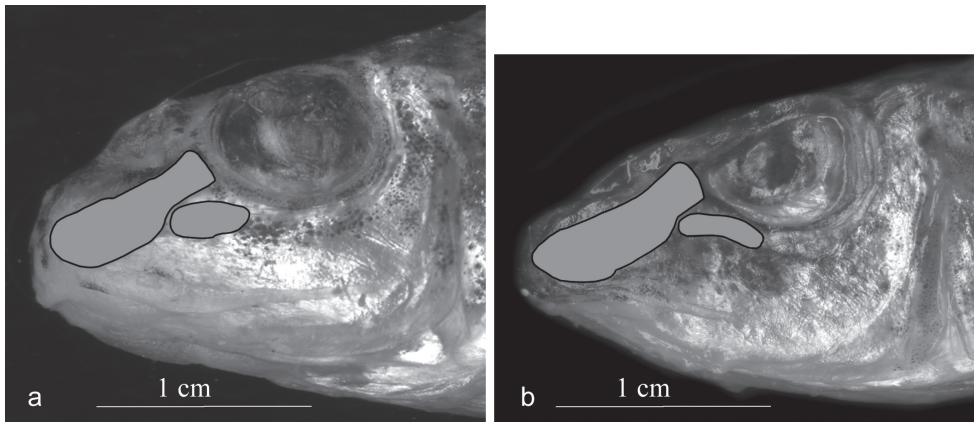


Figure 4. Lateral view of the head of *Romanogobio benacensis* (a) and *Gobio obtusirostris* (b); the 1st and 2nd infraorbital bones are shaded. Scale bar 1 cm.

(Bianco and Ketmaier 2005, Madeira et al. 2005, Yang et al. 2006, Tang et al. 2011, this study) most likely originates from the use of different sequence lengths (342 bp in Bianco and Ketmaier 2005 vs. 1141 bp in other studies). Similarly, a 657 bp COI fragment used in Geiger et al. (2012) could be less informative than a longer cytb fragment used in this study. A better resolution is expected using longer sequences in phylogenetic reconstructions although non-hierarchical relations can characterize some phylogenies no matter of the length of used sequences (Strimmer and von Haeseler 1997).

The Mirna population represents a single area of occurrence of *R. benacensis* out of its known distribution range in the south-east of the Soča (Isonzo) drainage. If the species is native in the Mirna River, this is the only occurrence of a native species belonging to the genus *Romanogobio* and the subfamily Gobioninae along the Croatian section of the Adriatic coast (the Dalmatia freshwater ecoregion *sensu* Abell et al. 2008). It may be an evidence of past connections between Istrian rivers and the paleo-Po drainage. A similar “paleo-Po” distribution is reported for the triotto *Leucos aula* (Bonaparte), the Padanian barbel *Barbus plebejus* Bonaparte, the alborella *Alburnus arborella* (Bonaparte) and some other fish species (Kottelat and Freyhof 2007), also for an amphibian, the Italian agile frog *Rana latastei* Boulenger (Gasc et al. 1997) and a freshwater decapod crustacean, the white-clawed crayfish *Austropotamobius pal-lipes* (Lereboullet) (Jelić et al. 2016b). However, a human mediated translocation of *R. benacensis* cannot be excluded; rather it is a supposition to be further investigated. For example, *G. obtusirostris* in the Ričica River (Lika Region, Adriatic basin) probably originates from the Danube drainage (Jelić et al. 2016a).

Only four specimens of *R. benacensis* were collected in spite of an intensive sampling effort. Since no other gudgeon species was reported in the Mirna River, an ongoing population extirpation by competition (e.g. with *G. gobio* as reported by Bianco and Ketmaier (2005) in Italy) can be excluded as a reason for low population density. Nevertheless, competition with non-native cyprinid species such as *P. parva*, or a pre-

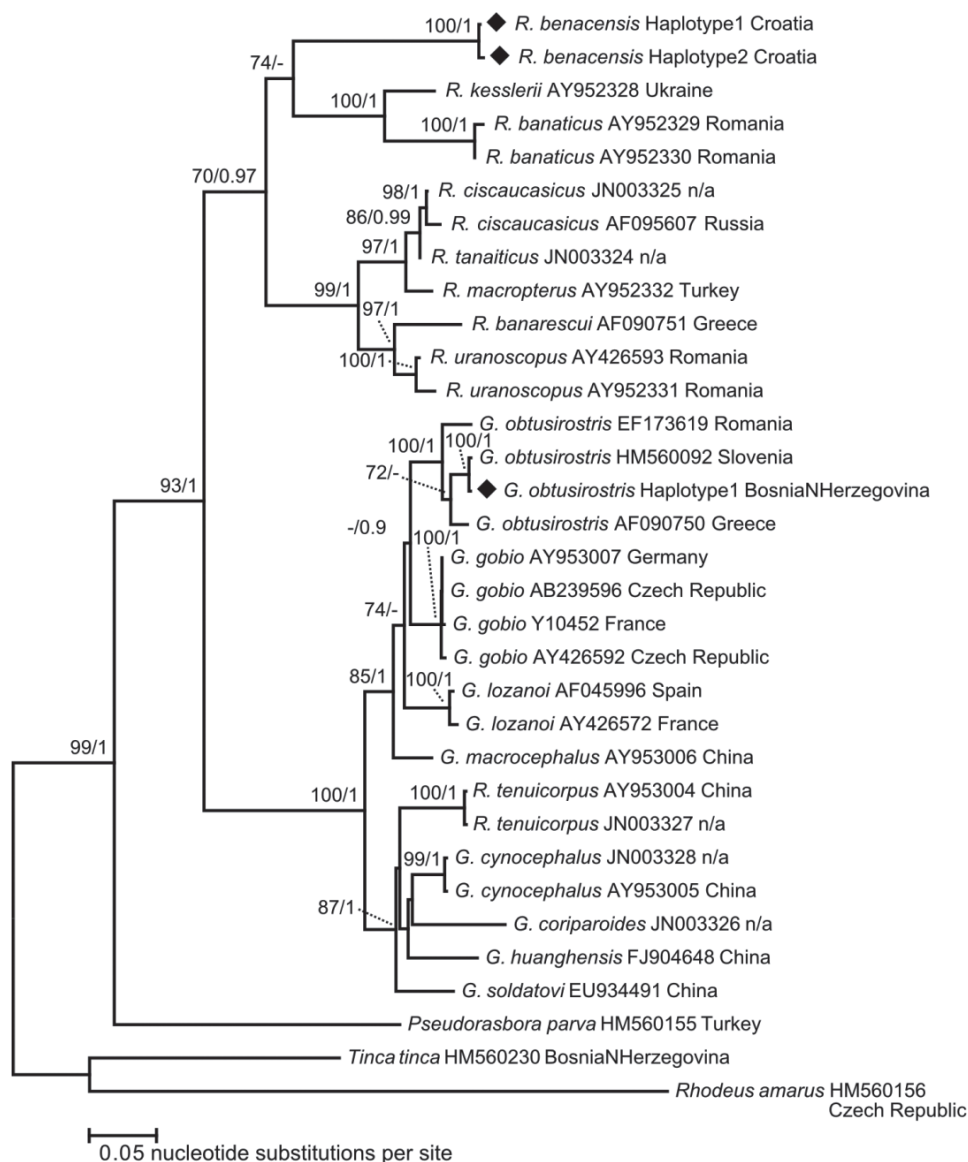


Figure 5. Result of DFA performed on 15 (8 meristic and 7 morphometric) distinguishing characters to classify Reka and Mirna samples.

dation by allochthonous piscivorous fish such as the pike *Esox lucius* (Linnaeus) or the pike-perch *Sander lucioperca* (Linnaeus) should not be excluded.

Therefore, having in mind that small-sized populations are more prone to extirpation due to genetic drift, extinction vortex, etc., it is necessary to implement systematical monitoring on the present *R. benacensis* population, accompanied with a more

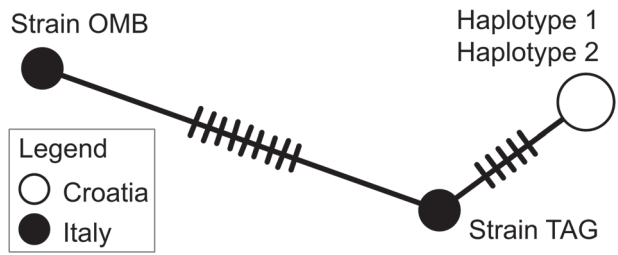


Figure 6. The MJ haplotype network of *Romanogobio benacensis*

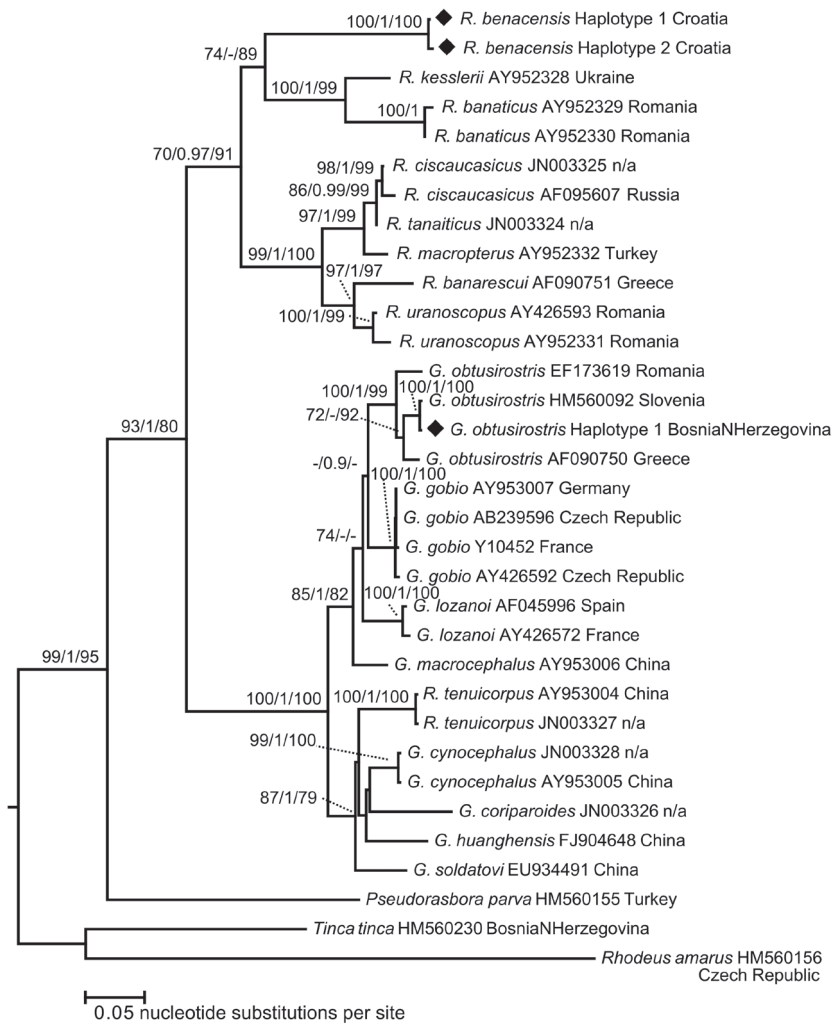


Figure 7. Phylogenetic tree inferred by ML analysis using cytb sequences of *Romanogobio* and *Gobio*. Newly obtained haplotypes in this study were marked by black rhombi. Node supports are given as bootstrap values (P) in ML and MP analyses (showing values ≥ 70) and posterior probabilities (pp) in IB (showing values ≥ 0.9).

intense sampling in order to reveal possible remaining populations and to characterize the gene pool of this endangered species, both crucial issues for further management and conservation.

Vernacular name. *Romanogobio benacensis* does not have any Croatian name as it has been only recently discovered in Croatian national territory. We offer “Talijanska krkuš” as its Croatian name, which originate from translation of vernacular name on English (the Italian gudgeon) and Italian (il gobione Italiano).

Acknowledgements

This research has been undertaken through research programmes of Croatian Biology Research Society (HDBI, Zagreb, Croatia) and Croatian Institute for Biodiversity (CIB, Croatia). AMN was supported by a contract from HDBI. We would like to thank Aleksandar Popijač and GEONATURA d.o.o. for help during the initial field work in Istria.

References

- Abell R, Thieme ML, Revenga C, Bryer M, Kottelat M, Bogutskaya N, Coad B, Mandrak N, Contreras Balderas S, Bussing W, Stiassny MLJ, Skelton P, Allen GR, Unmack P, Naseka A, Ng R, Sindorf N, Robertson J, Armijo E, Higgins JV, Heibel TJ, Wikramanayake E, Olson D, López HL, Reis RE, Lundberg JG, Sabaj Pérez MH, Petry P (2008) Freshwater ecoregions of the World: a new map of biogeographic units for freshwater biodiversity conservation. *Bioscience* 58(5): 403–414. <https://doi.org/10.1641/B580507>
- Bănărescu PM, Sorić VM, Economidis PS (1999) *Gobio gobio* (Linnaeus, 1758). In: Bănărescu PM (Ed) The freshwater fishes of Europe. Vol. 5/I. Cyprinidae 2. Part 1. *Rhodeus* to *Capoeta*. AULA Verlag, Wiebelsheim, 81–134. <https://doi.org/10.1093/oxfordjournals.molbev.a026036>
- Bandelt H, Forster P, Röhl A (1999) Median-joining networks for inferring intraspecific phylogenies. *Molecular Biology and Evolution* 16(1): 37–48.
- Bianco PG (1988) I Pesci d’acqua dolce d’Italia: note su un recente contributo. *Atti della Società italiana di scienze naturali e del Museo civico di storia naturale di Milano* 129: 146–158.
- Bianco PG (1991) Sui pesci d’acqua dolce del fiume Esino (Marche, Italia centrale). *Atti della Società italiana di scienze naturali e del Museo civico di storia naturale di Milano* 1325: 49–60.
- Bianco PG (2009) Threatened fishes of the world: *Gobio benacensis*. *Environmental Biology of Fishes* 84: 39–40. <https://doi.org/10.1007/s10641-008-9383-1>
- Bianco PG, Caputo V, Ferrito V, Lorenzoni M, Nonnis Marzano F, Stefani F, Sabatini A, Tancioni L (2013) IUCN Comitato Italiano. *Gobio benacensis*. <http://www.iucn.it/scheda.php?id=-1370993245> [Downloaded on July 7, 2016]
- Bianco PG, Ketmaier V (2001) Anthropogenic changes in the freshwater fish fauna of Italy, with reference to the central region and *Barbus graellsii*, a newly established alien species of Iberian origin. *Journal of Fish Biology* 59(sA): 190–208.

- Bianco PG, Ketmaier V (2005) Will the Italian endemic gudgeon, *Gobio benacensis*, survive the interaction with the invasive introduced *Gobio gobio*. *Folia Zoologica* 54(1): 42–49.
- Bianco PG, Taraborelli T (1984) *Gobio gobio benacensis* (Pollini, 1816) sottospecie valida per l'Italia (Pisces, Cyprinidae). *Bollettino del Museo Civico Storia naturale di Verona* 2: 525–536. [In Italian with English summary]
- Bianco PG (2014) Aggiornamento sistematico dei pesci d'acqua dolce autoctoni italiani: proposta di un workshop. *Italian Journal of Freshwater Ichthyology* 1: 133–162. [In English]
- Bogutskaya NG, Zupančič P, Bogut I, Naseka AM (2012) Two new freshwater fish species of the genus *Telestes* (Actinopterygii, Cyprinidae) from karst poljes in Eastern Herzegovina and Dubrovnik littoral (Bosnia and Herzegovina and Croatia). *ZooKeys* 180: 53–80. <https://doi.org/10.3897/zookeys.180.2127>
- Briolay J, Galtier N, Brito RM, Bouvet Y (1998) Molecular phylogeny of Cyprinidae inferred from cytochrome b DNA sequences. *Molecular Phylogenetics and Evolution* 9(1): 100–108. <https://doi.org/10.1006/mpev.1997.0441>
- Darriba D, Taboada GL, Doallo R, Posada D (2012) JModelTest 2: more models, new heuristics and parallel computing. *Nature Methods* 9(8): 772 pp. <https://doi.org/10.1038/nmeth.2109>
- Drummond AJ, Rambaut A (2007) BEAST: Bayesian evolutionary analysis by sampling trees. *BMC Evolutionary Biology* 7: 214 pp.
- Gasc J-P, Cabela A, Crnobrnja-Isailovic J, Dolmen D, Grossenbacher K, Haffner P, Lescure J, Martens H, Martínez Rica JP, Maurin H, Oliveira ME, Sofianidou TS, Veith M, Zuiderwijk A (Eds) (1997) *Atlas of Amphibians and Reptiles in Europe*. Societas Europaea Herpetologica and Muséum d'Histoire Naturelle (IEGB/SPN), Paris, 494 pp.
- Geiger M, Herder F, Manahan MT, Almada V, Barbieri R, Bohlen J, Casl-Lopez M, Delmastro GB, Denys GP, Dettai A, Doadrio I, Kalogianni E, Kärst H, Kottelat M, Kovačić M, Laporte M, Özuluğ M, Perdices A, Perea S, Persat H, Porcelotti S, Puzzo C, Robalo J, Šanda R, Schneider M, Šlechtová V, Stoumboudi M, Walter S, Freyhof J (2014) Spatial heterogeneity in the Mediterranean biodiversity hotspot affects barcoding accuracy of its freshwater fishes. *Molecular Ecology Resources* 14(6): 1210–1221. <https://doi.org/10.1111/1755-0998.12257>
- Goldman N, Anderson JP, Rodrigo AG (2000) Likelihood-based tests of topologies in phylogenetics. *Systematic Biology* 49: 652–670. <https://doi.org/10.1080/106351500750049752>
- Jelić D (2011a) Ihtiofauna rijeke Mirne i njenih pritoka. Report of Croatian Biological Research Society, Zagreb, 45 pp. [In Croatian with English summary]
- Jelić D (2011b) Popis vrsta slatkovodnih riba Republike Hrvatske, In: Ribe Hrvatske online portal Version 2012, Zagreb, www.ribe-hrvatske.com [In Croatian with English summary, Downloaded on 15.09.2015]
- Jelić D, Duplić A, Čaleta M, Žutinić P (2008) Endemske vrste riba jadranskog sliva (=Endemic fish of the Adriatic river system in Croatia). Croatian Environment Agency, Zagreb, 79 pp. [In Croatian with English summary]
- Jelić D, Jelić M (2016) *Telestes miloradi* Bogutskaya, Zupančič, Bogut and Naseka, 2012 and *Delminichthys ghetaidii* (Steindachner, 1882) re-discovered in Croatia, requiring urgent protection. *Journal of Applied Ichthyology* 31: 1133–1136. <https://doi.org/10.1111/jai.12879>

- Jelić D, Špelić I, Žutinić P (2016a) Introduced species community over-dominates endemic ichthyofauna of High Lika Plateau (Central Croatia) over a 100 year period. *Acta Zoologica Academiae Scientiarum Hungaricae* 62(2): 191–216. <https://doi.org/10.17109/AZH.62.2.191.2016>
- Jelić M, Klobučar GI, Grandjean F, Puillandre N, Franjević D, Futo M, Amouret J, Maguire I (2016b) Insights into the molecular phylogeny and historical biogeography of the white-clawed crayfish (Decapoda, Astacidae). *Molecular Phylogenetics and Evolution* 103: 26–40. <https://doi.org/10.1016/j.ympev.2016.07.009>
- Kishino H, Hasegawa M (1989) Evolution of the maximum likelihood estimate of the evolutionary tree topologies from DNA sequence data, and the branching order in Hominoidea. *Journal of Molecular Evolution* 29(2): 170–179. <https://doi.org/10.1007/BF02100115>
- Kottelat M (1997) European freshwater fishes. *Biologia (Bratislava)* 52(5): 1–271.
- Kottelat M, Freyhof J (2007) Handbook of European Freshwater Fishes. Kottelat, Cornol and Freyhof, Berlin, 646 pp.
- Leigh JW, Bryant D (2015) PopART: Full-feature software for haplotype network construction. *Methods in Ecology and Evolution* 6(9): 1110–1116. <https://doi.org/10.1111/2041-210X.12410>
- Leiner S, Povž M, Mrakovčić M (1995) Freshwater fish in Istrian peninsula. *Annales Series Historia Naturalis* 7: 215–222.
- Liu H, Yang J, Tang Q (2010) Estimated evolutionary tempo of East Asian gobionid fishes (Teleostei: Cyprinidae) from mitochondrial DNA sequence data. *Chinese Science Bulletin* 55(15): 1501–1510. <https://doi.org/10.1007/s11434-010-3159-7>
- Mace GM, Collar NJ, Gaston KJ, Hilton-Taylor C, Akçakaya HR, Leader-Williams N, Milner-Gulland EJ, Stuart SN (2008) Quantification of Extinction Risk: IUCN's System for Classifying Threatened Species. *Conservation Biology* 22(6): 1424–1442. <https://doi.org/10.1111/j.1523-1739.2008.01044.x>
- Machordom A, Doadrio I (2001) Evidence of a Cenozoic Betic-Kabilian connection based on freshwater fish phylogeography (*Luciobarbus*, Cyprinidae). *Molecular Phylogenetics and Evolution* 18(2): 252–263. <https://doi.org/10.1006/mpev.2000.0876>
- Madeira MJ, Gomez-Moliner BJ, Doadrio I (2005) Genetic characterization of *Gobio gobio* populations of the Iberian Peninsula based on cytochrome b sequences. *Folia Zoologica* 54(1): 5–12.
- Marčić Z, Buj I, Duplić A, Čaleta M, Mustafić P, Zanella D, Zupančič P, Mrakovčić M (2011) A new endemic cyprinid species from the Danube basin. *Journal of Fish Biology* 79(2): 418–430.
- Miller MA, Pfeiffer W, Schwartz T (2010) Creating the CIPRES Science Gateway for inference of large phylogenetic trees. In: Proceedings of the Gateway Computing Environments Workshop (GCE), 14 November 2010, New Orleans, LA, 1–8. <https://doi.org/10.1109/GCE.2010.5676129>
- Mrakovčić M, Brigić A, Buj I, Čaleta M, Mustafić P, Zanella D (2006) Crvena knjiga slatkovodnih riba Hrvatske (=Red Book of Croatian freshwater fish). Republic of Croatia, Ministry of Culture, Zagreb, 246 pp. [In Croatian with English summary]

- Mustafić P, Čaleta M, Mrakovčić M, Buj I, Zanella D, Mišetić S (2005) Distribution and status of the genus *Gobio* in Croatia. *Folia Zoologica* 54(1): 81–84.
- Naseka AM (1996) Comparative study on the vertebral column in the Gobioninae (Pisces, Cyprinidae) with special reference to its systematics. *Publ. Spec. Instituto Español de Oceanografía* 21: 149–167.
- Naseka AM, Bogutskaya NG, Poznjak VG (2002) *Romanogobio pentatrichus* Naseka et Bogutskaya, 1998. In: Bănărescu PM, Paepke HJ (Eds) *The Freshwater Fishes of Europe*. Vol. 5. Cyprinidae – 2. Pt.3. *Camassius* to *Cyprinus*: Gasterosteidae. AULA-Verlag, Wiebelsheim, 187–200.
- Naseka AM, Freyhof J (2004) *Romanogobio parvus*, a new gudgeon from River Kuban, southern Russia (Cyprinidae, Gobioninae). *Ichthyological Exploration of Freshwaters* 15: 17–23.
- Nei M, Kumar S (2000) *Molecular Evolution and Phylogenetics*. Oxford University Press, New York.
- Nylander JAA, Wilgenbusch JC, Warren DL, Swofford DL (2008) AWTY (are we there yet?): a system for graphical exploration of MCMC convergence in Bayesian phylogenetics. *Bioinformatics* 24(4): 581–583. <https://doi.org/10.1093/bioinformatics/btm388>
- Perea S, Böhme M, Zupančič P, Freyhof J, Šanda R, Ozuluğ M, Abdoli A, Doadrio I (2010) Phylogenetic relationships and biogeographical patterns in Circum-Mediterranean subfamily Leuciscinae (Teleostei, Cyprinidae) inferred from both mitochondrial and nuclear data. *BMC Evolutionary Biology* 10: 265 pp.
- Pizzul E, Specchi M, Valli G (1993) *Gobio gobio benacensis* (Pollini, 1816) (Osteichthyes, Cyprinidae) nelle acque del Friuli-Venezia Giulia. *Atti del museo civico di storia naturale di Trieste* 45: 163–168.
- Pollini C (1816) *Viaggio al Lago di Garda e al Monte Baldo in cui si ragiona delle cose naturali di quei luoghi aggiuntovi un cenno sulle curiosità del Bolca e degli altri monte Veronesi*. Tip. Mainardi, Verona, 152 pp. <https://doi.org/10.5962/bhl.title.53793> [In Italian]
- Povž M, Gregori A, Gregori M (2015) *Sladkovodne ribe in piškurji v Sloveniji* (= Freshwater fishes and lampreys of Slovenia). Zavod Umbra, Ljubljana, 293 pp. [In Slovenian]
- Povž M, Šumer S, Mrakovčić M, Mustafić P (2005) Present status and distribution of *Gobio* spp. in Slovenia. *Folia Zoologica* 54(1): 85–89.
- Ronquist F, Teslenko M, van der Mark P, Ayres DL, Darling A, Höhna S, Larget B, Liu L, Suchard MA, Huelsenbeck JP (2012) MrBayes 3.2: efficient Bayesian phylogenetic inference and model choice across a large model space. *Systematic Biology* 61(3): 539–542. <https://doi.org/10.1093/sysbio/sys029>
- Saitoh K, Sado T, Mayden RL, Hanzawa N, Nakamura K, Nishida M, Miya M (2006) Mitogenomic evolution and interrelationships of the Cypriniformes (Actinopterygii: Ostariophysi): the first evidence toward resolution of higher-level relationships of the world's largest freshwater fish clade based on 59 whole mitogenome sequences. *Journal of Molecular Evolution* 63 (6): 826–841. <https://doi.org/10.1007/s00239-005-0293-y>
- Schmidt HA, Strimmer K, Vingron M, von Haeseler A (2002) TREE-PUZZLE: maximum likelihood phylogenetic analysis using quartets and parallel computing. *Bioinformatics* 18: 502–504. <https://doi.org/10.1093/bioinformatics/18.3.502>
- Shimodaira H, Hasegawa M (1999) Multiple comparisons of log-likelihoods with applications to phylogenetic inference. *Molecular Biology and Evolution* 16: 1114–1116. <https://doi.org/10.1093/oxfordjournals.molbev.a026201>

- Stamatakis A (2014) RAxML Version 8: A tool for phylogenetic analysis and post-analysis of large phylogenies. *Bioinformatics* 30(9): 1312–1313. <https://doi.org/10.1093/bioinformatics/btu033>
- Strimmer K, Rambaut A (2002) Inferring confidence sets of possibly misspecified gene trees. *Proceedings of the Royal Society of London Series B-Biological Sciences* 269: 137–142. <https://doi.org/10.1098/rspb.2001.1862>
- Strimmer K, von Haeseler A (1997) Likelihood-mapping: a simple method to visualize phylogenetic content of a sequence alignment. *Proceedings of the National Academy of Sciences of the United States* 94: 6815–6819. <https://doi.org/10.1073/pnas.94.13.6815>
- Tamura K, Stecher G, Peterson D, Filipski A, Kumar S (2013) MEGA6: Molecular Evolutionary Genetics Analysis version 6.0. *Molecular Biology and Evolution* 30: 2725–2729. <https://doi.org/10.1093/molbev/mst197>
- Tang KL, Agnew MK, Chen WJ, Vincent Hirt M, Raley ME, Sado T, Schneider LM, Yang L, Bart HL, He S, Liu H, Miya M, Saitoh K, Simons AM, Wood RM, Mayden RL (2011) Phylogeny of the gudgeons (Teleostei: Cyprinidae: Gobioninae). *Molecular Phylogenetics and Evolution* 61(1): 103–124. <https://doi.org/10.1016/j.ympev.2011.05.022>
- Tavaré S (1986) Some probabilistic and statistical problems in the analysis of DNA sequences, In: Miura RM (Ed) *Lectures on mathematics in the life sciences*. Volume 17. American Mathematical Society, Providence (RI), 57–86.
- Yang J, He S, Freyhof J, Witte K, Liu H (2006) The phylogenetic relationships of the Gobioninae (Teleostei: Cyprinidae) inferred from mitochondrial cytochrome b gene sequences. *Hydrobiologia* 553: 255–266. <https://doi.org/10.1007/s10750-005-1301-3>
- Zardoya R, Doadrio I (1998) Phylogenetic relationships of Iberian cyprinids: systematic and biogeographical implications. *Proceedings of the Royal Society, London, series B, Biological Science* 265 (1403): 1365–1372. <https://doi.org/10.1098/rspb.1998.0443>
- Zardoya R, Doadrio I (1999) Molecular evidence on the evolutionary and biogeographical patterns of European cyprinids. *Journal of Molecular Evolution* 49 (2): 227–237. <https://doi.org/10.1007/PL00006545>
- Zupančič P, Bogutskaya NG (2002) Description of two new species, *Phoxinellus krbavensis* and *P. jadovensis*, re-description of *P. fontinalis* Karaman, 1972, and a discussion of the distribution of *Phoxinellus* species (Teleostei: Cyprinidae) in Croatia and Bosnia-Herzegovina. *Natura Croatica* 11 (4): 411–437.
- Zupančič P, Tisaj D, Lah LJ (2008) Rijetke i ugrožene slatkovodne ribe Jadranskog slijeva Hrvatske, Slovenije i Bosne i Hercegovine (= Rare and endangered freshwater fishes of Croatia, Slovenia and Bosnia and Herzegovina - Adriatic basin). AZV, Dolsko, 79 pp. [In Slovenian with English summary]

More new deep-reef basslets (Teleostei, Grammatidae, *Lipogramma*), with updates on the eco-evolutionary relationships within the genus

Carole C. Baldwin¹, Luke Tornabene², D. Ross Robertson³,
Ai Nonaka¹, R. Grant Gilmore⁴

1 Department of Vertebrate Zoology, National Museum of Natural History, Smithsonian Institution, Washington, DC, 20560, USA **2** School of Aquatic and Fishery Sciences, Burke Museum of Natural History and Culture, University of Washington, Seattle, WA, USA **3** Smithsonian Tropical Research Institute, Balboa, Republic of Panama **4** Estuarine, Coastal and Ocean Science, Inc., 5920 First Street SW, Vero Beach, FL, 32968, USA

Corresponding author: Carole C. Baldwin (baldwinc@si.edu)

Academic editor: D. Bloom | Received 24 October 2017 | Accepted 2 January 2018 | Published 16 January 2018

<http://zoobank.org/863BCE02-2C37-4DC2-9623-1517A1EE74D6>

Citation: Baldwin CC, Tornabene L, Robertson RD, Nonaka A, Gilmore GR (2018) More new deep-reef basslets (Teleostei, Grammatidae, *Lipogramma*), with updates on the eco-evolutionary relationships within the genus. ZooKeys 729: 129–161. <https://doi.org/10.3897/zookeys.729.21842>

Abstract

Two new *Lipogramma* basslets are described, *L. barrettorum* and *L. schrieri*, captured during submersible diving to 300 m depth off Curaçao, southern Caribbean. Superficially resembling *L. robinsi* in having 11–12 bars of pigment on the trunk, *L. barrettorum* is distinct from *L. robinsi* in having a stripe of blue-white pigment along the dorsal midline of the head (vs. a cap of yellow pigment), in patterns of pigment on the median fins, and in having 8–10 gill rakers on the lower limb of the first arch (vs. 11–12). *Lipogramma schrieri* is distinct from all congeners in having seven or eight dark bars of pigment on the trunk and broad, irregular, whitish blue markings on the dorsal portion of the head. The new species are genetically distinct from one another and from seven other *Lipogramma* species for which genetic data are available. A phylogenetic hypothesis derived from mitochondrial and nuclear genes suggests that the new species belong to a clade that also comprises *L. evides* and *L. haberi*. Collectively those four species are the deepest-living members of the genus, occurring at depths predominantly below 140 m. This study thus provides further evidence of eco-evolutionary correlations between depth and phylogeny in Caribbean reef fishes. Tropical deep reefs are globally underexplored ecosystems, and further investigation of Caribbean deep reefs undoubtedly will provide samples of species for which no genetic material currently exists and reveal more cryptic species diversity in the genus.

Keywords

Caribbean Sea, manned submersible, cryptic species, integrative taxonomy, phylogeny, ocean exploration, Deep Reef Observation Project (DROP)

Introduction

Baldwin et al. (2016) described two new species of western Atlantic *Lipogramma* basslets collected during diving to 300 m by the *Curasub* submersible, as part of the ongoing Deep Reef Observation Project (DROP) in the southern Caribbean. That brought the total number of species in the genus to 10. However, they noted that their deep-reef collections included two additional putative new species that superficially resemble *L. robinsi* Gilmore 1997. Further investigation has confirmed that these two species represent additional cryptic diversity in the Grammatidae, a family of usually small, brightly colored fishes restricted to deep reefs of the tropical northwest Atlantic Ocean. Here we describe the two new species of *Lipogramma* based on integrated morphological and molecular data, provide a revised phylogenetic hypothesis of relationships within the genus that includes *L. regia* (which we recently caught using the *Curasub* off St. Eustatius), comment on the eco-evolutionary history of the group based on the phylogenetic pattern of species' depth distributions, and present a revised key to the species of the genus.

Methods

Collecting and morphology. Basslets were collected using Substation Curaçao's manned submersible *Curasub* (<http://www.substation-curacao.com>). The sub has two flexible, hydraulic arms, one of which is equipped with a quinaldine/ethanol-ejection system and the other with a suction hose. Anesthetized fish specimens were captured with the suction hose, which empties into a vented plexiglass cylinder attached to the outside of the sub. At the surface, the specimens were photographed, tissue sampled, and fixed in 10% formalin. Measurements were made weeks to months after fixation and subsequent preservation in 75% ethanol and were taken to the nearest 0.1 mm with dial calipers or an ocular micrometer fitted into a Wild stereomicroscope. Selected preserved specimens were later photographed to document preserved pigment pattern and X-rayed with a digital radiography system. Images of parasitic cysts were made using a Zeiss Axiocam on a Zeiss Discovery V12 SteREO microscope. Counts and measurements follow Hubbs and Lagler (1947). Symbolism for configuration of supraneural bones, anterior neural spines, and anterior dorsal pterygiophores follows Ahlstrom et al. (1976): **USNM** = Smithsonian Institution, National Museum of Natural History; **UF** = Florida Museum of Natural History.

Molecular analyses. Tissue samples for 98 specimens assignable to nine species of *Lipogramma* were used for molecular analyses (Appendix 1). Tissues of *L. robinsi*,

L. rosea Gilbert, 1979 (in Robins and Colin 1979), and *L. flavescens* Gilmore & Jones, 1988 were not available. Tissues were stored in saturated salt-DMSO (dimethyl sulfoxide) buffer (Seutin et al. 1991). DNA extraction and cytochrome *c* oxidase subunit I (COI) DNA barcoding were performed for 98 specimens (i.e., for all available specimens except one *L. anabantoides* – Appendix 1) as outlined by Weigt et al. (2012). Four nuclear markers were amplified and sequenced—TMO-4C4, Rag1, Rhodopsin, and Histone H3—for 19 specimens of *Lipogramma*, and one or more of those genes was sequenced for an additional three specimens (Appendix 1). Primers and PCR conditions for the nuclear markers followed Lin and Hastings (2011, 2013). Sequences were assembled and aligned using *Geneious v. 9* (Biomatters, Ltd., Auckland). A neighbor-joining (NJ) network was generated for the COI data using the K2P substitution model (Kimura 1980) in the tree-builder application in *Geneious*. Mean within- and between-species K2P genetic distances were calculated from the COI data in *MEGA v. 7* (Kumar et al. 2015). Genetic distances were considered as corroborating morphology-based species delineation if the distances between species were ten or more times the intraspecific differences (Hebert et al. 2004). The alignments of COI and nuclear genes were concatenated and phylogeny was inferred using Bayesian Inference (BI), partitioning by gene. For the Bayesian analysis, substitution models and partitioning scheme were chosen using PartitionFinder (Lanfear et al. 2012) according to Bayesian Information Criterion scores. The chosen scheme had the following partitions and models: COI, HKY+I+G; Histone H3 plus Rhodopsin, HKY+G; TMO-4C4, K80+G; Rag1, K80+G. All partitions in the ML analysis received a GTR-GAMMA substitution model. The BI phylogeny was inferred in the program *MrBayes v. 3.2* (Ronquist et al. 2012) using two Metropolis-coupled Markov Chain Monte Carlo (MCMC) runs, each with four chains. The analysis ran for 10 million generations sampling trees and parameters every 1000 generations. Burn-in, convergence and mixing were assessed using Tracer (Rambaut and Drummond 2007) and by visually inspecting consensus trees from both runs. Outgroups for the phylogenetic analysis included two species of *Gramma* and several other genera from the Ovalentaria *sensu* Wainwright et al. (2012): *Acanthemblemaria* (Chaenopsidae), *Helcogramma* (Tripterygiidae), *Blenniella* (Blenniidae), and *Tomicodon* (Gobiesocidae).

To further corroborate the morphologically diagnosed species using our molecular data, we conducted a coalescent-based, Bayesian species-delimitation analysis (Yang and Rannala 2010, 2014). We used the computer program BP&P ver. 3.2 (Bayesian Phylogenetics and Phylogeography – Yang and Rannala [2010], Yang [2015]), which analyzes multi-locus DNA sequence alignments under the multispecies coalescent model (Rannala and Yang 2003). We used the five DNA alignments for the 22 *Lipogramma* specimens in BP&P, with each sequence in the alignments being assigned to one of nine groups *a priori*, based on diagnostic features of morphology and pigmentation. BP&P was then used to simultaneously infer a species tree and calculate posterior probabilities of different species-delimitation models, i.e., models comprising nine species, fewer than nine species (lumping multiple “morpho-species”), or more than nine species (splitting “morpho-species”).

Depth distributions. We updated the depth histogram for *Lipogramma* of Baldwin et al. (2017: fig. 10) with the new-species names (originally listed as “*L. ‘robinsi’* sp. 1” and “*L. ‘robinsi’* sp. 2”) and with new depth information for the new species and for *L. regia* based on submersible-caught specimens. Additionally, with resolution of the “*L. robinsi*” complex, we added *L. robinsi* based on depth information in the original description (Gillmore 1977).

Accession numbers. GenSeq nomenclature (Chakrabarty et al. 2013) and GenBank accession numbers for DNA sequences derived in this study are presented along with museum catalog numbers for voucher specimens in Appendix 1.

Taxonomy

Lipogramma barrettorum Baldwin, Nonaka & Robertson, sp. n.

<http://zoobank.org/B73F04C1-DBEB-4172-8E6E-71AC9625E76C>

English: Blue-Spotted Basslet; Spanish: Cabrillela manchado azul

Figures 1–3

Type locality. Curaçao, southern Caribbean.

Holotype. USNM 440439, 26.5 mm SL, tissue no. CUR16008, GenBank accession no. MG676227, Curasub submersible, sta. CURASUB16-33, Curaçao, west of Substation Curaçao downline, 12.083197 N, 68.899058 W, 161 m depth, 7 October 2016, C. Baldwin, B. Van Bebber, D. Pitassy & T. Devine.

Paratypes. USNM 406392, 24.5 mm SL, tissue no. CUR11392, Curasub submersible, sta. CURASUB11-06, Curaçao, off Substation Curaçao, 12.083197 N, 68.899058 W, 132–141 m depth, 31 May 2011, C. Baldwin, B. Van Bebber, A. Schrier & A. Driskell; UF 239254, 28.0 mm SL, tissue no. CUR11426, collection information same as USNM 406392; USNM 414914, 13.0 mm SL, tissue no. CUR12149, Curasub submersible, sta. CURASUB12-15, Curaçao, off Substation Curaçao, 12.083197 N, 68.899058 W, 123–160 m depth, 10 August 2012, C. Baldwin, B. Brandt, A. Schrier & P. Mace; USNM 431687, 25.2 mm SL, tissue no. CUR14079, Curasub submersible, sta. CURASUB-MISC14, Curaçao, off Substation Curaçao, 12.083197 N, 68.899058 W, no depth data, September 2014, Substation Curaçao staff; USNM 436460, 27.0 mm SL, Tissue no. CUR15125, Curasub submersible, sta. CURASUB15-21, Curaçao, off Substation Curaçao, 12.083197 N, 68.899058 W, 90–249 m depth (no discrete depth observation), 22 September 2015, C. Baldwin, B. Brandt & E. Duffy; USNM 436474, 10.2 mm SL, tissue no. CUR15139, Curasub submersible, sta. CURASUB15-27, Curaçao, Playa Forti, 12.368 N, 69.155 W, 50–246 m (no discrete depth observation), 29 September 2015, A. Collins, B. Brandt, A. Schrier & T. Devine.

Diagnosis. A species of *Lipogramma* distinguishable from congeners by the following combination of characters: pectoral-fin rays 15–16 (modally 16); gill rakers 12–14 (modally 12, 8–10 rakers on lower limb); four supraorbital pores present along dorsal

margin of orbit, a pore present between one above mid orbit and one above postero-dorsal corner of orbit; caudal fin rounded; body mostly yellow in life with 11 or 12 narrow brownish bars on trunk; posterior base of soft dorsal fin with large white- or blue-rimmed black ocellus; dorsal, anal and caudal fins yellow with blue/grey (brown in preservative) wavy bars or square-shaped spots. Pelvic fins blue/grey with scattered yellow-ringed dark spots. The new species is further differentiated genetically from congeners for which molecular data are available in mitochondrial COI and nuclear Histone 3, Rhodopsin, TMO-4C4, and RAG1.

Description. Counts and measurements of type specimens given in Table 1. Seven specimens examined, 10.2–28.0 mm SL. Dorsal-fin rays XII, 9 (last ray composite); anal-fin rays III, 8 (last ray composite); pectoral-fin rays 15–16, modally 16, 16 on both sides of holotype; pelvic-fin rays I,5; total caudal-fin rays 25 (13 + 12), principal rays 17 (9 + 8), spinous procurent rays 6 (III + III), and 2 additional rays (i + i) between principal and procurent rays that are neither spinous nor typically segmented; vertebrae 25 (10 + 15); pattern of supraneural bones, anterior dorsal-fin pterygiophores, and dorsal-fin spines 0/0/0+2/1+1/1/; ribs on vertebrae 3–10; epineural bones present on at least vertebrae 1–14 in holotype; gill rakers on first arch 12–14 (3–4 + 8–10), modally 12 (3+9 or 4+8), 12 (3+9) in holotype; upper-limb rakers and lowermost one or two rakers very small or present only as nubs, all other gill rakers elongate and slender with tooth-like secondary rakers as in *L. evides* Robins & Colins 1979 (Baldwin et al [2016: fig. 3]); pseudobranchial filaments ~4–7 (~5 in holotype), filaments fat and fluffy but poorly formed in most specimens; branchiostegals 6.

Spinous and soft dorsal fins confluent, several soft rays at rear of fin forming slightly elevated lobe that extends posteriorly beyond base of caudal fin. Pelvic fin, when depressed, extending posteriorly to point between base of second or third anal-fin spine and posterior base of anal fin, first pelvic-fin ray elongate. Dorsal profile from snout to origin of dorsal fin convex. Diameter of eye of holotype contained three times in head length. Pupil slightly tear shaped, with small aphakic space anteriorly. Scales extending anteriorly onto posterior portion of head, ending short of coronal pore. Scales present on cheeks, opercle, preopercle, interopercle, and isthmus. Scales lacking on top of head, snout, jaws, and branchiostegals. Scales large and deciduous, too many scales missing in most specimens to make accurate scale counts. In one paratype (USNM 436460) approximately 21 lateral scales between shoulder and base of caudal fin, approximately 4 scale rows on cheek, and approximately 9 scale rows across body above anal-fin origin. Scales on head and nape without cteni, scales on rest of body ctenoid. Fins naked.

Margins of bones of opercular series smooth, opercle without spines. Single row of teeth on premaxilla posteriorly, broadening to 2–3 rows anteriorly, teeth in innermost row smallest, some teeth in outer row enlarged into small canines. Dentary similar, holotype with 6 enlarged teeth in outer row near symphysis. Vomer with chevron-shaped patch of teeth. Palatine with long series of small teeth. Conspicuous pores present in infraorbital canal (2 pores), portion of supraorbital canal bordering dorsal portion of orbit (4), on top of head (1 median coronal pore), preopercle (at least 5),

Table 1. Counts and measurements of type specimens of *Lipogramma barrettorum* sp. n. Measurements are in percent SL. “Other Caudal Rays” include “i” – a slender, flexible, non-spinous, and typically non-segmented ray and “I” – a spinous procurent ray.

	USNM 440439	USNM 406392	UF 239254	USNM 414914	USNM 431687	USNM 436460	USNM 436474
	Holotype	Paratype	Paratype	Paratype (juvenile)	Paratype	Paratype	Paratype (juvenile)
SL	26.5	24.5	28.0	13.0	25.2	27.0	10.2
Dorsal-fin Rays	XII, 9	XII, 9	XII, 9	XII, 9	XII, 9	XII, 9	XII, 9
Anal-fin Rays	III, 8	III, 8	III, 8	III, 8	III, 8	III, 8	III, 8
Principal Caudal Rays	9+8	9+8	9+8	9+8	9+8	9+8	9+8
Other Caudal Rays	IIIi+iIII	IIIi+iIII	IIIi+iIII	IIIi+iIII	IIIi+iIII	IIIi+iIII	IIIi+iIII
Pectoral-fin Rays	16, 16	15, 15	16, 15	15, 16	16, 16	16, 16	16, 15
Gill Rakers	3+9=12	3+10=13	4+10=14	-	3+~9=12	4+8=12	-
Head Length	39.6	36.7	38.2	39.2	40.1	38.9	39.2
Eye Diameter	13.2	13.1	12.1	14.6	12.7	12.6	14.7
Snout Length	7.9	7.3	8.2	7.7	7.9	8.9	8.8
Depth at Caudal Peduncle	19.2	18.4	21.8	17.7	17.5	20.4	18.6
Depth at Pelvic-fin Origin	31.3	31.4	30.0	29.2	31.7	30.4	31.4
Length of Pectoral Fin	24.9	24.5	Broken	Broken	22.2	22.6	19.6
Length of Pelvic Fin	49.1	42.9	Broken	31.5	34.5	40.0	34.3
Length of 12 th Dorsal Spine	18.5	20.8	19.6	15.4	17.9	18.9	19.6

and lateral-line canal in the post-temporal region (3). The 4 supraorbital pores situated as illustrated by Baldwin et al. (2016: fig 4) for *L. evides*. Posterior nostril situated just ventral to anteriormost supraorbital pore, nostril a single large opening. Anterior nostril at apex of elongate narial tube and situated just posterior to upper lip. No lateral line present on body.

Coloration: *In life or deceased but prior to preservation* (Fig. 1): ground color of body brownish yellow, head darker than trunk, especially on underside. *Head*: dorsal midline of head with thin blue-white stripe beginning on lower lip, continuing on upper lip and over snout to nape; iris yellow, blue-white bars anterior and posterior to pupil; an indistinct yellow/brown bar from center of lower edge of iris to lower jaw, bar bordered anteriorly and posteriorly by smaller pale bars that extend up to top of eye. *Trunk*: 9–12 narrow dark bars between pectoral-fin base and caudal peduncle, bars about as wide as paler interspaces. *Dorsal fin*: yellow, with a thin blue-grey margin; series of straight, wavy, or irregular blue-grey bars on basal 2/3 of spinous dorsal fin; basal half of soft-dorsal with a large black ocellus complete ringed in blue-white pigment, ocellus extending onto trunk; distal half of fin with 2–3 rows blue-grey round-to square-shaped spots, these markings (here and on other unpaired fins) with pale centers and darker edges. *Anal fin*: yellow, with a thin blue-grey margin; 5–6 rows of blue-grey square-shaped spots between fin base and margin, some of which may fuse to form irregular lines. *Caudal fin*: yellow, with thin blue-grey posterior margin

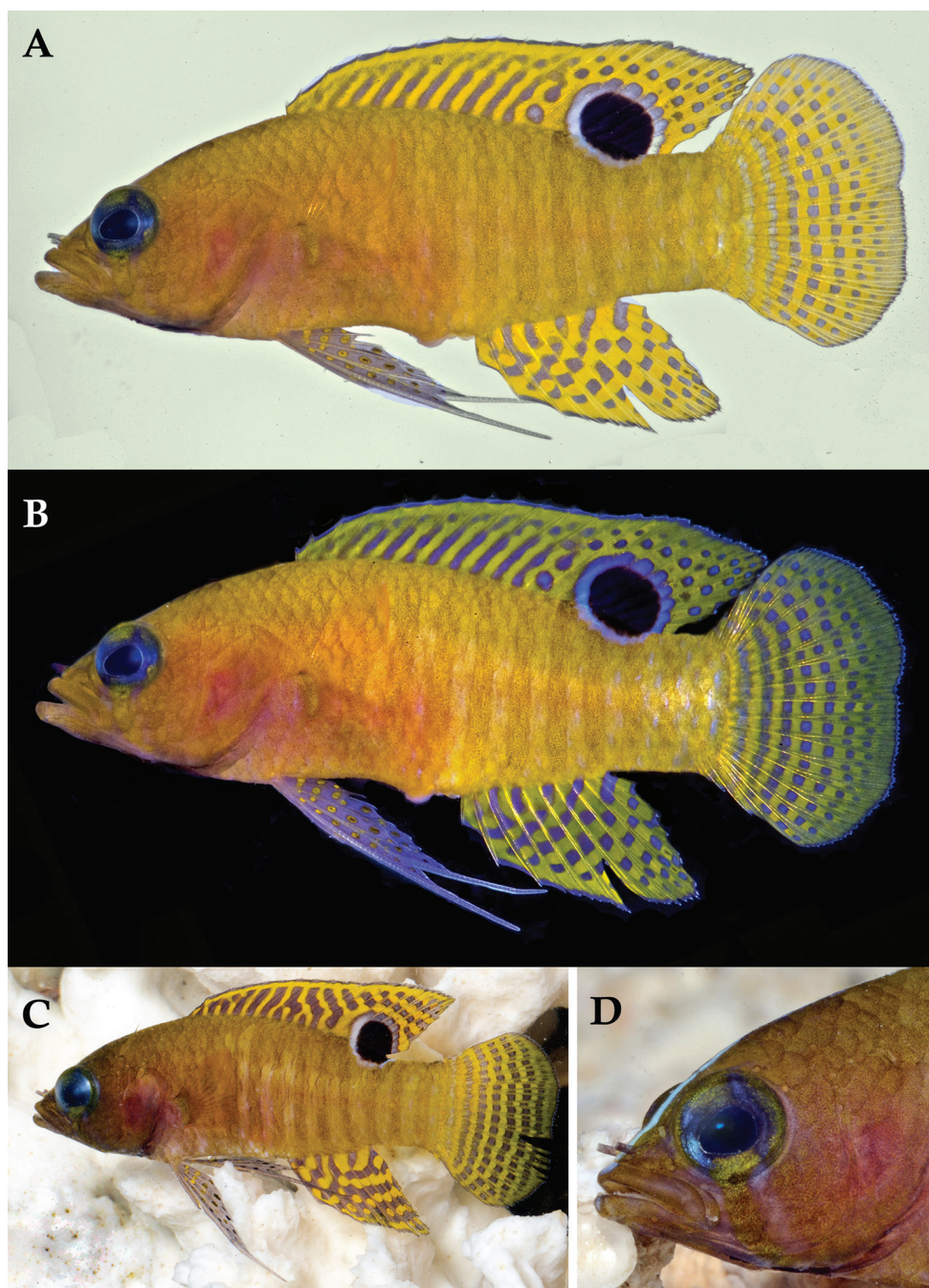


Figure 1. *Lipogramma barrettorum* sp. n. UF 239254, CUR11426, paratype, 28.0 mm SL **A** photographed against a light background and **B** against a dark background. Photographs by D. R. Robertson and C. C. Baldwin. **C** and **D** USNM 440439, CUR16008, holotype, 26.5 mm SL, aquarium photographs by Barry Brown.

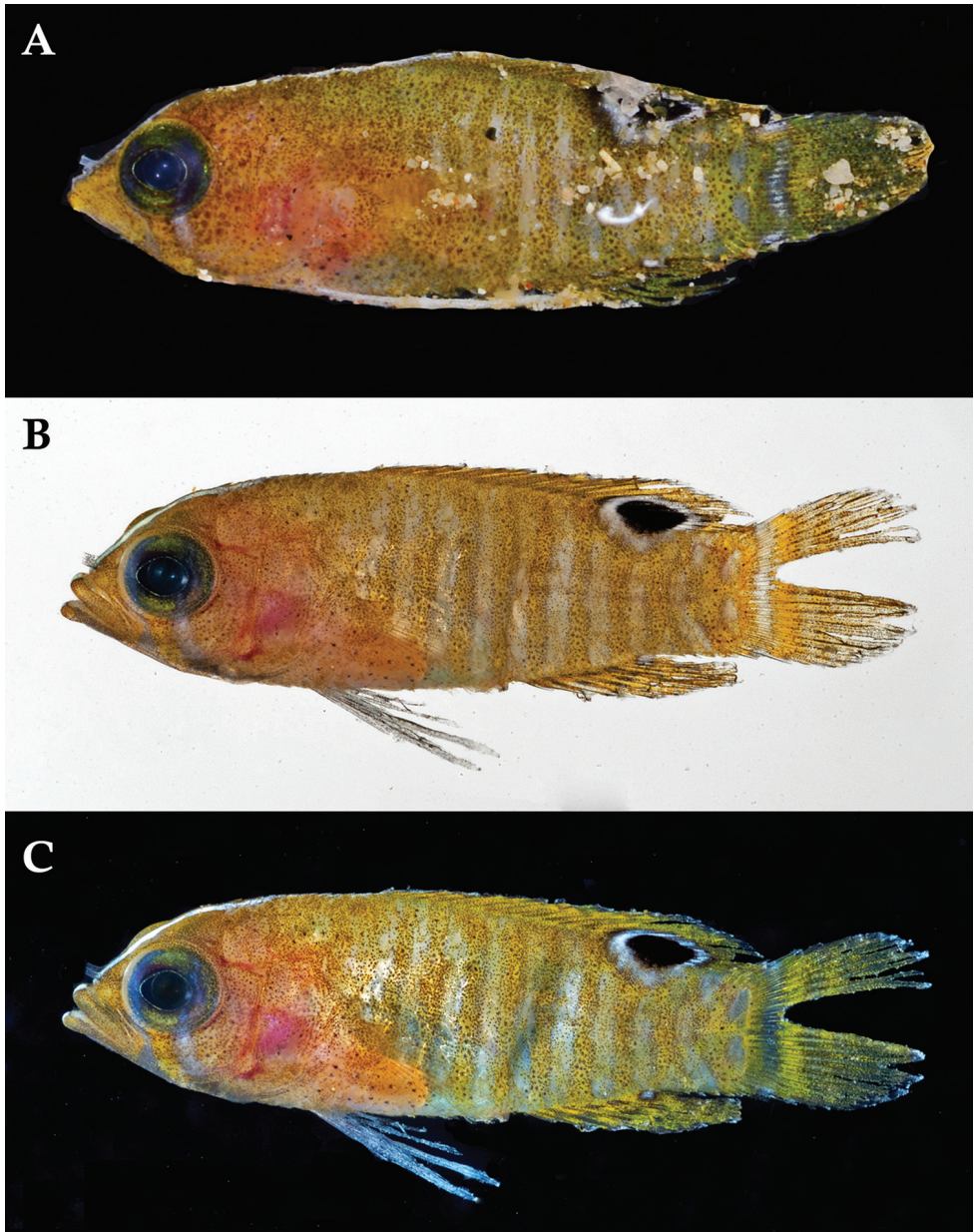


Figure 2. *Lipogramma barrettorum* sp. n. **A** USNM 436474, CUR15139, paratype, 10.2 mm SL **B** and **C** USNM 414914, CUR12149, paratype, 13.0 mm SL, photographed against light (**B**) and dark (**C**) backgrounds. Photographs by D. R. Robertson and C. C. Baldwin.

and 6–7 bars formed by vertical rows of blue-grey square-shaped spots on inter-radial membranes, basal two rows palest. *Pectoral fins*: translucent, base as dark as trunk bars. *Pelvic fins*: opposite color scheme to that of other fins, i.e., mostly blue-grey with yel-



Figure 3. Preserved holotypes of new *Lipogramma* species **A** *L. barrettorum*, USNM 440439, CUR16008, 26.5 mm SL **B** *L. schrieri*, USNM 431722, CUR14114, 49.7 mm SL. Photographs by C. C. Baldwin.

low spots along inter-radial membranes; proximally, spots with tiny black center; distally, dark centers larger, some spots appearing completely dark. *Juveniles*: the 12- and 15-mm SL paratypes (Fig. 2) with similar pigment pattern as adults. *Comment regarding live coloration*: photographed against a light background (Fig. 1A, C), “blue-grey” in description above = grey; photographed against a black background (Fig. 1B), “blue-grey” = blue. *Preserved coloration* (Fig. 3A): Head mostly brown, trunk mostly tan with darker tan to brown bars. Yellow portions of median fins in life clear in preservative, blue-grey markings on fins in life dark brown to black in preservative.

Distribution. Known only from specimens collected off Curaçao, southern Caribbean.

Habitat. Lives in or immediately above elevated rocky habitat with ample cracks or holes into which the fish retreated upon approach of the submersible. The holotype was collected at 161 m, which is the only discrete depth recording for the species. Depth ranges for two specimens were recorded as 123–160 m and 132–141 m, thus providing a potential total depth range of 123–161 m. Depth ranges for two additional specimens of 90–249 m and 50–246 m reflect depths visited during an entire

Table 2. Average Kimura two-parameter distance summary for species of *Lipogramma* based on cytochrome c oxidase I (COI) sequences analyzed in this study. Intraspecific averages are in bold.

	<i>L. barrettorum</i>	<i>L. regia</i>	<i>L. evides</i>	<i>L. schrieri</i>	<i>L. levinsoni</i>	<i>L. haberi</i>	<i>L. anabantoides</i>	<i>L. trilineata</i>	<i>L. klayi</i>
<i>L. barrettorum</i> (n=7)	0.003								
<i>L. regia</i> (n=1)	0.182	–							
<i>L. evides</i> (n=30)	0.099	0.201	0.002						
<i>L. schrieri</i> (n=7)	0.117	0.197	0.123	0.002					
<i>L. levinsoni</i> (n=15)	0.158	0.152	0.167	0.165	0.001				
<i>L. haberi</i> (n=3)	0.107	0.185	0.108	0.131	0.182	0.002			
<i>L. anabantoides</i> (n=2)	0.185	0.188	0.210	0.179	0.153	0.193	0.005		
<i>L. trilineata</i> (n=12)	0.214	0.207	0.242	0.246	0.227	0.235	0.254	0.005	
<i>L. klayi</i> (n=21)	0.253	0.243	0.253	0.253	0.248	0.264	0.239	0.240	0.003

submersible dive and provide little information relevant to establishing this species’ depth distribution.

Etymology. Named *Lipogramma barrettorum* in recognition of the support of Craig and Barbara Barrett for the Smithsonian’s Deep Reef Observation Project (DROP).

Common name. We propose blue-spotted basslet in reference to the numerous blue/grey markings on the dorsal, anal, and caudal fins in life.

Genetic comparisons. Table 2 shows average inter- and intraspecific divergences in COI among species of *Lipogramma* analyzed genetically in this study. Average intraspecific divergence among the seven specimens of *L. barrettorum* is 0.003 substitutions per site, and interspecific divergences between it and the other species for which data are available range from 9.9% (*L. evides*) to 25.3% (*L. klayi*).

Comments. The holotype has two cysts, one at the base of the uppermost left pectoral-fin ray and one about mid-way along the length of the elongate first left pelvic-fin ray (Fig. 4). The cysts or galls are likely parasitic, but further analysis is needed. No other cysts were observed on the holotype or paratypes.

***Lipogramma schrieri* Baldwin, Nonaka & Robertson, sp. n.**
<http://zoobank.org/4BB82A69-DE7F-438D-8DE3-740D00396C08>
English: Maori Basslet; Spanish: Cabrilleta maorí
Figures 3, 5, 6

Type locality. Curaçao, southern Caribbean.

Holotype. USNM 431722, 49.7 mm SL, tissue no. CUR14114, GenBank accession no. KX713790, Curasub submersible, sta. CURASUB 14-15, Curaçao, Jan Thiel Bay, 12.0746 N, 68.8825 W, 197 m, 19 September 2014, C. Baldwin, B. Brandt & A. Schrier.

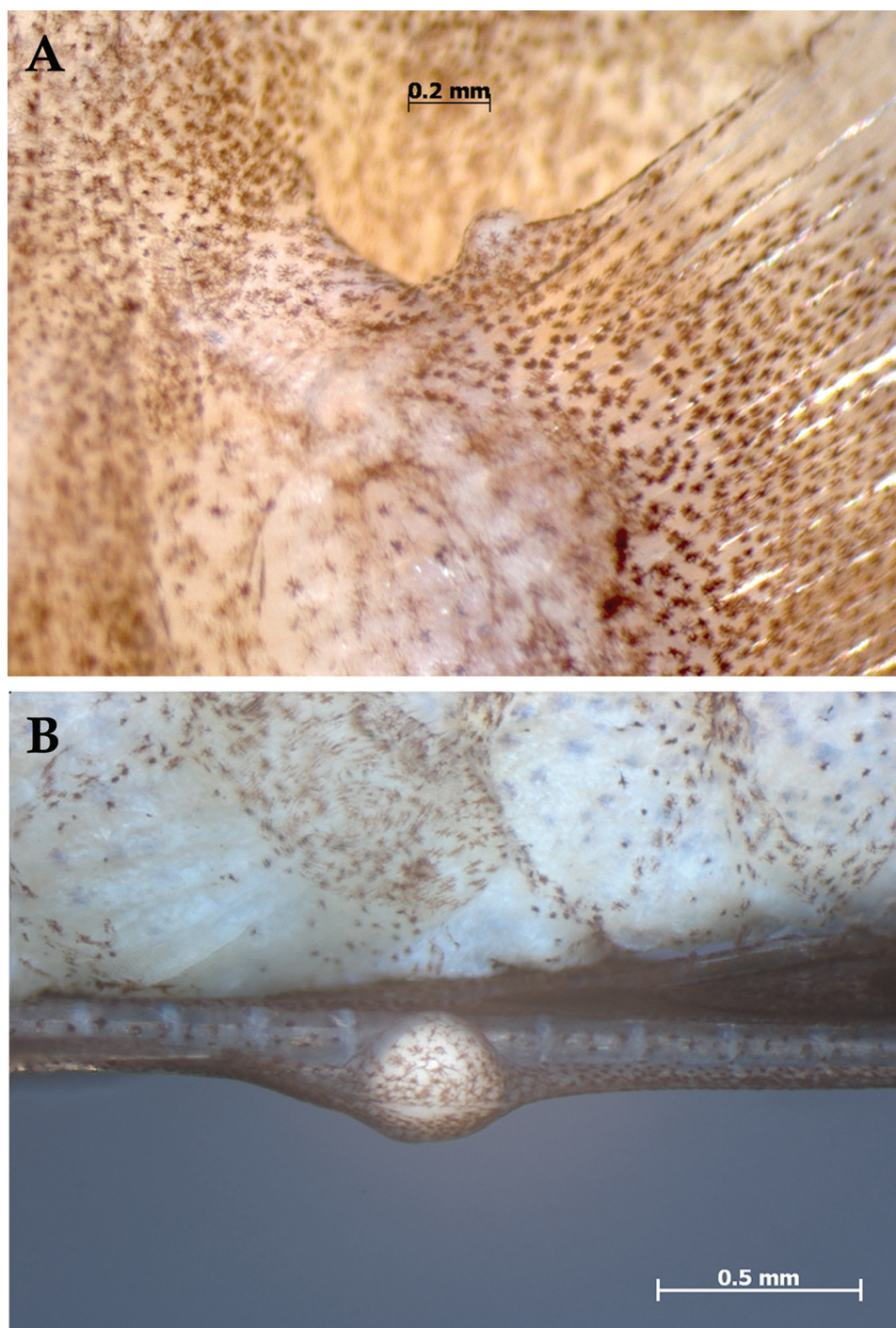


Figure 4. Cysts on fin rays of *Lipogramma barrettorum*, USNM 440439, CUR16008, holotype, 26.5 mm SL **A** left pectoral fin showing cyst on uppermost ray **B** elongate first left pelvic-fin ray showing cyst about midway along its length. Photographs by A. Nonaka.

Paratypes. USNM 414913, 56.0 mm SL, tissue no. CUR12101, Curasub submersible, sta. CURASUB12-12, Curaçao, east of Substation Curaçao downline, 12.0832 N, 68.8991 W, 156–290 m (no discrete depth observation), 7 August 2012, D. Pawson, B. Brandt, A. Schrier & C. Baldwin; USNM 414911, 61.9 mm SL, tissue no. CUR12316, Curasub submersible, sta. CURASUB12-MISC, Curaçao, off Substation Curaçao, 12.0832 N, 68.8991 W, no depth data, 21 May 2012, Substation Curaçao staff; UF 239255, 46.6 mm SL, tissue no. CUR12317, same collection information as USNM 414911; USNM 430035, 26.0 mm SL, tissue no. CUR13329, Curasub submersible, sta. CURASUB 13-31, Curaçao, west of Substation Curaçao downline, 12.0832 N, 68.8991 W, 177 m depth, 1 November 2013, C. Baldwin, B. Brandt, R. Robertson & C. Castillo; USNM 435299, 32.8 mm SL, tissue no. CUR15012, Curasub submersible, sta. CURASUB15-05, Curaçao, east of Substation Curacao downline, 12.0832 N, 68.8991 W, 173 m depth, 10 February 2015, C. Baldwin, B. Brandt, R. Robertson & C. Castillo; USNM 413864, 17.2 mm SL, tissue no. CUR12290, Curasub submersible, sta. CURASUB12-18, Curaçao, off Substation Curaçao, 12.0832 N, 68.8991 W, 207 m, 14 August 2012, C. Baldwin, B. Brandt, A. Schrier & A. Driskell.

Diagnosis. A species of *Lipogramma* distinguishable from congeners by the following combination of characters: pectoral-fin rays 16–17 (modally 16), gill rakers 11–13 (modally 12, 8–9 rakers on lower limb); four supraorbital pores present along dorsal margin of orbit, a pore present between one above mid orbit and one above posterodorsal corner of orbit; caudal fin rounded; body mostly tan to brown in life with 7 or 8 narrow darker brown bars on trunk; head with broad, irregular, whitish blue markings along dorsal midline from lower lip across upper lip and snout to nape; dark bar through eye bordered anteriorly and posteriorly by bluish-white bars; posterior base of soft dorsal fin with large white- or blue-rimmed black ocellus; dorsal and anal fins blue-grey with yellow spots or bars. Caudal fin mostly yellow with wide blue-grey margin and several bars comprising blue-grey mostly square-shaped spots. Pelvic fins grey/blue with scattered yellow-ringed dark spots. Juveniles with irregular white blotches of pigment on trunk and two triangular white blotches on caudal-fin base. The new species is further differentiated genetically from congeners for which molecular data are available in mitochondrial COI and nuclear Histone 3, Rhodopsin, TMO-4C4, and RAG1.

Description. Counts and measurements of type specimens given in Table 3. Seven specimens examined, 17.2–61.9 mm SL. Dorsal-fin rays XII, 9 (last ray composite); largest specimen (USNM 414911) with 9 pterygiophores in soft anal fin, but only 8 externally visible rays, the 8th appearing to represent fusion of two rays; anal-fin rays III, 8 (last ray composite); pectoral-fin rays 16–17, modally 16, 16 on both sides in holotype; pelvic-fin rays I, 5; total caudal-fin rays 25 (13 + 12), principal rays 17 (9 + 8), spinous procurent rays 6 (III + III), and 2 additional rays (i + i) between principal and procurent rays that are neither spinous nor typically segmented; vertebrae 25 (10 + 15); pattern of supraneural bones, anterior dorsal-fin pterygiophores, and dorsal-fin spines usually 0/0/0+2/1+1/1/, one paratype (USNM 435299) aberrant in having first two dorsal-fin spines supported in supernumerary association by separate pterygiophores

Table 3. Counts and measurements of type specimens of *Lipogramma schrieri* sp. n. Measurements are in percent SL. “Other Caudal Rays” include “i” – a slender, flexible, non-spinous, and typically non-segmented ray and “I” – a spinous procurent ray.

	USNM 431722 Holotype	USNM 413864 Paratype (juvenile)	USNM 414913 Paratype	USNM 414911 Paratype	UF 239255 Paratype	USNM 430035 Paratype	USNM 435299 Paratype
SL	49.7	17.2	56.0	61.9	46.6	26.0	32.8
Dorsal-fin Rays	XII, 9	XII, 9	XII, 9	XII, 9	XII, 9	XII, 9	XII, 9
Anal-fin Rays	III, 8	III, 8	III, 8	III, 8	III, 8	III, 8	III, 8
Principal Caudal Rays	9+8	9+8	9+8	9+8	9+8	9+8	9+8
Other Caudal Rays	IIIi+iIII	IIIi+iIII	IIIi+iIII	IIIi+iIII	IIIi+iIII	IIIi+iIII	IIIi+iIII
Pectoral-fin Rays	16, 16	16, 16	16, -	16, 16	16, 16	17, 17	16, 16
Gill Rakers	3+8=11	-	3+9=12	4+9=13	3+9=12	4+9=13	3+9=12
Head Length	38.6	36.1	33.9	36.0	37.6	37.3	38.7
Eye Diameter	11.7	15.1	11.4	12.1	10.9	13.5	14.0
Snout Length	10.1	6.4	8.8	9.1	9.0	8.5	7.9
Depth at Caudal Peduncle	19.7	19.8	20.4	21.0	20.2	20.0	19.2
Depth at Pelvic-fin Origin	32.8	31.4	31.8	31.8	32.2	32.3	31.4
Length of Pectoral Fin	20.9	21.5	20.9	22.9	Broken	22.7	21.7
Length of Pelvic Fin	Broken	39.5	40.4	40.6	Broken	39.6	39.0
Length of 12 th Dorsal Spine	15.7	19.2	23.6	18.9	19.7	22.3	20.7

vs. a single pterygiophore – 0/0/0+1+1/1+1/1/; ribs on vertebrae 3–10; epineural bones present on at least vertebrae 1–15 in holotype and two paratypes, difficult to assess in other specimens; gill rakers on first arch 11–13 (3–4 + 8–9), 11 (3 + 8) in holotype; upper-limb rakers and lowermost one or two rakers very small or present only as nubs, all other gill rakers elongate and slender with tooth-like secondary rakers as in *L. evides* (Baldwin et al. [2016: fig 3]); pseudobranchial filaments 7–11 (9 in holotype), filaments poorly or well developed (well developed in holotype); branchiostegals 6.

Spinous and soft dorsal fins confluent, several soft rays in posterior portion of fin forming slightly elevated lobe that extends posteriorly beyond base of caudal fin. Pelvic fin extending posteriorly to base of third anal-fin spine in preserved holotype when depressed, to middle or posterior portion of anal fin in aquarium photos (e.g., Fig. 5D). Dorsal profile from snout to origin of dorsal fin convex. Diameter of eye of holotype contained 3.3 times in head length. Pupil slightly tear shaped with small aphakic space anteriorly. Scales extending anteriorly onto top of head, ending short of coronal pore. Scales present on cheeks, operculum, and isthmus. Scales lacking on frontal region, snout, jaws, and branchiostegals. Scales large and deciduous, too many missing in most preserved specimens to make counts, but counts made from photographs of specimens prior to preservation indicate approximately 25–27 lateral scales between shoulder and base of caudal fin (27 in holotype), 5 cheek rows, and 12 rows across body above anal-fin origin. Scales on head and nape without cteni, scales on rest of body ctenoid. Fins naked.

Margins of bones of opercular series smooth, opercle without spines. Premaxilla with band of small conical teeth, band widest at symphysis, outer row with largest

teeth, 3 or 4 (4 in holotype) near symphysis enlarged. Dentary similar except 8 anterior teeth enlarge. Vomer with chevron-shaped patch of teeth, palatine with long series of small teeth. Conspicuous pores present in infraorbital canal (2 pores), portion of supraorbital canal bordering dorsal portion of orbit (4), on top of head (1 median coronal pore), preopercle (at least 5), and lateral-line canal in the posttemporal region (3). The 4 supraorbital pores situated as illustrated by Baldwin et al. (2016: fig 4) for *L. evides*. Posterior nostril situated just ventral to anteriormost supraorbital pore, nostril a single large opening. Anterior nostril at apex of elongate narial tube and situated just posterior to upper lip. No lateral line present on body.

Coloration: *In life or deceased but prior to preservation* (Fig. 5), ground color of body light brown. *Head:* dorsal midline of head with broad area of irregular, blue-white markings beginning on lower lip and continuing on upper lip and over snout to nape; a dark brown, pupil-width bar extending across orbit to lower jaw, this bar bordered on either side by thin whitish bar that runs from top of eye through front and rear of iris to lower jaw. *Trunk:* 7–8 narrow, dark-brown bars between posterior edge of operculum and caudal peduncle, bars narrower than paler interspaces. *Dorsal fin:* spinous dorsal and anterior portion of soft dorsal blue-grey with stripes comprising short yellow bars proximally and yellow spots distally; posterior portion of soft dorsal with large black ocellus ringed in blue-white pigment that extends onto trunk; several rows of yellow spots above ocellus. *Anal fin:* blue-grey, with yellow markings similar to those on spinous dorsal fin. *Caudal fin:* yellow, with vertical bars comprising blue-grey, square-shaped spots on interradial membranes on anterior 2/3 of fin; wide, blue-grey margin distally. *Pectoral fins:* most of fin translucent, base and anterior portion of fin dark. *Pelvic fins:* pale blue-grey to bright blue with yellow-ringed dark spots, spots mostly dark brown distally. *Juveniles:* An ontogenetic series from 17–33 mm SL is shown in Figure 6. The 17-mm SL specimen lacking body bars and with row of four large, irregular white blotches on or just below lateral midline of trunk, smaller white spots along back above that row, white spot at posterior base of anal fin, and two large, roughly triangular white blotches on caudal-fin base. First four dark trunk bars evident anteriorly in 26-mm SL juvenile, which has smaller white markings (spots vs. blotches). In 33-mm SL specimen, all trunk bars present, and remnants of each white caudal-fin blotch present as small white spot before indistinct pale vertical bar. *Comment regarding live coloration:* photographed against a light background (Fig. 5A–C), “blue-grey” in description above = grey; photographed against a darker background (Fig. 5D, E), “blue-grey” = blue. *Preserved coloration* (Fig. 3B): Head and trunk tan with darker tan to brown bars. Yellow portions of median fins in life clear in preservative, blue-grey markings on fins in life dark brown in preservative.

Distribution. Known only from specimens collected off Curaçao, southern Caribbean.

Habitat. Elevated rocky habitat with ample cracks or holes into which the fish retreated upon approach of the submersible. The holotype was collected at 197 m, and three paratypes were collected at 173–207 m. The range of 156–290 m recorded for another paratype reflects all depths visited on the submersible dive during which the specimen was collected and provides little relevant depth information.

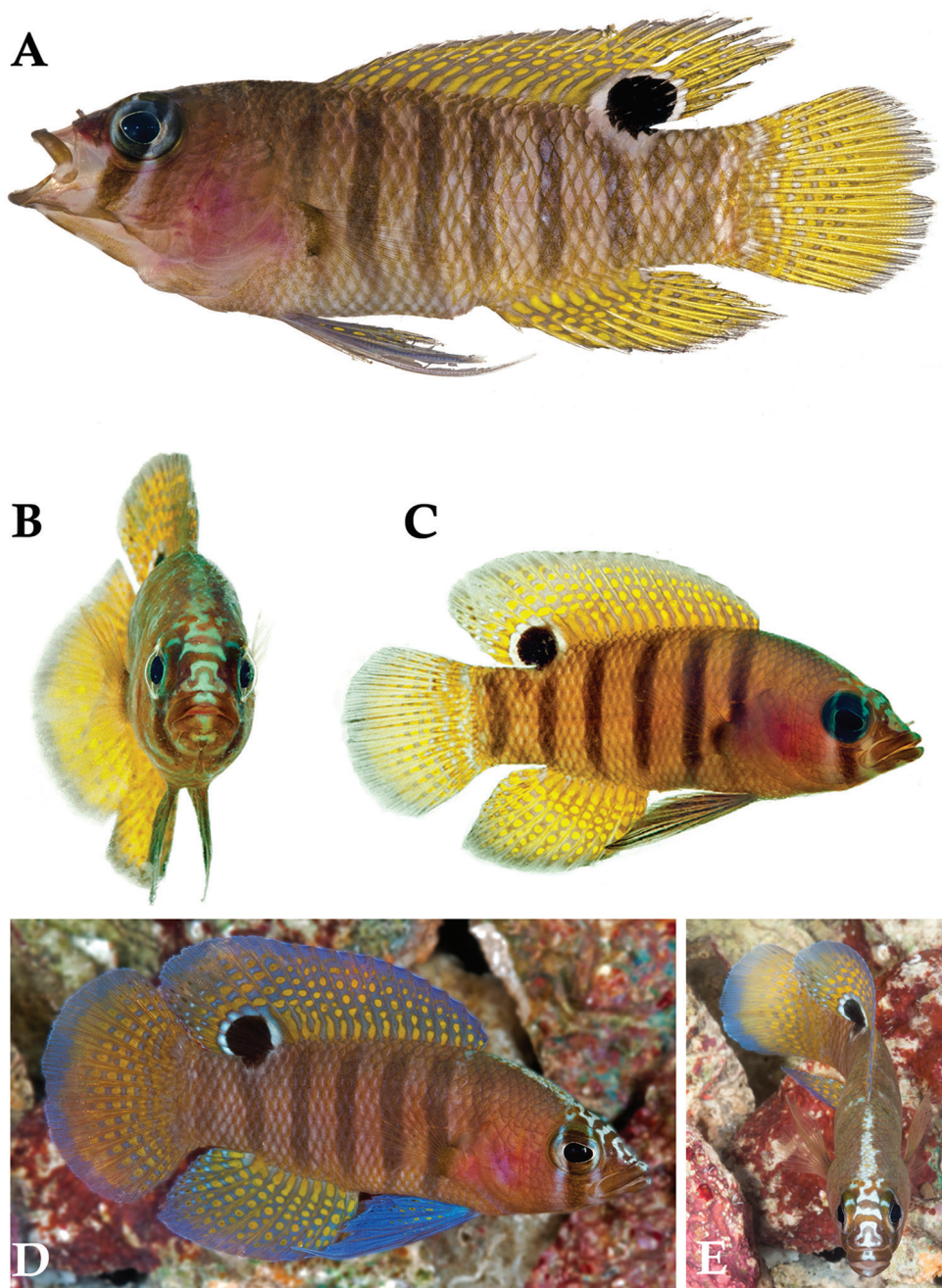


Figure 5. *Lipogramma schrieri* sp. n. **A** USNM 431722, CUR14114, holotype, 49.7 mm SL paratype, photograph by D. R. Robertson and C. C. Baldwin **B** and **C** specimen of unknown size collected off Curaçao (specimen not retained), aquarium photographs by Mac Stone **D** and **E** specimen of unknown size collected off Curaçao (specimen not retained), aquarium photographs by Barry Brown.

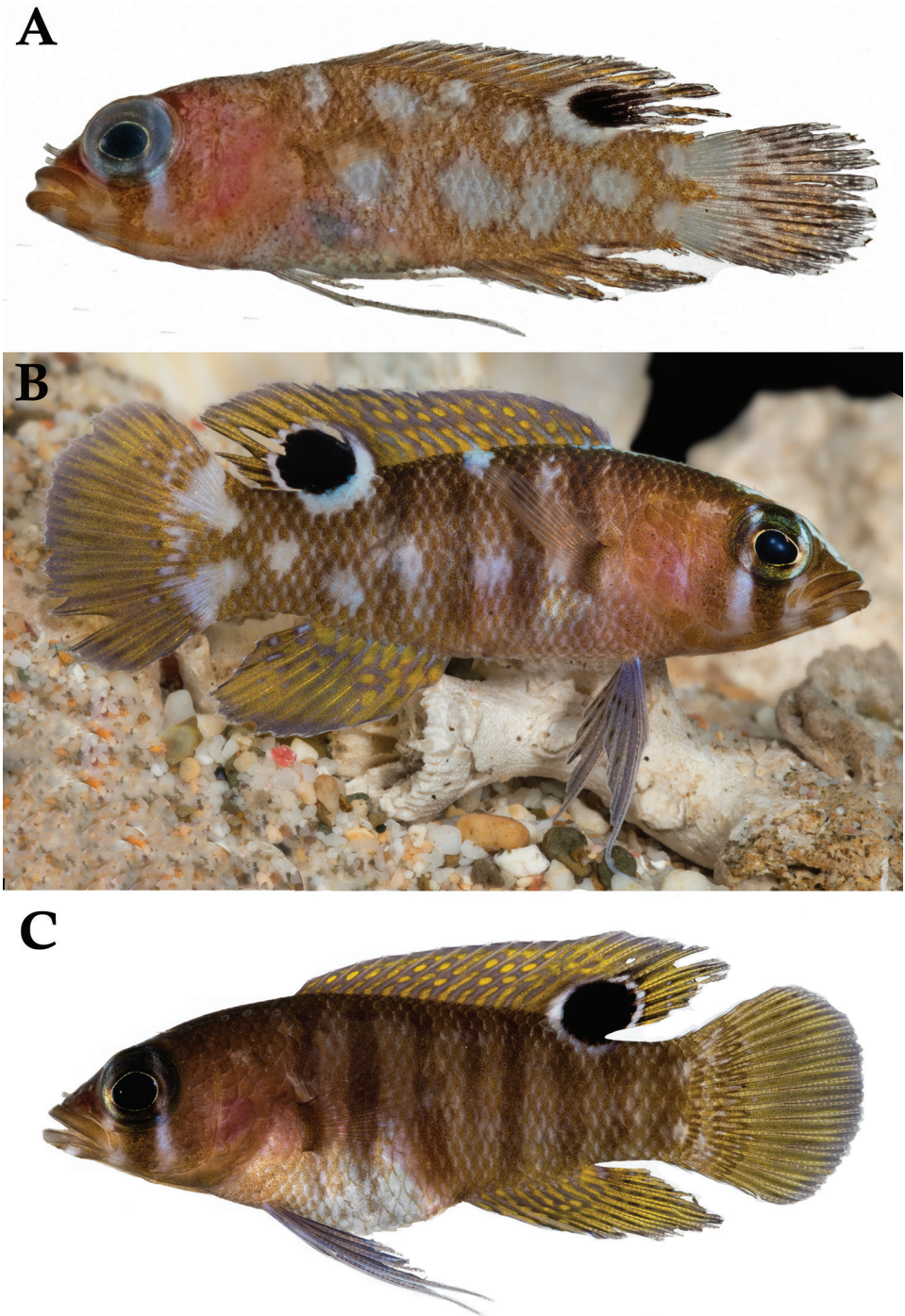


Figure 6. *Lipogramma schrieri* sp. n. **A** USNM 413864, CUR12290, paratype, 17.2 mm SL, photograph by D. R. Robertson and C. C. Baldwin **B** USNM 430035, CUR13329, paratype, 26.0 mm SL, photograph by Barry Brown **C** USNM 435299, CUR15012, paratype, 32.8 mm SL, D. R. Robertson and C. C. Baldwin.



Figure 7. *Lipogramma* sp. from Cuba, RGG uncataloged, 52.5 mm SL, collected at Cayos Los indios, JSLII Dive 3069, 296 m, 27 Dec 1997, R. G. Gilmore and R. Robins. Drawing by R. G. Gilmore.

Etymology. Named *Lipogramma schrieri* in honor of Adriaan (Dutch) Schrier, owner of Substation Curaçao. Although the *Curasub* submersible was not built originally for scientific research, Dutch's enthusiastic support of research use of his sub has exponentially expanded our understanding of fish and invertebrate faunas of Caribbean mesophotic and deeper reefs.

Common name. We propose Maori Basslet, in reference to the similarity of the markings on the dorsal midline of the forehead to the beautiful facial tattoo of the Maoris, indigenous Polynesian people of New Zealand.

Genetic Comparisons. Table 2 shows average inter- and intraspecific divergences in COI among species of *Lipogramma* analyzed genetically in this study. Average intraspecific divergence among the seven specimens of *L. schrieri* is 0.002 substitutions per site, and interspecific divergences between it and the other species for which data are available range from 11.7% (*L. barrettorum*) to 25.3% (*L. klayi*).

Comments. A 52.5 mm SL *Lipogramma* (RGG uncataloged), collected at 296 m in 1997 by one of us (RGG) and Richard Robins off Cuba (Fig. 7), could be a specimen of *L. schrieri*. It has a similar color pattern, including seven dark body bars, the “maori” pattern of pigment on top of the head (based on examination of the preserved specimen), and similar pattern of fin pigment. However, this specimen has yellow pigment around the eye (vs. brown in *L. schrieri*), yellow pigment in a triangular-shaped subocular bar (vs. brown pigment in a rectangular-shaped bar), and a yellow pectoral-fin base (vs. dark brown). Furthermore, the Cuban specimen has 15 pectoral-fin rays on each side vs. 16–17 (modally 16) in *L. schrieri*, and 14 total gill rakers vs. 11–13 in *L. schrieri*. Further study is needed to determine if this specimen represents a variant of *L. schrieri* or an additional cryptic species in the genus.

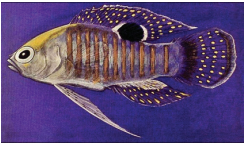
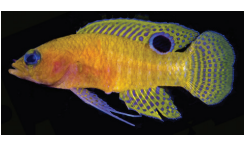

Discussion

Morphological comparisons. *Lipogramma barrettorum*, *L. robinsi*, and *L. schrieri* differ from all congeners in having at least seven dark trunk bars. A comparison of major morphological and pigmentation differences among those three species is provided in Table 4. They are easily separable from one another on the basis of live or fresh color patterns, most notably the following: (1) the presence of 7–8 dark brown trunk bars against a tan background in *L. schrieri*, 10–12 tan/yellow bars against a flesh to greenish background in *L. robinsi*, and 11–12 light brown bars against a yellow background in *L. barrettorum* (trunk bars also evident in preserved specimens); (2) the presence of a bright yellow nape in *L. robinsi*, a blue-white stripe from the tip of the lower jaw to the base of the dorsal fin in *L. barrettorum*, and irregular, broad, blue-white markings from the tip of the lower jaw to the nape in *L. schrieri* (stripe in *L. barrettorum* and irregular markings in *L. schrieri* also evident in preserved specimens); (3) the presence of a distinct dark bar through the eye in *L. schrieri*, no such bar in *L. robinsi*, and an indistinct bar in *L. barrettorum* (orbital bar, when present, also evident in preserved specimens); and (4) median fins transparent with yellow spots in *L. robinsi*, yellow with blue/grey spots in *L. barrettorum*, and blue/grey with yellow spots in *L. schrieri*. *Lipogramma robinsi* can further be distinguished from the other two species by having more lower-limb gill rakers on the first arch (11–12 vs. 8–9 in *L. schrieri* and 8–10 in *L. barrettorum*) and usually having fewer pectoral-fin rays (15 vs. modally 16 in *L. schrieri* and *L. barrettorum*). Based on available material, *Lipogramma schrieri* reaches a larger size (~62 mm SL) than *L. robinsi* (~22 mm SL) and *L. barrettorum* (~25 mm SL).

Species delimitation and phylogeny. Comparative morphological analysis supports the recognition of *L. barrettorum* and *L. schrieri* as distinct species, and combinations of diagnostic morphological features that distinguish them from all other *Lipogramma* species are provided in the species descriptions above. Molecular data for the nine *Lipogramma* species for which genetic data existed prior to this study (Baldwin et al. 2016) or was generated in this study (*L. anabantoides*, *L. barrettorum*, *L. evides*, *L. haberi*, *L. klayi*, *L. levinsoni*, *L. regia*, *L. schrieri*, *L. trilineata*) unequivocally support the presence of nine species (molecular data not available for *L. flavescens*, *L. roseum* and *L. robinsi*). The neighbor-joining network (Suppl. Material 1) derived from COI data shows nine distinct lineages with very high genetic distances between lineages (10–27%, mean = 19%), which are at least 20 times greater than variation in COI within lineages (range 0.1–0.5%, mean = 0.3%). The molecular phylogeny from the Bayesian analysis of the concatenated dataset (Fig. 8) was identical in topology to the BP&P coalescent-based species-tree analysis. The BP&P analysis also had overwhelming support for a nine-species model (posterior probability 0.996) versus models with fewer or more species.

Eco-evolutionary relationships. The two new species, *L. barrettorum* and *L. schrieri*, belong to a clade that includes *L. evides* and *L. haberi*. Collectively the members of this clade are the deepest-living species in our analysis, occurring at depths predominantly below 140 m (Figure 9). Sister to this clade is a group comprising *L. levinsoni*, *L. anabantoides*, and *L. regia*, species that inhabit depths predominantly shallower than 150 m, in

Table 4. Summary of major morphological and pigmentation differences among *Lipogramma robinsi*, *L. barrettorum* sp. n., and *L. schrieri* sp. n.

ADULT	<i>L. robinsi</i>	<i>L. barrettorum</i>	<i>L. schrieri</i>
			
SL in preservative	To 22 mm	To 25 mm	To 62 mm
Gill Rakers	14–16, 11–12 on lower limb	12 (12–14), 8–10 on lower limb	12 (11–13), 8–9 on lower limb
Pectoral-fin rays	15	16 (15–16)	16 (16–17)
Body ground color	Translucent green to flesh	Yellow to yellowish brown	Tan/brown
Head coloration in life	Grey-brown; top of head bright yellow without blue-white marks Dark bar through eye to mouth absent	Yellow-brown; top of head with median blue-white stripe Dark bar through eye to mouth indistinct	Pale brown; top of head with blue-white "tattoo" marks Dark bar through eye to mouth strong
Trunk in life	10–12 narrow yellow bars, narrow interspaces	11–12 narrow brown bars, narrow interspaces	7–8 narrow brown bars, wide interspaces
Dorsal Fin in life	Transparent with yellow spots; margin white Soft dorsal: black ocellus with white front & rear edges	Yellow with blue-grey wavy bars and spots; margin grey-blue Soft dorsal: black ocellus ringed with blue-white	Blue-grey with yellow spots and short bars; margin blue-grey Soft dorsal: black ocellus ringed with blue-white
Anal fin in life	Translucent; base white; rows yellow spots	Yellow with blue-grey spots and wavy lines; margin blue-grey	Blue-grey with yellow spots and bars; margin blue-grey
Caudal Fin in life	Translucent; base yellow, center with yellow spots, margin white	Yellow with bars of blue-grey spots; blue-grey margin.	Yellow with bars of blue-grey spots; margin blue-grey
Pectoral fins in life	Translucent	Translucent	Translucent; base dark
Pelvic fins in life	White; rows black spots	Blue-grey with yellow-ringed dark spots	Pale blue-grey to blue with yellow-ringed dark spots
JUVENILE	Not known	Known from 10–13 mm (preserved SL) specimens	Known from 17–33 mm (preserved SL) specimens
Trunk	Not known	Similar to adult	Scattered white spots and blotches on trunk and base of caudal fin, blotches roughly in two rows of four in smallest juvenile (17 mm SL); anterior trunk bars first evident in 26-mm SL juvenile paratype
Anal fin	Not known	Similar to adult	Similar to adult except more yellow distally
Caudal fin	Not known	Similar to adult	Mostly yellow with blue-grey margin and 2 large triangular white blotches on base

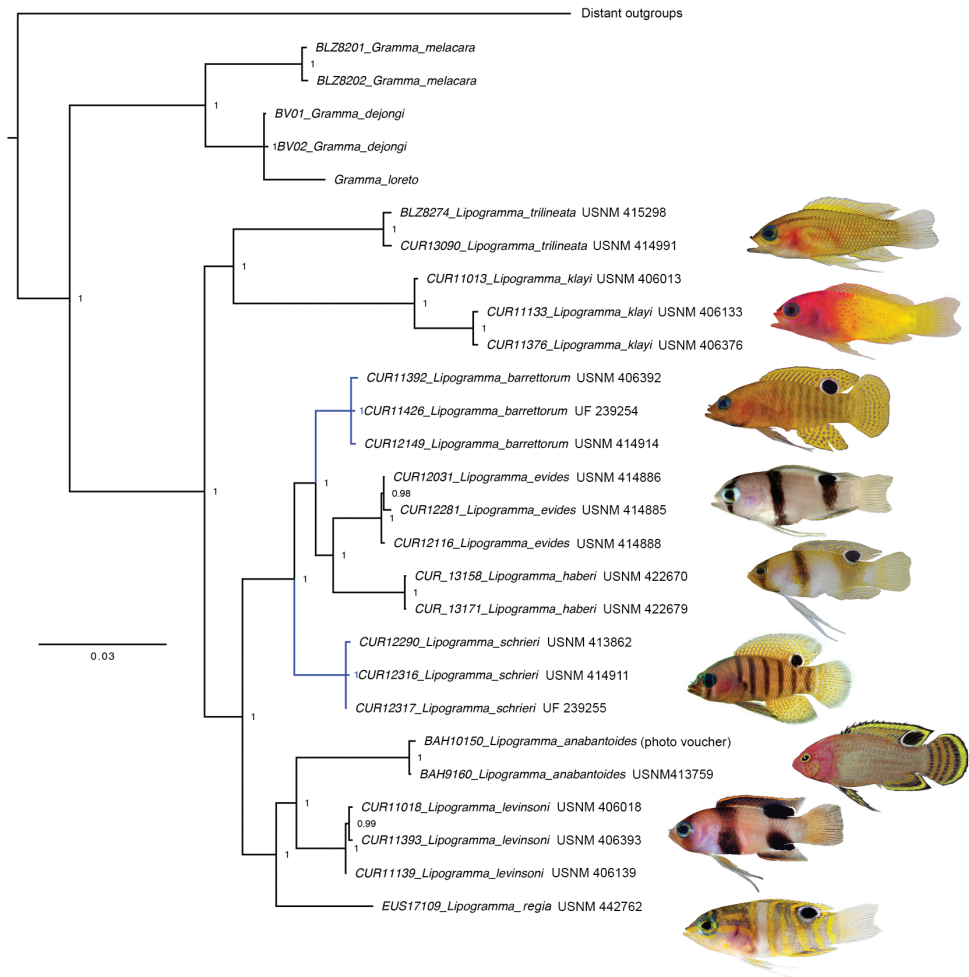


Figure 8. Bayesian Inference molecular phylogeny of nine species of *Lipogramma* based on combined mitochondrial and nuclear genes. Numbers of individuals analyzed for each species are given in Appendix 1, along with the genes sequences for each individual. Topology is identical to that from BP&P species-tree analysis. Support values are Bayesian posterior probabilities (above) and bootstrap values (below). Nodes without labels have 1.0 posterior probability and 100 bootstrap values. Photographs or illustrations by C. C. Baldwin, R. G. Gilmore, D. R. Robertson, C. R. Robins, and M. Stone.

the zone traditionally referred to as mesophotic coral ecosystems (MCEs—30–150 m; Kahng et al. 2010). A second shallow/MCE (< 150 m) clade that is sister to both those clades comprises *L. trilineata* and *L. klayi*. There is clear habitat partitioning by depth within both shallow clades, particularly between sister species: *L. trilineata* vs *L. klayi* and *L. levinsoni* vs *L. anabantoides*. Based on available data, there is no clear depth partitioning evident within the more speciose *L. evides* clade. We note, however, that these depth distributions are based on collections and observations of different species from different locations. Hence, we cannot rule out the possibility that some of the differences in depth distributions in Figure 9 represent location effects rather than depth partitioning.

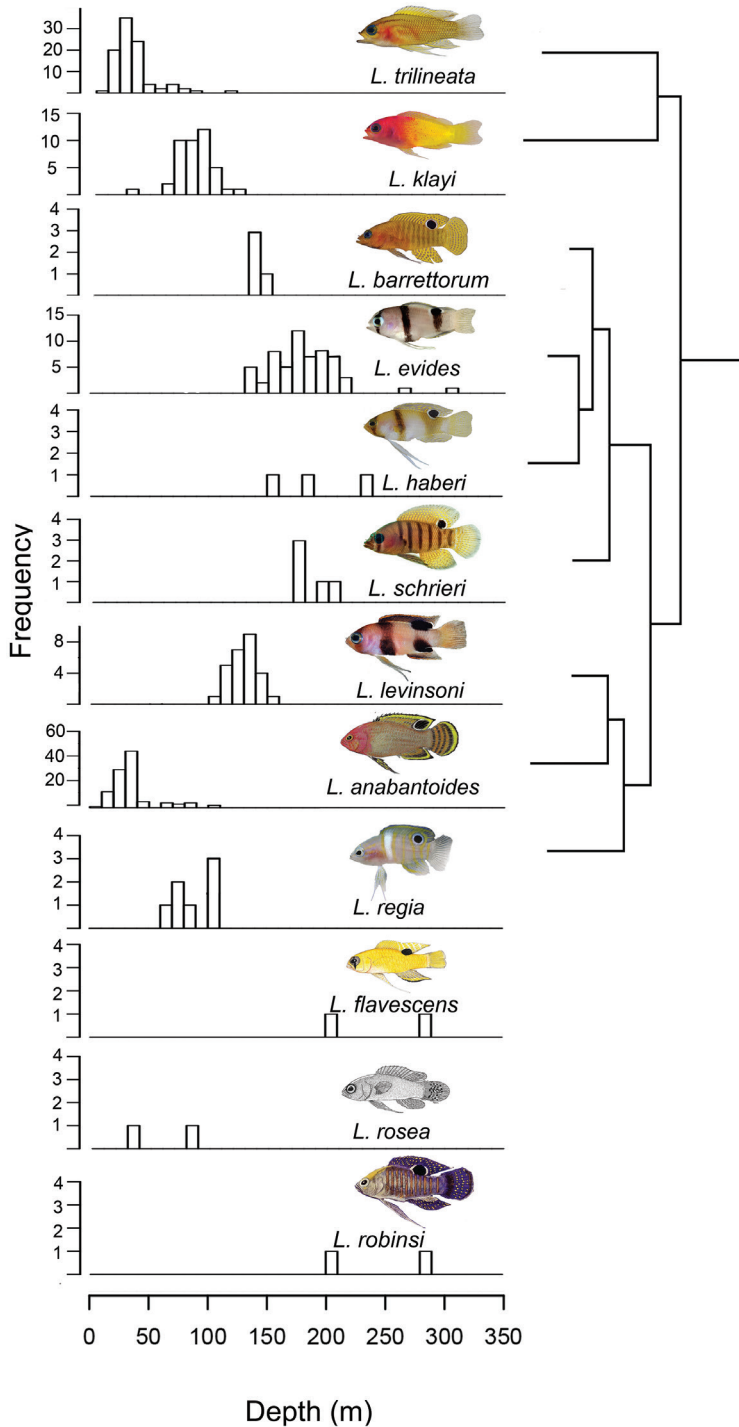


Figure 9. Eco-evolutionary histogram for species of *Lipogramma* showing phylogenetic distribution of species' depth ranges. Photographs or illustrations by C. C. Baldwin, R. G. Gilmore, Gilmore (1997: fig. 1), Mooi and Gill (2002: fig. 9), D. R. Robertson, and M. Stone.

In addition to depth, we have observed distinct interspecific variation in the types of substrata with which some of these species associate and the nature of their associations with substrata. Off Curaçao, *Lipogramma klayi* is a very commonly observed species, especially on the upper level of vertical faces or slopes of ~30–60° that are heavily indented with small caves and overhangs and festooned with gorgonians and other growth. We have commonly seen it occupying the same habitat at Bonaire, Dominica, Roatan, and St. Eustatius. Its sister species, *L. trilineata* is much more cryptic than *L. klayi*. It is rarely observed, as it tends to stay close to ceilings of cavities, whether those are caves or small holes formed in large rock or coral heads. Within the clade comprising the two new species, *L. evides* and *L. levinsoni* are commonly associated with small patches of cobble scattered among rocky areas, whereas *L. barrettorum* and *L. schrieri* are associated with elevated rocky habitat with ample cracks or holes. Finally, two of us (LT and DRR) recently observed multiple instances of *L. flavescens* off Roatan sitting on coarse sand, meters away from shelter, in areas of sand and scattered small low patches of rock.

Baldwin et al. (2016) noted that members of the large clade comprising all *Lipogramma* species except *L. trilineata* and *L. klayi* are characterized by a dark ocellus on the posterior base of the dorsal fin. Based on this character, a relatively shallow depth range, and a modal count of 17 rays in the pectoral fin, they hypothesized that *L. regia* (not sampled in that study) is most closely related to *L. anabantoides* and *L. levinsoni*. The present phylogenetic analysis includes a recently collected specimen of *L. regia* and supports this hypothesis. Baldwin et al. (2016) also hypothesized that *L. flavescens* may be part of the deep-dwelling clade comprising *L. evides*, *L. haberi*, *L. barrettorum*, and *L. schrieri* (the last two as “*Lipogramma ‘robinsi’*” in their phylogeny) and, based on the deep depth-range of *L. flavescens*, a dark ocellus on the dorsal fin, bright yellow body coloration, a dark bar through the eye, and a low gill-raker count (15–16), possibly most closely related to *L. haberi*. Collection of fresh material of *L. flavescens* would provide the genetic material needed to test their hypotheses. We note that *L. robinsi* is likely part of this deep-dwelling clade as well, based on the presence of a dorsal-fin ocellus, a barring pattern on the body similar to that of *L. schrieri* and *L. barrettorum*, and its depth range (although the latter is based on very few specimens). Fresh material of *L. robinsi* for genetic analyses is also desirable. In addition, more information is needed on the depth distributions of all of the less common species, particularly to determine the extent of habitat partitioning within locations, as well as its consistency between locations.

Submersible exploration. Effective capture of fish specimens during deep-sea submersible dives has only been realized since 1982 with the *Johnson Sea-Link* submersibles and, much more recently, with the *Curasub*. Fresh and often living specimens are brought to the surface, providing quality material for color photography and genetic analyses to investigate phylogenetic relationships and evolutionary trends. Capture of cryptobenthic species, including gobiids (Baldwin and Robertson 2015; Tornabene et al. 2016a, 2016b; Tornabene and Baldwin 2017), blennioids (Baldwin and Robertson 2013), grammatids (Gilmore and Jones 1988; Gilmore 1997; Baldwin et al. 2016b;

this study), serranids (Baldwin and Johnson 2014, Baldwin and Robertson 2014), and scorpaenids (Baldwin et al. 2016a) using manned submersibles is allowing unprecedented examination of microhabitat relationships, depth and temperature preferences, and biogeography, along with comparative morphology and molecular phylogenetic relationships in previously unknown or inaccessible species. We cannot overemphasize the value of these manned undersea operations to increasing our knowledge and understanding of tropical deep-reef fish assemblages.

Revised key to the species of *Lipogramma* (modified from Mooi and Gill 2002)

Photographs or illustrations by C. C. Baldwin, R. G. Gilmore, Gilmore (1997: fig. 1), Mooi and Gill (2002: fig. 9), D. R. Robertson, and M. Stone.

- 1 Posterior base of soft dorsal fin with prominent dark spot, ocellus, or elongate blotch **2**
- Soft dorsal fin without prominent markings **10**
- 2 With prominent black bar through eye **3**
- Without prominent black bar through eye **7**
- 3 Trunk without bars, body yellow above, white below *flavescens*



- Trunk with bars **4**
- 4 Trunk with 2 bars **5**
- Trunk with 7–8 bars *schrieri*



- 5 Bar through eye wide, encompassing entire eye; trunk bars of equal intensity, often hourglass shaped; pectoral-fin rays modally 17, gill rakers modally 19..... *levinsoni*



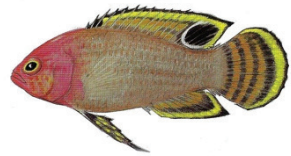
- Bar through eye narrow, encompassing only pupil; anterior trunk bar more pronounced than posterior bar, neither bar hourglass shaped; pectoral-fin rays modally 16, gill rakers 15–16 or 20–21 **6**
- 6 Posterior trunk bar a broad, yellowish inverted triangle; gill rakers modally 15–16 ***haberi***



- Posterior trunk bar a black rectangle; gill rakers modally 20–21 ***evides***



- 7 Trunk without bars; head reddish, trunk grey-brown ***anabantoides***



- Trunk with bars; head and trunk not colored as above **8**
- 8 Trunk with 6 yellow bars, anterior 5 extending onto dorsal fin and 3rd-5th extending onto anal fin; head with two prominent broad yellow stripes behind eye; top of head without yellow cap ***regia***



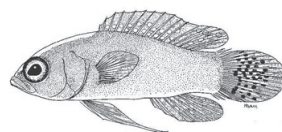
- Trunk with 10 to 12 bars, none extending onto dorsal or anal fins; head without broad yellow stripes behind eye, and top of head with or without yellow cap **9**
- 9 Median fins transparent with yellow spots; top of head with yellow cap, without median blue-white stripe; lower-limb gill rakers 11–12 ***robinsi***



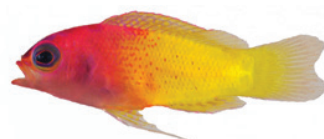
- Median fins yellow with blue-grey spots; top of head without yellow cap, with median blue-white stripe; lower-limb gill rakers 8–10.....***barrettorum***



- 10 Dorsal fin XI, 6–7; circum-peduncular scales 16; head and body yellow to rose colored, caudal fin yellow with dark spots, dorsal and anal fins red with pale spots.....***rosea***



- Dorsal fin XII–XIII, 8–10; circum-peduncular scales 18 to 21; not colored as above.....**11**
- 11 Strongly bicolored, purplish red anteriorly, yellow posteriorly; no stripes on head; scales in lateral series 29 to 35; gill rakers 20 to 21; anal-fin soft rays 8; upper caudal-fin spines 4 or 5***klayi***



- Uniformly yellowish, 3 blue stripes on head: one along dorsal midline from snout to dorsal-fin, one from top of each eye to shoulder and anterior portion of trunk; lateral scales 25 to 29; gill rakers 13 to 18; anal-fin soft rays 7; upper caudal-fin spines 3 ***trilineata***



Acknowledgments

We thank Bruce Brandt, Barry Brown, Cristina Castillo, Loretta Cooper, Tico Christiaan, Tommy Devine, Brian Horne, Dave Johnson, Rob Loendersloot, Dan Mulcahy, Diane Pitassy, Laureen Schenk, Adriaan “Dutch” Schrier, and Barbara van Bebbber for assistance in various ways with this study. Portions of the laboratory and/or computer work were conducted in and with the support of the L.A.B. facilities of the National Museum of Natural History. Funding for the Smithsonian Institution’s *Deep Reef Observation Project* was provided internally by the Consortium for Understanding and Sustaining a Biodiverse Planet to CCB, the Competitive Grants for the Promotion of

Science program to CCB and DRR, the Herbert R. and Evelyn Axelrod Endowment Fund for systematic ichthyology to CCB, and STRI funds to DRR. Externally the research was funded by National Geographic Society's Committee for Research and Exploration to CCB (Grant #9102-12) and the Prince Albert II of Monaco Foundation grant to CCB. This is Ocean Heritage Foundation/Curacao Sea Aquarium/Substation Curacao (OHF/SCA/SC) contribution number 32.

References

- Ahlstrom EH, Butler JL, Sumida BY (1976) Pelagic stromateoid fishes (Pisces, Perciformes) of the eastern Pacific: Kinds, distributions, and early life histories and observations on five of these from the northwest Atlantic. *Bulletin of Marine Science* 26: 285–402.
- Baldwin CC, Robertson DR (2013) A new *Haptoclinus* blenny (Teleostei, Labrisomidae) from deep reefs off Curacao, southern Caribbean, with comments on relationships of the genus. *ZooKeys* 306: 71–81. <https://doi.org/10.3897/zookeys.306.5198>
- Baldwin CC, Johnson GD (2014) Connectivity across the Caribbean Sea: DNA barcoding and morphology unite an enigmatic fish larva from the Florida Straits with a new species of sea bass from deep reefs off Curaçao. *PLoS ONE* 9(5): e97661. <https://doi.org/10.1371/journal.pone.0097661>
- Baldwin CC, Robertson DR (2014) A new *Liopropoma* sea bass (Serranidae: Epinephelinae: Liopropomini) from deep reefs off Curaçao, southern Caribbean, with comments on depth distributions of western Atlantic liopropomins. *Zookeys* 409: 71–92 <https://doi.org/10.3897/zookeys.409.7249>
- Baldwin CC, Robertson DR (2015) A new, mesophotic *Coryphopterus* goby (Teleostei: Gobiidae) from the southern Caribbean, with comments on relationships and depth distributions within the genus. *Zookeys* 513: 123–142. <https://doi.org/10.3897/zookeys.513.9998>
- Baldwin CC, Pitassy DE, Robertson DR (2016a) A new deep-reef scorpionfish (Teleostei: Scorpaenidae: *Scorpaenodes*) from the southern Caribbean with comments on depth distributions and relationships of western Atlantic members of the genus. *Zookeys* 606: 141–158. <https://doi.org/10.3897/zookeys.606.8590>
- Baldwin CC, Robertson DR, Nonaka A, Tornabene L (2016b) Two new deep-reef basslets (Teleostei, Grammatidae, *Lipogramma*), with comments on the eco-evolutionary relationships of the genus. *Zookeys* 638: 45–82 <https://doi.org/10.3897/zookeys.638.10455>
- Chakrabarty P, Warren M, Page LM, Baldwin CC (2013) GenSeq: An updated nomenclature and ranking for genetic sequences from type and non-type sources. *ZooKeys* 346: 29–41. <https://doi.org/10.3897/zookeys.346.5753>
- Gilmore RG (1997) *Lipogramma robinsi*, a new basslet from the tropical western Atlantic, with descriptive and distributional notes on *L. flavescens* and *L. anabantoides* (Perciformes: Grammatidae). *Bulletin of Marine Science* 60: 782–788.
- Gilmore RG, Jones RS (1988) *Lipogramma flavescens*, a new grammid fish from the Bahama Islands, with descriptive and distributional notes on *L. evides* and *L. anabantoides*. *Bulletin of Marine Science* 42: 435–445.

- Hebert PDN, Stoeckle MY, Zemplak TS, Francis CM (2004) Identification of birds through DNA barcodes. *PLoS Biology* 2: 1657–1663. <https://doi.org/10.1371/journal.pbio.0020312>
- Hubbs CL, Lagler KF (1947) Fishes of the Great Lakes region. Cranbrook Institute of Science Bulletin No. 26.
- Kahng SE, Garcia-Sais JR, Spalding HL, Brokovich E, Wagner D, Weil E, Hinderstein L, Toonen RJ (2010) Community ecology of mesophotic coral reef ecosystems. *Coral Reefs* 29: 255–75. <https://doi.org/10.1007/s00338-010-0593-6>
- Kimura M (1980) A simple method for estimating evolutionary rates of base substitutions through comparative studies of nucleotide sequences. *Journal of Molecular Evolution* 16: 111–120. <https://doi.org/10.1007/BF01731581>
- Kumar S, Stecher G, Tamura K (2015) MEGA7: Molecular Evolutionary Genetics Analysis version 7.0 for bigger datasets. *Molecular Biology and Evolution* 33: 1870–1874. <https://doi.org/10.1093/molbev/msw054>
- LANFAR R, Calcott B, Ho SYW, Guindon S (2012) PartitionFinder: Combined selection of partitioning schemes and substitution models for phylogenetic analyses. *Molecular Biology and Evolution* 29: 1695–1701. <https://doi.org/10.1093/molbev/mss020>
- Lin H-C, Hastings PA (2011) Evolution of a Neotropical marine fish lineage (Subfamily Chaenopsinae, Suborder Blennioidei) based on phylogenetic analysis of combined molecular and morphological data. *Molecular Phylogenetics and Evolution* 60: 236–248. <https://doi.org/10.1016/j.ympev.2011.04.018>
- Lin H-C, Hastings PA (2013) Phylogeny and biogeography of a shallow water fish clade (Teleostei: Blenniiformes). *BMC Evolutionary Biology* 13: 210. <https://doi.org/10.1186/1471-2148-13-210>
- Mooi RD, Gill AC (2002) Grammatidae. In: Carpenter KE (Ed.) The living marine resources of the western Central Atlantic. Volume 2 Bony fishes part 1 (Acipenseridae to Grammatidae). FAO Species Identification Guide for Fishery Purposes, 1370–1373.
- Rambaut A, Drummond AJ (2007) Tracer. <http://beast.bio.ed.ac.uk/Tracer>
- Randall JE (1963) Three new species and six new records of small serranoid fishes from Curaçao and Puerto Rico. *Studies on the Fauna of Curacao and other Caribbean Islands* 19: 77–110. [Pls. 1–3]
- Rannala B, Yang Z (2003) Bayes estimation of species divergence times and ancestral population sizes using DNA sequences from multiple loci. *Genetics* 164: 1645–1656.
- Robins CR, Colin PL (1979) Three new grammid fishes from the Caribbean Sea. *Bulletin of marine Science* 29: 41–52.
- Ronquist F, Teslenko M, van der Mark P, Ayres DP, Darling A, Höhna S, Larget B, Liu L, Suchard MA, Huelsenbeck JP (2012) MrBayes 3.2: efficient Bayesian phylogenetic inference and model choice across a large model space. *Systematic Biology* 61: 539–542. <https://doi.org/10.1093/sysbio/sys029>
- Seutin G, White BN, Boag PT (1991) Preservation of avian blood and tissue samples for DNA analyses. *Canadian Journal of Zoology* 69(1): 82–90. <https://doi.org/10.1139/z91-013>
- Tornabene L, Robertson DR, Baldwin CC (2016a) *Varicus lacerta*, a new species of goby (Teleostei, Gobiidae, Gobiosomatini, Nes subgroup) from a mesophotic reef in the southern Caribbean. *Zookeys* 596: 143–156. <https://doi.org/10.3897/zookeys.596.8217>

- Tornabene L, Van Tassell JL, Gilmore RG, Robertson DR, Young F, Baldwin CC (2016b) Molecular phylogeny, analysis of character evolution, and submersible collections enable a new classification for a diverse group of gobies (Teleostei: Gobiidae: *Nes* subgroup), including nine new species and four new genera. *Zoological Journal of the Linnean Society* 177(4): 764–812. <https://doi.org/10.1111/zoj.12394>
- Wainwright PC, Smith WL, Price SA, Tang KL, Sparks JS, Ferry LA, Kuhn KL, Eytan RI, Near TJ (2012) The evolution of pharyngognath: a phylogenetic and functional appraisal of the pharyngeal jaw key innovation in labroid fishes and beyond. *Systematic Biology* 61: 1001–1027. <https://doi.org/10.1093/sysbio/sys060>
- Weigt LA, Driskell AC, Baldwin CC, Ormos A (2012) DNA barcoding fishes. Chapter 6 In: Kress WJ, Erickson DL (Eds) *DNA Barcodes: Methods and Protocols*, *Methods in Molecular Biology* 858: 109–126. https://doi.org/10.1007/978-1-61779-591-6_6
- Yang Z, Rannala B (2010) Bayesian species delimitation using multilocus sequence data. *Proceedings of the National Academy of Sciences of United States of America* 107: 9264–9269. <https://doi.org/10.1073/pnas.0913022107>
- Yang Z, Rannala B (2014) Unguided species delimitation using DNA sequence data from multiple loci. *Molecular Biology and Evolution* 31: 3125–3135. <https://doi.org/10.1093/molbev/msu279>
- Yang Z (2015) The BPP program for species tree estimation and species delimitation. *Current Zoology* 61(5): 854–865. <http://dx.doi.org/10.1093/czoolo/61.5.854>

Appendix I

Links between DNA voucher specimens, GenBank accession numbers, and DNA sequences of *Lipogramma* derived for use in this study. BAH = Bahamas, BLZ = Belize, CUR = Curaçao, DOM = Dominica, EUS = St. Eustatius, TIK = Curaçao.

CatalogNumber	TissueNumber	Species	GenBank COI	GenBank H3	GenBank TMO-4C4	GenBank Rag1	GenBank Rhodopsin	GenSeq designation
Photo Voucher Only	BAH10150	<i>Lipogramma anabanooides</i>	KX713732	KX713823	KX713880	KX713842	KX713862	genseq-5
USNM 413759	BAH9160	<i>Lipogramma anabanooides</i>		KX713824	KX713881	KX713843	KX713863	genseq-4
USNM 420334	BLZ5340	<i>Lipogramma anabanooides</i>	KX713733	-	-	-	-	genseq-4
USNM 414886	CUR12013	<i>Lipogramma evides</i>	KX713750	-	-	-	-	genseq-4
USNM 414889	CUR12031	<i>Lipogramma evides</i>	KX713751	KX713834	KX713891	KX713852	KX713872	genseq-4
USNM 414883	CUR12044	<i>Lipogramma evides</i>	KX713752	-	-	-	-	genseq-4
USNM 414884	CUR12050	<i>Lipogramma evides</i>	KX713753	-	-	-	-	genseq-4
USNM 414887	CUR12078	<i>Lipogramma evides</i>	KX713754	-	-	-	-	genseq-4
USNM 414890	CUR12084	<i>Lipogramma evides</i>	KX713755	-	-	-	-	genseq-4
USNM 414888	CUR12116	<i>Lipogramma evides</i>	KX713757	KX713835	KX713892	KX713853	KX713873	genseq-4
USNM 414882	CUR12118	<i>Lipogramma evides</i>	KX713758	-	-	-	-	genseq-4
USNM 414878	CUR12276	<i>Lipogramma evides</i>	KX713760	-	-	-	-	genseq-4
USNM 414881	CUR12280	<i>Lipogramma evides</i>	KX713761	-	-	-	-	genseq-4
USNM 414885	CUR12281	<i>Lipogramma evides</i>	KX713762	KX713837	KX713894	KX713855	KX713875	genseq-4
USNM 414879	CUR12288	<i>Lipogramma evides</i>	KX713763	-	-	-	-	genseq-4
USNM 414876	CUR12353	<i>Lipogramma evides</i>	KX713767	-	-	-	-	genseq-4
USNM 421602	CUR13100	<i>Lipogramma evides</i>	KX713771	-	-	-	-	genseq-4
USNM 426769	CUR13233	<i>Lipogramma evides</i>	KX713779	-	-	-	-	genseq-4
USNM 426770	CUR13234	<i>Lipogramma evides</i>	KX713780	-	-	-	-	genseq-4
USNM 426771	CUR13265	<i>Lipogramma evides</i>	KX713781	-	-	-	-	genseq-4
USNM 426737	CUR13266	<i>Lipogramma evides</i>	KX713782	-	-	-	-	genseq-4
USNM 426746	CUR13279	<i>Lipogramma evides</i>	KX713785	-	-	-	-	genseq-4
USNM 426709	CUR13286	<i>Lipogramma evides</i>	KX713786	-	-	-	-	genseq-4
USNM 426722	CUR13294	<i>Lipogramma evides</i>	KX713787	-	-	-	-	genseq-4

CatalogNumber	TissueNumber	Species	GenBank COI	GenBank H3	GenBank TMO-4C4	GenBank Rag1	GenBank Rhodopsin	GenSeq designation
Photo Voucher Only	CUR15032	<i>Lipogramma evides</i>	KX713793	-	-	-	-	genseq-5
Photo Voucher Only	CUR15055	<i>Lipogramma evides</i>	KX713795	-	-	-	-	genseq-5
Photo Voucher Only	CUR15057	<i>Lipogramma evides</i>	KX713796	-	-	-	-	genseq-5
Photo Voucher Only	CUR15060	<i>Lipogramma evides</i>	KX713798	-	-	-	-	genseq-5
Photo Voucher Only	CUR15061	<i>Lipogramma evides</i>	KX713799	-	-	-	-	genseq-5
USNM 434771	CUR15091	<i>Lipogramma evides</i>	KX713811	-	-	-	-	genseq-4
USNM 434783	CUR15103	<i>Lipogramma evides</i>	KX713813	-	-	-	-	genseq-4
USNM 434784	CUR15104	<i>Lipogramma evides</i>	KX713814	-	-	-	-	genseq-4
USNM 431313	TIK003	<i>Lipogramma evides</i>	KX713822	-	-	-	-	genseq-4
USNM 422670, paratype	CUR13158	<i>Lipogramma haberi</i>	KX713775	-	-	KX713860	-	genseq-2
USNM 422679, holotype	CUR13171	<i>Lipogramma haberi</i>	KX713776	-	-	KX713861	-	genseq-1
USNM 434772, paratype	CUR15092	<i>Lipogramma haberi</i>	KX713812	-	-	-	-	genseq-2
USNM 406013	CUR11013	<i>Lipogramma klayi</i>	KX713737	KX713826	KX713883	KX713845	KX713865	genseq-3
USNM 406133	CUR11133	<i>Lipogramma klayi</i>	KX713740	KX713828	KX713885	KX713847	KX713867	genseq-3
USNM 406134	CUR11134	<i>Lipogramma klayi</i>	KX713741	-	-	-	-	genseq-3
USNM 406375	CUR11375	<i>Lipogramma klayi</i>	KX713744	-	-	-	-	genseq-3
USNM 406376	CUR11376	<i>Lipogramma klayi</i>	KX713745	KX713830	KX713887	KX713849	KX713869	genseq-3
USNM 422669	CUR13112	<i>Lipogramma klayi</i>	KX713772	-	-	-	-	genseq-3
USNM 422676	CUR13113	<i>Lipogramma klayi</i>	KX713773	-	-	-	-	genseq-3
USNM 422690	CUR13114	<i>Lipogramma klayi</i>	KX713774	-	-	-	-	genseq-3
Photo Voucher Only	CUR15064	<i>Lipogramma klayi</i>	KX713800	-	-	-	-	genseq-5
Photo Voucher Only	CUR15066	<i>Lipogramma klayi</i>	KX713801	-	-	-	-	genseq-5
Photo Voucher Only	CUR15068	<i>Lipogramma klayi</i>	KX713802	-	-	-	-	genseq-5
Photo Voucher Only	CUR15069	<i>Lipogramma klayi</i>	KX713803	-	-	-	-	genseq-5
Photo Voucher Only	CUR15070	<i>Lipogramma klayi</i>	KX713804	-	-	-	-	genseq-5
Photo Voucher Only	CUR15075	<i>Lipogramma klayi</i>	KX713805	-	-	-	-	genseq-5
Photo Voucher Only	CUR15076	<i>Lipogramma klayi</i>	KX713806	-	-	-	-	genseq-5
Photo Voucher Only	CUR15077	<i>Lipogramma klayi</i>	KX713807	-	-	-	-	genseq-5
Photo Voucher Only	CUR15084	<i>Lipogramma klayi</i>	KX713810	-	-	-	-	genseq-5

CatalogNumber	TissueNumber	Species	GenBank COI	GenBank H3	GenBank TMO-4C4	GenBank Rag1	GenBank Rhodopsin	GenSeq designation
USNM 438687	DOM16036	<i>Lipogramma klayi</i>	KX713817	-	-	-	-	genseq-4
USNM 438741	DOM16090	<i>Lipogramma klayi</i>	KX713819	-	-	-	-	genseq-4
USNM 438742	DOM16091	<i>Lipogramma klayi</i>	KX713820	-	-	-	-	genseq-4
USNM 438803	DOM16152	<i>Lipogramma klayi</i>	KX713821	-	-	-	-	genseq-4
USNM 406011	CUR11011	<i>Lipogramma levinsoni</i>	KX713735	-	-	-	-	genseq-3
USNM 406012	CUR11012	<i>Lipogramma levinsoni</i>	KX713736	-	-	-	-	genseq-3
USNM 406018, paratype	CUR11018	<i>Lipogramma levinsoni</i>	KX713738	KX713827	KX713884	KX713846	KX713866	genseq-2
USNM 406019	CUR11019	<i>Lipogramma levinsoni</i>	KX713739	-	-	-	-	genseq-3
USNM 406139, holotype	CUR11139	<i>Lipogramma levinsoni</i>	KX713742	KX713829	KX713886	KX713848	KX713868	genseq-1
USNM 406140, paratype	CUR11140	<i>Lipogramma levinsoni</i>	KX713743	-	-	-	-	genseq-2
USNM 406393, paratype	CUR11393	<i>Lipogramma levinsoni</i>	KX713747	KX713832	KX713889	KX713851	KX713871	genseq-2
USNM 406394	CUR11394	<i>Lipogramma levinsoni</i>	KX713748	-	-	-	-	genseq-3
USNM 426784, paratype	CUR13183	<i>Lipogramma levinsoni</i>	KX713777	-	-	-	-	genseq-2
USNM 426754	CUR13184	<i>Lipogramma levinsoni</i>	KX713778	-	-	-	-	genseq-3
USNM 426774	CUR13267	<i>Lipogramma levinsoni</i>	KX713783	-	-	-	-	genseq-3
USNM 426730	CUR13268	<i>Lipogramma levinsoni</i>	KX713784	-	-	-	-	genseq-3
Photo Voucher Only	CUR15031	<i>Lipogramma levinsoni</i>	KX713792	-	-	-	-	genseq-5
Photo Voucher Only	CUR15058	<i>Lipogramma levinsoni</i>	KX713797	-	-	-	-	genseq-5
USNM 438703	DOM16052	<i>Lipogramma levinsoni</i>	KX713818	-	-	-	-	genseq-4
USNM 440439, holotype	CUR16008	<i>Lipogramma barretoi</i>	MG676227	-	-	-	-	genseq-1
USNM 406392, paratype	CUR11392	<i>Lipogramma barretoi</i>	KX713746	KX713831	KX713888	KX713850	KX713870	genseq-2
UF 239254, paratype	CUR11426	<i>Lipogramma barretoi</i>	KX713749	KX713833	KX713890	-	-	genseq-2
USNM 414914, paratype	CUR12149	<i>Lipogramma barretoi</i>	KX713759	KX713836	KX713893	KX713854	KX713874	genseq-2
USNM 431687, paratype	CUR14079	<i>Lipogramma barretoi</i>	KX713789	-	-	-	-	genseq-2
USNM 436460, paratype	CUR15125	<i>Lipogramma barretoi</i>	KX713815	-	-	-	-	genseq-2
USNM 436474, paratype	CUR15139	<i>Lipogramma barretoi</i>	KX713816	-	-	-	-	genseq-2
USNM 431722, holotype	CUR14114	<i>Lipogramma schrieri</i>	KX713790	-	-	-	-	genseq-1
USNM 414913, paratype	CUR12101	<i>Lipogramma schrieri</i>	KX713756	-	-	-	-	genseq-2
USNM 414911, paratype	CUR12316	<i>Lipogramma schrieri</i>	KX713765	KX713839	KX713896	KX713857	KX713877	genseq-2

CatalogNumber	TissueNumber	Species	GenBank COI	GenBank H3	GenBank TMO-4C4	GenBank Rag1	GenBank Rhodopsin	GenSeq designation
UF 239255, paratype	CUR12317	<i>Lipogramma schrieri</i>	KX713766	KX713840	KX713897	KX713858	KX713878	genseq-2
USNM 430035, paratype	CUR13329	<i>Lipogramma schrieri</i>	KX713788	-	-	-	-	genseq-2
USNM 435299, paratype	CUR15012	<i>Lipogramma schrieri</i>	KX713791	-	-	-	-	genseq-2
USNM 413864, paratype	CUR12290	<i>Lipogramma schrieri</i>	KX713764	KX713838	KX713895	KX713856	KX713876	genseq-2
Photo Voucher Only	BLZ8127	<i>Lipogramma trilineata</i>	JQ841643	-	-	-	-	genseq-5
Photo Voucher Only	BLZ8128	<i>Lipogramma trilineata</i>	JQ841642	-	-	-	-	genseq-5
USNM 415245	BLZ8168	<i>Lipogramma trilineata</i>	JQ841645	-	-	-	-	genseq-4
USNM 415298	BLZ8274	<i>Lipogramma trilineata</i>	JQ841646	KX713825	KX713882	KX713844	KX713864	genseq-4
Photo Voucher Only	BLZ8343	<i>Lipogramma trilineata</i>	JQ841644	-	-	-	-	genseq-5
USNM 404204	BLZW204	<i>Lipogramma trilineata</i>	KX713734	-	-	-	-	genseq-4
USNM 414989	CUR13082	<i>Lipogramma trilineata</i>	KX713768	-	-	-	-	genseq-3
USNM 414990	CUR13089	<i>Lipogramma trilineata</i>	KX713769	-	-	-	-	genseq-3
USNM 414991	CUR13090	<i>Lipogramma trilineata</i>	KX713770	KX713841	KX713898	KX713859	KX713879	genseq-3
Photo Voucher Only	CUR15034	<i>Lipogramma trilineata</i>	KX713794	-	-	-	-	genseq-5
Photo Voucher Only	CUR15078	<i>Lipogramma trilineata</i>	KX713808	-	-	-	-	genseq-5
Photo Voucher Only	CUR15079	<i>Lipogramma trilineata</i>	KX713809	-	-	-	-	genseq-5
USNM 442762	EUS17109	<i>Lipogramma regium</i>	MG676228	-	-	-	-	genseq-4

Supplementary material I

Figure S1

Authors: Carole C. Baldwin, Luke Tornabene, D. Ross Robertson, Ai Nonaka, R. Grant Gilmore

Data type: (measurement/occurrence/multimedia/etc.)

Explanation note: Neighbor-joining network based on COI sequences of *Lipogramma* species investigated in this study. Scale-bar units are substitutions per site.

Copyright notice: This dataset is made available under the Open Database License (<http://opendatacommons.org/licenses/odbl/1.0/>). The Open Database License (ODbL) is a license agreement intended to allow users to freely share, modify, and use this Dataset while maintaining this same freedom for others, provided that the original source and author(s) are credited.

Link: <https://doi.org/10.3897/zookeys.729.21842.suppl1>

